DEVELOPMENT OF A PROCESS ROUTE FOR THE BENEFICIATION OF MALLAM AYUBA MANGANESE DEPOSIT TO FERROMANGANESE FEED GRADE

BY

YARO, SHEHU ALIYU

A thesis submitted to the Postgraduate School, Ahmadu Bello University, Zaria in partial fulfilment of the Requirements for the award of the degree of Doctor of Philosophy in the Department of Metallurgical Engineering, Faculty of Engineering.

1998

DECLARATION

I, Shehu Aliyu Yaro do hereby declare that this thesis is the result of my original research work. All works of other authors referred to in the course of the research have been appropriately acknowledged and properly referenced. And to the best of my knowledge and understanding this thesis or part of it has not been submitted to any other institution or organization for the award of a higher degree.

Shehu Aliyu Yaro

CERTIFICATION

This thesis entitled "Development of a process route for the Beneficiation of Mallam Ayuba Manganese deposit" by SHEHU ALIYU YARO. Meets the regulation governing the award of the degree of Doctor of Philosophy of the Ahmadu Bello University, Zaria and is approved for its contribution to knowledge.

Dr. I. A. Madugu
Chairman, Supervisory Committee — Date: 4/3/98

Dr. O. B. Oloche
Member, Supervisory Committee — Date: 4/3/98

Dr. I. A. Madugu
Head of Department — Date: 4/3/98

Dean, Postgraduate School — Date: 4/9/98

DEDICATION

Dedicated to Almighty Allah who make all things possible and to my late Mother Nana Asama'u who took the burden of sending me to School.

ACKNOWLEDGEMENT

I am grateful to my Supervisor and Head of Department, Dr. I. A. Madugu who inspite of his tight schedule of work has been able to spare his time and energy to go through the work, profer academic insights and also for his moral and financial support in the course of carrying out the research. Working with him has been my most demanding academic Adventure.

My sincere appreciation to the World Bank Project Implementation Office A.B.U. Zaria and the National Universities Commission for the 9 months fellowship at the Camborne School of Mines, University of Exeter where most of the analyses were carried out and without this fellowship this work would have remained a dream. I also extend my gratitude to Dr. C.V. Phillips Research Director Camborne School of Mines who arranged the programme and Dr. B. A. Wills who provided supervision and guidance during my stay at the School. My appreciation also goes to the persons of Tony Clark and Tony Ball both of Mineral processing and Instrumental Analytical Laboratories respectively at the School.

I would also like to acknowledge the help of Dr. Muhammad Bala Dewu, Dr. J.O.T. Adewara and Dr. O. B. Oloche for their advice and guidance while conducting and writing the project. My deep gratitude to my former Head of Department, Prof. A. K. Oyinlola for recommending me for the 9 months fellowship.

In the course of carrying this work, I have had the opportunity of meeting people who contributed directly or indirectly to its successful completion and space will not permit me to mention their names. Their contributions are hereby acknowledged.

ABSTRACT

A process route for the beneficiation of Mallam Ayuba Manganese deposit located in Kaduna State, Nigeria was developed. By this route a low grade manganese concentrate which can be used in the production of spiegeleisen using the blast furnace process was produced.

Based on the chemical, size/assay and mineralogical analyses carried out in this study, it was established that Mallam Ayuba Manganese deposit is a low grade ore containing only 23%Mn_3O_4 with high amoaunt of SiO_2 (38.68%). The deposit also contains moderate amount of sulphur (0.01%) and phosphorous (P205) (0.49%). From these analyses it was also established that the constituent minerals of the ore, are uniformly distributed, finely dessiminated and intermittently associated with each other.

Liberation and grindability tests, revealed that no meaningful degree of liberation could be achieved because of the high degree of interlocking and intergrowth between the individual mineral grains. These tests also gave the average work index of the ore over particle size range -75 to -lOOOuM to be 13.12kwh/st.

Concentration tests by gravity and froth flotation techniques with the aim of producing a concentrate for ferromanganese production did not yield the desired results. This is because the concentrates produced assay low manganese and high SiO_2 However, a low grade concentrate which can be used in the production of spiegeleisen(low grade ferromanganese) was produced by the process of lime-clinkering .This low grade concentrate can also be smelted with the Itakpe iron ore concentrate to produce a high manganese pig iron.

TABLE OF CONTENTS

	PAGES
DECLARATION	ii
CERTIFICATION	iii
DEDICATION	iv
ACKNOWLEDGEMENT	v
ABSTRACT	vi
TABLE OF CONTENTS	vii
LIST OF TABLES	xi
LIST OF FIGURES	xiv
LIST OF PLATES	xvii
LIST OF APPENDICES	xix
LIST OF ABBREVIATIONS	xx
CHAPTER ONE:	
1.0 **INTRODUCTION**	1
1.1 Nigerian Manganese Deposit	5
1.2 Mallam Ayuba Manganese Deposit	8
1.3 Common Manganese Bearing Minerals	8
1.4 Classification of Manganese Ores/Concentrates	12
1.5 Manganese Nodules	13
CHAPTER TWO:	
2.0 **LITERATURE REVIEW**	16
2.1 Sampling in Metallurgical Industries	16
2.2 Chemical Analysis of Metallurgical Raw Materials	21
2.3 Analytical Methods used in Metallurgical Analysis	21
2.4 X-ray Florescence Spectrometry [XRFS]	22
2.5 Scanning Electron Microscopy (SEM)	23
2.6 X-ray Powder Diffraction (XRD)	24

2.7 Comminution 26

2.8 Grindability Tests 29

2.8.1 Work Index Methods 29

2.9 Mineral Beneficiation Unit Processes ... 32

2.10 Gravity Concentration Processes 33

2.10.1Concentration Criterion in Gravity Separation 35

2.11 Heavy Liquid Tests 35

2.11.1 Simple Sink-Float Analysis 36

2.11.2 Complete Sink-Float Analysis 36

2.11.3 Density Gradient Analysis 37

2.11.4 Density Curves 38

2.11.5 CUM. % Assay Against Wt. of Sink Curves ... 38

2.11.6 Elementary Assay Curves/Characteristics Assay Curves 39

2.12 Theoritical Background on the Use of Release Technique in Liberation Studies ... 39

2.13 Froth Flotation 44

2.13.1 Column Flotation 48

2.14 Magnetic Method of Separation 50

2.14.1 Principles of Magnetic Separation ... 50

2.15.0 Physical and Physio-Chemical Separation Processes Used in the Beneficiation of Manganese Ores 52

2.15.1 Manganese Beneficiation by Gravity Methods 53

2.15.2 Flotation of Manganese Ores 54

2.15.3 Manganese Benefication by Magnetic Method 57

2.16 Some of the Hydrometallurgical Processes Developed for the Beneficiation of Manganese Ores 58

2.17 Pyrometallurgical Processes for manganese Beneficiation 61

2.18 Other Processes 65

2.19 Thermal Pre-Treatments Given to Silicate

	Bearing Minerals Prior to Beneficiation ...	66
2.20	Lime-Clinkering Process	67
2.21	Electrometallurgy of Manganese ...	69
2.22	Beneficiation of Manganese Nodules ...	70
2.23	Ferroalloy Production	71
2.23.1	Manganese Ferroalloy Production ...	72
2.23.2	High Carbon Ferromanganese Production ...	72
2.23.3	Low and Medium Carbon Ferromanganese Production	73
2.23.4	Silico-Manganese Production	73
2.23.5	Conclusion	74
CHAPTER THREE:		
3.0	**EXPERIMENTAL TECHNIQUES**	75
3.1	Introduction	75
3.2	Sample Taking at the Field ...	75
3.3	Preparation of Bulk Sample for Chemical Analysis	75
3.4	Chemical Analysis by XRFS ...	78
3.5	Size/Assay Analysis	79
3.6	Mineralogical Analyses	86
3.6.1	Sample Preparation for SEM Analysis	90
3.7	Liberation Size Determination ...	90
3.7.1	Determination of Liberation Size using Release Analysis Technique	96
3.8	Heavy Liquid Tests	103
3.9	Gravity Separation Test	107
3.9.1	Gravity Concentration Using Shaken Table ...	107
3.9.2	Gravity Concentration Using Mozley Separator	110
3.10	Determination of Bond Work Index (W_i) ...	113
3.11	Granulatory Tests	124
3.12	Froth Flotation Tests	126

3.13	Lime - Clinkering Process	131
CHAPTER FOUR:		
4.0	**RESULTS AND DISCUSSIONS**	136
4.1	Chemical Analysis	136
4.2	Size/Assay Analyses	137
4.3	Mineralogical Investigations	139
4.4	Heavy Liquid Tests	149
4.5	Liberation Size Studies	150
4.6	Gravity Separation Tests	168
4.7	Granulatory Test	177
4.8	Froth Flotation Tests	179
4.9	Grindability Tests	180
4.10	Lime-Clinkering Processes	185
CHAPTER FIVE:		
5.0	**CONCLUSIONS AND RECOMMENDATIONS** ...	199
5.1	Introduction	199
5.2	Conclusions	201
5.3	Recommendations	204
	References	207
	Appendices	220

LIST OF TABLES

			PAGES
Table 1.1	-	Important manganese bearing minerals and their properties ...	11
Table 1.2	-	Typical Composition of a Metallurgical Grade Ore/Concentrate. ...	13
Table 1.3	-	Typical composition of manganese nodules from different ocean floors	15
Table 2.1	-	Gravity Separation Processes and their approximate effective particle size range for their applications	34
Table 3.1	-	Full Chemical Analysis of the Raw Ore as determined by XRFS ...	79
Table 3.2	-	Results of Size/Assay Analysis for Manganese	81
Table 3.3	-	Results of Size/Assay Analysis for Silica	82
Table 3.4	-	Results of Size/Assay Analysis for Iron	83
Table 3.5	-	Distribution of Mn, Fe and S_1O_2 in the various Size Fractions	84
Table 3.6	-	Summary of Results of Size/Assay Analysis	85
Table 3.7	-	Full Mineralogical Analysis of the Ore	88
Table 3.8	-	Distribution of Minerals in the various Size Fractions from by XRD Analysis	88
Table 3.9	-	Distribution of Manganese into the Sink, Float for various Size Fractions produced by heavy liquid Tests ...	92
Table 3.10	-	Distribution of Silica into the Sink, Float for various Size Fraction produced by heavy liquid Test ...	93
Table 3.11	-	Distribution of Iron into the Sink, Float for various Size Fraction produced by heavy liquid Test ...	94
Table 3.12	-	Distribution of Mn, SiO_2 and Fe into the Sink and Float or various Size Fraction produced by heavy Liquid Test	95

Table 3.13	-	Release Analysis for Manganese ...	97
Table 3.14	-	Release Analysis for Silica ...	99
Table 3.15	-	Release Analysis for Iron ...	101
Table 3.16	-	Characteristic Curves for Manganese at various Size Fractions ...	105
Table 3.17	-	Metallurgical Balance for Manganese Separation carried out using laboratory Scale shaken table at various Size Fraction	108
Table 3.18	-	Metallurgical Balance for the S_1O_2 Separation carried out using Mozley Separator at various Size Fractions	109
Table 3.19	-	Metallurgical Balance for the Manganese Separation carried out Using Mozley Separator at Various Size Fractions ...	111
Table 3.20	-	Metallurgical Balance for S_1O_2 Separation carried out using laboratory Scale shaken Table at various Size Fractions	112
Table 3.21	-	Particle Size Analysis of the Feed to the Ball Mill for Work index Determination	117
Table 3.22	-	Particle Size Analysis of the Mill Discharge for work index determination at 75µM Size Fraction	118
Table 3.23	-	Particle Size Analysis of the Mill discharge for work index determination at 1000µM	119
Table 3.24	-	Particle Size Analysis of the Mill Discharge for work index Determination at 500µM	120
Table 3.25	-	Bond work index calculation sheet for 100µM Size Fraction	121
Table 3.26	-	Bond Work index calculation sheet for 500µM Size Fraction	122
Table 3.27	-	Bond work index calculation for 75µM Size Fraction	123
Table 3.28	-	Granulatory Test Results ...	125
Table 3.29	-	Chemical Analysis of Concentrate and	

Tailing produced by Flotation Using Armac-C Collector 127

Table 3.30 - Chemical Analysis of the Concentrate and Tailings produced by Flotation Using Aerofloate 64 Collector ... 128

Table 3.31 - Chemical Analysis of the Concentrate and Tailings produced Using Armac-T Collector 129

Table 3.32 - Metallurgical Balance for the Flotation Tests 130

Table 3.33 - Chemical Analysis of the Concentrate produced from the Lime - Clinkering Process 133

Table 3.34 - Chemical Analysis of the Tailings Produced from the lime - Clinkering Process 134

LIST OF FIGURES

			PAGES
Figure 1.1	-	Schist belts of Northern Nigeria	6
Figure 1.2	-	Location of Major Identified Manganese Ore Deposits in Nigeria	9
Figure 2.1	-	Theoretical Density Curve for completely liberated minerals ...	39
Figure 2.2	-	Theoretical Density Curve for Completely Locked up Minerals ...	39
Figure 2.3	-	Theoretical Density Curve for Partially Liberated Minerals ...	41
Figure 2.4	-	Theoretical Characteristics Curve for completely liberated Minerals	41
Figure 2.5	-	Theoretical Characteristics Curve for Completely Locked Minerals	42
Figure 2.6	-	Theoretical Characteristics Curve for Partially Liberated Minerals	42
Figure 2.7	-	Single Sample Vector Diagram	44
Figure 2.8	-	Addition of Vectors ...	44
Figure 2.9	-	Theoretical Release Analysis Curves	46
Figure 2.10	-	Principle of Froth Flotation ...	48
Figure 2.11	-	Column Flotation Cell	50
Figure 2.12	-	Principles of Magnetic Separation	51A
Figure 3.1	-	Sampling Procedures	77
Figure 3.2	-	Flow diagram of the Lime - Clinkering Process	132
Figure 4.1	-	A plot of CUM. % Distribution against CUM. % weight for µM and SiO_2 ...	138

Figure 4.2	-	Plot of % Distribution against Particle size for Mn, SiO_2 and Fe	138A
Figure 4.3	-	XRD Diffraction Pattern of the Ore	140
Figure 4.4	-	X-ray Spectrum of a Mineral Phase in the Ore	145
Figure 4.5	-	X-ray Spectrum of a mineral phase in the Ore	146
Figure 4.6	-	X-ray Spectrum of a mineral phase in the Ore	147
Figure 4.7	-	X-ray Spectrum of a mineral phase in the Ore (Hollandite) ...	148
Figure 4.8	-	Plot of % Distribution against size Fraction for Mn, SiO_2 and Fe in the Float	151
Figure 4.9	-	Plot of % Distribution against Size Fraction for Mn, SiO_2 and Fe in The Sink	152
Figure 4.10	-	Density Curve for Manganese ...	154
Figure 4.11	-	Characteristic Curve for Manganese	155
Figure 4.12	-	CUM. % Assay against Wt of Sinks Curves	156
Figure 4.13	-	Release analysis curve for Manganese Liberation ...	158
Figure 4.14	-	Release analysis curve for Iron Liberation	159
Figure 4.15	-	Release analysis curve for SiO_2 liberation	160
Figure 4.16	-	Grade - Recovery plot for Mn and SiO_2 at -63 + 45 µM Size Fraction	170
Figure 4.17	-	Grade - Recovery plot for Mn and SiO_2 at -45 µM Size Fraction	171
Figure 4.18	-	Grade - Recovery plot for Mn and SiO_2 at -125 +90 µM Size Fraction	172
Figure 4.19	-	Grade - Recovery plot for Mn and SiO_2 at -90 +60µM Size Fraction	173
Figure 4.20	-	A Comparison of Grade - Recovery Curves for Manganese at various Size	

Fraction 174

Figure 4.21 - A Comparisons of Grade - Recovery Curves for Silica at various Size Fractions 175

Figure 4.22 - A plot logarithmic of Grinding Against CUM. 80% passing for Granulating test 178

Figure 4.23 - Semi-logarithmic plot of the feed to the ballmill for wi determination 181

Figure 4.24 - Semi-logarithmic plot of the ballmill discharge for wi determination at 75μM 182

Figure 4.25 - Semi - logarithmic plot of the Ballmill Discharge for wi Determination at 500μM ... 183

Figure 4.26 - Semi - logarithmic plot of the ballmill discharge for Wi at 1000μM 184

Figure 4.27 - Variation of work index with Size Fraction 186

Figure 4.28 - X-ray spectrum of the Tailings of the lime - clinkering process 188

Figure 4.29 - X-ray Spectrum of the concentrate of the lime clinkering process 189

Figure 4.30 - X-ray Spectrum of phase A (Light Phase) 189A

Figure 4.31 - X-ray Spectrum of Phase B (Grey Phase) 190

Figure 4.32 - X-ray Spectrum of Phase C (Dark Grey Phase) 191

Figure 4.33 - X-ray Spectrum of the Single Phase Produced at $\frac{CaO-3P_2O_5}{SiO_2} = 1.0$ 198

LIST OF PLATES

			PAGES
Plate I	-	Highly magnified Backscattered Electron Image (BEI) of the lump sample of the Ore	142
Plate II	-	Electron Photomicrograph of the Lump Sample of the Ore Showing some of the Minerals in the Ore	143
Plate III	-	Electron Photomicrograph of the Ore Showing a single phase of Hollandite Mineral	144
Plate IV	-	Electron Photomicrograph of the Sinks (+3.0) Tests at particle Size Fraction -63 + 45μM	161
Plate V	-	Backscattered Electron Image of the Sinks (+3.0) at the particle Size Fraction -63 + 45μM	162
Plate VI	-	Electron Photomicrograph of the ground Ore (-125 + 90μM)	163
Plate VII	-	Electron Photomicrograph of the ground Ore (-100μM)	164
Plate VIII	-	Electron Photomicrograph of the Gravity concentrate Shaking Table ...	165
Plate IX	-	Electron Photomicrograph of the Gravity concentrate (-45μM) Mozley Separator ...	166
Plate X	-	Electron Photomicrograph of the Gravity Tailings (-45μM) Mozley separator	167
Plate XI	-	Electron Photomicrograph of the clinker produced at $\frac{CaO-3(P_2O_5+Al_2O_3)}{SiO_2} = 2.0$	192
Plate XII	-	Backscattered Electron Image (BEI) of the clinker produced at $\frac{CaO-3(P_2O_5+Al_2O_3)}{SiO_2}=2.0$	194
Plate XIII	-	Electron Photomicrograph of the clinker Produced at $\frac{CaO-3(P_2O_5+Al_2O_3)}{SiO_2} = 1.4$	195

Plate XIV – Electron Photomicrograph of the clinker produced at $\frac{CaO-3(P_2O_5+Al_2O_3)}{SiO_2} = 1.4$ Showing Individually Phases of A & B 196

Plate XV – Electron Photomicrograph of the Clinker Produced at $\frac{CaO-3(P_2O_5+Al_2O_3)}{SiO_2} = 1.0$ 197

LIST OF APPENDICES

Appendix I	-	XRD patterns for the sample of the ore ground to various Size Fractions from - 1000µM to +45µM.
Appendix II	-	A printouts from the master sizer of the results of granulatry Tests of the Ore ground for various times.
Appendix III	-	Specifications for Battery and Chemical Grade Ore/Concentrate.

ABBREVIATIONS

AIMME:	American Institute of Mining and Metallurgical Engineers.
AIME:	American Institute of Mining Engineers
SME:	Society of Mining Engineers
USBM:	United States Bureau of Mines
SEM:	Scanning Electron Microscopy
XRFS:	X-ray Fluorescence Spectrophotometry
XRD:	X-ray diffraction (Diffractometer)
CAMMET:	Canadian Metallurgical Quarterly
IMM:	Institution of Mining and Metallurgy
US:	United States
µM:	Micron Meter (10^{-6}M).
CUM.:	Cumulative
Wt:	Weight

CHAPTER ONE

INTRODUCTION

The importance of manganese in steel making dates from shortly after the introduction of the Bessemer process in 1856 when the Ferroalloy spiegeilesen was first used to introduce manganese into steel to overcome hot shortness. At present 90% of the total world production of manganese is used in the metallurgical industries (1). It is mainly consumed in these industries in the form of ferromanganese for deoxidation, desulphurisation and alloying.

Manganese is a strategic metal as most of the industrialised nations depend on the less developed nations for their continuous supply of manganese. In fact metallurgical grade manganese ores are located in only four countries, Gabon, South Africa, Australia and Brazil (1). For use in the metallurgical industries the manganese ore/concentrate must meet certain minimum requirements in terms of manganese, silica, alumina, sulphur and phosphorous content.

Despite the fact that reports from Geological Survey of Nigeria (2), Raw Materials Research and Development Council and Steel Raw Materials Exploration Agency showed that Nigeria is blessed with large reserves of proven and unproven manganese deposits. The local steel industries have continued

to depend on imported sources of manganese. This is because the local manganese deposits are low grade and require upgrading before they could be used. The challenge is the development of technology which could recover manganese from those low grade deposits. This is the aim of this work and requires detailed study of the various processes for recovering manganese from low grade manganese sources.

At present, limited or no research has been carried out on the beneficiation of the manganese ores in the proven reserves(3). It is therefore important that these types of studies are conducted. They will go a long way in helping the government conserve its limited foreign exchange. Also through such studies the technology for the beneficiation will be acquired by indigenous Engineers and Technician which will contribute towards our much sought technological take off and economic self reliance.

It is the aim of this research work to look into the feasibility of beneficiating one of these Ores (Mallam Ayuba deposit) so as to produce a concentrate that can be used for ferromanganese production. Physical, physio-chemical, pyrometallurgical, and combination of these processes were used in the course of the research. However, emphasis was laid on the physical separation processes. This is justified by the fact that these processes are relatively cheap and effective with less environmental hazards.

The work was started by carrying out a full chemical analysis of the Ore with the aim of establishing its chemical composition and grade. The chemical analysis revealed that the Ore is low grade assaying only about 23% Mn_3O_4 and contains high amount of Silica (36.8%) and Alumina (11.0%), while the phosphorus and sulphur contents of 0.04% and 0.01% respectively is within the acceptable limit. The chemical analysis was followed by Size/Assay analysis which was to determine the distribution of constituent minerals of the Ore in the various size fractions with the aim of establishing the possibility of using a waste rejection technique in its concentration. The results of the Size/Assay analysis revealed that all the constituent minerals of the Ore are uniformly distributed in all the size fractions. The use of waste rejection technique was therefore ruled out because any attempt to reject the gangue material at coarse sizes would result in the loss of appreciable amounts of valuable minerals.

Mineralogical analyses using optical microscopy, X-ray Diffraction technique and Scanning Electron Microscopy for the purpose of identifying the constituent minerals of the Ore, their grain size distribution and the degree of associations of the valuable and gangue minerals were also carried out. The results revealed that the most abundant manganese bearing minerals in the ore are spessartine ($3MnO.\ Al_2O_3.3SiO_2$) and Almandine [$3\ (FeO,MnO).\ Al_2O_3.3SiO_2$] while psilomelane [(Ba, K)

(Mn_8O1_6) (OH)] occurs in small amounts. Other manganese bearing minerals were also recorded. The results also showed that these minerals are finely disseminated and associated with each other requiring very fine grinding before liberation could be achieved. Liberation studies by heavy liquid methods and Release Analysis Technique were carried out with the view of determining the liberation size of the ore for purposes of comminution and beneficiation. The results of this test showed that it is impossible to achieve good degree of liberation because the valuable and the gangue minerals are finely disseminated and interlocked with each other.

Grindability tests for the determination of grinding characteristics (work index) of the ore carried out over particle size range - 75µm, -500µm and -1000µm gave the work indeces of the ore over these particle size ranges as 10.5, 12.83 and 16.02 Kwh/st respectively. These values indicate that the ore is soft, the softness increasing with decreasing particle size.

Physical and Physio - Chemical separation tests involving gravity and Froth Flotation techniques carried out could not produce a concentrate suitable for ferromanganese production. This is because the concentrates produced assay high silica and low manganese. But a process which involved production of clinker after heating the ore with calculated amount of lime followed by grinding of the clinker and Magnetic separation of the two phases in the clinker gave a product which could serve

as feed for ferromanganese production. This process is called lime-clinkering process. The two phases in the clinker are the magnetic phase which constitute metal oxides in a complex magnetic spinel with the typical formula (Fe,)O. (Fe, Mn, Al)$_2$O$_3$ and the non-magnetic fraction constituting mainly dicalcium silicate (2CaO. SiO$_2$), tricalcium phosphates (3CaO. P$_2$O$_5$) and calcium Alumino silicate (3CaO.Al$_2$O$_3$. SiO$_2$) containing most of the silica (gangue).

The mangetic spinel phase containing essentially all the manganese as oxides can be used in several different applications. It can be fed to the blast furnace (Ajaokuta) with the Itakpe Iron ore concentrate to produce a high manganese pig iron. It may also be smelted directly to a low manganese alloy (spiegeilesen) or can undergo a two-stage smelting operation in which it will be reduced to a pig iron and a standard ferromanganese. This concentrate is also amenable to leaching and the manganese can be recovered in metallic form by hydrometallurgical means. The non-magnetic tailings comprising mainly calcium Alumina silicate and calcium disilicate can be used in cement manufacture or as refractory material.

1.1 NIGERIAN MANGANESE DEPOSITS

Most of the metallic bearing minerals in Nigeria are contained in the Schist belts or the basement complex. The Schist belts include Birnin Gwari, Kushaka, Igara, Maru and Maska, (Figure 1.1.). Major occurences of manganese bearing



A —— Ruwan-doruwa.
B —— Maraba hill.
C —— Maru belt.
D —— Chad formation.
E —— Maska belt.
F —— Unguwar mallam ayuba.
G —— Tudu kudu hill.

FIG 1-1- MAP OF NORTHERN NIGERIA SHOWING THE SCHIST BELTS

minerals have been reported in these Schist belts with minor occurences in the gneisses of the Oban Massif and the Fika shales of the sedimentary chad formation [4].

In Nigeria, the manganese bearing minerals occur mostly within the metasedimentary belts of the Schists formation as gondite type or as banded iron formation [5]. They were formed as a result of the precipitation of manganese minerals in clay and sandstones sediments under low pH-Eh conditions in an early geosychinal basin which was later metamorphosed in the green schist facies in the sediments and in the granulite facies in the gneises to form spessertine-quartzite-phyllite and spessertine-gneisses respectively.

The genesis of manganese bearing minerals depends on so many factors vis-a-vis environment of depositon, tectonic settings, climatic and biogenic conditions, conditions of temperature, pH and Eh. Basically there are three main environments of manganese deposition: the Igneous, Sedimantary and Metamorphic environments, Sedimentary and metamorphic depositions being the most important and usually contain manganese bearing minerals in economic quantities.

Available results of study show that in Nigeria most of the manganese deposits are of metamorphic origin. These include Tudun Kudu and Unguwar Mallam Ayuba in the Maska belt, Ruwan Doruwa and Maraba Hill in the Maru belt [2]. Others are the supergene enrichment manganese deposit of Igarra formation within the schist belt of South-Western Nigeria [3] and

manganese oxides deposit of sedimentary origin in association with gypsum in the Fika shales and those of Birnin Gwari, Kushaka and Massive Oban hills of present Cross River State [5]. Figure 1.2 is a map of Nigeria showing the location of major identified Manganese Ore deposits.

1.2 MALLAM AYUBA MANGANESE DEPOSIT

The Mallam Ayuba Manganese deposit is located in the Maska Schist belt, (Figure 1.1) in a village about 20km from Gangara - a border town between Kaduna and Katsina State, Nigeria.

Alot of Geological work has been carried out and published on this deposit. Geological mapping on a scale of 1: 50,000 has been carried out using normal reconnaissance technique of photogeological interpretation supplemented by field traverse. Mucke and Okujeni, [4] have published some work on the formation and origin of the deposit. Field investigation of this mineralisation was reported in the area by Wright *et al*[5]. The field investigations have covered an area of about 500 km^2 comprising of topographic sheets.

1.3 COMMON MANGNESE BEARING MINERALS

The manganese bearing minerals consist of carbonates, silicates and a large number of oxides, hydrated oxides and compound oxides with other metals. In the carbonates, for example, ($MnCo_3$) and silicates e.g. Rhodonite ($MnSio_3$) and

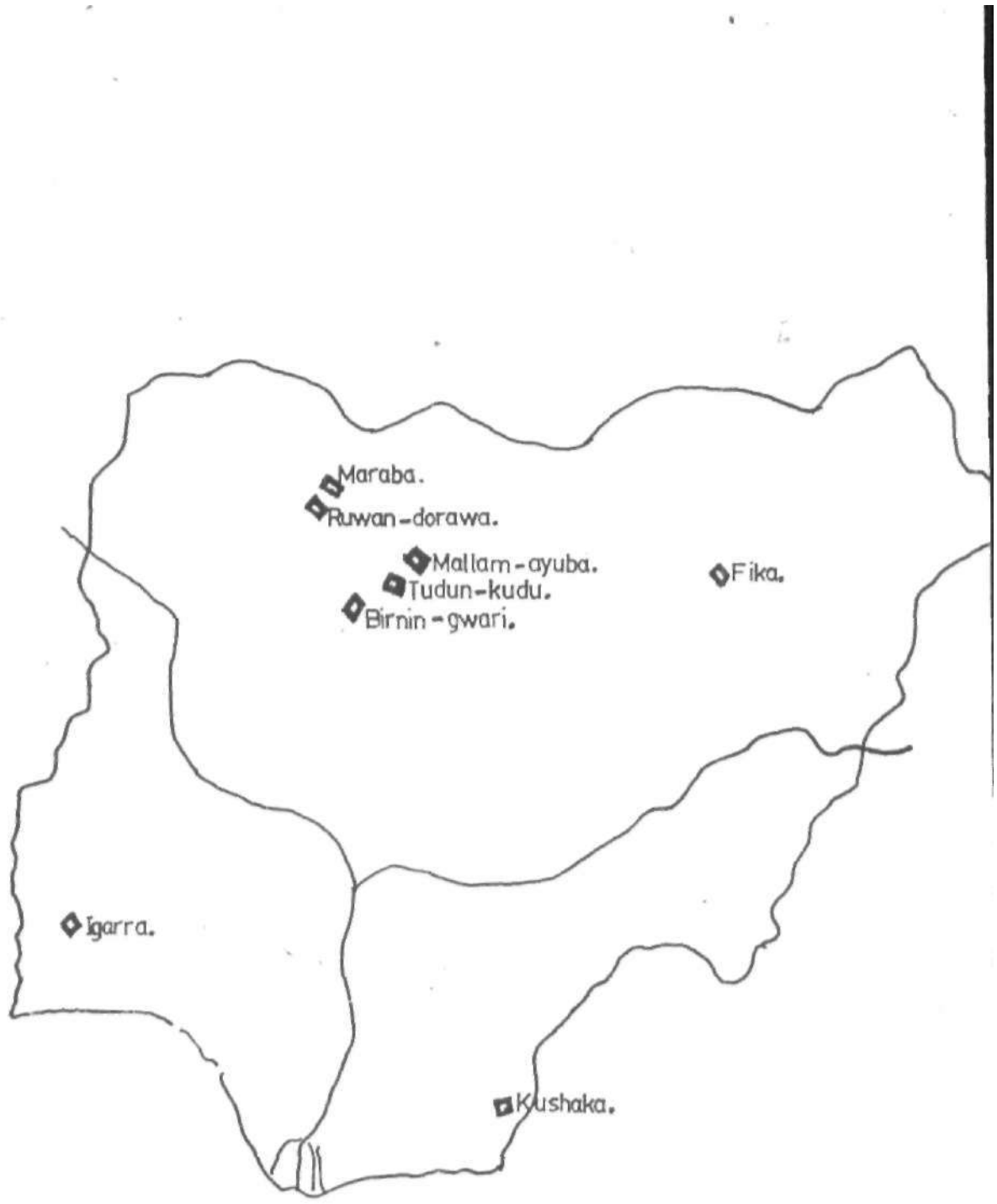


FIG.12- MAP OF NIGERIA SHOWING LOCATION OF MANGANESE DEPOS

Spessartite [$Mn_3\ Al_2\ (Sio_3)_4$], the manganese is divalent. But in the oxides it is mostly in a higher state of oxidation mainly tetravalent (Mn^{4+}). The silicate occurences presently are of no commercial value because they are very expensive to beneficiate. The carbonates and oxides are the commercially treatable minerals [6].

The oxides and the hydrated oxides of the high valency manganese are the principal sources of manganese. They usually occur in complex association with other compounds such that their mineralogy is usually difficult to understand. They include those manganese minerals which contain only manganese, oxygen and hydrogen as in pyrolusite (MnO_2), hausmanite (Mn_3O_4) and manganete [MnO (OH)]. There is also psilomelane which is an oxide-hydroxide of Ba, K and Pb and then Mn^{2+} with the general chemical formular [Ba, k, pb) (Mn1 $Mn_8O_{16}\ (OH)_4$]. Psilomelane are black and frequently fine grained, retaining adsorbed water and salts. They are intergrown with each other and with finely hydrated silicious iron minerals and alumino silicates [7]. The Ba - rich psilomelane [(Ba, Mn) (Mn_8O_{16} $(OH)_4$] is called Hollandite, the k - rich [(K, Mn) (Mn_8O_{16} $(OH)_4$)] is known as cryptomelane while the Pb - rich [(Pb, Mn) (Mn_8O_{16} $(OH)_4$)], Coronadite. In the psilomelane, the divalent Mn^{2+} may be substituted by Fe, Cu, Zn, etc. Other manganese bearing minerals include Lithiophorite [(Al, Fe, Ba, Mn, Li) $(OH)_2$ MnO_2]. The name Lithiophorite is contested most especially in phases in which

Li is absent. Jakobsite $(Mn, Fe)_3O_4$, bixbyite $(Mn,Fe)_2O_3$, Franklinite $(Fe,Mn)_2O_4$, Golaxite $(Mn\ Al_2O_4)$, Braunite $[3(Mn,Fe)_2O_3.\ MnSiO_3]$ etc [8]. Table 1.1 gives the most common manganese bearing minerals and some of their properties.

Table: 1.1 Properties of important manganese minerals

Meneral	Formula	Colour	Mn (%)	Hard-ness	Specific gravity
Pyrolusite	MnO	Steel grey to black	63.2	6-7	5
Ramdellite	MnO_2	Dark grey to black	63	3	4.7
Polianite	Mn_2O_3	Black to steel grey	N.A	6-6.5	5
Manganite	$Mn_2O_3H_2O$	Black to steel grey	62	4	4.3
Cryptomelane	KMn_8O_{16}	Black to steel grey	45-60	5-6	4.3
Psilomelane	$BaMn_9O_{16}2H_2O$	Black to dark grey	N.A	5-6	4.4-4.7
Hausmanite	$MnMn_2O_4$	Brown to Black	72	4.8	4.7-5.0
Braunite	$3Mn_2O_3MnSiO_3$	Brown to Black	50-60	6.0-6.5	4.7-4.9
Bixbyite	$(Mn,Fe)_2O_3$	Black	30-40	6	5
Jacobsite	$MnFe_2O_4$	Black	24	6	4.6
Hollandite	$BaMn_8O_{16}$	Black to steel grey	N.A	6	4.5-5.0
Coronadite	$PbMn_8O_{16}$	Black to steel grey	N.A	5.2-5.6	4.5-5.0
Rhodochrosite	$MnCO_3$	Red-rose to brown	48	3.5-4.5	3.3-3.6
Rhodonite	$MnSiO_3$	Pink	42	5.5-6.5	3.4-3.6
Alabandite	MnS	Iron-black	N.A	3.5-4	3.95
Spessartite	$3MnO.Al_2O_3 3SiO_2$	Brawnish-red	33.3	4.1-4.3	7.0-7.5

Source: "Manganese - the other uses" Stanley A. Weiss [8].

1.4 CLASSIFICATION OF MANGANESE ORES/CONCENTRATES

The term manganese ore is used to describe ores assaying more than 35%Mn. While Ores containing 10-35%Mn are termed ferruginous manganese ores and those containing less than 10%Mn are known as manganiferrous iron ores.

Beneficiated manganese concentrates are classified into three types: Metallurgical, Battery and Chemical grade. The metellurgical grade concentrates contain 38-55%Mn with 48%Mn taken as the standard for pricing. The quality of the metallurgical grade concentrate also depends on the Mn:Fe ratio and on the concentration of impurities like Alumina, phosphorous and silica. In fact metallurgical grade manganese concentrates should ideally have a Mn:Fe ratio of 7.5:1 and should contain less than 0.2% phosphorous for the production of standard ferromanganese. Table 1:2 gives the specifications for the metallurgical grade manganese ores/concentrates.

Battery and chemical grade manganese ores/concentrates have smilar composition to metallurgical grade ore/concentrates. However, for these applications the manganese content are expressed as MnO_2 [1]. The specifications for these applications are given in Appendix 3.

TABLE 1.2: SPECIFICATIONS FOR METALLURGICAL GRADE manganese ore/concentrate

Constitutuent (% Dry Basis)	Assay
Mn_3O_4, Minimum	66.6
Fe, Maximum	6
Al_2O_3, Maximum	7
Al_2O_3, + SiO_2 Maximum	11
Al, Maximum	0.18
P, Maximum	0.19
Cu + Pb + Zn, Maximum	0.3

1.5 MANGANESE NODULES

Parts of the ocean floor contain vast resources of manganese and other metals. These metals are contained in spheres of Cryptocrystalline material (do not form minerals) known as manganese nodules. The nodules are not only an important source of manganese but also of copper, nickel and cobalt. They are composed mainly of manganese oxide, iron hydroxides, nickel, cobalt and copper. Table 1.2 gives a typical composition of a manganese nodule [9].

Manganese nodules are formed in-situ by small nuclei on the ocean floor, such as Fragments of pumice, Coral, Volcanic ash and mammalian skeletons. Concentric bands of Iron and manganese oxides accumulate by precipitation from the ocean water. As these oxides precipitate they absorb and hence trap other metal ions, especially manganese, copper, nickel, cobalt etc from the ocean water and because of these trapped metal

ions the nodules are referred to as polymetallic nodules [11].

Nodules formation is favoured where sedimentation of detrital material is slow or non-existence and this coincides with some of the deepest parts of the Ocean. It is estimated that the ocean floor is littered with over 3 billion tonnes of potato sized nodules. The exploration and exploitation of these sea-bed mineral reserves is regulated by the United Nations. The United Nations has already declared some of the deep sea beds as Economic Exclusion Zones and Common heritage of mankind, [14].

Mining of the nodules as described above requires processing plants and the location of these plants is expected to depend mainly on the availability of inexpensive energy and chemicals rather than the traditional consideration of proximity to mine or market. Currently, the Japanese are believed to be close to commercial exploitation of the polymetallic nodules.

Table 1.2: Typical Composition of Manganese Nodules from the Different Ocean Floors.

	North Paciifc % Assay	South Pacific % Assay	East Pacific % Assay	Atlants/ Indian Ocean % Assay
Manganese	24.60	15.10	14.50	16.28
Nickel	1.28	0.51	0.50	0.54
Copper	1.16	0.23	0.06	0.26
Cobalt	0.23	0.34	0.42	0.26

CHAPTER TWO

2.0 LITERATURE REVIEW

2.1 SAMPLING IN METALLURGICAL INDUSTRIES

INTRODUCTION

Sampling is the means by which small amount of material is taken from the main bulk in such a way that it represents the bulk of the material. The basic purpose of sampling is to obtain a small fraction of a large quantity of material for laboratory analysis and that this small fraction should represent the average composition of the bulk of the material. Sampling is of great significance in metallurgical analysis in all types of analysis since it will be of no use if the portion of material analysed does not represent the bulk of the material.

A sample may be defined as a small portion of relatively large mass containing the same ingredient in the same proportions that occur in the bulk material. In metallurgical analysis sampling is carried out in order to achieve one of the following aims.

1. To ascertain the chemical composition of the metallurgical material e.g. Ores, Alloys, Slags etc.
2. To check whether a metallurgical product meets certain requirements.
3. For detecting impurities and contamination in metallurgical material.
4. For routine checks in metallurgical operations.

SAMPLE PREPARATION AND TAKING IN METALLURGICAL INDUSTRIES

The raw materials and finished products of metallurgical industries from which samples are taken vary greatly in their composition and therefore sampling of these materials is quite complicated most especially when a sample of 0.5 - 1kg is to be taken from 50-250 tons of materials and these materials contain unevenly distributed constituents. However samples should be taken from a material after it has been reduced to the smallest particle size.

When sampling, the bulk of material should be prepared without bringing any change in its essential characteristics, for example in the case of ores and other similar materials there is the need for series of crushing and grinding before the sample is taken. In carrying out crushing and grinding precautions should be exercised to avoid:

1. Contamination from grinding and crushing media.
2. Chemical change taking place in the sample as the heat of grind may result in the decomposition of carbonates, hydrates or oxidation of constituents e.g. sulphur or absorption of carbon dioxide.

TYPES OF SAMPLING

There are two types of sampling for metallurgical purposes.

1. Moisture sampling.
2. Assay sampling.

Moisture Sampling: Since metallurgical accounting requires accurate knowledge of the dry weights of solids and most metallurgical materials contain moisture to vary degrees. There is the need for determination of moisture content of a particular material. The moisture and assay samples should be prepared from the same material.

Grab samples are usually taken for purpose of moisture determination. The samples are then immediately weighed when wet, then dried at a suitable temperature until all hygroscopic water is driven off and then weighed again. The difference in weight represents moisture content and is expressed as

$$\% \text{ moisture} = \frac{\text{wet weight} - \text{dry weight}}{\text{wet weight}} \times 100$$

The drying temperature should not be so high so as not to bring about physical or chemical change in the material.

Assay Sampling: Assay samples are taken for purposes of chemical analysis. Most samples taken are for this purpose. Samples for assaying should be taken from the material when it has been reduced to the smallest particle size consistent with the process. Usually these samples are taken from flow streams since a ground pulp is easier to sample and will give more accurate results.

Method of Calculating Minimum Weight of Sample to be taken

Since sampling is dependent on probability then the more frequently the incremental sample is taken the more accurate

the final sample will be.

GY developed a sampling method which takes into account the particle size of the material, the mineral content, the shape of the material and the degree of liberation of the mineral in calculating the size of the sample to be taken to give the required degree of accuracy. GY's basic sampling equation is given by

$$\frac{ML}{L-M} = \frac{Cd^3}{S^2} \qquad \text{.....(1)}$$

Where

M = minimum weight of the sample required in grams.

L = The gross weight of the material to be sampled.

C = Sample constant for the material to be sampled.

d = Dimension of the largest pieces in the material to be sampled in cm.

S = Statistical error that can be tolerated in the assay of the sample.

Since in most cases the minimum weight of the sample required in grammes is small in relation to L. Then equation (1) proximates to

$$M = \frac{Cd^3}{S^2} \qquad \text{.....(2)}$$

The sampling constant C is specific to the material being sampled taking into account the mineral content and degree of liberation given by the relationship.

$$C = fglm$$

Where

f = shape factor which equals to 0.5 for all ores except gold for which it equals to 0.2.

g = factor dependent on particles size range

l = liberation factor which has values of 0 for completely homogenous material and 1.0 for completely heterogenous material. It is calculated from the expression.

$$l = (L/d)$$

where L is the size in centimetres at which the mineral is liberated and d the dimension of the largest pieces in the ore to be sampled.

M is the mineralogical composition factor which is calculated from the expression.

$$M = \frac{1-a}{a}\,[(1-a)r + at)]$$

where r and t are the mean densities of the valuable mineral and the gangue mineral respectively, a is the fractional average mineral content of the material being sampled. It is determined by assaying a number of samples of the material.

The Gy's sampling equation assumes that samples are taken at random and without bias. The equation gives the minimum theoretical weight of sample which must be taken. However, this equation is most applicable to sampling from ores, transported on conveyors or in pulp streams rather than heap

deposits which are partly inaccessible to the sampler[28].

2.2 Chemical Analysis of Metallurgical Raw Materials

Chemical Analysis of a Metallurgical raw material like an ore is very important, because from this analysis the assay as well as the amount and type of impurities associated with the are determined. These parameters play a major role in the development of a process route for the benefication of the ore. Determination of chemical composition of an ore is usually the first step to be taken for its beneficiation.

2.3 Analytical Methods used for Metallurgical Analyses

Metallurgical analyses involve the qualitative as well as the quantitative analysis of various metallurgical raw materials like ores and products like metals, alloys and slags. The analytical methods employed in metallurgical analysis can be broadly classified into two

(i) Classical methods.

(ii) Instrumental methods.

In the instrumental methods of analysis, measurement is made upon the system as a whole. A particular physical or chemical property of the system is measured in order to get the desired analytical results. Comparisons of the samples for analysis with standard samples of known composition is necessary in this method.

The most common instrumental analytical techniques used are Atomic Absorption Spectrophotometry (AAS), X-Ray Fluorescence Spectrometry (XRFS), X-Ray Diffraction (XRD), Scanning Electron Microscopy (SEM), Electron Probe Micro Analysis (EPMA).

2.4 XRFS: X-Rays Fluorescence Spectrometry

This technique works on the principle that when a material is Irradiated by X-rays, electrons are ejected from the atoms making up the material. The vacancies created by these ejected electrons are then filled by other electrons either from the higher shells within the atom or outside the atom. These electrons lose energy mainly in the form of radiation or X-rays. The X-rays will have a precisely defined energy and the wavelength or (velocity of the electron) are related by the Plank's energy equation

$$E_1 - E_2 = hc. \qquad (1)$$

Where

E_1 = Former Energy level of the electrons before filling the vacancy.

E_2 = New energy level of the electrons after filling the vacancy.

h = Plank's constant

c = Velocity of light.

As the energies or wavelengths are characteristics of the

atoms of the elements emitting the X-rays, they are used for qualitative analysis while the intensity of these characteristics X-rays is related to the concentration of the particular element in the material and is used for quantitative elemental analysis (15, 16, 17, 18).

2.5 SCANNING ELECTRON MICROSCOPY

This method is used to study the properties of materials at microspic level. The most important applications are the investigation of the micro-structure and analysis of inhomogeneity such as defects, dislocation, submicroscopic precipitates, inclusions, domains etc. It is also used for determining the composition of individual grains of particles and surface properties like topography.

In SEM, a small area of the specimen of a material is irradiated with direct electron beam and characteristics X-rays are produced which are used for the qualitative and quantitative analysis. The most important of the produced electrons (X-rays) called Backscattered or primary reflected electrons are detected and amplified. The output from this, is a function of the composition of the area irradiated by electron beam.

The intensity of Backscattered electron signals is dependent on the atomic number of the specimen and specimen surface of different chemical composition will produce different signal intensities and appear different on the SEM

screen. The signal intensities are used for quantitative analysis [19].

Before the analysis an optical microscopic is used to view and mark the position or area of interest on the specimen. The specimen is then introduced into the machine (SEM) where an electron beam is focused unto the specimen by a system of electromagnetic lenses and by means of deflection coils. The electron beam is made to scan across several lines to cover a rectangular area enclosing the marked area of interest. The quantitative analysis of that particular point of interest on the specimen is then carried out using crystal spectrometers which collect all the signals from that point and record them. The recorded signals are used for identification and quantitative analysis of the sample [20].

2.6 X-RAY POWDER DIFFRACTION (DIFFRACTOMETER)

X-ray diffraction analysis is a non-destructive methods of analysis. It is use for both qualitative and quantitative analysis of materials. This method can be used to determine the actual compound/compounds presents in a material and can also distinguish the different crystal forms of the compounds. However, this technique is only applicable to crystalline solids [22,23].

It is based on the diffraction of X-rays by polycrystalline solids and the reflections are called powder diffractometry. X-rays are deflected by crystals

when the condition satisfying the Braggs equation are fulfilled. The Braggs equation is given by:

$$X = \frac{2d \sin Q}{n} \qquad (2)$$

where

d = interplaner (lattice) space of Bragg angle

Q = Angle between the family of planes and the X-ray in the reflecting position

X = X-rays wavelength

n = an integer called order of reflection.

When a sample of crystalline material is bombarded with X-rays and Braggs conditions are satisfied, some of the X-rays are deflected and they emerge with wavelength n from the crystals while all other wavelengths are either absorbed by the crystals or passes through it and are lost. These characteristics X-rays which are deflected by the crystals are detected by a detector and registered and displayed on paper chart recorder as series of peaks (X-rays patterns). Each compound has a unique X-ray powder pattern because the line position depends on the unit cell size and the type of atoms present and their intensities of powder lines are used for qualitative phase analysis while quantitative phase analysis depends on the accurate determination of the line intensity [24, 25].

For purpose of carrying out chemical analysis using one of the above discussed methods. The sample of the ore is usually ground to powder form through a series of crushing and grinding operations known as comminution. Comminution is a very important stage in mineral beneficiation and is discussed in the following section.

2.7 COMMINUTION

This is one of the two fundamental operations in mineral processing. Because most valuable minerals are finely disseminated and intimately associated with the gangue they need to be liberated before separation can be effected and this is achieved by a process called comminution. It involves the gradual reduction in size of the particles until the clean particles of the minerals can be separated by such methods available. Comminution in mineral processing takes place as a sequence of crushing and grinding processes [27].

The theory of comminution is mainly concerned with the relationship between energy input and the product particles size produced from a given feed size. This theory continues to be a rich field of controversy. Many theories have been proposed but the greatest problem has been the fact that most of the energy input to the comminution is absorbed by the machines themselves and only a small proportion of the energy is used in real

particle breakage. For example, it has been shown that [28] in a ballmill, only 1% of the energy input is used in grinding while the rest is used in the movement of the machine parts and production of heat.

One of the earliest theory of comminution is that of Rittinger [29] which states that the energy consumed in particle breakage is proportional to the area of new surface produced. The surface area of a given weight of particle of uniform diameter is inversely proportional to the diameter (1/d) and the useful work input is also proportional to 1/d, hence Riltinger's energy equation is given by:

$$E = K\left\{\frac{1}{D_2} - \frac{1}{D_1}\right\} \qquad (3)$$

Where E = is the energy input

D_1 = is the initial particle diameter

D_2 = is the final particle diameter and

K = is a constant.

Kick [29] however proposed that the work needed, in particle breakage is proportional to the reduction in volume of the particles concerned. If d1 is the diameter of the feed particle and d2 is the diameter of the product particles, then the reduction ratio is given by d1/d2 and according to Kick's law, the energy required to achieve that reduction ratio is proportional to $R/\log_{10}2$.

It is instructive to note that in practice, these

theories have failed to meet actual commercial crushing and grinding processes. A third theory was therefore proposed by Bond [30]. According to Bond's theory the work input is proportional to the new crack tip length produced and equals the work represented by the product minus that presented by the feed. In particles of similar shape, the crack tip length is equivalent to the square root of one-half the surface area, and the new crack length is proportional to:

$$\frac{1}{\sqrt{P}} - \frac{1}{\sqrt{F}}$$

where P = the diameter in microns which 80% of the product passes

F = The diameter in micrometres which 80% of the feed passes and Bond's energy equation is given by:

$$W = \frac{10W_i}{\sqrt{P}} - \frac{10W_i}{\sqrt{F}} \qquad (4)$$

Where Wi is the work index, a comminution parameter which expresses the resistance of the ore to crushing and grinding. Wi is the energy in Kwh/t required to reduce the ore from theoretical infinite feed size to 80% passing 100μm. W is the work input or energy required to achieve that particle breakage.

plant-scale comminution equipment. The work index has also been used widely to evaluate the grinding efficiency in operating plants. Although the Bond grindability test though provides an accurate measure of ore grindability however the test procedure is time consuming. This method involves the use of a standard laboratory ballmill specifically made for the purpose, with a specified charge of balls of different diameters. The ore is ground in this ballmill for various revolutions of the mill. However, when making plant evaluations a simplified procedure requiring less time can be adequate provided the simplicity does not affect the accuracy.

Several methods to simulate the Bond work index parameter are used and some have been reported in the literature. Smith and Lee [32] for example, used batch type grindability tests to arrive at the work index. The batch-type test results were found to compare favourably with the standard grindability test data. The potential advantage being that less time is required to determine the work index using this method.

Another method of determining work index was reported by Barry and Bruce [35]. Their method requires the use of a reference ore whose work index is known using the Bond's comminution equation 4.
The work index of the unknown ore is determined when the work input W is the same for identical sample weights of

the reference and unknown ore, ground under the same conditions in a laboratory ballmill. The energy input of the unknown equal to the energy input of the reference. For the above conditions where r and u denote reference and unknown ores respectively, the following holds:

$$W_r = W_u = W_{i_r}\left[\frac{10}{\sqrt{P_r}} - \frac{10}{\sqrt{F_r}}\right] = W_{i_u}\left(\frac{10}{\sqrt{P_u}} - \frac{10}{\sqrt{F_u}}\right] \qquad (4)$$

where W_r = energy input in grinding the reference ore

W_u = energy input in grinding the test ore

W_{ir} = work index of the reference ore

W_{iu} = work index of the test ore

F_r = 80% passing feed of the reference ore

F_u = 80% passing feed of the test ore

P_r = 80% passing product of the reference ore

P_u = 80% passing product of the test ore

Therefore, the work index of the unknown ore is then:

$$W_{i_u} = W_{i_r}\left[\left(\frac{10}{\sqrt{P_r}} - \frac{10}{\sqrt{F_r}}\right)/\left(\frac{10}{\sqrt{P_u}} - \frac{10}{\sqrt{F_u}}\right)\right] \qquad (6)$$

This method is a relatively simple procedure and is called the comparative method of determining the grindability parameter. In mineral beneficiation, comminution operation is immediately followed by separation processes. These are discussed in the

following section.

2.9 MINERAL BENEFICIATION: UNIT PROCESSES

For purposes of beneficiation of any type of ore for its minerals or metal values and for the design of accompanying flowsheet(s), the separation unit processes which are involved can be broadly classified into:

Physical separation

Gravity, Magnetic, Electrostatic, Electronic, Fine Particle separation

Chemical Separation

Leaching, Precipitation, Solvent Extraction, Ion-Exchange, Carbon Adsorption, Electrowinning, Autoclaving, Chlorination.

Biological Extraction

Bacterial leaching

Pyrometallurgical Extraction

Roasting, Smelting, Refining, Thermal Decomposition, Thermal Pre-treatments

Combinations

Roast - Leach - Solvent Extraction - Electrowinning etc.

Based on the relevant data obtained from geological and mineralogical investigations, laboratory and pilot plant concentration tests are conducted from which a conceptual flowsheet is prepared, incorporating one or a combination of the above unit processes for the beneficiation of the ore(s). In the following sections,

the principles underlying some of these separation methods are discussed

2.10 GRAVITY CONCENTRATION PROCESSES

Gravity concentration processes are those processes for the separation of minerals of different specific gravity by inducing variance movement in response to the force of gravity and one or more forces, natural or applied with the assistance of a flowing film. They are widely used alone or in combination with other processes, in particular flotation, magnetic separation and/or chemical treatment. The main disadvantage of gravity separation processes is the recovery of fines and it is inherent in the process itself. Even with the more sophisticated slime gravity concentrators the practical lower limit of particle size which can be handled is still about 10μM [36,37]. Table 1.3 gives the list of major and modern gravity processes currently employed with the size range of feed material that can be effectively separated by each [38].

Gravity separation processes are effective, practical and economical in the treatment of so many ores. But their applicability to the processing of any specific ore alone or in combination with other processing methods must be determined from thorough knowledge of the mineralogical composition and

characteristics of representative samples of the ore and from careful and comprehensive testing, [39,40].

Table 2.1: Gravity separation processes and approximate effective particle size range [38].

Process/equipment	Effective particle size range in (MM)		
Dense medium separation			
i. Static type	2.0	-	50.0
ii. Dynamic type	3.0	-	20.0
Reichert Cone	1.0	-	20.0
Reichert/Vickers spirals	0.07	-	1.0
Shaking Tables	0.07	-	2.0
Slime box	0.2	-	12.0
Pinched Sluice	0.07	-	2.0
Bartles-Mozley table	0.005	-	0.1
Cross belt Separator	0.005	-	0.1
GET Duplex Separator	0.02	-	0.1
Centrifugal Separators			
i. Horizontal type	0.005	-	0.1
ii. Vertical type		-	4.1

2.10.1 CONCENTRATION CRITERION IN GRAVITY SEPARATION

In assessing the feasibility of concentrating two or more minerals by gravity method, a simple relationship known as Concentration Criterion (CC) is used. CC is defined as:

$$CC = [(\sigma_h - \sigma_f)/(\sigma_L - \sigma_f)] \qquad (7)$$

Where CC = Concentration Criterion

σ_h = s.g of heavy minerals

σ_L = s.g of Light Minerals

σ_f = s.g of Separating Medium

When the value of cc $\geq \pm$ 2.5 then it is possible to concentrate the two minerals under consideration using this method.

For determining the amenability of any ore to gravity separation at laboratory scale, heavy liquids tests are some of the methods employed. Heavy liquid tests are briefly discussed in the next section.

2.11 HEAVY LIQUID TESTS

Heavy liquid tests involve the separation of mineral mixtures into fractions of varying specific gravities. Liquid of varying specitic gravities are prepared in incremental step and representative sample of the crushed or ground ore are introduced into the liquid of highest

2.11.4 Density Curves

These curves are produced by plotting cumulative percent weight of sinks against the density of separation. They give the cumulative percent weight of sinks to be expected at any density of separation. They are in most cases used for determining the degree of liberation of minerals. For example, for liberation studies in the case of an ore in which the minerals are completely liberated, the curve takes the form of a double step line (Figure 2.1). If however, neither of the minerals is liberated, the curve will be a single vertical step at the specific gravity of the ore as in Figure 2.2. In practical situations where there are various degree of liberation, the shape of the curves usually lie between the two extremes as in figure 2.3

2.11.5 Cumulative Percent Assay Against Weight of Sinks Curves

These curves are produced by plotting cumulative percent assay of sinks against cumulative percent weight of sinks for each density of separation. These curves give both the assay and the quantity of sinks that would result at a particular density of separation.
They are used in conjunction with density curves to produce the percent weight and assays of two products of separation at any given density.

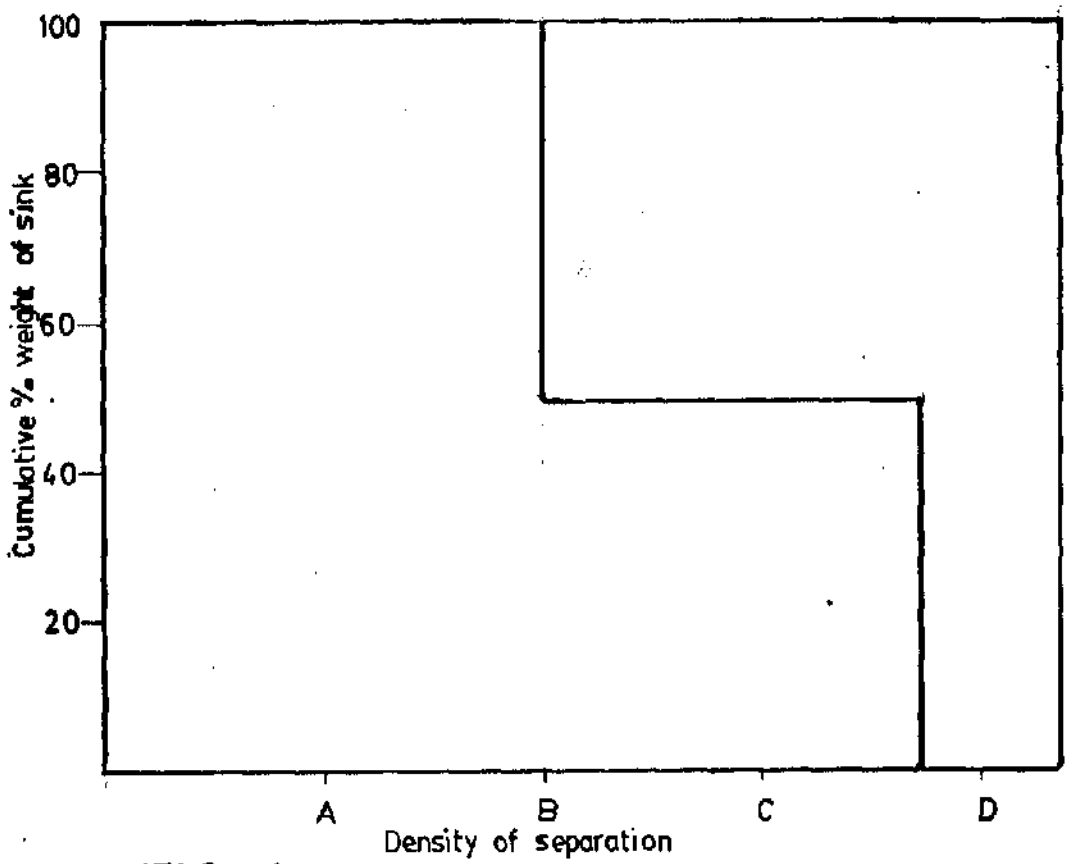


FIG. 2.1 – Theoritical density curve for completely liberated mineral.

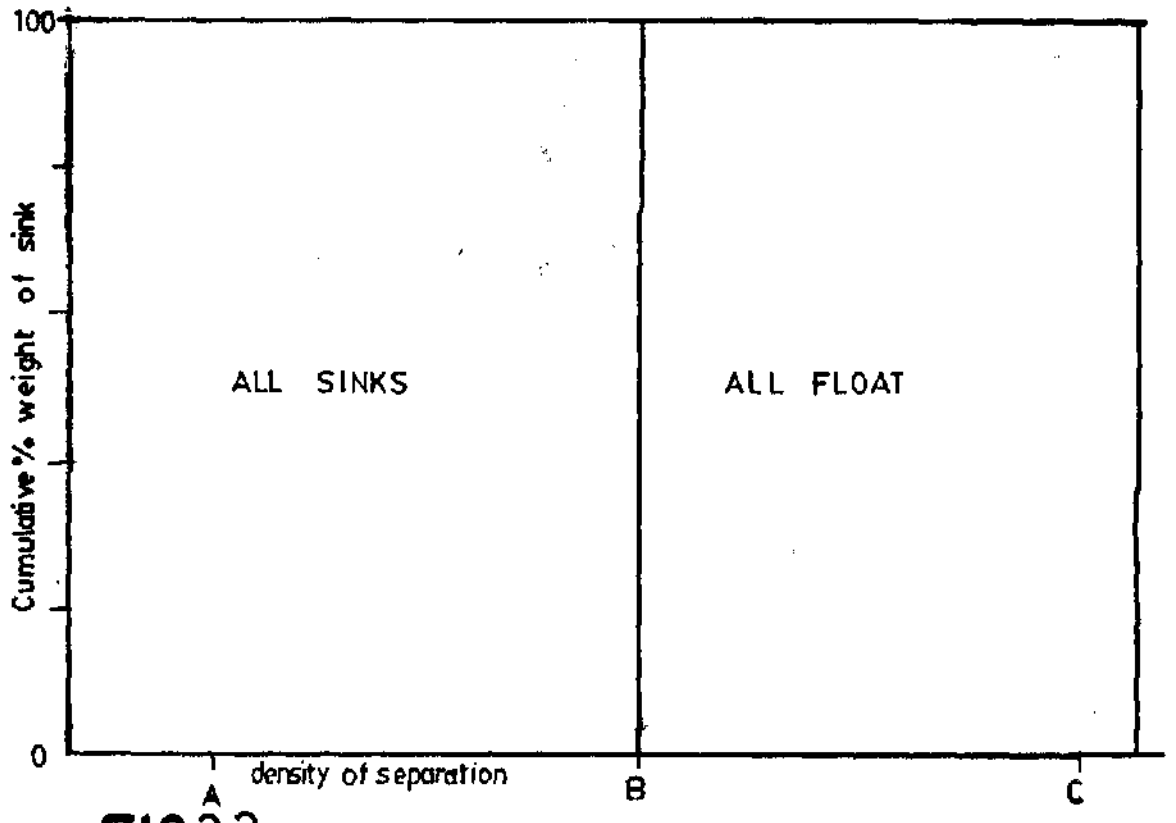


FIG. 2·2 Theortical density curve for completely locked up mineral for an ore of density B

2.11.6 Elementary Assay Curves or Characteristics Assay Curve

Elementary Assay Curves otherwise known as characteristic assay curves are produced by plotting the actual determined assays of each fraction against the average cumulative percent weight of each sink fraction. The average cumulative percent weight of each sink fraction is taken as the cumulative weight of previous fraction plus one half of the percent weight of the fraction in question. This is done because the assay refers to the whole of the weighings between the densities. Ideally, for a situation in which the minerals are completely liberated the curve is a perfect single step (Figure 2.4). For a material which contain liberated minerals the curve will be represented by (Figure 2.5) a straight line connecting the minimum assay at 100% sinks and maximum assay of 0% sinks. For a mixture of liberated and unliberated minerals, the curves are usually sigmoid in shape, Figure 2.6.

2.12 THEORETICAL BACKGROUND ON THE USE OF RELEASE ANALYSIS TECHNIQUE IN LIBERATION STUDIES

The release - Analysis curve otherwise known as Grade - Gradient plot is based upon metallurgical separation which are represented by Vectors. Figure 2.7 is a single sample Vector diagram in which the horizontal line BC represents the weight of the sample and is proportional to the length of the Vector BC. The mass of the metal contained in the sample is

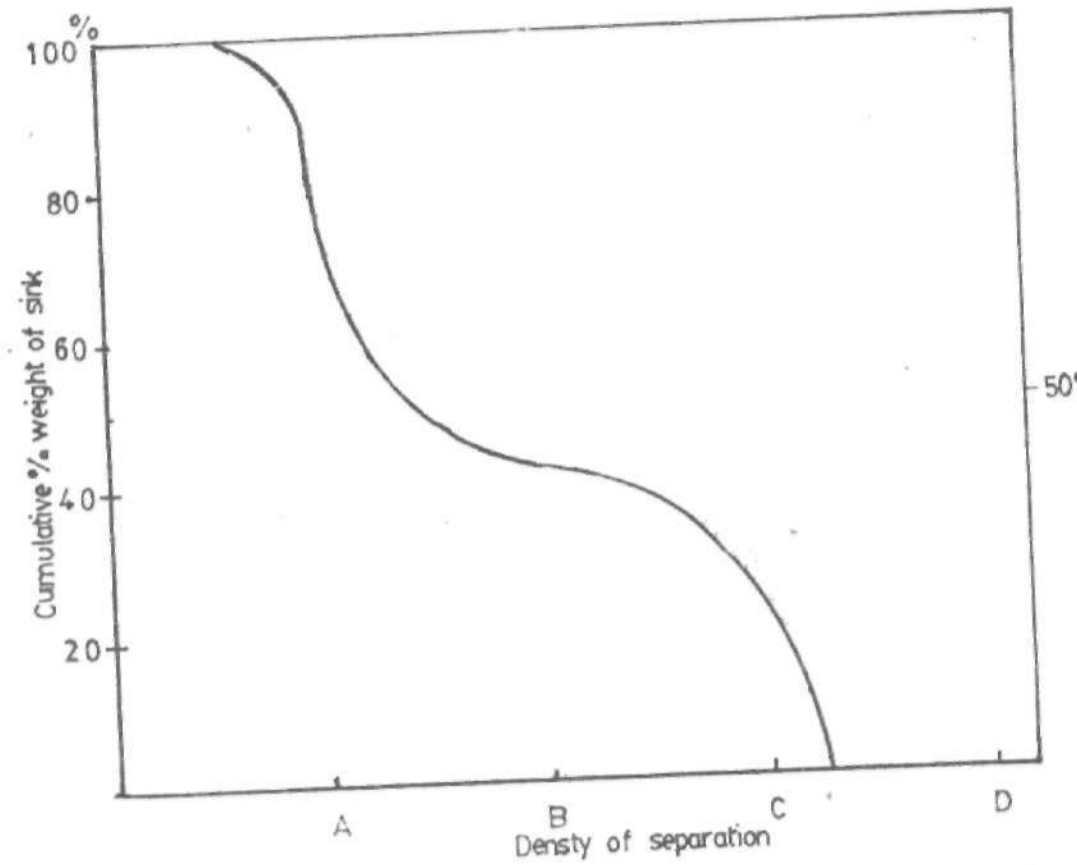


FIG2·3-Theoretical density curve for Partially liberated minerals.

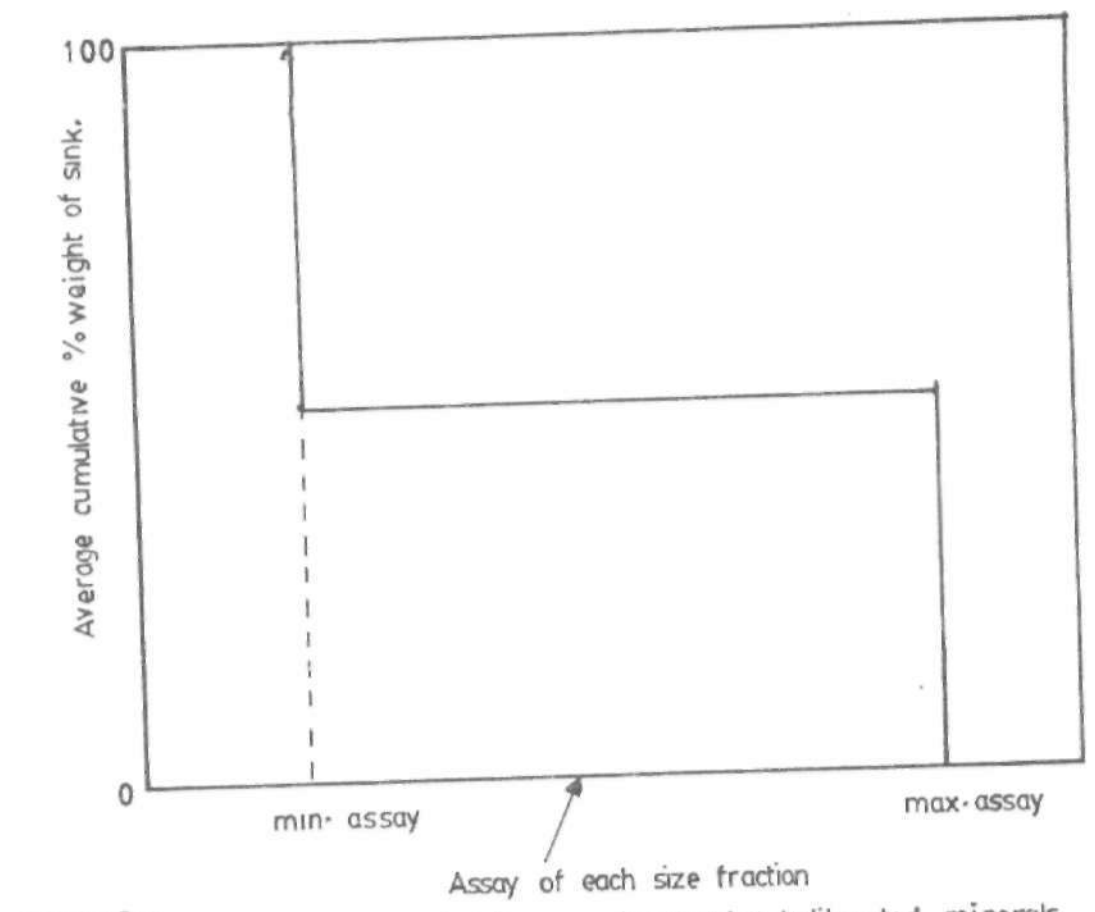


FIG2·4—Theoretical characteristic curve for completely liberated minerals

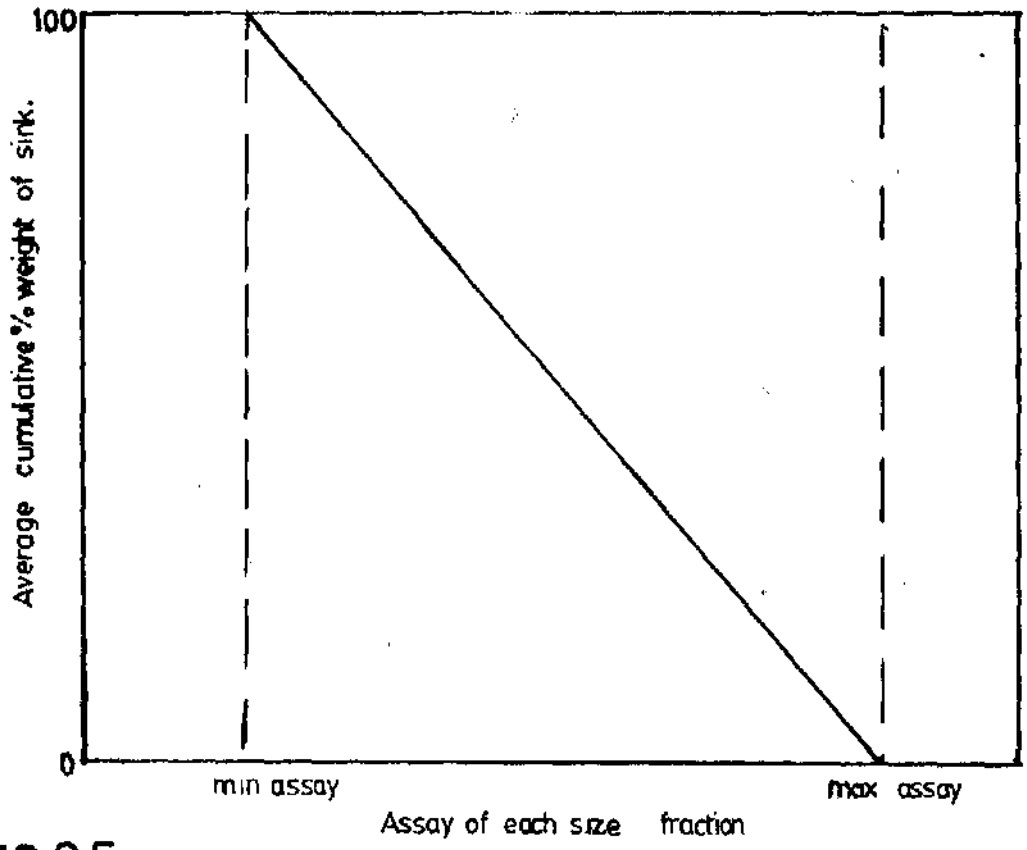


FIG.2·5— Theoretical characteristic curve for unliberated minerals.

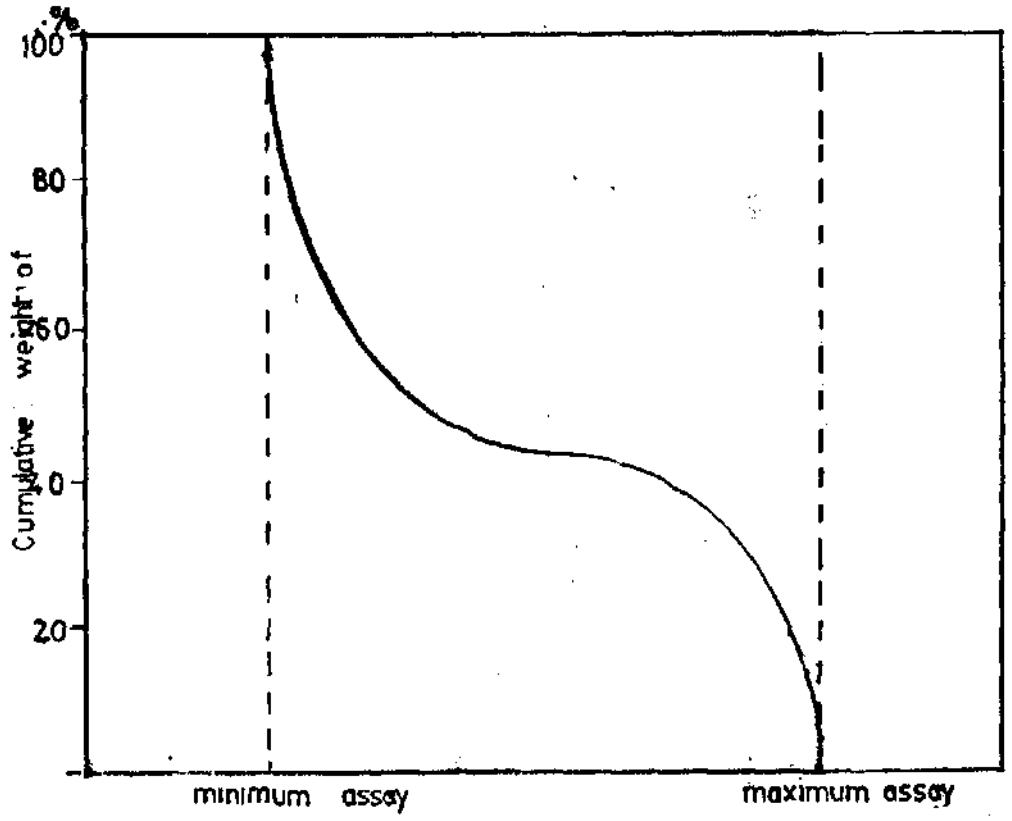
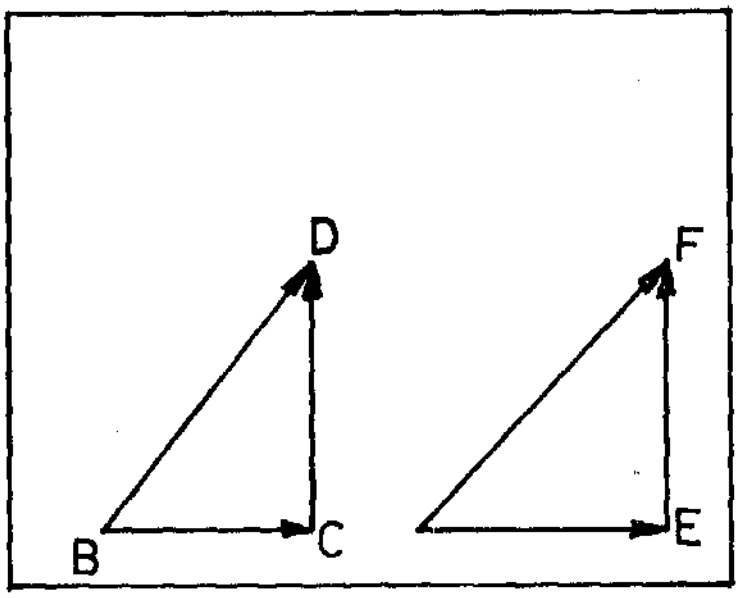


FIG.2·6 - Theoretical characteristic curve for partially liberted minerals

represented by the vertical Vector CD. While the resultant Vector BD is equivalent to the grade (% metal) of the sample. In the same Figure, assuming that DEF is another sample separation vector. Since the two components vectors are formed in the same plane then the law of vector addition applies. And the resultant vector for the two sample vectors will be given by Figure 2.8 in which the sum of weight of both samples BC and DE will be given by vector BG. Conversely the mass of the metal contained in the two samples will be represented by line GF. Whereas the resultant sum of the vectors BC + CD, DE + EF and BG + GF are BF, DF and BF. The resultant vectors BD, DF represent the grade of each individual sample while resultant vector BF represents the composite grade of the two samples.

Based on these diagrams, the steepness of gradient of any of the diagrams or resultant diagram is a function of the metal content of the sample such that overall concentrates containing higher percentage of metal would be represented by steeper vectors. And conversely, tailings containing little metal values would be represented by shallow vectors. The feed grade will be represented by the total summation of all horizontal and vertical vectors in the original feed sample.

In the applications of these vector diagrams in studying the liberation of mineral values, the component containing highly liberated minerals will be represented by one steep gradient of the liberated components and a shallow tailings



Single sample .

FIG 2·7 Vector diagrams .

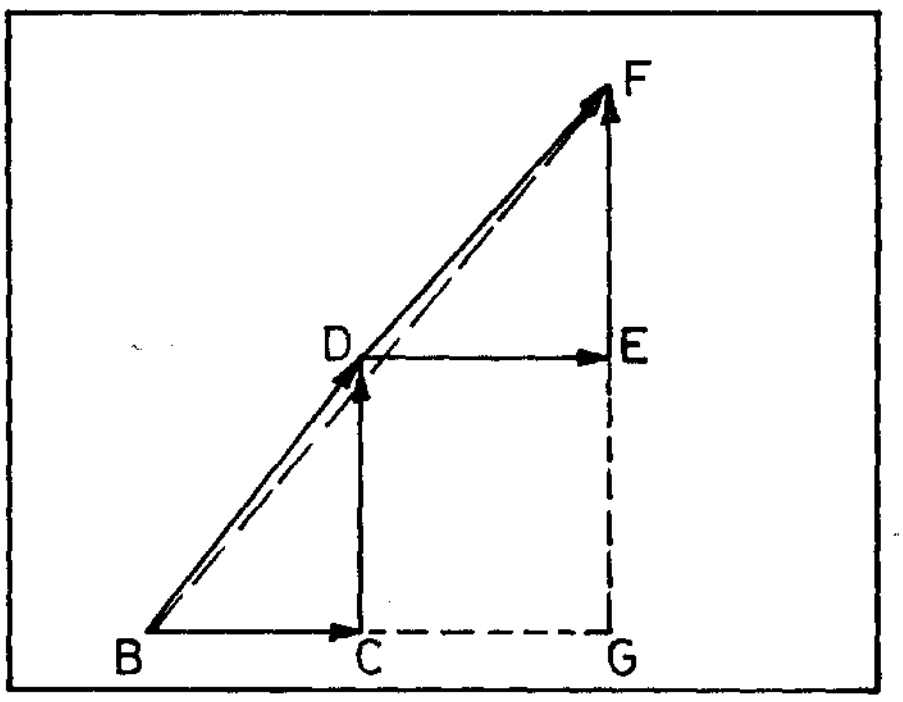


FIG 2·8 Addition of vectors .

gradient. Components in which the mineral particles are partially liberated are represented by a simple shallow gradient. In Figure 2.9 is shown a hypothetical Grade Gradient plots for a metal value that has been separated after being ground to various size fractions. The separation was carried out at various size fraction in order to determine at which of the size fractions is the metal value completely freed from the gangue. Plot A indicates a situation in which the metal values are highly liberated while plots B and C indicate just liberated mineral while E indicated partial liberation and F represents situation where there is no liberation at all (Feed).

2.13 FROTH FLOTATION

Froth flotation is a process for separating valuable minerals from gangue minerals based on the utilisation of differences in the physio-chemical surface properties of the particles of the various minerals. It is the most widely used technique for mineral beneficiation. It is a selective process and is used in the treatment of large tonnages of low grade and complex ores (28).

Froth flotation is carried out in an aqueous medium in which the minerals are treated with certain reagents so that the inherent differences in their surface properties become apparent. Air is then blown through the medium and the mineral particles which have affinity

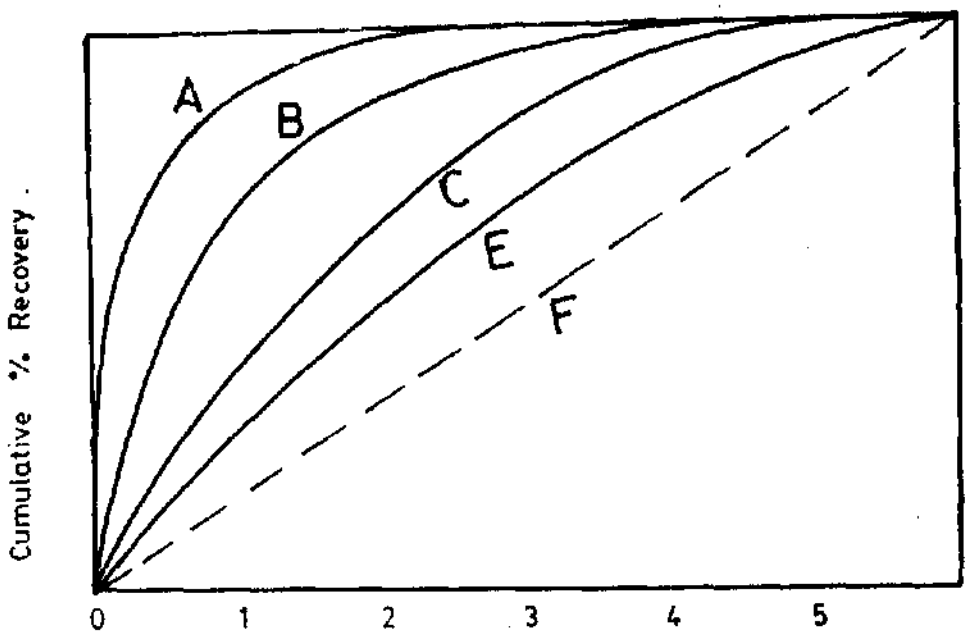


FIG.2.9- Theoretical release analysis curves .

for air (aerophilic) stick to the air bubbles as they rise through and are brought to the surface while particles of other minerals remained in suspension (Figure 2.10).

In froth flotation separation, the valuable mineral is usually transferred to the froth leaving the gangue in the aqueous medium. This is known as direct flotation while in some cases however the gangue is transferred to the froth fraction and it is known as reverse flotation (45,46).

The key to the successful operation of a froth flotation process lies in the correct selection of the chemicals to be added to the aqueous medium. Some of the chemicals affect process in the aqueous medium while others affect process in the froth phase.

Figure 2.10 illustrates the principle of froth flotation. In this system the agitation and aeration are provided by the means of a rotating impeller on a vertical shaft. The process is divided into three phases, the mixing and aeration phase, separation phase and concentration phase. In the first phase air is drawn in by positive suction down the pipe into cell and sheared into small bubbles which become laden with mineral particles. As the bubbles rise the hydrophobic minerals are separated from those wetted with water in the separation phase 2. Phase 3 is the concentration phase which is relatively quiescent. Here the

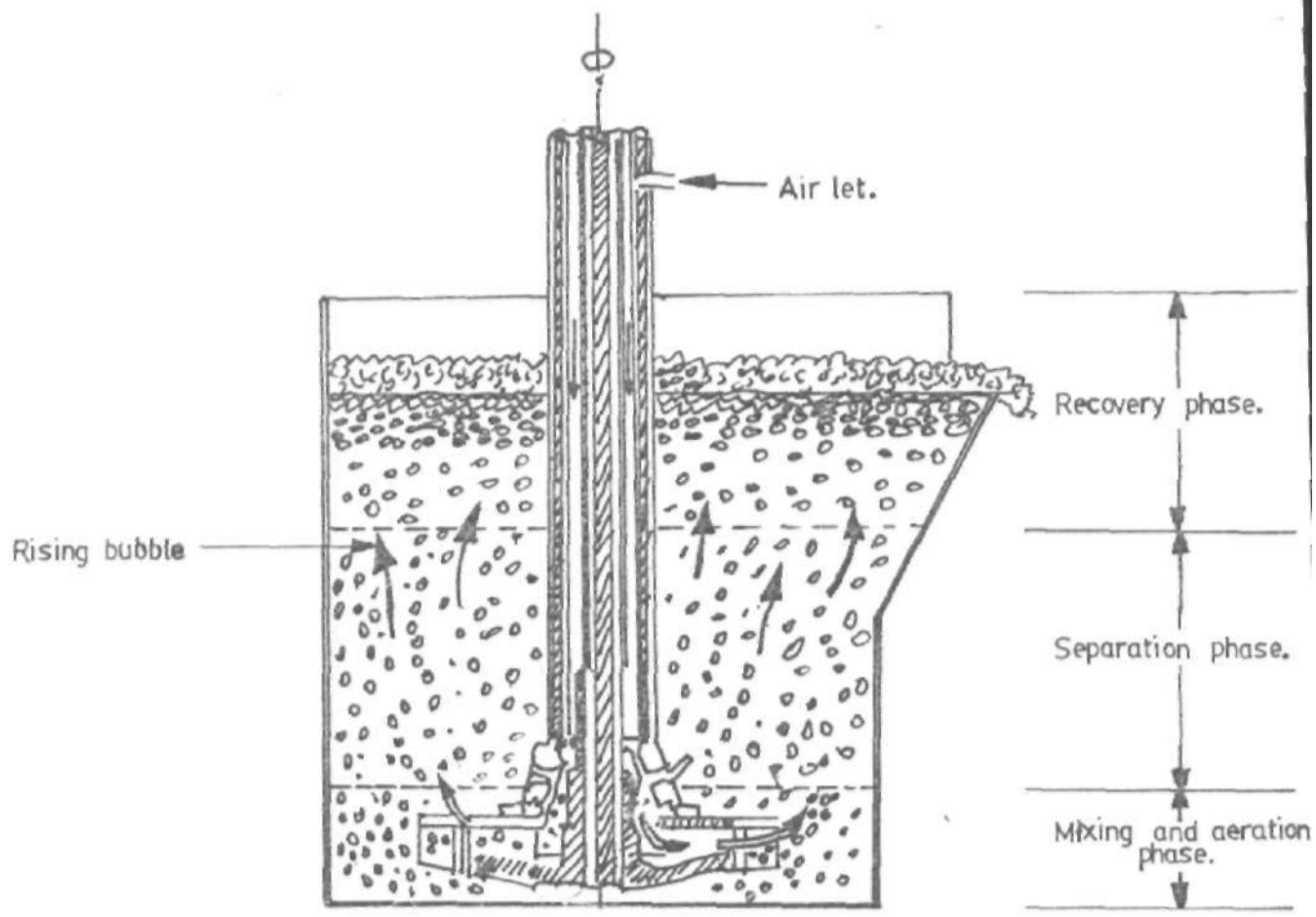


FIG 2.10- A simple diagram illustrating the principle of froth flotation

concentrate is enriched in the froth and collected.

2.13.1 COLUMN FLOTATION

The advent of column flotation cells has been one of the most significant advances in froth flotation technology in the last decade. It is part of the attempt of finding solution to the treatment of very fine particles and are usually installed at the final cleaning stages in most flotation circuits. It can in a single separation step achieve a product recovery and quality (grade) equivalent to what can be obtained in a multistage flotation using conventional cells. In addition, it has low capital costs, low operating costs, occupies less plant space and more adaptable to automatic control than the conventional cells, [49,50].

A typical configuration of a column flotation cell is given in Figure 2.11. It consists of two distinct zones: collection/recovery and cleaning zones.

At the collection zone, the particles suspended in the descending water phase contact a rising swarm of air bubbles produced by a bubble generator at the base of the column. Floatable particles collide with and adhere to the bubbles and are transported to the cleaning zone just above the feed point. Non-floatable particles are collected from the base of the column as tailings. Some gangue particles which are loosely attached to the

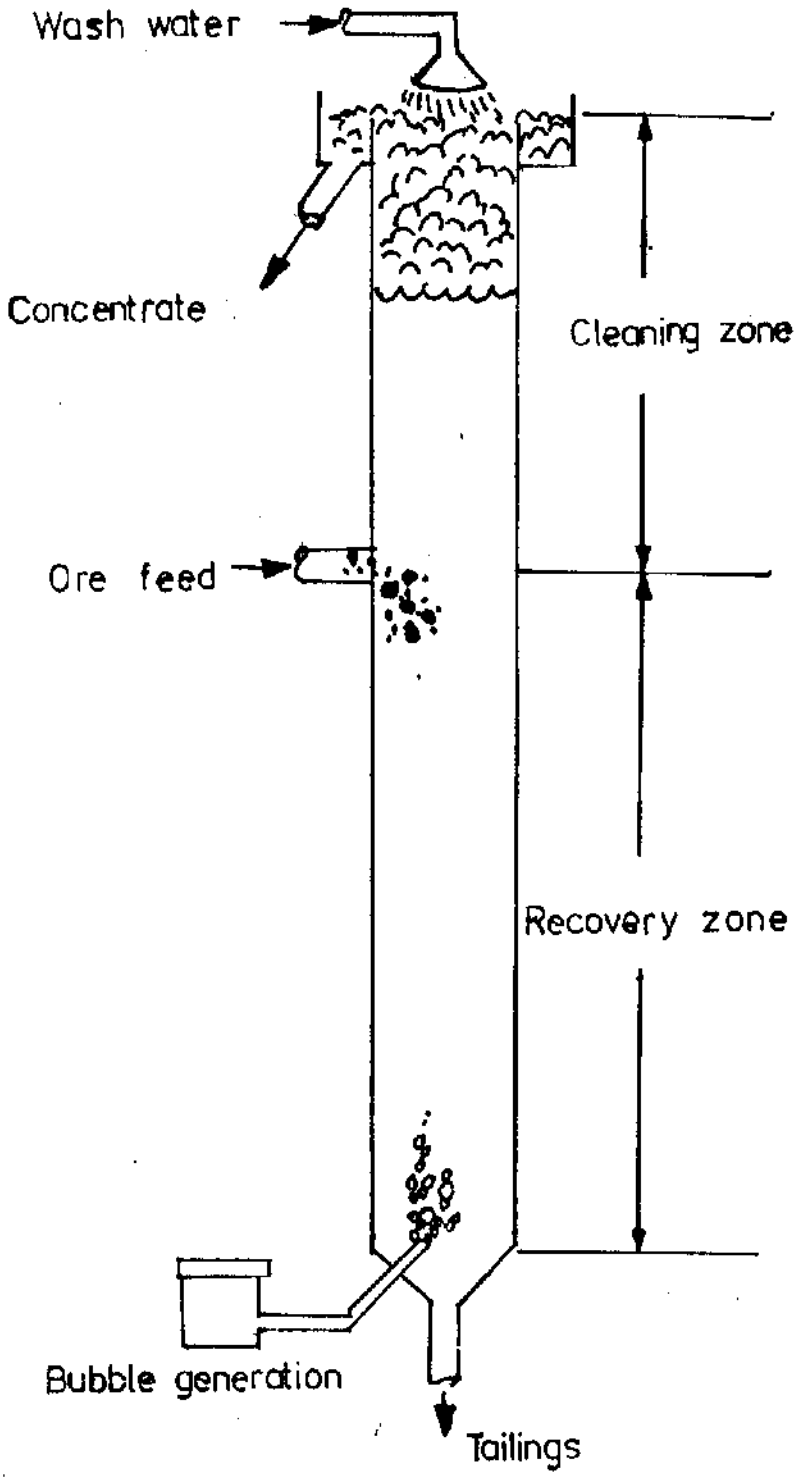


FIG.2.11 - A COLUMN FLOTATION CELL.

bubbles or entrained in the bubbles are washed back into the recovery zone thereby minimizing the contamination of the concentrate [51].

2.14 MAGNETIC SEPARATION METHOD

Magnetic method of separation of minerals exploits the difference in magnetic properties between the constituent minerals in the ore. The concentration is achieved by passing a mixture of the mineral particles through a non-homogenous magnetic field which results in either preferential retention or deflection of the magnetisable particles [55].

For purposes of magnetic separation, minerals are classified into three main groups based on their response to a magnetic field. Ferromagnetic minerals which are strongly attracted by a magnetic field and sometimes retain the magnetism even when removed from the field. Paramagnetic minerals which are weakly attracted by a magnetic field and diamagnetic minerals which are repelled along the lines of magnetic force to a point where the intensity is negligible (56,57).

2.14.1 PRINCIPLES OF MAGNETIC SEPARATION

Figure 2.12 Illustrates basically the principle of magnetic separation in which the mineral is acted upon by several external forces with a dominant magnetic force.

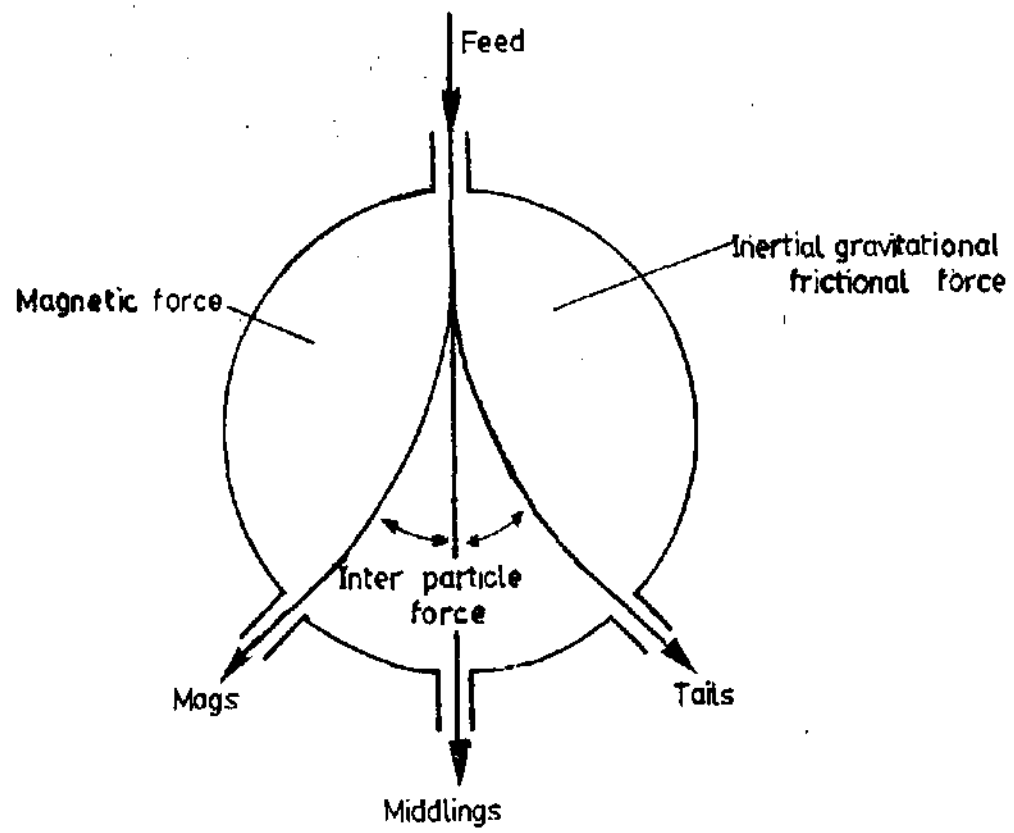


FIG.2·12— Principle of magnetic separation.

The separation of one mineral from another depends upon their motion in response to the dominant force and other competing forces namely gravitational, frictional, inertia and centrifugal. From the diagram, it can be seen that in the case of separation involving ferromagnetic minerals in the magnetic field of a separator, the magnetic force acting on the particles must be greater than the sum of all the other competing forces. As a result of which the mineral will be attracted to the magnet. For non-magnetic mineral the magnetic force will be smaller than the sum of all the competing forces and the mineral will then be repelled away from the magnetic field [58].

2.15 PHYSICAL AND PHYSIO-CHEMICAL SEPARATION PROCESSES USED IN THE BENEFICIATION OF MANGANESE ORES

Several beneficiation methods have been developed for the beneficiation of different types of manganese ores taking into cognisance the grade, mineralogy gangue type etc. These processes include gravity separation, magnetic separation, froth flotation, hydrometallurgical and pyrometallurgical processes. The susceptability of any manganese ore to beneficiation by one of these methods is a major determinant in the development of a process route for its concentration.

The amenability of any type of ore to beneficiation depends on its mineralogical characteristics. These

characteristics include grain size of the minerals, gangue type and their association with the valuable minerals. For purposes of beneficiation by any of the above mentioned methods, manganese ores can be classified into four categories [65].

(1) Simple ores containing light gangue minerals which are coarsely liberated and amenable to concentration by simple methods involving one treatment route only.

(2) Ferruginous ores containing principally ferruginous minerals which need magnetising reduction and magnetic separation.

(3) Garnetiferous ores requiring electrostatic separation or flotation.

(4) Complex ores. These types of ores require complicated treatment routes which may include chemical processes like leaching.

2.15.1 Beneficiation of Manganese Ores by Gravity Methods

This method of beneficiation is only applicable to simple ores in which there is a specific gravity difference between the valuable minerals and the gangue and in situation where liberation is achieved at coarse sizes. It is usually a pre-concentration process in which the valuable minerals are separated from the gangue at as coarse a size as possible using a relatively cheap method. This is an effective physical concentration

technique, whereby the major portion of the gangue is discarded which may entail some loss of valuables. The concentrated product is then subjected to more costly processing methods for the ultimate extraction of the valuable minerals, metals and by-products.

The gravity separation flowsheets, usually incorporates scrubbing section to remove the slimes, followed by size reduction using crushers and simple gravity separation using Jigs and Drums. This simple treatment scheme is only applicable to high grade, coarsely liberated manganese ores from Gabon, Brazil and South Africa [66] that presently dominate the manganese market because of their low production costs. In situations where fine fractions containing silicious or bauxitic gangue particles are present, dynamic gravity separators like Dutch State Mines (DSM) cyclones, Dyna-Whirlpool and Tri-flow separators are used to recover and improve the quality of the fine valuable minerals [68,69]. This is the situation at the African Manganese Nsuta, Ghana where Dyna-Whirlpool and Humprey's spirals are used. The middlings produced at this plant after the primary separation are upgraded by the use of high intensity magnetic separators which remove the weakly magnetic MnO_2 minerals.

2.15.2 FLOTATION OF MANGANESE MINERALS

Manganese ore flotation is not easy, as clay slimes

prove troublesome and the removal of the gangue particles is often a formidable process. The oxides and hydroxides minerals of manganese show little flotation activity. The works of Renzhumin [70] on the flotation of manganese minerals revealed that manganite, braunite and rhodocrosite are the easiest manganese minerals to float. The study also shows that pyrolusite and wad are the most difficult to float, even though good responses were obtained for the pyrolusite after peptising the slimes with oxatic acid and sodium silicate [71].

Fuersteneu and Rice [72] also studied the electro-kinetic and flotation behaviour of pyrolusite using sodium dodecyl & sulphonate and dodecyl ammonium chloride as collector. They obtained good responses in both acidic (PH=4) and alkaline (PH=8.5) conditions. They attributed the response in acidic condition to be due to the collectors and that in alkaline condition to the chemisorption of the reagents on the mineral surface.

Rhodonite ($MnSiO_3$) has also been floated by Palmer *et al.* [73]. While the flotation of other high silica manganese ores has been reported [74] to be adversely affected by slimes and the desliming as a preliminary step before flotation is very important. Kharlamov *et al* [75] also carried out considerable research on trying to establish the relative order of flotation of manganese oxide minerals. In their studies they established that

flotation susceptibility with anionic collectors decreases in the order of manganate, pyrolusite and psilomelane. This order was established using oleic acid and tride cyclic acids as collectors.

LIU YAO *et al* [76] of the Mananshan Mining Research Institute of China reported using a variety of collectors for flotation of manganese oxide minerals. The collectors used include oxidised paraffin soap, alkali residue, petroleum sodium sulphonate, calcium sulphonate and a combination of these reagents. They concluded that petroleum sodium sulphonate and calcium sulphate have good selectivity but poor collectivity while oxides paraffin is a powerful collector with poor selectivity. Good flotation responses were obtained using the mixture of petroleum sodium sulphate with oxidised paraffin and calcium sulphonate with oxidised paraffin.

Flotation has been used in several plants for the beneficiation of manganese minerals in the past. The discovery and development of large high grade manganese deposits in Gabon, Brazil, South Africa and Australia, in the 1950s and 60s which do not require major beneficiation affected these plants which used the relatively expensive flotation methods. However, flotation and other complex expensive beneficiation techniques will undoubtedly be used in the near future when these high grade and easily processed deposits would

have been exhausted.

2.15.3 MANGANESE BENEFICIATION BY MAGNETIC METHOD

The ores treated by this method of beneficiation are mainly Ferruginous manganese ores. It is one of the cheapest methods and is carried out by reduction roast, followed by removal of the magnetic Iron-rich fraction. During the roasting, oxides of Iron are converted to magnetite while most of the higher oxides of manganese are converted to manganous oxide (MnO) by gaseous reduction in the temperature range of 400^0 - 600^0 C. The gases used for reduction are pure hydrogen, carbon monoxide, producer gas or furnace gases. The reaction is exothermic in nature, the released energy is what is usually used in the reduction and preheating of the feed once the process starts [79], thus the process is self sustaining.

The reduced ore is then comminuted to the required economic liberation size. The grinding of the reduced ore is much cheaper because it is softer than the raw ore. After comminution the material is subjected to low-intensity magnetic separation in which the iron-rich fraction is separated as the magnetic, while the manganese rich fraction the Non-magnetic [81].

2.16 SOME OF THE HYDROMETALLURGICAL PROCESSES DEVELOPED FOR THE BENEFICIATION OF MANGANESE ORES

There have been several processes both at laboratory, pilot and plant stages for the beneficiation of manganese Ores by hydrometallurgical methods. One of the early works was that of leaver (83), who developed a flowsheet which involved comminution of the Ore followed by reduction calcination then leaching with HCl and precipitation of $MnCO_3$. The reactions for the leaching and precipitation are:

$MnO + 2HCl$ ------> $MnCl_2$ (aq) + H_2O (8) and

$MnCl_2 + Na_2CO_3$ ------> $MnCO_3 + 2NaCl$. (9)

The precipitated $MnCO_3$ is then sintered to Mn_3O_4.

Marshal (86) also developed a process for the Republic Steel Corporation America in which he used hydrogen chloride for selective chloridising of Manganese in Manganiferrous Ores using a mixture of Hcl and $H_2O(g)$, followed by leaching with water and precipitation of $MnCl_2$ crystals on evaporation. The $MnCl_2$ was then converted to MnO with the regeneration of Hcl.

A similar process initiated by Macmillan (87) and fully investigated by United States Bureau of Mines involved using Hcl and HNO_3 for chloridisation and all the subsequent unit operations were the same as in the method of Marshal (86). Conley (89) also reported using chlorine gas for chloridisation before leaching with

water. Calcium chloride and sodium chloride salts were also used in an attempt to avoid the use of Hcl because of its corrosion problem by Bradley Wilson (90).

Ammonia based processes were also investigated by individual researchers and Corporations. Fox et al (92) successfully used Nitrogen dioxide in leaching Manganese bearing materials. In the investigation, after wet grinding, the material was nitrated with NO_2 (gas) resulting in the formation of $Mn(NO_3)_2(aq)$ which was then evaporated to $Mn(NO_3)$ and followed by decomposition to MnO_2 with the release of NO_2 gas.

Nossen (94) also used Nitric acid in leaching Manganese oxide carbonate and silicious Ores. The Unit Operations involved, reduction of higher Manganese oxides to lower oxides then followed by leaching, evaporation and decomposition producing MnO_2 as in Fox's process. Using the same process Macmillan (95) employed a mixture of HNO_3- NO_2 in leaching and the leached solution was purified in autoclaves before recovery of the manganese values.

Dean and levate (96, 97) investigated the use of a mixture of NH_3 - CO_2 -H_2O. This process was tested at pilot stage by the United States Bureau of Mines and is currently being used at Industrial scale by the Manganese chemical Corporation of America. Ammonium sulphate was also used in leaching manganese Ore by

Broadley (101, 102) who developed the process for Broadley-Fitch Corporation of America and operated a pilot plant at Minnesota School of Mines. A similar process was developed by Sweet (103) in which ammonia was used in leaching, after the Ore had been roasted with SO_2 gas. This process which later came to be known as Sweet Ammonia Process had been used in recovering manganese from complex manganese carbonate and modules.

Also, Stringham and Summers (104) developed a technique of ammonium salts roast for the recovery of manganese from various types of manganese sources including manganese silicate. Ammonium salts like $(NH_2)_2SO_4$ and NH_4HF_2 were used depending on the nature of the manganese sources. The process involved roasting the material at 450^0C to 550^0C with excess ammonium salts and manganese bearing mineral were converted to either $MnSO_4$ or $Mncl_2$ depending on the type of ammonium salts used. The calcined Ore was then water leached and the leached solution purified. $MnCO_3$ was then precipitated on addition of $(NH_4)_2CO_3$.

The precipitated MnCO3 was then calcined to Mn_3O_4.

Several sulphur dioxide based processes have been investigated. One of them is the popular sulphur dioxide drum - leach process investigated by Van Barneveld (107) and developed by the United State Bureau of Mines (107). In this process, the Ore was ground down to 730µm and leached with hot SO_2 gas in a counter

current flow of the ground ore and hot SO_2 gas. The pregnant solution containing the manganese value was evaporated to precipitate $MnSO_4.2H_2O$ crystals. The precipitated $MnSO_4.2H_2O$ crystals were then calcined to Mn_3O_4. A similar process was investigated by Allen (108) but in his process the leached solution was purified in autoclaves in order to obtain a highly purified solution.

A dithionate leach process was developed by Ravit et al. (109) in which the roasting stage was eliminated. In this process the manganese Ore was leached with SO_2 in a dithionate solution (CaS_2O_6). As soon as the manganese is taken into solution, the $MnSO_4$ formed was attached to the dithionate and converted to MnS_2O_6 and $CaSO_4$ was precipitated according to the reaction:

$$MnSO_4 + CaS_2O_6 \text{ ------> } MnS_2O_6 + CaSO_4 \qquad (9)$$

$Ca(OH)_2$ is then added to MnS_2O_6 solution precipitating $Mn(OH)_2$ while CaS_2O_6 is regenerated as follows:

$$MnS_2O_6 + Ca(OH)_2 \text{ ------> } Mn(OH)_2 + CaS_2O_6. \quad (10)$$

The $Mn(OH)_2$ was then calcined to Mn_3O_4

2.17 PYROMETALLURGICAL PROCESSES FOR THE BENEFICIATION OF MANGANESE ORES

Pyrometallurgical processes are applicable to any manganiferrous raw materials but they are specially well suited to beneficiation of low grade silicious manganese ores and slags as most chemical processes cannot effectively cope with large quantities of silica normally found in these ores

(114). Even though, these processes cannot produce pure manganese metal, they are capable of producing high quality synthetic manganese concentrates and valuable ferroalloys.

In the pyrometallurgical beneficiation of manganese ores, a two-stage reduction process developed by the Broken Hill proprietary of Australia (115) for the recovery of manganese from slags of open-hearth furnaces. At the first stage, smelting was carried out at a temperature range of 1100^{0}C to 1500^{0}C in which iron was selectively reduced producing a manganese rich slag. The slag was then reduced at temperature range of 1600^{0}C to 1650^{0}C under basic conditions. This process has been tested up to the Pilot plant stage and overall manganese recovery of up to 65% has been achieved and Ferromanganese assaying up to 70% Mn produced (116).

Another important pyrometallurgical process is the stage by stage selective smelting as developed by Udy (117). In this process, the ore was calcined with Lime at a temperature range 1100^{0}C to 1200^{0}C for the reduction of the higher manganese oxides to divalent manganese states. The reduced product was then smelted at 1300^{0}C to 1600^{0}C producing slag rich in manganese with small amount of Iron and a metal phase rich in Iron. The slag was further smelted producing a high grade ferromanganese.

A process for the smelting of a high silica manganese ore to silicomanganese was investigated by Banning et al (118) and

Hoskma et al (116) for the United States Bureau of Mines as a means of utilising low grade high silica manganese ore deposits of the United Stated of America. In this process, the ore after concentration was smelted at 1550^0C reducing Iron, Silica and Manganese Oxides. The manganese oxides was than used in ferromanganese production.

Similarly, a two stage matte smelting flow sheet has been developed by Torgeson et al (119) for the United States Bureau of Mines. In this process, in the first stage smelting the MnO_2 was reduced to (MnS.FeS) on addition of FeS_2 according to the reaction.

$$MnO_2 + FeS_2 + C \text{ -----> } (MnS.FeS) + CO_2 + \text{Slag} + \text{Pig Iron} \quad (11)$$

At the second stage, the (Mns.Fes) was converted to (MnO.MnS) on addition of sufficient amount of Mn_3O_4 according to the reaction.

$$(MnS.FeS) + C + Mn_3O_4 \text{ ------> } (2MnO.2MnS) + CO_2 \quad (12)$$

The (MnO.MnS) was then calcined to Mn_3O_4. A similar process was developed by Lofquist (120, 121). In his process the ore was converted to spiegeleisen before being oxidised and sulphurdised to (MnO.MnS). Buehl et al (128) and Royers et al (129) also reported similar processes except that in their processes, after the ore has been converted to spiegeleisen, the spiegeleisen was preferentially oxidised. These process had been used in recovering manganese from rhodonite $MnSiO_3$ which on heating, the $MnSiO_3$ partially dissociates to MnO and SiO_2 which are reduced to metal, while other free silicates are only slightly reduced and remain in

the slag forming stable silicates with the basic oxides.

A process for the recovery of manganese from manganese silicate using high-intensity Arc decomposition was investigated by Harris et at (122). In this process, the ore, after milling was extruded into electrodes and used as anodes in a high intensity Arc furnace at a temperature of 7000^0C to 10000^0C. At these temperatures atoms of manganese, silicon and oxygen are vaporised. As the vapour moves into cooler part of the Arc tail flame, the elements recombined into their simple oxides and are swept out of the furnace and collected in suitable dust filters, producing essentially a mixture of submicron sized particles of MnO and SiO_2.

Schoenaub (123) and Rupport (124) proposed and patented a process for the recovery of manganese by decomposition of manganese silicate with excess lime. In their proposal the manganese bearing silicate was mixed with excess amount of lime and roasted at 1350^0C producing a clinker containing two phases. One comprising mainly of the silica and phosphorus as dicalcium silicate ($2CaO.SiO_2$) and tricalcium phosphate ($3CaO.3P_2O_5$). The other phase contains the metal oxides in a complex magnetic spinel of which $(Mg, Fe)O.(Fe, Mn,Al)_2O_3$ is typical. The spinel phase was then separated from the Tailings after grinding by magnetic method.

Another method of beneficiating manganese bearing silicate was designed by Carosella (125). He designed a

process to treat Rhodonite and other silicious manganese ores and slags. The process involves melting at a temperature of about 1200^{0}C to 1500^{0}C of the silicious material, followed by quenching of the molten product in a series of water sprays so as to produce finely divided amorphous product ($MnO.SiO_2$). The manganese in the amorphous products is bivalent and can easily be smelted or leached. Therefore, if the manganese in the material is not in the bivalent stage, a reduction smelting is necessary.

Scortecci et al (126) have developed a process for the recovery of Iron from low grade silicious Iron ores using carbonaceous solid reductants which was later applied for the beneficiation of low-grade Ferromanganese ores to produce an enriched manganese slag and a metal phase rich in the (FeMn). The slag was then smelted to a richer manganese ferroalloy.

2.18 OTHER PROCESSES

There are several attempts of recovering manganese through the use of reducing agents other than the usual reducing gases. Veglio and Toro [130] reported having successfully leached pyrolusite (MnO_2) with sulphuric acid using sucrose as a reducing agent. This process is an upspring of the study of bioleaching of pyrolusite utilising heterotrophic mixed cultures in which sucrose was used as the energic substrate [131].

Biological leaching of low-grade manganese ores has also been reported by a number of investigators including Madgwick [132], Eirlich [133], Gupta and Eirlich [134] Agate and Desphande [135] and Hart and Madgwick [136]. In a typical biological leaching technique, Baglin *et al.* [137] reported leaching several low-grade manganese ores using molasses as source of nutrients for the micro-organisms. Several micro-organisms are capable of solubilising manganese via bio-reduction. These micro-organisms can be natured to the ore or introduced as Isolated cultures from soils, fresh water or marine environment. Most of the bio-reduction studies carried out were conducted in Flasks and batch reactors and only a few were conducted using low-cost insitu leaching.

2.19 Thermal Pre-Treatments Giving to Silicate Bearing Minerals Prior to Beneficiation

Metallurgical important silicates bearing minerals are usually subjected to certain thermal pretreatments prior to beneficiation so as to induce physical changes in their structures. The nature and intensity of the thermal pretreatments depend on whether the silicates are hydrated or unhydrated. The hydrated silicates in most cases are heated to about 500^0C to expel hydroxyl groups from the crystalline structure in the form of water vapour leaving behind a porous solid having a large

surface area which can easily be leached with dilute acids.The unhydrated silicates can be treated in two ways either by melting and quenching to obtain a glassy structure that can be readily crushed, ground and leached with acids or heated to a temperature below the melting point to effect a phase transformation which will result in volume change and the product will become porous which can also be easily crushed and leached. In some thermal pre-treatments some fluxing agents e.g. lime are added which fluxes the silica immediately after decomposition producing two phases of metallic oxides. These two phases are usually separated using one of the concentration techniques [138].

2.20 Lime-Clinkering Process

The lime clinkering process in general is based on the principle that manganese silicates like spessartime will be decomposed into ferrites, manganites and other compounds, when mixed with excess lime and heated to high temperature above 1350^{0}C.

One of the most important unit operations of the lime clinkering process involves adjusting the composition of the feed to a range of certain critical proportion given by the basicity ratio B, where B equals

$$\frac{CaO - 3(P_2O_5 + Al_2O_3)}{SiO_2} \qquad (13)$$

The range of values of B has been given by Schoenaub [123] to be 1.7 to 2.0. The next unit operation is the treating of the prepared material to pyrochemically displace the manganese, followed by grinding to render it separable by magnetic method producing a concentrate rich in manganese and iron and tailings rich in the silica and Alumina.

To understand the chemical mechanism by which the manganese is recovered from the ore by this process, it is necessary to note some of the characteristics of reaction in slag chemistry. Slags although chcmically complex, on crystallising will form relatively few crystal phases. In the lime clinkering process the slag form during the heating contains two solid phases, one composed chiefly of silica, Alumina and phosphorous as dicalcum silicate ($2CaO.SiO_2$), calcium Alumina silicate ($CaO.Al_2O_3$).SiO_2) and tricalcium phosphate ($3CaO.P_2O_5$). While the second phase contain the rest of the metal oxides in a complex magnetic spiniel of typical formular $(Fe)O.(Fe,Mn,Al)_2O_3$.

The clinker produced is then crushed and ground and the two phases separated by magnetic method. The crushing and grinding liberates the magnetic spinel which can be recovered in several phases through a megnetic separator.

2.21 ELECTROMETALLURGY OF MANGANESE

The commercial production of high purity metallic manganese for use in special steels and Non-ferrous alloys production which require manganese free of both carbon and iron from the leach ores is usually by electrolytic deposition. This is because of the high reactivity of manganese metal when compared with its associated gangue mainly iron and silicon.

The gangue makes production of high purity metal from lean ores by pyrometallurgical route an impossible task. Also, because of the high affinity of manganese metal for oxygen it has to be smelted under reducing conditions and smelting at high temperatures under reducing conditions results in the reduction of Iron oxides, silica and dissolution of carbon. The usual practice is to produce a high grade product from these lean ores by pyrometallurgy and then the high grade product is further treated to recover the manganese metal by a combination of hydrometallurgy (leaching) and Electrometallurgy (aqueous electrolysis). The manganese ore or any manganese rich product is first roasted to reduce the manganese from high oxides to soluble manganese dioxide which is then leached using sulphuric acid usually recycled from the electrowinning circuit. Ammonia is added to precipitate iron and alumina impurities while impurities like arsenic, copper, zinc

are removed by precipitation with hydrogen sulphide. The purified liquor is then electrolysed in diaphragm cells containing stainless steel cathodes with semi mirror finish for easy stripping of the manganese metal while the anodes are made from a Pb/Ag alloy of composition 99% Pb and 1% Ag. In order to minimise the deposition of manganese dioxide at the anodes, holes are drilled in them to generate higher current densities than at the cathodes [143].

In fused salt electrolysis, the manganese metal is produced by electrolysing rich manganese ore or concentrates in an electrolytic cell containing calcium fluoride and lime. The flourspar is added to maintain the desired fused salt composition while the lime is to neutralise the silica contained in the ore/concentrates. Another important future source of manganese is the manganese nodules. The beneficiation route for this source of manganese is different from the conventional source. The possible beneficiation method is briefly reviewed in the following section.

2.22 BENEFICIATION OF MANGANESE NODULES

The fact that manganese nodules are found underneath the sea and when collected contain appreciable amounts of water, suggests that their treatment by pyrometallurgical methods would not be practical because of the cost of drying. Their high porosity [200m^3/g] suggests that,

hydrometallurgical methods could be more suitable.

While the processing of manganese ores is always for the recovery of manganese values, that of manganese nodules may not only be for the manganese values but for the recovery of other metals like copper, nickel and cobalt. This is economically very important because treatment of the nodules for the sole recovery of manganese values is not economically viable without the recovery of the associated metal values. The manganese nodules may therefore be treated in practically the same way as copper oxides, nickel laterites etc.

2.23 FERRO-ALLOY PRODUCTION

Ferro-alloys are produced by reducing the ore/concentrate containing the metal in the oxide form in the blast furnace and electric arc submerged furnaces. The electric arc furnace process is the most widely used method accounting for more than 70% of ferro-alloy production. The electric arc furnace for ferro-alloy production uses three-phase voltage with three graphite consumable electrodes.

The reducing agents used in ferro-alloy production include Carbon, Silicon and Aluminium. Carbon is the most common reducing agent used most especially in situations where its content is not a limiting factor. Reduction with Silicon and Aluminium is called metallothermic

reduction and is used when ferroalloys with low carbon is desired, for example, in speciality steels and non-ferrous-alloys.

2.23.1 Manganese Ferro-Alloy Production

Manganese is mainly consumed in the Metallurgical industry in the form of high-carbon ferromanganese containing 78-80%Mn with about 6.7% carbon. Silico-manganese assaying about 65-68%Mn with less than 2%C. Manganese is also consumed in the metallurgical industry as medium (80-85%Mn) and low carbon (85-90%Mn) ferromanganese in speciality steels and aluminium-manganese alloys.

2.23.2 High Carbon Ferromanganese Production

High carbon ferromanganese are produced mainly by electro-thermit reduction in submerged electric-arc furnaces and in blast furnace type operations. The manganese bearing material which may be a manganese ore/concentrate is mixed with coke fines and charged into the furnace. The manganese oxide in the concentrate is reduced by the coke fines through the following stages:

MnO_2---- Mn_2O_3---- Mn_3O_4---- MnO---- Mn_3C (14)

Under the reducing conditons and high temperature in the electric arc furnace the MnO and FeO then interact with the solid carbon according to the following reaction.

$$MnO + C \text{ --- } CO + Mn \quad (15)$$

$$FeO + C \text{ --- } CO + Fe \quad (16)$$

Ferromanganese is generally produced by fluxless smelting in which no slag forming components are added to the charge. The produced alloy and slag are tapped simultaneously from the furnace. The slag is usually low in phosphorous as most of the phosphorous in the ore/concentrate is also reduced during the smelting.

2.23.3 Low and Medium Carbon Ferromanganese Production

Low and medium carbon ferromanganese are produced by several methods. One of the early methods involved reacting silico-manganese with high grade manganese ore/concentrate that has been fused in an electric furnace. With the recent technological development low and medium carbon ferromanganese are produced by decarburisation of standard high carbon ferromangenese. This is achieved by top blowing with oxygen in a basic oxygen furnace (BOF). This type of ferromanganese is also produced by fused salt-electrolysis of a mixture containing manganous oxide made from manganese ore.

2.23.4 Silico-Manganese Production

Smelting silico-manganese is a similar process to smelting high-carbon ferromanganese in a submerged-arc furnace. However, in the production of silico-manganese

a more silicious charge is desired by using ores with high silica content or ores with added quartz. In integrated operations, slag from the ferromanganese furnace with relatively high manganese content, is fed to the silico-manganese furnace along with ore and coke.

Conclusion

From the litereture reviewed on the beneficiation of manganese ores in this chapter, it can be concluded that several methods have been developed for the beneficiation of different types of manganese ore deposits. The choice of a particular method depends on so many factors which include, the nature of occurrence of the manganese ore, the grade of the ore, mineralogy, the type and amount of impurities, the degree of association of the valuable minerals with gangue and finally the application to which the beneficiation product will be put to.

The next Chapter discusses the various procedures followed in carrying out the experimental work involved in this research.

CHAPTER THREE

3.0 EXPERIMENTAL TECHNIQUES

3.1 Introduction

This chapter explains the various procedures followed in carrying out the tests, analyses and investigations conducted in this work.

3.2 Sample Taking at the Field

For the purpose of carrying out this work, fifty kilograms (50 kg) sample of the ore was taken from the four trenches dug at the deposit by Steel Raw Material Research and Exploration Agency formerly known as National Steel Council. These four trenches were the sampling points during the exploration studies.

3.3 Preparation of the Bulk Sample for Chemical Analysis

Out of the 50 kg sample taken for the project, a representative sample for the total analysis was taken by crushing the whole 50 kg in a big laboratory jaw crusher. The crushed product was screened using a 25mm aperture screen. The +25mm fraction was retained while the -25mm fraction was further crushed using a cone crusher in closed circuit with a screen of aperture 4mm. A representative sample of 1 kg was riffled out of the -4mm and the remaining -4mm was retained.

The -4mm 1 kg sample was crushed in a jaw crusher in closed circuit with a screen of aperture 1mm reducing it all to -1mm. A 250g sample was ground in a Tema Mill in a 250cc pot for 10 seconds and 50 g sample taken out of the Milled product. The 50g sample was further ground in a tema mill in 100cc pot for 3 minutes before taken for chemical analysis. Figure [3.1] shows the procedure for the sampling.

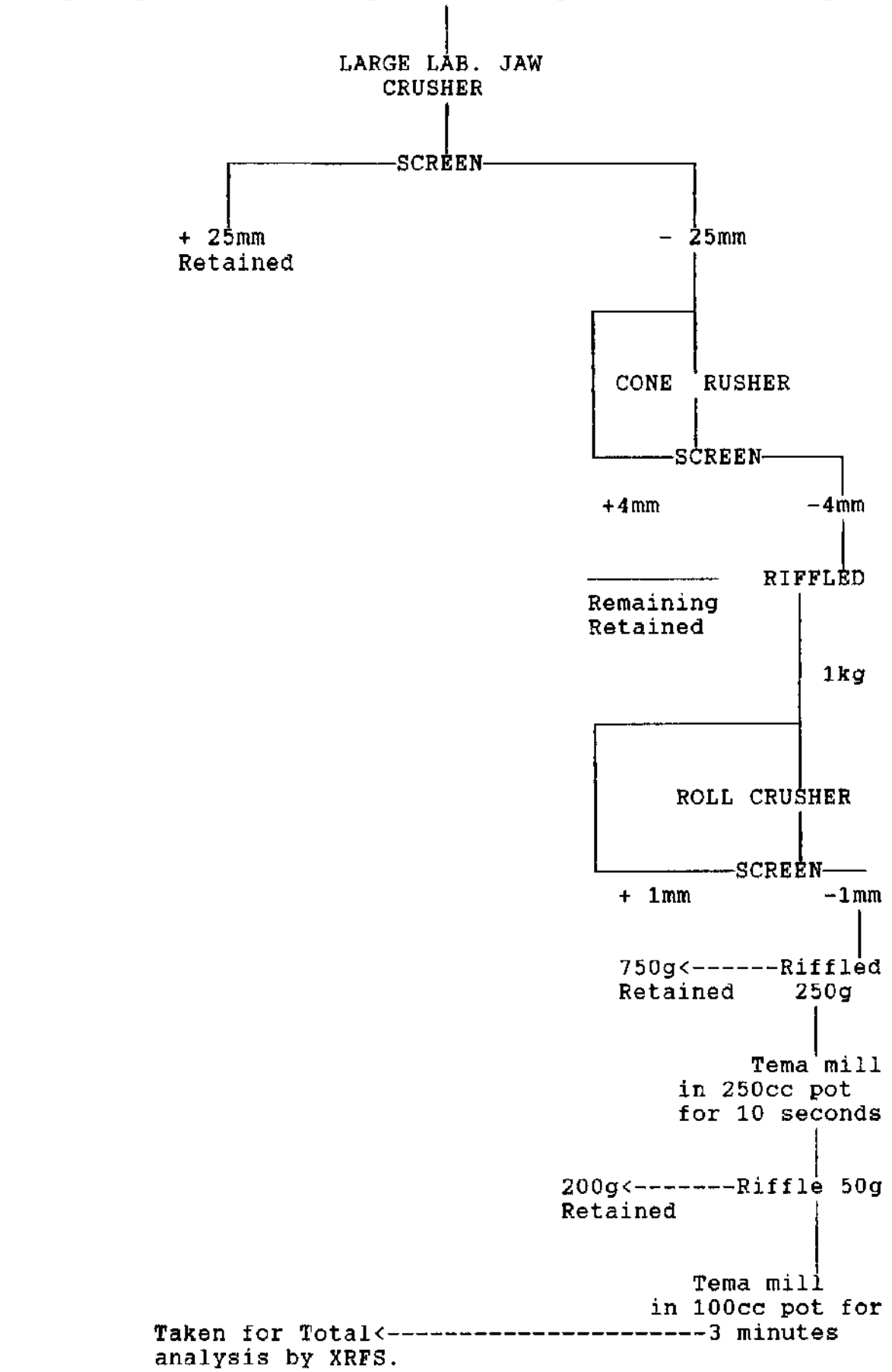


Fig. 3.1: Schematic Diagram for Sampling Procedure

3.4 CHEMICAL ANALYSIS

The test was carried out to determine the full chemical composition and grade of the ore using a phillips PW 1212 X-ray flourescence spectrophotometer (XRFS).

Standards in the form of pellets were produced by taking portion of the sample ground in the tema mill and mixing it with a binder consisting of wax and polystyrene resin. The mixtures were pressed into discs producing the pellets. The XRFS machine was calibrated using those standards. Then a representative sample of the ore was taken, mixed with the binder, pressed into a pellet and then introduced into the machine and its chemical composition was determined. These standards were kept and used in the subsequent analysis. The result of the chemical analysis is given in Table 3.1.

Table 3.1:Chemical analysis of the raw ore as determined by X-ray fluorescence spectrophotometry.

Compound/Mineral	% Assay
Mn_3O_4	23.0
SiO_2	36.4
Fe_2O_3	14.8
Al_2O_3	11.0
CaO	0.89
MgO	0.63
BaO	0.58
K_2O	0.14
TiO_2	0.53
P_2O_5	0.49
Cr_2O_3	0.04
Cu	0.03
Ni	0.03
S	0.01
LOI (Loss On Ignition)	10.91

NOTE: The above assay result does not mean that all the elements occurred as the given compounds in the analysis.

3.5 SIZE ASSAY ANALYSIS

The size/assay analysis was carried out to determine the distribution of the various minerals specifically, Manganese, Silica and Iron bearing minerals of the ore in the various size fractions. The analysis was used to obtain information on the possibility of using waste rejection techniques so as to reject the gangue minerals at as coarse a size as possible using simple crushing and screening operations. It was also used to obtain clues on the liberation sizes of the various minerals in the ore and their degree of associations

A representative sample of the ore which has been crushed to - 4mm was riffled out and 1250g was taken for the analysis. The size analysis was carried out using standard screen designation sieve series consisting of 14 size fractions ranging from + 2.8mm to - 45µM. The series being (+ 2.8mm, - 2.8+2.0mm, - 2.0+1.4mm, - 1.4+1.0mm, - 1000+710µM, 710+500µM, - 500+355µM, - 355+250µM, - 180+125µM, - 125+ 90µM, - 90+63µM, - 45µM. The size analysis was performed dry for the material from +2.8mm to + 125µM. For the - 125µM material the analysis was performed wet. The amount of material retained on each sieve size was collected and weighed and a representative sample taken from each and ground in a Tema mill before they were taken for chemical analysis.

Each sample was analysed for manganese, silica and iron. The assay results of each fraction together with their weight were then used in determining the distribution of manganese, silica and Iron into the various size fractions. The results are shown in Tables 3.2 to 3.6.

Table 3.2 Size/Assay analysis for manganese

particle size (μM)	Weight (g)	Weight %	Commu-lative weight	Assay % Mn	Manga-nese Unit	Cummu-lative Mn Unit	%Mn distri-bution
+2800	292.3	24.0	24.0	16.9	49.40	49.4	23.5
-2800+2000	199.9	16.4	40.4	17.1	34.20	83.6	16.3
-2000+1400	126.8	10.4	50.8	17.6	22.32	105.92	10.6
-1400+1000	87.6	7.2	58.0	17.7	15.51	121.42	7.4
-1000+710	62.7	5.2	63.2	18.0	11.29	132.71	5.4
-710+500	48.7	4.0	62.2	17.8	8.67	141.38	4.1
-500+355	38.4	3.2	70.4	18.0	6.91	148.29	3.3
-355+250	45.6	3.8	74.2	18.3	8.35	156.64	4.0
-250+180	60.3	5.0	79.2	19.3	11.64	168.28	5.5
-180+125	65.5	5.4	84.6	18.7	12.25	180.53	5.82
-125+90	62.5	5.1	89.7	15.0	9.35	189.91	4.5
-90+63	66.3	5.5	95.2	18.8	12.46	202.37	5.9
-63+45	39.2	3.2	98.4	12.2	4.78	207.15	2.3
-45	20.0	1.7	100.0	16.3	3.26	210.41	1.6
FEED	1215.8	100.0		17.3	210.41		100.0

Table 3.3 Size/Assay analysis for SiO_2

Particle size (μM)	Weight (g)	Weight %	Commu-lative weight	Assay $\%SiO_2$	Silica Unit	Cummu-lative SiO_2 Unit	$\%SiO_2$ distri-bution
+2800	292.3	24.0	24.0	38.3	111.95	111.95	24.7
-2800+2000	199.9	16.4	40.4	38.3	75.56	188.51	16.9
-2000+1400	126.8	10.4	50.8	38.1	48.31	236.82	10.6
-1400+1000	87.6	7.2	58.0	36.6	32.06	268.88	7.1
-1000+710	62.7	5.2	63.2	35.7	22.38	291.26	4.9
-710+500	48.7	4.0	67.2	35.2	17.14	308.40	3.8
-500+355	38.4	3.2	70.4	33.7	12.94	321.34	2.9
-355+250	45.6	3.8	74.2	33.0	15.05	336.39	3.3
-250+180	60.3	5.0	79.2	30.9	18.63	355.02	4.1
-180+125	65.5	5.4	84.6	32.1	21.03	376.05	4.6
-125+90	62.5	5.1	89.7	43.2	27.0	403.05	6.0
-90+63	66.3	5.5	95.2	40.0	26.25	429.57	5.8
-63+45	39.2	3.2	98.4	45.6	17.88	447.45	3.9
-45	20.0	1.7	100.0	33.1	6.62	454.07	1.5
FEED	1215.8	100.0		37.4	454.07		100.0

Table 3.4 Size/Assay analysis for Fe.

particle size (μM)	Weight (g)	Weight %	Commu-lative wt. %	Assay % Fe	Fe Unit	Cummu-lative FeUnit	%Fe distri-bution
+2800	292.3	24.0	24.0	10.2	29.82	29.82	23.2
-2800+2000	199.9	16.4	40.4	10.3	20.59	50.41	16.0
-2000+1400	126.8	10.4	50.8	11.0	13.95	64.36	10.8
-1400+1000	87.6	7.2	58.0	10.7	9.37	73.73	7.3
-1000+710	62.7	5.2	63.2	11.20	7.02	80.75	5.5
-710+500	48.7	4.0	62.2	11.0	5.36	86.11	4.2
-500+355	38.4	3.2	70.4	11.5	4.42	90.53	3.4
-355+250	45.6	3.8	74.2	11.3	5.15	95.68	4.0
-250+180	60.3	5.0	79.2	11.1	6.69	102.37	5.2
-180+125	65.5	5.4	84.6	10.4	6.81	109.18	5.3
-125+90	62.5	5.1	89.7	9.9	6.19	115.37	4.8
-90+63	66.3	5.5	95.2	9.2	6.10	121.94	4.7
-63+45	39.2	3.2	98.4	11.4	4.47	125.94	3.5
-45	20.0	1.7	100.0	13.5	2.7	128.64	2.1
FEED	1215.8	100.0		17.3	210.41		100.0

Table 3.5 Distribution of Mn, Fe and SiO_2 in various size fractions

particle size (µM)	Commulative Weight %	CUMMULATIVE % DISTIRBUTION Manganese	Silica SiO_2	Iron Fe
-2800+2000	24.0	23.5	24.7	23.2
-2000+1400	40.0	39.8	41.6	39.2
-1400+1000	50.8	50.4	52.2	50.0
-1000+710	63.2	63.2	64.2	62.8
-710+500	67.2	67.3	68.0	67.0
-500+355	70.4	70.3	70.9	70.4
-355+250	74.2	74.6	74.2	74.4
-250+180	79.2	80.1	78.3	79.6
-180+125	84.6	85.6	82.9	84.9
-125+90	89.7	90.4	88.9	89.7
-90+63	95.2	96.3	94.7	94.7
-63+45	98.4	98.6	98.6	97.9
-45	100.0	100.0	100.0	100.0

Table 3.6: Summary of Results of Size/Assay Analyses

Particle size in (μM)	ASSAY %Mn	% Fe	% SiO_2
+2800	16.9	10.2	38.3
-2800+2000	17.1	10.3	38.3
-2000+1400	17.6	11.0	38.1
-1400+1000	17.7	10.7	36.6
-1000+710	18.0	11.2	35.7
-710+500	17.8	11.0	35.2
-500+355	18.0	11.5	33.7
-355+250	18.3	11.3	33.0
-250+180	19.3	11.1	30.2
-180+125	18.7	10.4	32.1
-125+90	15.0	9.9	43.2
-90+63	18.8	9.2	40.0
-63+45	12.2	11.4	45.6
-45	16.3	13.5	33.1

3.6 MINERALOGICAL ANALYSIS

The mineralogical analysis carried out involved Identifying the major, minor and trace minerals, allocation of each element to each mineral, determining the qualities of each mineral and also the grain size distribution of the minerals of economic importance. The detailed mineralogy of the ore was determined using optical microscopy, Scanning Electron Microscopy (SEM) and X-ray Diffraction techniques.

For the optical microscopy thin sections of the uncrushed lumps and representative sample of the ore were prepared. The polished and thin sections were examined in a transmitted light, and only a few phases were identified. The polished sections were then taken for detailed examination by Scanning Electron Microscope (SEM) using back scatter energy dispersive X-ray analyser. The scanning electron microscopy was carried out using a combridge instruments S600 stereoscan fitted with a link system 860 energy dispersive spectrometer. While the X-ray diffraction was conducted using a phillips diffractometer. The XRD Diffraction pattern of the sample of the ore was obtained. Also the X-ray Spectra of some of the phases identified in the ore were also produced. Scanning electron Photomicrographs were also taken using various magnifications in order to aid

identification of the various phases.

Powder representative sample of the ore of various size fractions were prepared for analysis using the X-ray Diffractometer. The tracings of the powder patterns were obtained and used in identifying the various minerals in the ore using a computer programme which enables the comparison of tracings of the powder patterns obtained from the samples with standard powder patterns of several minerals. The powder patterns are given in Appendix 3 and the results in Tables 3.7 and 3.8.

TABLE 3.7 MINERALOGICAL ANALYSIS OF THE ORE

Mineral	Amount	Chemical formula
(1) Spessartine	Major	$Mn_3Al_2(SiO_4)_3$
(2) Almandine Manganon	Minor	$(Fe,Mn)_3Al_2(SiO_4)_3$
(3) Psilomelane		
- Hollandite		$(Ba,Mn)(Mn_8O_{16})(OH)_2$
- Cryptomelane		$(K,Mn)(Mn_8O_{16})(OH)_2$
(4) Quartz (Free silica)	Major	SiO_2
(5) Manganon	Trace	(Fe, Mn) + OY
(6) Lithiophorite	Trace	$(Al,Ba,Fe,Mn)(OY)MnO_2$
(7) Hematite	Trace	Fe_2O_3
(8) Pyrite		
(inclusion in Quartz)	Trace	FeS_2
(9) Galaxite	"	$MnAl_2O_4$
(10) Knorringite	"	$Mg_3Cr_2(SiO_4)_3$
(11) Manganon ilmenite	"	$(Fe,Mn)TiO_3$
(12) Ringowoodite	"	$MgSiO_4$
(13) Monozite (Lanthanide)	"	$LnPO_4$
(14) Arsenopyrite	"	-
(15) Limonite	"	FeO.OH

Table 3.8: Distribution of minerals into various size fractions produced from XRD analysis.

Particle Size (μM)	Sample Number	Mineral Detected by XRD
-1000 + 710	Y/8520	Quartz (SiO_2) Spessartine {$Mn_3 Al_2 (SiO_4)$}
-710 + 500	Y/8521	Almandine Manganon {$(Fe,Mn)_3 Al_2 (SiO_4)$} Quartz (SiO_2)
-500 + 355	Y/8522	Quartz (SiO_2) Knorringite $Mg_2 Al_2 (SiO_4)_4$ Galaxite ($Mn Al O_4$
-355 + 250	Y/8523	Spessartine {$Mn_3 Al_2 (SiO_4)_3$} Quartz (SiO_2)
-250 + 180	Y/8524	Knorringite $Mg_3 Cr_2 (SiO_2)$ Quartz (SiO_2)
-180 + 125	Y/8525	Knorringite {$Mg_3 Cr_2 (SiO_4)_4$ Almandine Manganon {$(FeMn)_3 Al_2 (SiO_4)_3$} Spessartine {$Mn_3 Al (SiO_4)_3$} Galaxite ($Mn Al_2 O_4$ Quartz (SiO_2) Spinel, Ferrian Mg (Al, Fe) Spinel
-125 + 90	Y/8526	Almandine, Manganon $(Fe,Mn)_3 Al_2 (SiO_4)_3$ Knorringite {$Mg_3 Cr_2 (SiO_4)_3$} Galaxite ($Al_2 O_4$) Quartz $(SiO)_2$
-90 + 63	Y/8527	Quartz (SiO_2) Almandine, Manganon $(Fe,Mn)_3 Al_2 (SiO_4)_3$ Galaxite ($Mn Al_2 O_4$)
-63 + 45	Y/8528	Quartz (SiO_2) Spessartine {$Mn_3 Al_2 (SiO_4)_3$}

3.6.1 SAMPLE PREPARATION FOR SEM

When Non-conductive specimens are examined in SEM, they tend to collect a surplus of electrons on their surfaces and become negatively charge, as these electrons build up the image quality of specimens is badly affected. The built up electrons sometimes deflect or repel the electron mirror or some of these electrons can escape from the specimen after a considerable delay causing a spurious charging and the means of eliminating it is either to use a lower energy beam or coat the specimen with a high energy beam.Since it is essential to achieve this, coating the specimen is the only alternative way of eliminating this phenomena [21].

The most commonly used materials for coating the specimens include: gold, gold/palladium alloy and carbon. Throughout this work all specimens for SEM analysis were coated with carbon using a vacuum evaporation unit. The specimens are placed in a vacuum chamber in which a few strands of carbon fibre are held in contact. The carbon is then heated using a high current source and as it evaporates it is deposited on the specimens.

3.6 LIBERATION SIZE DETERMINATION

Two methods were used for the determination of the liberation size of the ore. The methods are:

(i) Heavy liquid methods

(ii) Release analyses method

The heavy liquid method for the determination of liberation size involved carrying out size analysis of the ore, followed by heavy liquid analysis of each size fraction at a density of 3.0 kg L-1. This density was chosen because most manganese minerals have density greater than 3.0 kg L-1 and will settle to the sink while the main gangue silica with a density of 2.65 kg L-1 will be in the float fraction.

For the purpose of carrying out this test, nine size fractions (-1000+710µM, -710_500µM, -500+355µM, -355+250µM, -250+180µM, -180+125µM, -125+90µM, -90+63µM, -63+45µM) of the representative sample of the ore were prepared. 50g of each of the size fraction was subjected to heavy liquid test at the given density. Sinks and floats of each size fraction were collected, weighed and analysed for manganese, silica and iron by XRFS. Powder samples of the sinks and floats of each size fractions were also analysed by X-ray Diffractometer. Polished sections of the sinks and floats fractions of each of the size fractions were produced and examined under scanning electron microscope.

The heavy liquid of density 3.0 kg L-1 used in this study was prepared by mixing D1 - Idomethane of density 3.3 kg L-1 with acetone of lower density. The results of the heavy liquid tests are given in tables 3.9 to 3.12.

Table 3.9:Distribution of Manganese into Various Size Fractions Produced from Heavy Liquid Tests.

Size Fractions (µM)	FEED Wt (g)	FEED Assay %Mn	FEED Mn Unit	SINK Wt (g)	SINK Ass %Mn	SINK Mn Unit	SINK % Distr.	FLOAT Wt (g)	FLOAT Ass %Mn	FLOAT Mn Unit	FLOAT % Distr.
-1000+710	54.51	18.0	981.18	4.8	18.8	654.24	66.7	19.1	13.8	263.94	33.3
-710+500	51.25	17.8	912.25	26.1	19.1	498.51	54.7	24.6	13.8	263.94	45.3
-500+355	52.68	18.0	948.24	31.1	19.5	606.45	64.0	21.0	16.3	341.79	36.0
-355+250	52.58	18.3	962.21	36.9	19.9	734.31	76.3	15.5	14.7	227.90	23.7
-250+180	55.16	19.3	1064.21	38.6	20.0	772.0	72.5	17.2	17.0	292.60	27.5
-180+125	62.72	18.7	1172.86	44.1	20.2	890.82	76.0	18.7	15.0	282.04	24.0
-125+90	54.30	15.0	814.50	36.1	19.3	696.73	85.5	18.1	6.5	117.77	14.5
-90+63	55.90	18.8	1050.51	28.5	17.9	510.15	48.6	27.6	19.6	540.77	51.4
-63+45	55.2	12.2	673.44	30.6	15.3	468.18	69.5	23.9	8.6	205.26	30.5

Table 3.10:

Distribution of SiO_2 into Various Fractions Produced from Heavy Liquid Tests

Size in (μM)	FEED			SINK				FLOAT			
	Wt (g)	Assay %SiO_2	Silica Unit	Wt (g)	Assay %SiO_2	Silica Unit	% Distr.	Wt (g)	Assay %SiO_2	Silica Unit	% Distrib.
-1000+710	54.51	53.7	1946.01	34.8	34.0	1183.20	60.80	19.1	39.9	762.81	39.2
-710+500	51.25	35.2	1804.0	26.1	33.8	882.18	48.90	24.6	37.5	921.82	51.1
-500+355	62.68	33.7	1775.32	31.1	32.4	1007.64	56.70	21.13	6.6	767.72	43.3
-355+250	52.58	33.0	1735.14	36.9	29.1	1073.79	61.91	5.5	42.7	661.35	38.1
-250+180	55.16	30.9	1642.64	38.6	28.3	1092.38	66.5	17.2	32.0	550.26	33.5
-180+125	62.72	32.1	2013.31	44.1	27.7	1221.57	60.7	18.7	42.3	791.74	39.3
-125+90	54.30	43.2	2345.75	36.1	30.2	1090.22	46.5	18.1	69.4	1255.53	53.5
-90+63	55.90	40.0	2236.0	28.5	33.7	943.35	42.2	27.6	46.4	1255.53	53.5
-63+45	55.20	45.6	2517.12	30.6	43.3	1324.98	52.6	23.9	49.9	1192.14	47.4

Table 3.11

Distribution of Fe into Sink and Float.

	FEED			SINK				FLOAT			
Size Fraction µM	Wt (g)	Assay %Fe	Fe Unit	Wt (g)	Assay %Fe	Fe Unit	% Distr.	Wt. (g)	Assay %Fe	Fe Unit	% Distr
-1000+710	54.51	11.2	610.51	34.8	12.1	471.08	69.00	19.1	9.9	189.43	31
-710+500	51.25	11.0	563.75	26.1	12.0	313.2	55.6	24.6	10.2	250.55	44.6
-500+355	52.68	11.5	605.82	31.1	12.6	391.86	64.7	21.0	10.2	213.96	35.3
-355+250	52.58	11.3	594.15	36.9	13.0	479.7	80.7	15.5	7.3	114.45	19.3
-250+180	55.16	11.1	590.08	38.6	12.2	470.92	79.8	17.2	6.9	119.16	20.2
-180+125	62.72	10.4	652.29	44.1	12.4	546.84	83.8	18.7	5.6	105.45	16.2
-125+90	54.30	9.9	537.57	36.1	12.7	458.47	85.3	18.1	4.4	79.10	14.7
-90+63	55.90	9.2	514.28	28.5	12.9	67.65	71.5	27.6	5.3	146.63	28.5
-63+45	55.45	11.4	629.28	30.6	11.8	361.08	57.4	23.9	11.2	268.2	42.6

Table 3.12

Distribution of Mn, SiO_2 and Fe into Sink and Float.

	SINK %DISTRIBUTION			FLOAT %DISTRIBUTION		
Size Fraction In µM	Manganese	Silica	Iron	Manganese	Silica	Iron
1000+710	7.6	6.6	8.0	3.1	4.2	3.6
710+500	5.8	4.9	5.9	4.8	5.2	4.7
500+355	7.1	5.6	7.4	4.0	4.2	4.0
355+250	8.6	5.9	9.0	2.6	3.7	2.2
250+180	9.0	6.1	8.9	3.5	3.0	2.3
180+125	10.3	6.8	10.3	3.2	4.4	1.9
125+90	8.2	6.0	8.7	1.4	7.0	1.5
90+63	5.9	5.3	6.9	6.3	7.2	2.8
63+45	5.5	7.3	6.8	2.4	6.6	5.1
TOTAL	68	54.5	71.9	32.0	45.5	28.1

3.7.1 DETERMINATION OF LIBERATION SIZE USING RELEASE ANALYSIS TECHNIQUE

The aim of this analysis was to determine the liberation size of the ore at various size fractions ranging from -355 to +45μM, using Release analyses technique on data obtained from the Mozley mineral separator.

After grinding and sizing of the ore to the required size fractions, separation tests were carried out using the Mozley Laboratory Mineral Separator. Using the result of the separation test Release analysis table were drawn up using the relationship.

$$C.U.W = \sum \left(\frac{C}{Ff} \times 100\right) \qquad (8)$$

$$C.U.M.\ \%\ Recovery = \sum \left[\frac{Cc}{Ff} \times 100\right] \qquad (9)$$

Where:

C.U.W. = Cummulative Unit Weight

C.U.M % Recovery = Cummulative % Recovery

F = Weight of the Feed

C = Weight of the Concentrate

f = Assay of the Feed

c = Assay of the Concentrate

The results generated are given in tables 3.13 and 3.14 Using these results Release analysis curves were produced and compared with theoretical liberation curve given in figure 2.9.

Table 3.13 Release Analysis Data for Manganese at various size fractions.

S.G	Wt(g)	Wt%	Assay %Mn	Metal Value	% Recovery	Cummulative Recovery	Unit Wt	Cumulative Unit Wt
				-355+250 µM				
-3.3	65.8	32.1	21.2	4394.96	36.0	36.0	1.70	1.70
-3.3+3.0	87.8	42.8	19.1	1676.98	43.3	79.3	2.30	4.0
-3.0+2.8	33.3	11.4	16.1	536.13	13.8	93.1	0.86	4.86
-2.8	28.3	13.8	9.5	268.85	6.9	100.0	0.73	5.59
Total	215.2			6876.92				
				-250+180 µM				
+3.3	127.2	57.0	21.1	2683.92	63.0	63.0	2.99	2.99
-3.3+3.0	51.7	23.2	19.4	1002.98	23.5	68.5	1.21	4.20
-3.0+2.8	20.6	9.2	16.6	341.96	8.0	94.4	0.48	4.68
-2.8	23.8	10.7	9.7	280.86	5.5	100.0	0.56	5.24
TOTAL	223.3	100.0	4259.72					
				-180+125 µM				
+3.3	198.1	71.9	20.2	4001.62	73.3	78.3	3.88	3.88
-3.3+3.0	46.9	17.0	16.1	755.09	14.8	93.1	0.92	4.80
-3.0+2.8	24.3	8.8	11.7	284.31	5.6	98.7	0.48	5.28
-2.8	6.3	2.3	11.2	70.56	1.4	100.0	0.12	5.40
TOTAL	275.6	100.0	5111.58					

Table 3.13 cont.

-125+90 µM

+3.3	94.1	47.1	21.7	2041.97	63.6	63.6	2.93	2.93
-3.3+3.0	37.6	18.8	17.2	646.72	20.1	83.7	1.17	4.10
-3.0+2.8	18.7	9.4	14.1	263.67	8.2	91.9	0.58	4.68
-2.8	49.6	24.8	5.2	257.92	8.0	100.0	1.55	6.23
TOTAL	200	100.0		3210.28				

-90+63 µM

+3.3	94.2	46.4	17.9	1684.39	64.6	64.6	3.61	3.61
-3.3+3.0	28.3	13.9	17.4	492.42	18.9	83.5	1.09	4.8
-3.0+2.8	24.6	12.1	7.7	189.42	7.3	90.8	0.94	5.75
-2.8	55.9	27.5	4.3	240.37	9.2	100.0	2.15	7.89
TOTAL	203	100.0		2606.6				

-63+45 µM

S.g	Wt(g)	Wt%	assay %Mn	Metal Value	% Recovery	Cummulative Recovery	Unit Wt	cumulative Unit Wt
+3.3	88.1	46.2	16.2	1488.89	22.16	27.16	0.95	0.95
-3.3+3.0	30.5	16.0	13.0	396.50	36.3	63.9	1.27	2.22
-3.0+2.8	26.2	13.7	7.0	183.46	15.7	79.6	0.48	2.7
-2.8	45.9	24.1	5.0	234.09	20.4	100.0	0.41	3.11
TOTAL	190.7	100.0		2302.94				

Table 3.14 Release of Analysis Data for SiO_2 at various size fractions

-355+250 µM

S.g	Wt(g)	Wt %	%SiO_2	Metal Value	% Recovery	Cummulative Recovery	Unit Wt	cumulative Unit Wt
-2.8	65.8	30.5	50.0	1415.0	20.4	20.46	0.95	0.95
-3.0+2.8	87.8	40.8	32.7	1088.91	15.7	36.1	0.27	2.22
-3.3+3.0	33.3	15.5	23.7	2519.86	36.3	72.4	0.48	2.7
+3.3	28.3	13.2	29.1	1914.78	27.6	100.0	1.41	3.11
TOTAL	215.2			6938.55				

-250+180 µM

-2.8	23.8	10.7	49.6	1180.48	17.11	17.16	0.34	0.34
-3.0+2.8	20.6	9.2	29.6	609.76	8.8	25.9	0.30	0.64
-3.3+3.0	51.7	23.22	27.6	1426.92	20.8	46.7	0.75	1.36
+3.3	127.2	57.01	29.01	3688.8	53.3	100	1.84	3.23
TOTAL	223.7			6905.96				

-180+125 µM

-2.8	6.3	2.3	46.9	295.47	3.4	3.4	0.07	0.07
-3.0+2.8	24.3	8.8	48.1	1168.83	13.3	16.7	0.28	0.35
-3.3+3.0	46.9	17.02	35.2	1650.88	18.8	35.5	0.53	0.88
+3.3	198.1	71.91	28.7	5685.47	64.6	100.0	2.25	3.13
TOTAL	275.6			8800.65				

Table 3.14 cont.

					-125+90 µM			
-2.8	49.6	24.8	74.7	3705.12	44.2	44.2	0.59	0.59
-3.0+2.8	18.7	9.4	38.4	716.08	8.6	52.8	0.22	0.81
-3.3+3.0	37.6	18.82	33.5	1259.6	15.0	67.8	0.45	1.26
+3.3	94.1	47.1	28.6	2691.20	32.1	100.0	1.12	2.38
TOTAL	200			8800.65				
					-63+45 µM			
-2.8	45.9	46.2	74.2	3405.78	32.1	32.1	0.43	0.43
-3.0+2.8	28.2	16.0	65.9	1726.58	16.3	48.4	0.25	0.68
-3.3+3.0	30.5	13.7	36.2	1104.1	10.4	58.8	0.29	0.97
+3.3	88.1	24.1	49.7	4378.57	41.1	100.0	0.83	1.8
TOTAL				10615.03				
					-90+63 µM			
-2.8	55.9	27.5	78.4	4382.56	41.6	41.6	0.53	0.53
-3.0+2.8	24.6	112.1	64.5	1586.7	15.0	56.6	0.23	0.76
-3.3+3.0	28.3	13.9	35.0	990.5	9.4	66.0	0.27	0.03
+3.3	94.3	46.4	38.1	3389.02	34	100.0	0.89	1.92
TOTAL				10548.73				

Table 3.15

RELEASE ANALYSIS DATA FOR IRON

Product	Wt(g)	Wt%	Assay SiO_2	Metal Value	% Recovery	Cum.% Recovery	Unit Weight	Cum.Unit Weight
				-355+250 µM				
Concentrate	65.8	30.6	11.0	723.80	28.3	28.3	2.57	2.57
Middling 1	87.8	40.8	12.9	1132.62	44.2	72.5	3.43	6.00
Middling 2	33.3	15.5	13.0	432,9	16.9	89.4	1.30	7.30
Tailing	28.3	13.2	9.6	271.68	10.6	100.0	1.11	8.41
Total								
				-250+180 µM				
Concentrate	127.2	57.0	11.0	1399.20	55.4	55.4	5.03	5.03
Middling 1	51.1	23.2	12.6	651.42	25.6	81.2	2.05	7.08
Middling 2	20.6	9.2	12.7	261.62	10.4	91.6	0.82	7.90
Tailing	73.8	10.7	124.2	214.4	8.2	100.0	0.94	8.84
Total	223,3		100.0					
				-180+125 µM				
Concentrate	98.1	71.9	11.1	2198.91	72.11	72.11	6.50	6.50
Middling 1	46.9	17.0	11.8	553.42	18.2	90.3	1.54	6.04
Middling 2	24.3	8.8	9.7	135.71	7.7	98.0	0.80	8.84
Tailing	6.3	2.5	9.7	61.11	2.0	100.0	0.20	9.04
Total		275.6	100.0		3049.11			

Table 3.15 (Cont'd) **RELEASE ANALYSIS DATA FOR IRON**

Product	Wt(g)	Wt%	Assay SiO_2	Metal Value	% Recovery	Cum.% Recovery	Unit Weight	Cum.Unit Weight
-125+90μM								
Concentrate	94.1	47.1	11.1	1044.51	54.3	54.3	4.89	4.89
Middling 1	37.6	18.8	11.7	439.92	22.9	77.2	1.85	6.84
Middling 2	18.7	9.4	11.3	211.31	11.0	88.2	0.97	7.81
Tailing	49.6	24.8	4.6	228.16	11.9	100.0	2.57	10.38
Total		200.0	100.0		1923.9			
-90+63 μM								
Concentrate	94.2	46.5	10.4	979.68	56.8	56.8	5.58	5.58
Middling 1	28.3	13.9	11.8	333.94	19.4	76.2	1.93	7.51
Middling 2	24.6	12.1	6.91	109.74	9.9	85.1	1.66	9.17
Tailing	55.9	27.5	4.3	240.37	14.0	100.0	2.9-	12.07
-63+45μM								
Concentrate	88.1	46.2	9.4	828.14	52.4	52.4	5.58	5.58
Middling 1	30.5	16.0	11.7	355.68	22.5	74.9	1.93	7.51
Middling 2	26.2	13.7	6.7	152.44	10.3	85.2	1.66	9.17
Tailing	45.9	24.1	5.1	234.09	14.8	100.0	2.90	12.07
				234.09				
Total		190.7			1580.35			

3.8 HEAVY LIQUID TESTS

The heavy liquid test was carried out to determine the amenability of the ore to gravity concentration and also to prepare washability curves which would be used in assessing the performance of the proposed gravity separation process. The test was also to be used in selecting the optimum particle size range for the proposed gravity separation process.

The tests were carried out on six different size fractions: -355+250μM, -250+180μM, -180+125μM, -125+90μM -90+63μM and -63+45μM using liquid densities of 3.3, 3.0 and 2.8 kg L^{-1}, which gave four fractions of +3.3, -3.3+3.0 and -2.8. The particle size fractions -355 to +125μM were prepared by dry sieving while -125 to +45μM by wet sieving so as to remove slimes which will affect the tests by increasing the density of the liquids.

The different density fractions were prepared by mixing proportional amount of D1 - Iodomethane and acetone and the densities were checked again after each run and adjusted when necessary before the next run.

After preparation of the heavy liquids with the desired densities.Samples of the ore so prepared were introduced into the heavy liquids beginning with the heaviest liquid fraction. The sink from this fraction was collected, washed with acetone,

dried and weighed while floats from it were introduced into the next liquid of lower density. The procedure was repeated to the lowest selected density. The four different density fractions collected for each particle size fraction were analysed for Mn, and density characteristic curve table was drawn up given in table 3.16.

Density and characteristics assay curves were produced using the experimental data. These curves were then matched with theoretical density and characteristics curves (Figures 2.1 to 2.6) and the degree of liberation achieved was estimated.

Table: 3.16 Characteristic cuves for Mn. at various size fractions.

-355+250 µM

S.g	Wt(g)	Cumm. %Wt	Assay %wt	%Mn	Unit Mn	Cumm. Unit	Cumm. %Mn	Cumm. Wt(g)	Charact. Assay
+3.3	65.8	32.1	32.1	21.2	1394.96	1394.96	21.2	65.8	16.05
-3.3+3.0	87.8	42.8	74.9	19.1	1676.98	3071.94	20.0	153.6	53.5
-3.0+2.8	23.3	11.4	86.3	16.1	536.13	3608.07	20.4	176.9	80.6
-2.8	28.3	13.8	100.0	9.5	268.85	3876.92	18.9	205.2	93.2
TOTAL	205.2	100.0			4394.96				

-250+180µM

+3.3	127.8	57.0	28.5	21.2	2683.92	2683.92	21.1	127.2	28.5
-3.3+3.0	51.2	23.2	80.2	19.4	1022.98	3686.9	20.6	178.9	68.6
-3.0+2.8	20.6	9.2	89.4	16.6	341.96	4028.86	20.2	199.5	84.8
-2.8	28.8	10.7	100.0	9.7	230.86	4209.72	19.1	223.3	94.8
TOTAL	223.3	10.7			4259.72				

-180+125µM

+3.3	198.1	71.9	71.9	20.2	4001.62	4001.62	20.2	198.1	35.95
-3.3+3.0	46.9	17.0	88.9	16.1	755.09	4756.91	19.4	245.0	80.4
-3.0+2.8	24.3	8.8	97.7	11.7	284.31	5041.02	18.7	269.3	93.3
-2.8	6.3	2.3	100.0	11.2	70.56	5711.58	18.6	275.6	98.85
TOTAL	275.6	100.0			5111.58				

Table 3.16 (Cont'd)

-125 + 90µM

S.g	Wt(g)	%Wt	Cum%Wt	Assay %Mn	Unit of Mn	Cumulative Units	Cumulative % Mn	Cumulative (Wt)(g)	Characteristic Assay
+3.3	94.1	41.1	47.1	21.7	2041.97	2041.97	21.7	94.1	23.55
-3.3+3.0	37.6	18.8	65.9	17.2	646.72	2688.69	20.4	131.7	56.5
-3.0+2.8	18.7	9.4	75.3	14.1	263.67	2952.36	19.6	150.4	70.6
-2.8	49.6	24.8	100.1	5.2	257.92	3210.28	16.1	200	87.7
TOTAL	200				3210.28				
				-90 + 63µM					
+3.3	94.2	46.4	46.4	17.9	1684.39	1684.39	17.9	94.2	23.20
-3.3+3.0	28.3	13.9	60.3	19.4	492.91	2176.81	17.8	122.5	53.35
-3.0+2.8	24.6	12.1	72.4	7.7	169.42	2366.23	16.1	147.1	66.35
-2.8	55.9	275	100.0	4.3	240.37	2606.6	12.8	203.0	86.15
TOTAL	203.08				2606.6				
				- 63 + 45µM					
+3.3	88.1	46.2	46.2	16.9	1488.89	1488.89	16.9	88.1	23.1
-3.3+3.0	30.5	62.2	62.2	13.0	396.5	1885.39	15.6	118.6	45.2
-3.0+2.8	26.2	75.9	75.9	17.0	183.34	2068.85	14.3	144.8	69.1
-2.8	45.9	100	100	5.0	234.09	2302.94	12.1	190.7	88.0
	150.7				2302.94				

3.9.2 GRAVITY CONCENTRATION USING MOZLEY SEPARATOR

The test was undertaken using 50g of the ore which has been ground and sized into -125+90μM, -90+63μM,-63+45μM and -45μM size ranges. Appropriate adjustments for the treatment of each size ranges were made where necessary to the motion mechanisms (amplitude, inclination, frequency, knock tension etc.). The sized material was then placed at the top edge of the deck and gently wetted using a wash bottle. Irrigation water was introduced at approximately 800ml/min. The deck was set in motion and the minerals of different density were allowed to separate. Wash water was manually controlled so that the heaviest minerals form a small point at the head of this deck and the lighter minerals travel on a wider band towards the tailings launder. The separation permitted the segregation of different density fractions while Timed - samples were taken after every 5 minutes. Each Time-sample was then dried, weighed and assayed for Mn, and SiO_2. The results are shown in Tables 3.19 and 3.20.

Table 3.19: Metallurgical Balance for Manganese using mozley separator

PRODUCT	wt(g)	% Mn	Metal Content	Cumulative Metal Recovery	% Cummula-tive	Cumulative Wt	Cumulative Assay
			-125+90 µM				
Concentrate	16.4	21.5	352.6	332.6	47.9	47.9	16.4	21.5
Middling	7.5	21.0	101.2	503.8	20.5	68.4	23.9	21.3
Middling	10.8	14.3	154.44	658.24	21.0	89.4	34.7	19.1
Tailing	8.0	9.8	78.4	736.64	10.6	100.0	42.7	17.4
Total	42.4		736.64		100.00			
			-90+63 µM				
Concentrate	22.6	20.8	470.08	470.08	60.6	60.6	22.6	20.8
=	13.3	15.2	202.16	672.24	26.1	86.7	35.9	18.7
=	5.7	11.1	63.27	735.51	8.2	94.9	41.6	17.6
=	4.8	8.3	39.84	775.35	5.1	100.0	46.4	16.7
Total	46.4		777.35		100.00			
			-63+45µM				
Concentrate	11.9	22.9	272.51	272.51	39.7	39.7	11.9	22.9
=	9.1	12.0	109.2	381.71	15.9	55.6	21.0	18.2
=	9.6	11.2	107.52	489.23	15.7	71.3	30.6	16.0
=	21.4	9.2	196.88	686.11	28.7	100.0	52.0	13.2
Total	52.0		686.11		100.00			
			-45µM				
Concentrate	6.4	21.9	140.16	140.16	18.1	18.1	6.4	21.9
=	3.2	14.30	45.76	185.92	5.9	24.0	9.6	21.9
=	11.6	13.5	156.6	342.52	20.3	44.3	21.2	16.2
=	33.1	13.0	430.3	772.82	55.7	100.0	54.3	14.2
Total	54.3		772.82		100			

Table 3.20 Metallurgical Balance for the SiO_2 using Mozley separator

PRODUCT	wt(g)	Cummulative wt(g)	Assay %SiO_2	Metal Content	Cummulative Metal Value	Recovery %	Cummulative %Recov.	Cumulative Assay
-90+63 µM								
Concentrate	16.4	16.4	31.2	511.68	511.68	30.1	30.1	31.2
Middling	7.2	23.6	31.0	223.2	734.88	13.1	43.2	31.1
Middling	10.8	34.4	47.8	516.24	1251.12	30.4	73.6	36.4
Tailings	8.0	42.4	55.8	446.4	697.52	26.3	100.0	40.0
Total	42.4			1697.52				
-63+45 µM								
Concentrate	22.6	22.6	34.2	772.92	722.92	43.9	43.9	34.2
Middling	13.3	35.9	29.1	387.03	1159.95	22.0	65.9	32.3
Middling	5.7	41.6	49.2	280.44	1440.39	15.9	81.8	34.6
Tailings	4.8	46.4	66.8	320.64	1761.03	18.2	100.0	38.0
Total	46.4			1761.03		100.0		
-45µM								
Concentrate	11.9	11.9	27.9	332.01	332.01	13.1	13.1	27.9
Middling	9.1	21.0	42.3	384.93	716.94	15.2	28.3	34.1
Middling	9.6	30.6	57.0	547.2	1264.14	21.5	49.8	41.3
Tailings	21.4	52.0	59.7	1277.58	2541.42	50.3	100.0	48.9
Total	52.0			2541.42				
-125+90 µM								
Concentrate	6.4	6.4	27.3	174.72	174.74	8.5	8.5	27.3
Middling	3.2	9.6	43.9	140.48	315.2	6.8	15.3	32.8
Middling	11.6	21.2	34.8	403.68	718.88	19.6	34.9	33.9
Tailings	33.1	54.3	40.5	1340.55	2059.43	65.1	100.0	37.9
Total	54.3			2059.43				

3.10 DETERMINING OF WORK INDEX USING BONDS METHOD

The equipment use for the test consists of:

(1) An F.C.B. special laboratory scale Bico-Braun ball mill.

(2) A complete set up standard screen designation

(3) A precision balance

(4) An F.C. Bond ball mill discharge which consists of 285 iron balls ranging in size from 38mm to 19mm in diameter with a total weight of 125gm. The calculated distribution of number of balls so as to arrive at the given specification is given below:

Ball diameter	Number of balls	% distribution by number
38mm	25	8.8
32mm	39	13.7
25mm	60	21.0
22mm	68	23.9
19mm	98	21.6
TOTAL	285	100

DETERMINATION OF THE SIZE DISTRIBUTION OF FEED TO THE BALL MILL:

1kg of the representative sample which has been crushed to -4.0mm was taken by riffling. A dry screen analysis of this sample was run using the standard screen designation series consisting of 14 fractions of size ranging from +2.8mm to -45mm. The amount of material returned on each sieve size was weighed. Cumulative weight percent retained were calculated

from which cumulative weight per cent passing were also calculated. The results are given in Table 3.21.

DETERMINATION OF THE MATERIAL WEIGHT OF THE ORE TO BE FED TO THE BALL MILL:

The test stipulates that the initial weight of the feed to the ballmill must corresponds to the weight of 700cm^3 of the ore compacted in a 1000ml graduated cylinder. The -4.0mm crushed ore was introduced into the 1000ml graduated cylinder. The cylinder was shaken and the ore was compacted to the level of 700ml. The ore was poured out from the cylinder and its weight was determined using the precision balance was found to be 1227.7g.

DETERMINING THE WEIGHT(G) OF SIEVE UNDER SIZE THAT MUST BE PRODUCED AT 250% OF CIRCULATING LOAD:

The bond test also assumes that the grinding operations are carried out in closed circuit with a Circulating Load (CL) of

250%, circulating load is given by:

$$CL = \frac{\text{Wt. of Fresh Feed} - \text{Wt. of Prod. under size}}{\text{Weight of Fresh Feed}} \times 100$$

For a circulating load of 250%, assuming an initial weight of 1 and x weight of product under size will be produced, then

$$CL = \left\{ \frac{1 - x}{x} \right\} \times 100 = 250 \qquad (20)$$

Assuming that the grinding operation has attained steady state during which there is no accumulation and the rate at which the material is fed equals to the

rate at which the product is produced. Then

$$CL = \frac{1 - x}{X} = 2.5$$

$$X = \frac{1}{3.5}$$

for an initial weight of 1227.7

$$X = \frac{1227.7}{3.5} = 350.8g$$

. . The amount of under size required to be produced

= 350.8g

TEST-RUN AND TABULATION OF RESULTS:

A dry representative sample weighing 1227.7g taken from the -4.0mm crushed ore was placed in the standard Bond ball mill and ground dry for an initial period of 200 revolutions at a mill speed of 70revs/mins. The mill was then dumped and the ball charge were screened to remove the ground ore. The ground ore was then dry sieved by hand on a 75µM sieve. After sieving the -75µM material was weighed and the weight was recorded. The ball charge were returned to the mill with the over size material and a fresh feed of the weight equal to the amount of under size material removed. The mill was then set at the same speed but for different revolutions. This procedure was repeated through subsequent cycles until a constant circulating load of 250% was attained.

After attaining a constant circulating load of 250% the under size material from the last three cycles were combined and dry sieve analysed. The

results were plotted as cumulative percentage weight passing against the sieve size in micrometers and are given by tables 3.21 to 3.24. Tables were prepared as shown in Tables [3.25 to 3.27], to save all the data and to maintain a close check of the fluctuations of the product under size versus circulating load. The bond work index was then calculated using the following empirical equation.

$$W_i = \frac{44.5}{(P_1)^{0.23} \times (G_{bp})^{0.82} \times \left(\frac{10}{\sqrt{P_2}} - \frac{10}{\sqrt{F_2}}\right)} \quad (21)$$

where W_i = Ball Mill work index at the given size fraction

P_1 = Size openings in micronmeter of the sieve

G_{bp} = The average grams of product under size per revolutions obtained from the last three cycle Tests

P^2 = Size opening in microns at which 80% of last three grinding cycle sieve under size product passes

F_2 = Size opening in micron at which 80% of fresh ballmill feed passes.

Using the above procedure for the three samples the bond work index was determined for three different size fractions of 75μM, 500μM and 1000μM.

Table 3.21:Particle size analysis of Feed to the Bond Ballmill for Wi determinator.

Size (µM)	Weight (g)	Cummulative	Wt. % Retained	Cummulative Wt. % Passing
+ 2800	292.3g	292.3	24.0	76
- 2800 + 2000	199.9g	492.3	40.5	59.5
- 2000 + 1400	126.8g	619.0	50.9	41.1
- 1400 + 1000	87.6g	706.6	58.1	41.9
- 1000 + 710	62.7g	769.3	63.3	36.7
- 710 + 500	48.7g	818.0	67.3	32.7
- 500 + 355	38.4g	856.4	70.4	29.6
- 355 + 250	45.6g	902.0	74.2	28.5
- 250 + 180	60.3g	962.3	79.2	20.8
- 180 + 125	65.5g	1027.8	84.5	15.5
- 125 + 90	62.5g	1090.3	89.7	10.3
- 90 + 63	66.3g	1156.6	95.1	4.9
- 63 + 45	39.2g	1195.8	98.4	1.6
- 45	20.0g 1215.8g	1215.8	100.00	0

Table 3.22:Particle Size Analysis of Mill Discharge for Work Index Determination for 75µM Size Fraction.

particle size in µM	Wt. (g)	Cummulative Weight. (g)	Cummulative Weight. % retained	Cummulative Weight. % Passing
- 75+63	35.5	35.5	34.1	65.9
- 63+45	22.0	57.5	55.2	44.8
- 45	46.6	107.1	100	-
TOTAL	104.1			

Table 3.23: Particle size analysis of mill discharge for Wi calculation at 1000µM.

Size fraction in µM	Weight. (g) retained	% Weight Retained	Cummulative Weight Retained	Cummulative Weight % Passing
- 1000+710	31.17	8.8	8.8	91.2
- 710+500	24.52	6.9	15.7	84.3
- 500+355	20.54	5.8	21.5	78.5
- 355+250	43.57	12.3	33.8	66.2
- 250+180	39.67	11.2	45.0	55.0
- 180+125	52.69	14.9	59.9	40.1
- 125+90	48.17	13.6	73.5	26.5
- 90+63	30.82	8.7	82.2	17.8
- 63+45	25.23	7.1	89.3	10.7
- 45	37.82	10.7	100.0	0
TOTAL	354.4			

Table 3.25: Bond Work Index Calculation Sheet for 1000µM

	MILL FEED							
	B	C	D	E	F	G	H	I
CYCLE	NEW FEED(g)	<1000 µM (g)	1000 µM O/S	REVS	TE1000 in DISCH.	- 1000 PROD (F-D	U/SPROD PER REV (G÷E)	% GRC LOAD (B-F F
1	1227.7	516.63	164.80	100	683.6	167.97	1.67	80.0%
2	683.6	287.61	63.69	110	419.11	132.0	1.21	192.9%
3	419.11	176.0	174.80	120	394.4	218.4	1.82	211.3
4	894.4	165.60	185.20	130	408.7	243.1	1.87	200.4
5	408.7	171.60	178.20	100	369.6	198.0	1.80	232.2
6	369.6	155.20	195.60	100	337.2	182.0	1.82	264.0
7	337.2	141.60	209.20	100	351.6	210.0	2.1	249.1
8	351.6	147.70	203.10	100	347.7	200.0	2.0	253.1
9	347.7	146.00	204.80	100	356.0	210.0	2.1	245.0
10	356.0	149.52	201.30	100	349.5	200.0	2.0	251.3 F

Table 3.26: Bond Work Index Calculation Sheet For 500µM

	MILL FEED							
	B	C	D	E	F	G	H	I
CYCLE	NEW FEED(g)	<500µM (g)	500µM O/S	REVS	TE1500 in DISCH.	-500PROD (F-D)	U/SPROD PER REV (G÷E)	% GRC LOAD $(\frac{B-F}{F})$
1	1227.7	386.2	-35.4	200	594.2	208	1.04	106.5
2	594.2	184.2	166.6	100	318.3	134	1.34	285.8
3	318.3	98.7	252.1	110	330.8	232.1	2.11	271.1
4	330.8	102.6	248.2	120	343.2	240.6	2.01	248.5
5	343.2	106.4	244.4	120	347.3	241.2	2.01	253.5
6	347.3	107.7	243.1	120	352.5	244.8	2.04	248.4
7	352.5	109.9	240.9	120	355.86	246.0	2.04	245.0
8	355.86	110.32	240.5	120	352.72	242.4	2.02	248.1
9	352.72	109.34	241.5	120	349.34	240.0	2.01	251.4
10	349.34	108.3	242.5	120	349.5	241.2	2.01	201.1

Table 3.27: Bond Work Index Calculation Sheet For 75µM

	MILL FEED 350.8							
	B	C	D	E	F	G	H Gbp	I
CYCLE	NEW FEED(g)	75µM (g)	75µM O/S	REVS	TE1 75 in DISCH.	- 75PROD (F-D)	U/SPROD PER REV (G÷E)	% GRC LOAD $\frac{(B-F)}{F}$
1	1227.7	92.10	258.7	200	353.7	261.6	1.31	247.1
2	353.7	26.53	324.3	170	260.3	233.8	1.38	371.6
3	260.3	19.52	531.28	180	290.4	270.9	1.51	322.8
4	290.4	21.78	329.0	190	335.4	313.6	1.65	266.0
5	335.4	25.20	325.6	200	367.6	342.4	1.71	234.1
6	367.6	27.60	323.2	195	340.8	313.2	1.61	260.2
7	340.8	25.56	325.2	200	350.3	324.8	1.62	250.5
8	350.3	26.3	324.5	200	349.2	322.9	1.75	251.61
9	349.2	26.2	324.6	200	351.8	325.6	1.63	249.0

3.11 GRANULOMETRY TESTS

The granulatory test was used to determine:

(1) Mesh of grind necessary for mineral liberation.

(2) Granulatory versus grinding time relationship.

For the purpose of carrying out this test in this study, 15kg of the ore was reduced to 100% passing 2.5mm. This weight was then riffled into 500 ± 5g samples. The samples were ground in a laboratory Rod Mill in open circuit at a solid density of 60% solids for various times ranging from 2 to 6 minutes at 80% of the critical speed of the mill. The grinding time (2 - 6min) was arrived at from the determined work index of the ore. After each grinding cycle the pulp was poured into a bucket and the rods were washed. The ground pulp was then agitated and a representative sample taken which was then introduced into a MALVERN Master Sizer.

The master sizer automatically carried out the particle size analysis of the pulp sample and produced a print out of the particle size distribution, cumulative % passing against size fraction and a Histograph of the particle size distribution. The results of these tests are given in Appendix 2 while the summary is given in table 3.28.

A plot of 80% cumulative passing versus the logarithm of the grinding time was also produced. This plot was used in determining the required time necessary to produce a desired mesh of grind.

Table 2.28: Summary of results of granulatory Test.

Grinding Time Minutes	Cummulative 80% Passing µM	Log. Grinding Time
4	56	0.00
3.5	83	0.54
3.0	118	0.48
2.5	135	0.40
2.0	170	0.30

3.12 FROTH FLOTATION TEST

The three (3) different types of reagents were used. The reagents are Armac C, Armac T and Aerofloat 64. 500g sample of the ore was used for each batch run of the experiment in carrying out this test. Each sample was ground for 4 minutes such that 80% passing - 63µM product would be produced and used as the feed to the flotation tests using the same laboratory Rod Mill with the same charge. A grinding time of 4 minutes was arrived at based on the laboratory grinding tests data so that size 80% passing -63µM was produced.

After grinding the Rods were washed using warm water and the pulp was transferred into the 2 litre Denver Flotation cell container and warm water added to dilute the pulp to 30% solids. The warm water was used to help in the activation of silica. After this operation, the pH was adjusted to 11 using Lime $Ca(OH)_2$. The lime also provides Ca^{2+} which are activators for silica. The reagent/collector was then added and the pulp was conditioned for 10 minutes before air was passed through. At the end of the flotation the floats and the sinks were collected, filtered, dried, weighed and analysed by XRFS. The results of the tests are given in tables 3.29 to 3.32.

Table 3.29:Full chemical analysis of the concentrate and Tailings Produced from Flotation using Armac (C) Collector.

Constituent	% of Constituent in	
	Concentrate	Tailings
MnO	27.49	7.39
Al_2O_3	15.29	4.22
Fe_2O_3	15.64	6.45
SiO_2	28.02	75.06
CaO	1.70	0.15
MgO	0.40	0.06
TiO_2	0.70	0.05
K_2O	1.17	0.04
Ba_2O	0.57	0.12
Cr_2O_3	0.06	0.12
S	0.03	0.00
P_2O_5	0.46	0.67
Ni	0.02	0.01
LOI	6.56	5.54

Table 3.30 :

Full chemical analyses of concentrate and tailings obtained from flotation test using Aerofloat 64 collector

Constituent (s)	% Constituent in	
	Concentrate	Tailings
MnO	26.52	8.39
Al_2O_3	14.2	6.27
Fe_2O_3	15.93	7.12
SiO_2	32.08	71.5
CaO	1.8	0.13
MgO	0.34	0.08
TiO_2	0.68	0.73
K_2O	0.05	0.14
BaO	0.61	0.09
S	0.04	0.0
P_2O_5	0.50	0.70
Cr_2O_3	0.08	0.01
Ni	0.04	4.56
L:O:I	6.81	

Table 3.32: Summary of the Results of Flotation Tests.

Type of Reagent	Weight (g)		Wt. %	
	Concentrate	Tailings	Concentrate	Tailings
Armac (C)	401.6	96.8	80.6	19.4
Armac (T)	396.8	101.7	79.6	20.4
Aerofloate 64	390.6	108.2	78.3	21.7

3.13 LIME-CLINKERING PROCESS

For the purpose of carrying out this test samples of the ore were crushed and ground to -355μM and then thoroughly mixed with lime to produce a mixture which satisfies the given ratio.

$$\frac{CaO - 3(P_2O_5+Al_2O_3)}{SiO_2} = 2.0 \quad \ldots\ldots\ldots\ldots\ldots\ldots (22)$$

This requirement must be met in order to have enough CaO for the Stoichiometric formation of ($2CaO.SiO_2$), ($CaO, 2P_2O_5$) and ($CaO.Al_2O_3.SiO_2$).

The mixed material so prepared was then poured into laboratory size Alumina silicate crucibles lined with carbon. The crucibles were then transferred into a gas fired furnace at a temperature of about 1350^{0}C where they were left for two hours until the mixture become molten. The molten mixture was further heated to allow for the reactions to take place. The furnace was then put off and the molten clinker air cooled before removal from the furnace.

The cooled clinker was crushed and ground to unlock the two phases and then subjected to magnetic separation to separate the two phases. In figure 3.2 is shown a simple block diagram of the various stages involved in this process. Full chemical analyses of the separated fractions were carried out and the results are given in tables 3.33 and 3.34. Electron photomicrographs were also taken of the separated fractions to aid in identifying the various structures in the fractions. X-ray spectra of the many phases in the clinker were also produced which helped in determining the composition of the phases.

Table 3.33:

Full Chemical analysis of the magnetic concentrate produced by the clinker process.

Constituent	Assay %
Fe_2O_3	31.2
Mn_3O4	38.3
Al_2O_3	6.2
TiO_2	0.43
K_2O	0.06
MgO	0.70
BaO	0.33
S	0.05
P_2O_5	0.02
Cu	0.01
Ni	0.01
CaO	12.7
SiO_2	8.3

Table 3.34:

Full chemical analysis of the Non-magnetic (Tailings) of the Lime-clinkering process.

Constituent	Assay %
SiO_2	39.6
CaO	39.1
Al_2O_3	13.2
TiO_2	0.3
K_2O	0.58
MgO	0.01
BaO	0.26
S	0.17
P_2O_5	0.76
Cu	0.03
Ni	0.02
Fe_2O_3	5.8
Mn_3O_4	7.6

CHAPTER FOUR

RESULTS AND DISCUSSIONS

4.1 CHEMICAL ANALYSIS

Table 3.1 shows the chemical analysis of the Mallam Ayuba Manganese ore. The manganese content of the ore is expressed in terms of Mn_3O_4 and the Iron as Fe_2O_3. From the table it can be seen that there are substantial amount of Iron, Aluminium and SiO_2 associated with the manganese ore. The percentage of the Silica represents both free Silica which occurs as quartz and chemically combined silica which occurs either with manganese or Alumina and Iron.

The following elements Calcium, Magnesium, Barium, Potassium, Phosphorous and Titanium occur as minor elements while chromium, copper, Nickel and sulphur occur in trace quantities. The amount of material Lost On Ignition (LOI = 11%) is substantial due to the presence of volatiles like chlorides and zinc which were detected by SEM (Figure 4.6) but not during the chemical analysis and most importantly water of hydration.

Based on this chemical analysis, the ore does not meet the specification of a metallurgical grade manganese Ore (Table 1.2). This is because the ore assays high silica (36.4%), Alumina (11.0%) and low manganese (Mn_3O_4) (23.0%). However, the sulphur (0.01%) and Phosphorous (0.04%) assays

are within the acceptable range. It is therefore clear that there is a need for the ore to be beneficiated before it could be used for ferromanganese production.

4.2 *SIZE/ASSAY ANALYSIS*

Table 3.6 gives the size/Assay analysis of the ore in which, each given size fraction was assayed for Mn, Fe and SiO_2. Tables 3.2 to 3.4 give the distribution of each of these elements in each size fraction and Table 3.5 gives a summary of the cumulative weight percentage and cumulative percentage distribution for the various elements. Figures 4.1 to 4.3 are the graphs of the percentage distribution against cumulative percentage weight.

From these results, it is clear that Mn, Fe and SiO_2 are equally and uniformly distributed in all the size fractions which suggest that to achieve optimal concentration of the manganese minerals by mere crushing and sizing/classification will not work. For example, from the results in table 3.6 it is clear that any attempt to reject material of size range greater than 1000µm will result in losing up to 50.8 % of the total manganese content. This represents a recovery of only about 50% which is not good enough. Hence, waste rejection technique will not be feasible in this case as liberation will not be achieved at as coarse a size as possible. This enterpretation is also clear from (Figures 4.1 and 4.2) where there is approximately a linear relationship for both SiO_2 and

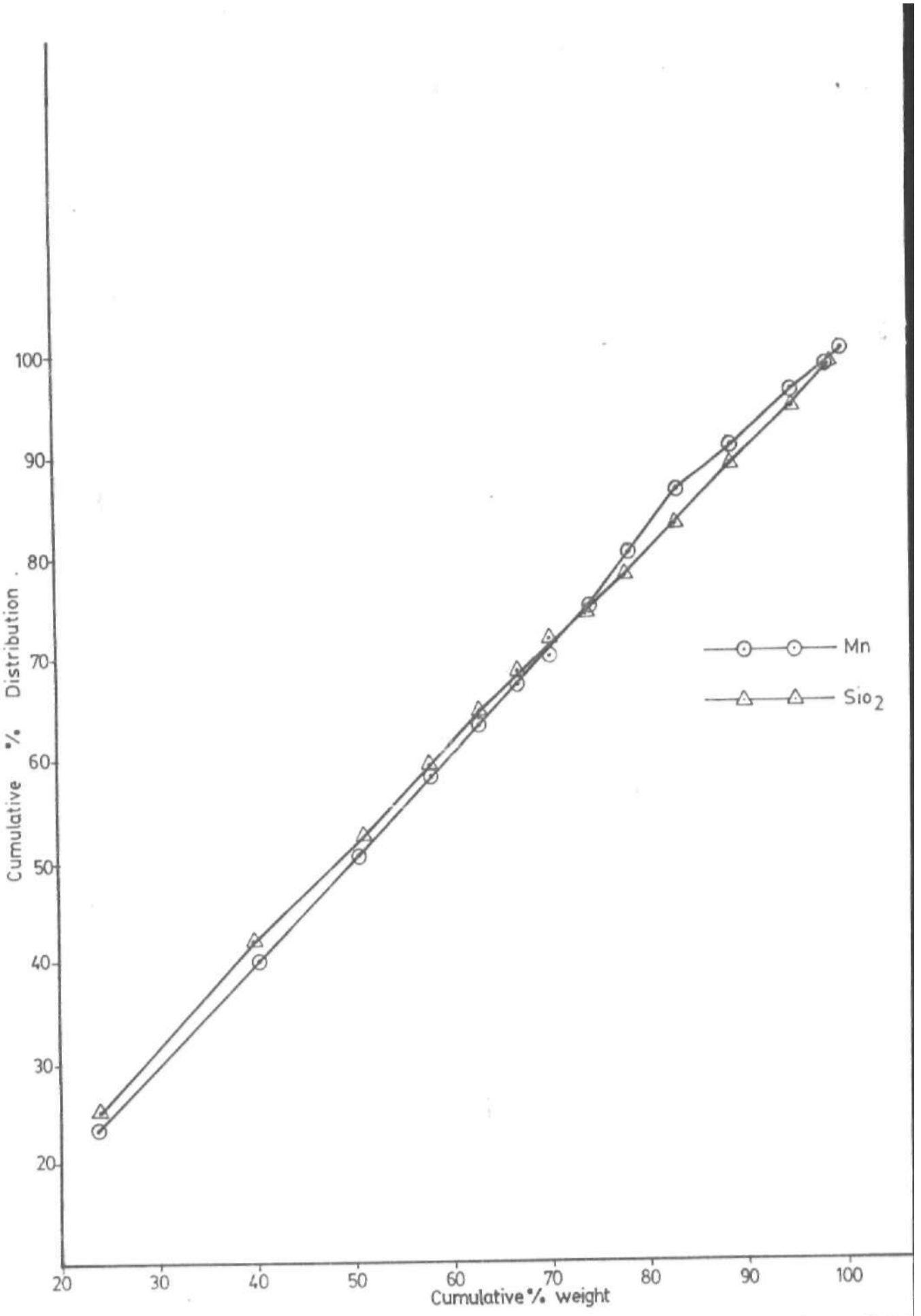


FIG4.1 – A plot of cumulative distribution against cumulative % weight for Mn & S_iO

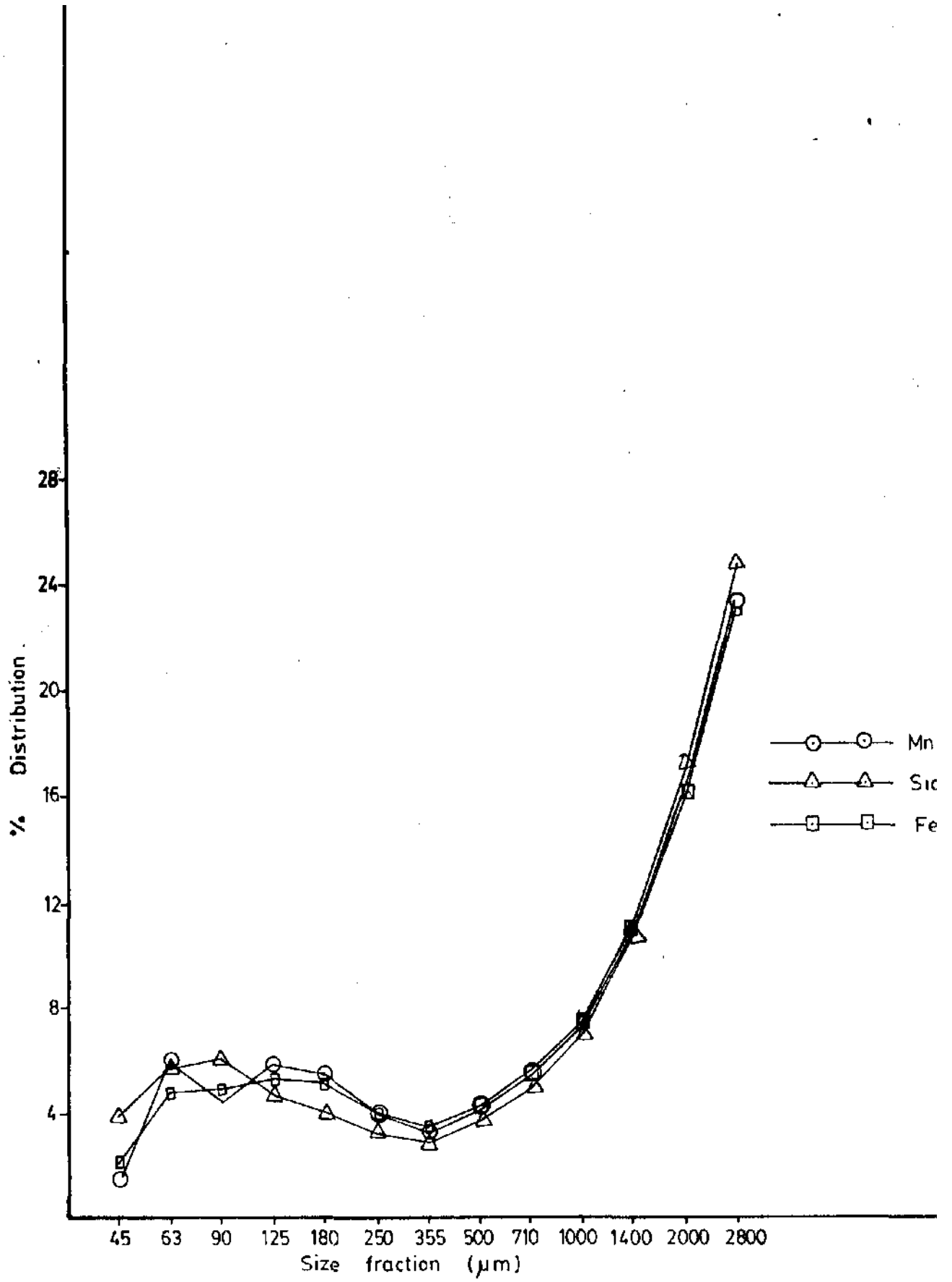


FIG 4·2—Plot of %distribution against particle size for Mn, S_1O_2&Fe

Mn in the plots of percentage distribution against cumulative percentage weight. Any attempt to reject some amount of SiO_2 at the coarser size fractions would result in the loss of about the same amount of manganese.

4.3 MINERALOGICAL INVESTIGATION

Table 3.7 shows the qualitative mineralogical composition of the ore. The Table is derived from the results of XRD and SEM. From this table it is clear that the major manganese bearing mineral in this ore is spassartine/almandine. This mineral stoichiometrically contains at most 33% manganese by composition, while iron, Alumina and SiO_2 account for the remaining percentage. The next in abundance of the manganese bearing mineral in the ore after spessartine is psilomelane which is an isomorphous solid - solution of cryptomelane and Hollandite. This mineral however occurs only in minor amount. In addition to these two there are trace amounts of other manganese bearing minerals like lithiophorite, manganon, manganon cemenite and galaxite. All these trace manganese bearing mineral put together account for less than 5% of the ore.

Silica is the main gangue and occurs both as chemically combined in the spessartine/almandine and as free silica (Quartz).

Figure 4.3 is the XRD diffraction pattern of the ore. From this Figure, it is clear that there are only three

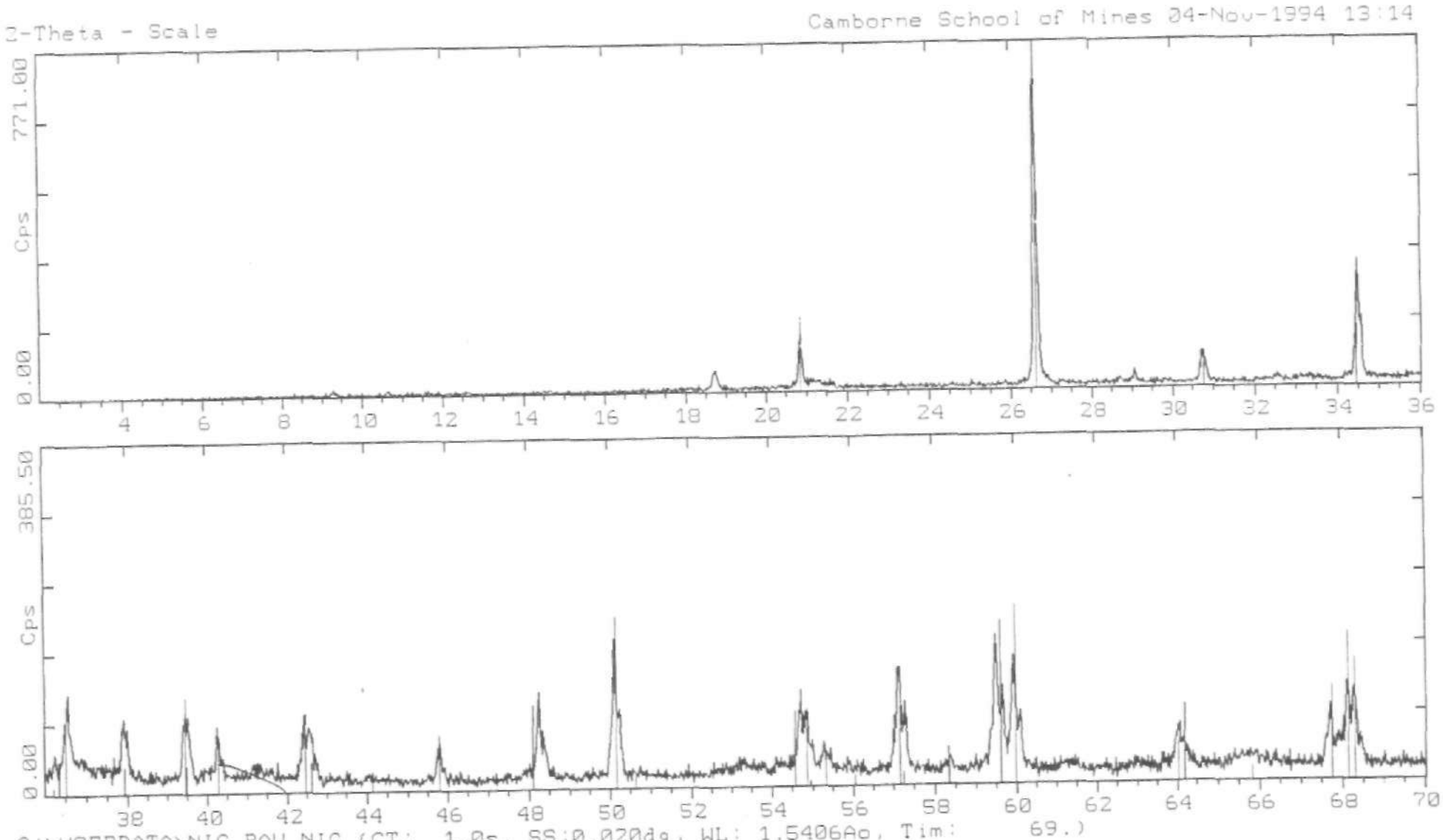


Figure 4.3: XRD Diffraction pattern of the Ore.

minerals in the ore spessartine, Galaxite and Quartz. The reason being that the XRD machine cannot detect any minerals of composition below 5% and most of these minerals in the ore occure in trace amounts.

Plates i, ii, iii, are the SEM photomacrographs of the ore taken at different magnifications. From these micrographs it can be seen that a wide range of phases could be identified which were not detected by XRD. The phases identified include psilomelane and Hollandile identified in the photomicrograph by numbers 1 and 3 respectively in Plate i. Also it is clear from these Figures that the mineral phases are finely dessiminated and intermittently intergrown with each other, which implies that very fine grinding is necessary in order to achieve any degree of liberation. Also looking at micrograph in Plate iii - the back scattered election image (BEI) of the sample of the ore. The ore is highly porous, the high porosity of the ore is exhibited by the presence of pores.

The X-rays spectra (EDX) of some of the mineral phases are given in Figures 4.4 to 4.7. Except for Figure 4.7 which is clearly a spectrum of Hollandite ($BaMnO_5$), all other spectra are too complex to be identified. This is because, the size of most of the minerals, that is their crystal size is less than 10μM and the diameter of the generation of the X-rays for SEM is about 10μM which means that some of the X-ray spectra are for more than one phase. The spectrum is generated

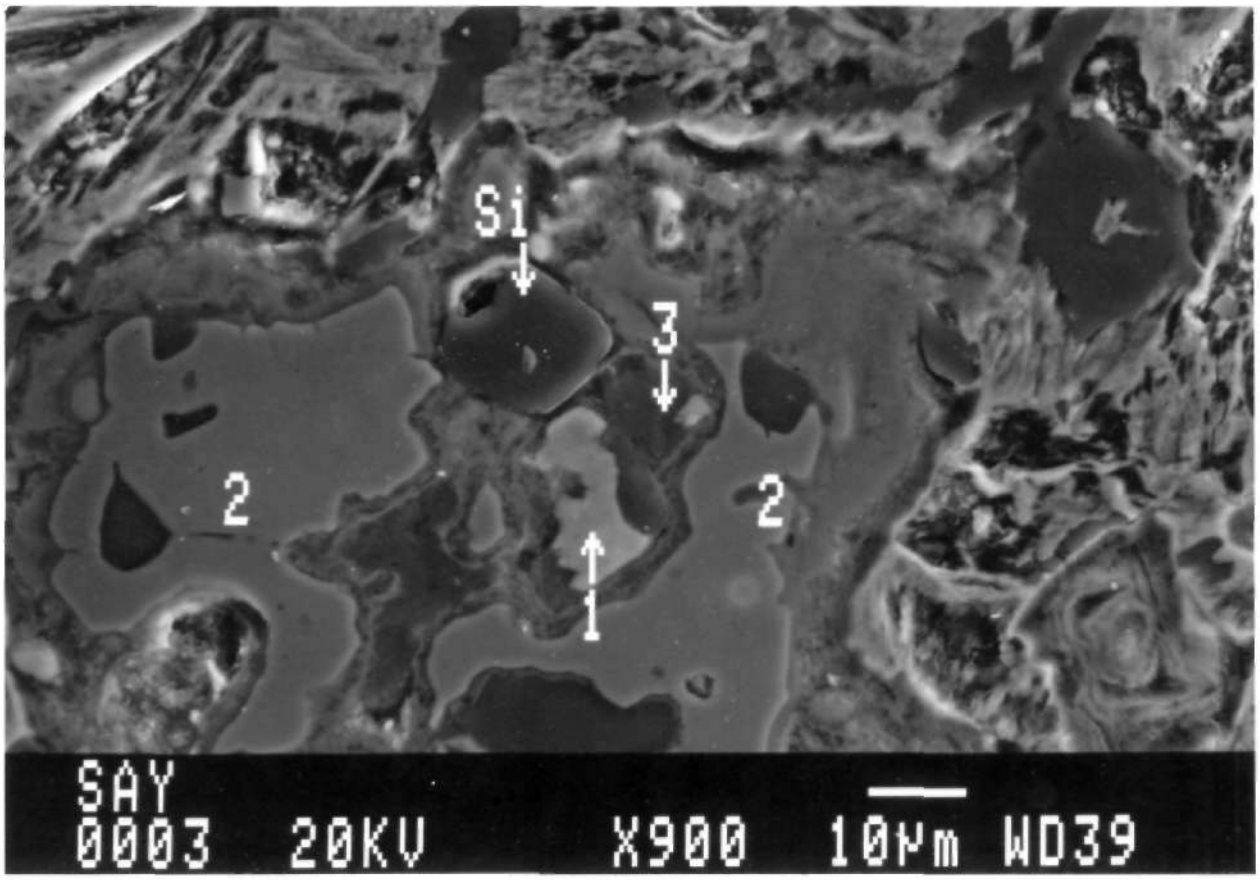


Plate I: Electron Photomicrograph of the ore in which some mineral phases were identified as follows:

1 - Psilomelane

2 - Spessartine/almandine

3 - Hollandite

4 - Quartz

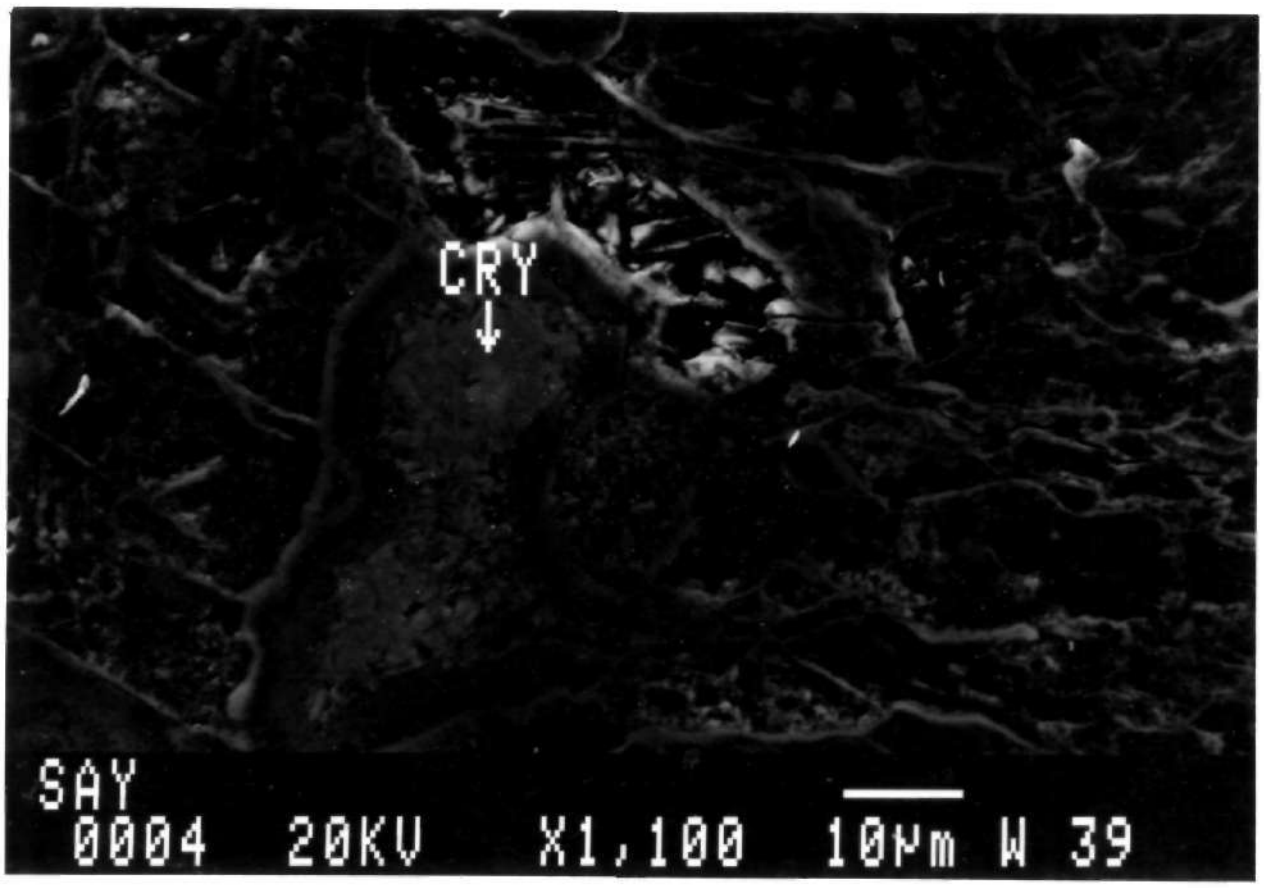


Plate II: Highly magnified Electron Photomicrograph of the lump sample of the ore showing a phase of hollandite mineral. This particle is approximately about 50µm.

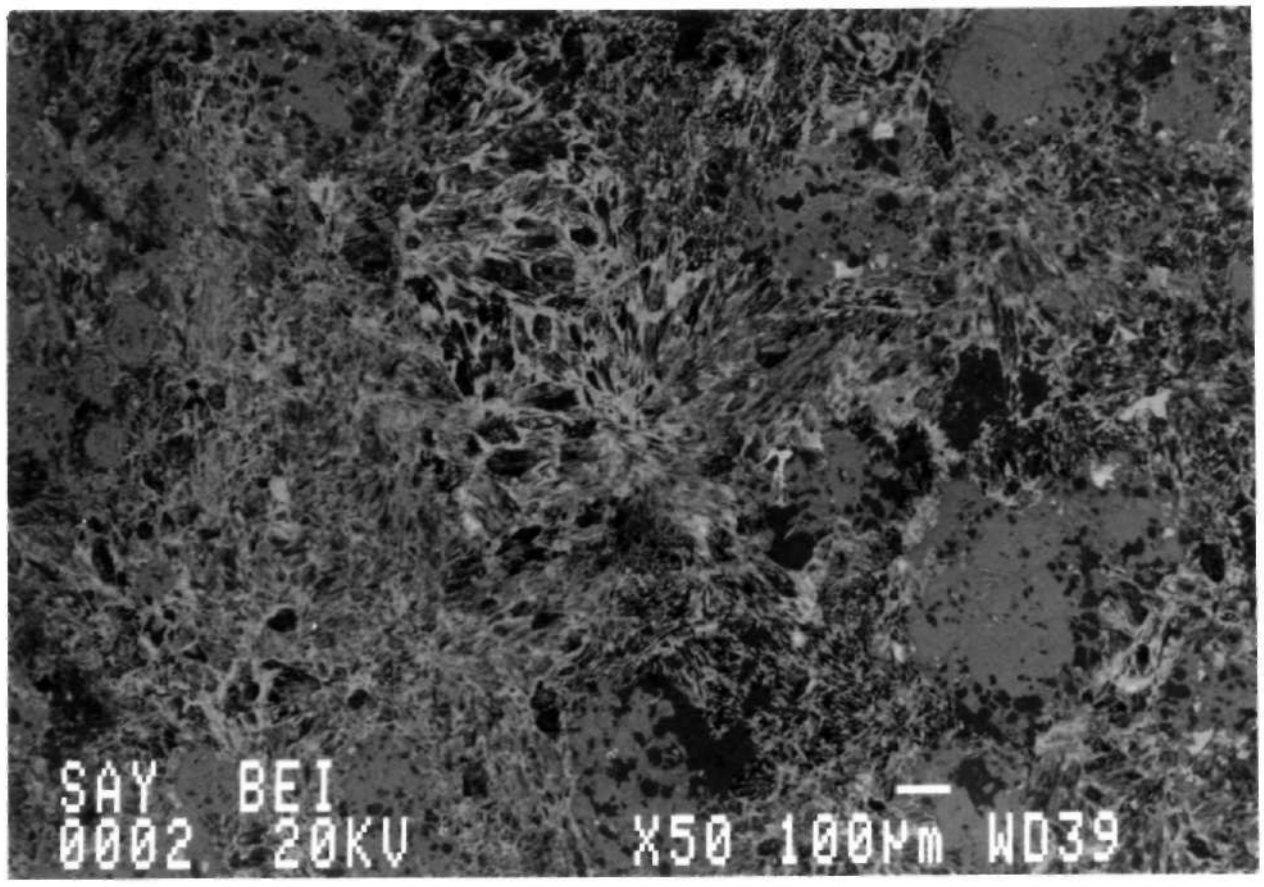


Plate III: Scanning Electron Photomicrograph of the Backscattered Electron Image [BEI] of the lump sample of the ore showing:

Light phase - Psilomelane

Grey Phase - Spessartine/almandine

Dark Phase - Quartz

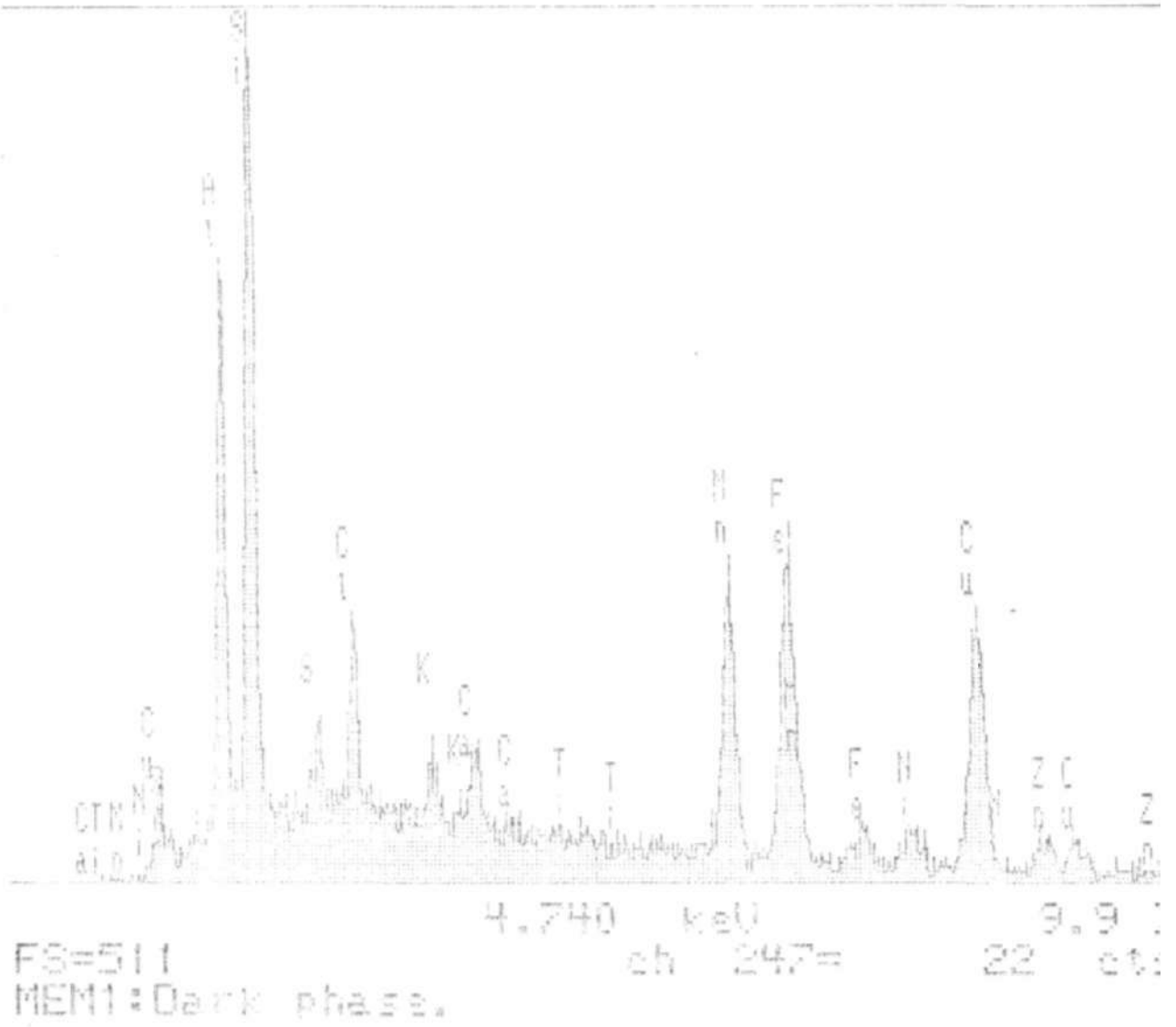


Figure 4.4: X-ray Spectrum of a complex mineral phase in the ore which could not be identified.

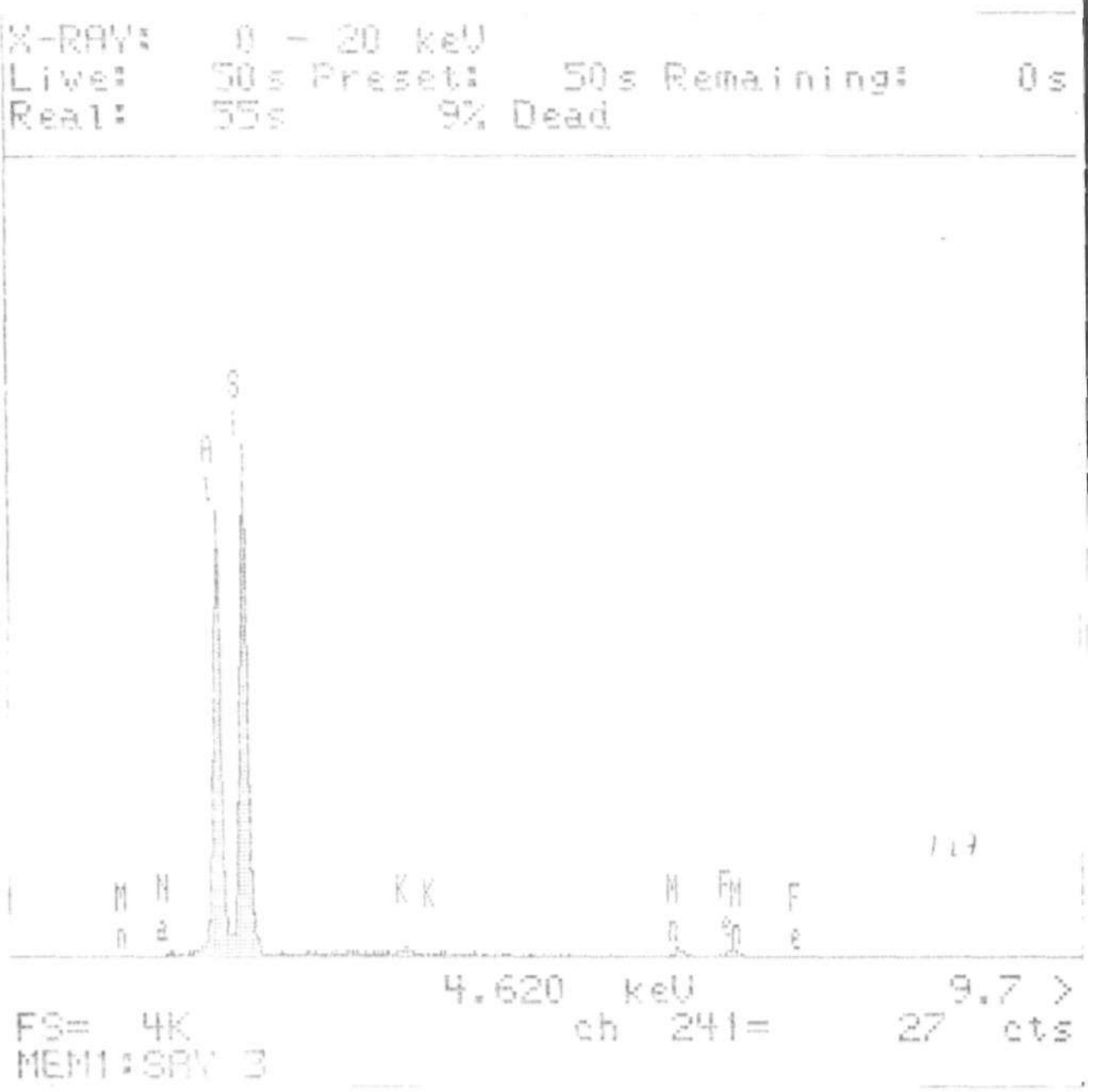


Figure 4.5: X-ray Spectrum of another complex mineral phase in the ore.

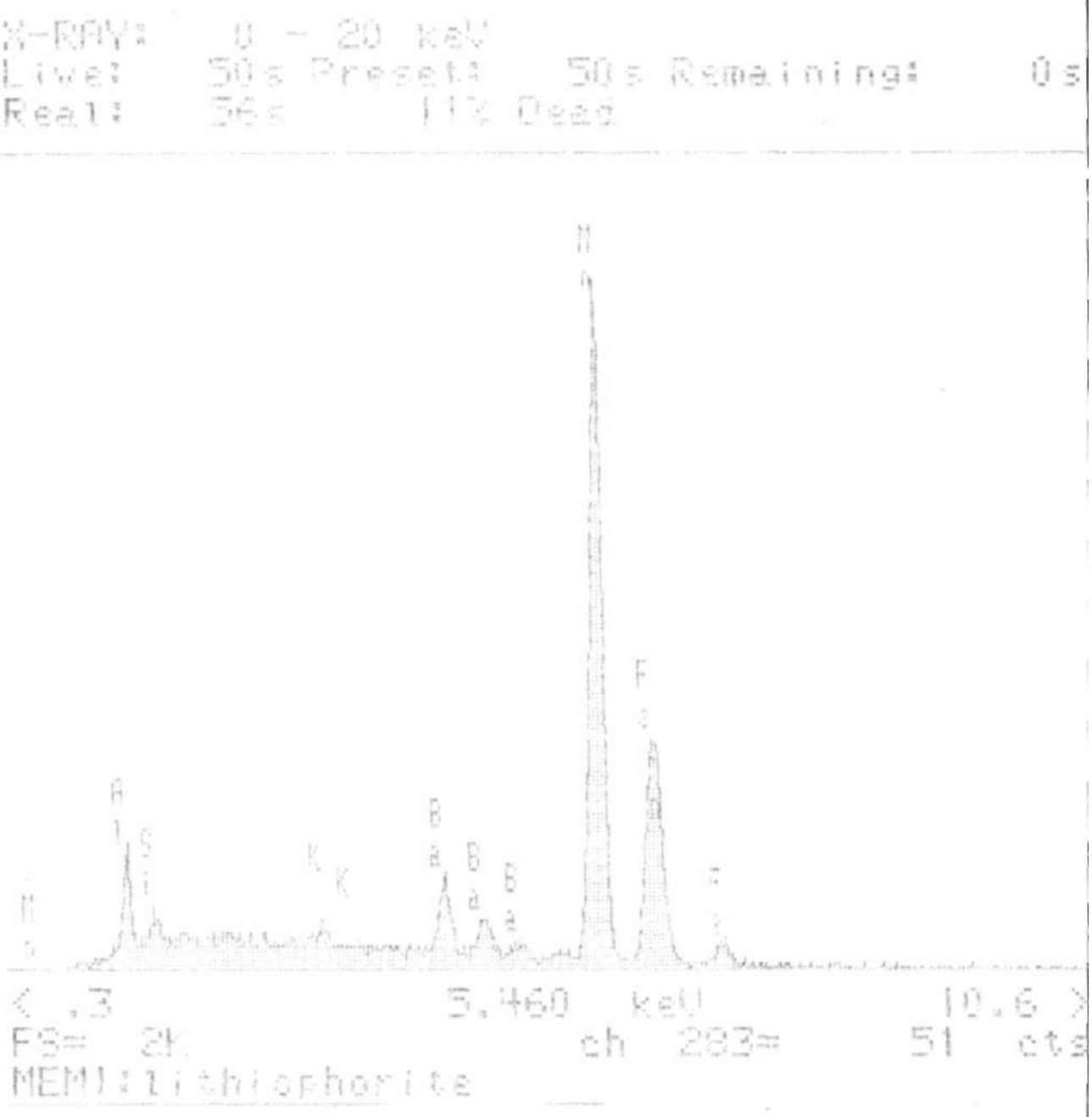


Figure 4.6: X-ray Spectrum of a mineral phase identified to be Lithiophorite.

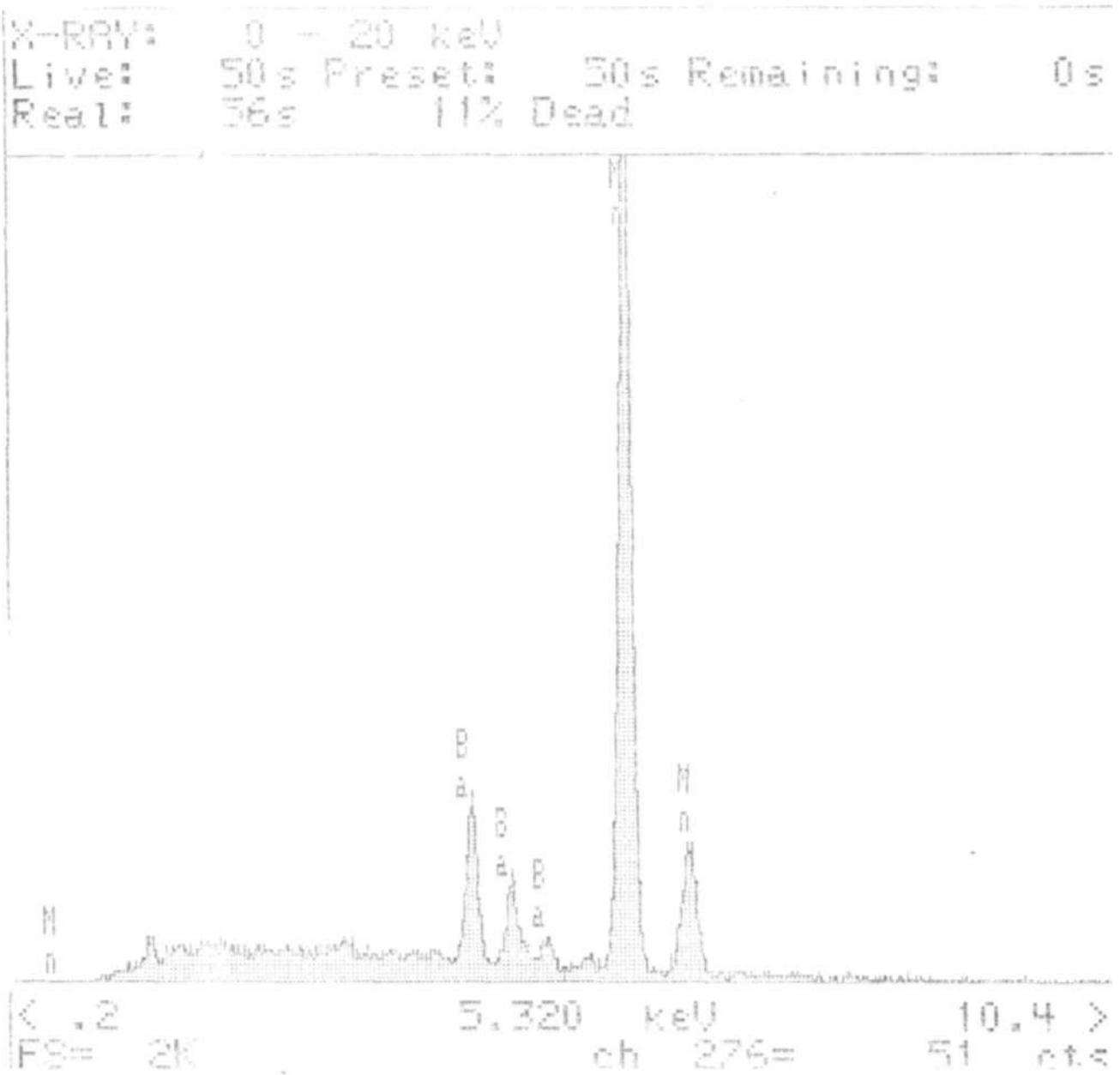


Figure 4.7: X-ray Spectrum of another mineral phase identified to be Hollandite

$\underline{\Gamma}(Ba, Mn)(Mn_8O_{16}(OH)_4\underline{]}$

from a volume with diameter of about 5µM, hence each spectra may present an average of several crystals.

In order to fully understand the complex mineralogy of the ore which is a crucial factor in liberation and separation processes; representative sample of the ore were ground and XRD analysis of each size fraction was carried out. Table 3.8 shows the various size fractions and the minerals detected in each size fraction. From this table most of the minerals present in the ore were Identified and the XRD diffraction patterns are given in the appendix 1.

4.4 HEAVY - LIQUID TESTS

Tables 3.9 to 3.12 are the results of the heavy liquid tests carried out. Table 3.9 gives the distribution of Manganese in the feed, sink and float at size fractions ranging from 1000µM + to +45µM. Tables 3.10 and 3.11 give those of Iron and silica. Table 3.12 is a summary of the distribution of the three elements into the sink and float fractions for all sizes.

From Table 3.9, it is evident that more of the manganese is distributed into the sink than in the float at all the size fractions. This is because the manganese bearing minerals are heavier than the gangue minerals. As for silica (Table 3.10), the same trend was observed as with the manganese. This was rather unexpected because ideally, silica being lighter than manganese minerals, should have all been collected in the

float. The interpretation of this is that the most of the silica in the ore does not occur as free silica but as compound with other elements. These compounds may be as heavy as the manganese bearing minerals.

Table 3.11 shows the distribution of Iron into the sink and float and reveals that a substantial proportion of it is distributed into the sink than in the cases of manganese and silica. This is very interesting as the assay of ore gave the percentage of Iron in it to be about 14.8% Fe_2O_3 while its mineralogy revealed that Iron compounds occurred in trace amounts (Table 3.7). The large proportion of Iron must have come from the compound Almandine Manganon [$(Fe, Mn)_3 Al_2(SiO_4)_3$] which is a manganese bearing mineral in which some of the manganese has been substituted by Iron.

Figures 4.8 and 4.9 are the graphs of percentage distribution against the size fractions for Mn, Fe and SiO_2 into the sink and float. A careful examination of these graphs will reveals that the Mn, SiO_2 and Fe peaks occur at the same size fractions showing that all the three elements occur in the same proportion hence as a compound.

4.5 LIBERATION STUDIES

The liberation studies were conducted using two separation techniques: Heavy liquids and the mozley laboratory separator. The data from the heavy liquids were analysed by plotting density and elementary assay curves while those from the mozley separator were analysed using release

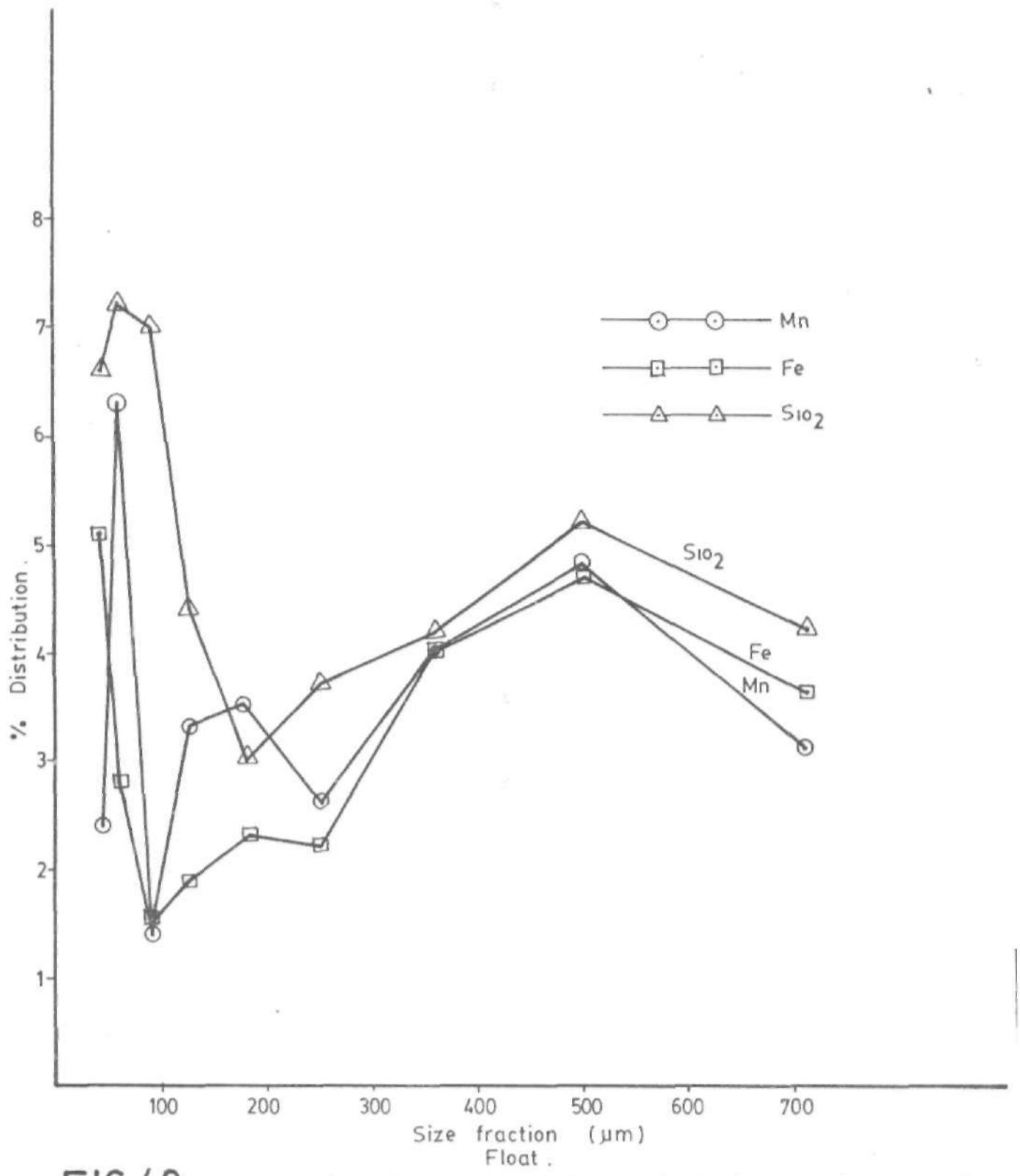


FIG.48— A Plot of % distribution against size fraction in the float for Mn, S_iO_2 & Fe.

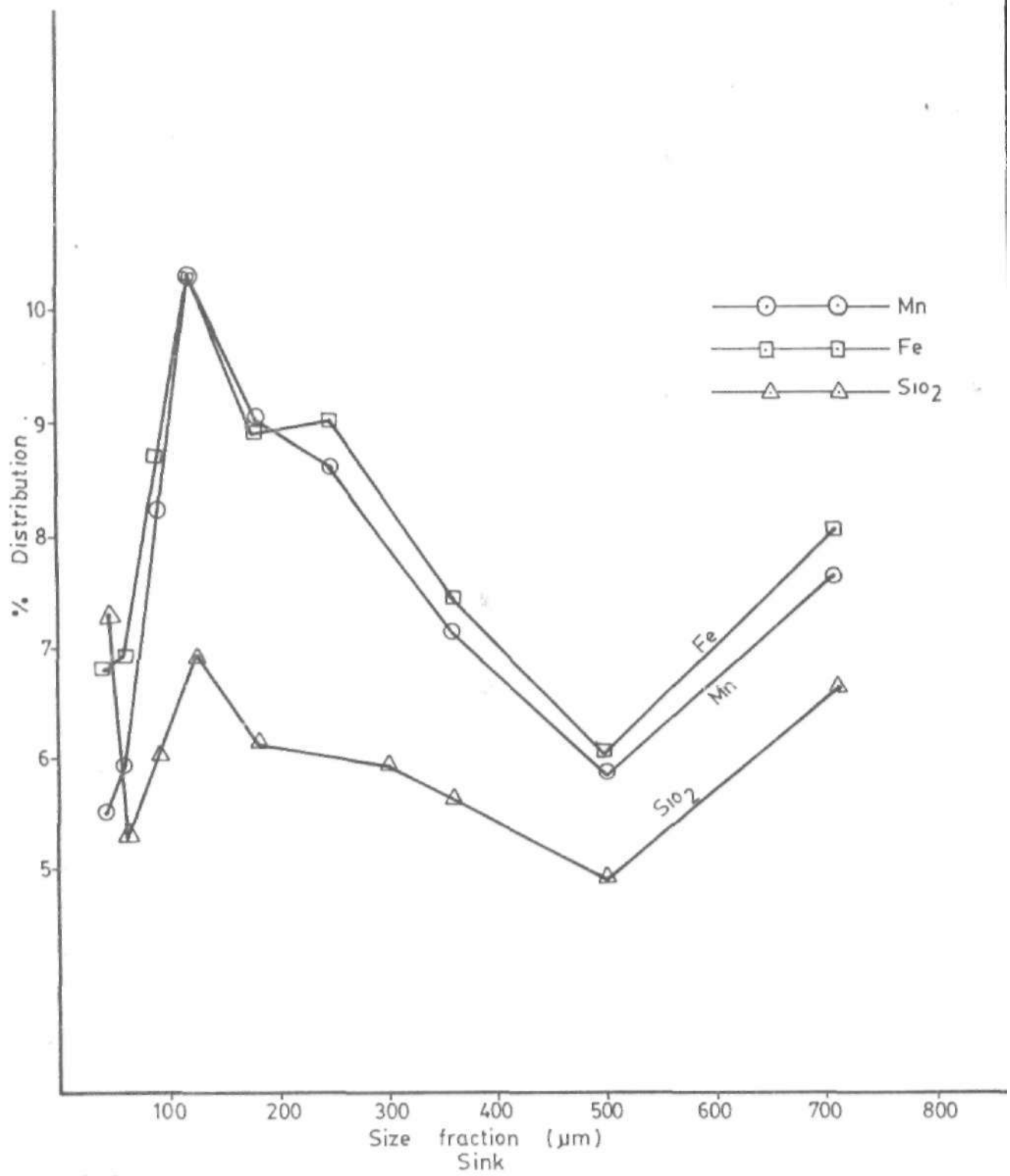


FIG.4·9 - A Plot of % distribtion against size of fraction for Mn, Fe & S_iO_2 in the sink fraction.

analysis technique.

For the liberation study using heavy liquids, a single heavy liquid was initially used from which only a sink and a float were obtained which were analysed for heavy and light minerals the results of which are given in Tables 3.9 to 3.12. From these results it is impossible to draw conclusions as regards the liberation of the minerals in the ore. Therefore, a full scale sequential tests involving liquids of different densities was undertaken. The results of these tests are shown in Table 3.13. These results were used in plotting density and elementary assay curves which are given in Figures 4.10 to 4.12 respectively.

A careful examination of these curves and comparing them with the theoretical density and assay characteristics curves (Figures 2.5 to 2.10) indicates that there is very little liberation of the manganese minerals at the various size fractions considered. This can be seen by a thorough examination and careful comparison of the experimental curves (Figures 4.10 to 4.12) which shows that, they all match theoretical curves for partial liberation cases given in Figures 2.5 to 2.8. This is expected because the mineralogical studies have shown that there is a high degree of interlocking between the constituent minerals of the ore. Also the mineralogical studies have shown that, the valuables (Manganese bearing Minerals) and the gangue are finely dessiminated with grain size sometimes less than 10μm and

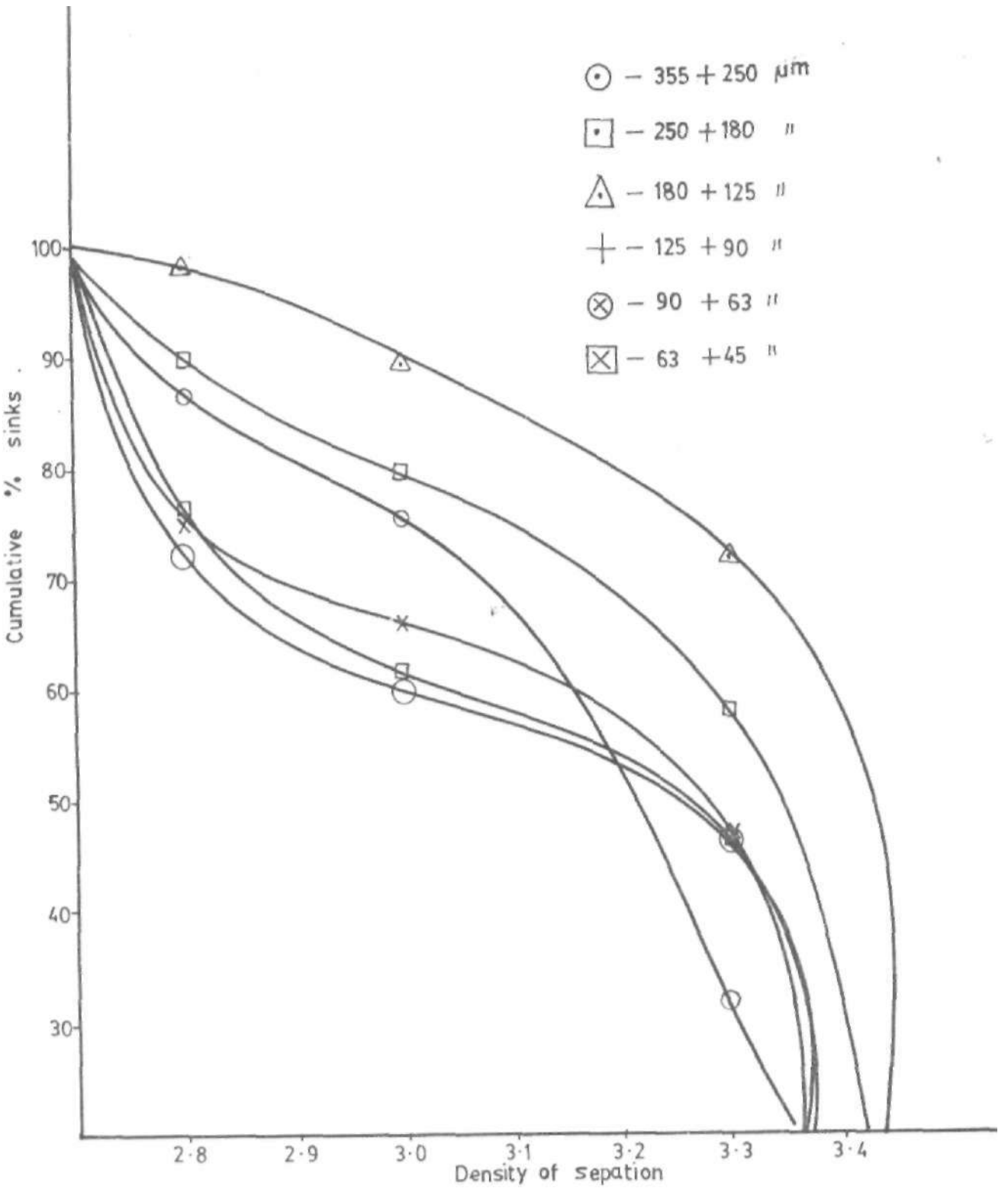


FIG 4.10 — Density curve for manganese

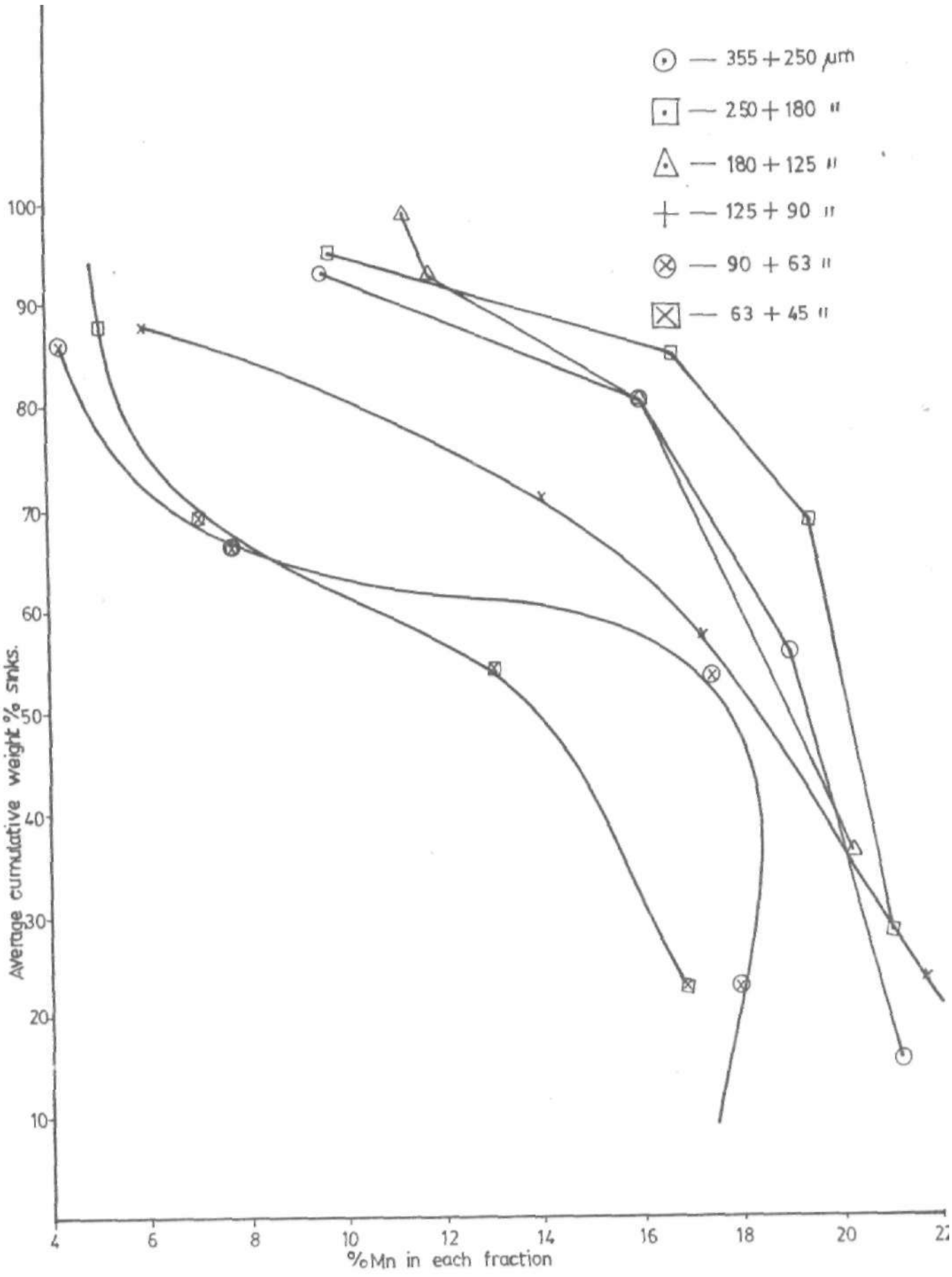


FIG. 4·11—— Characteristic curve for manganese

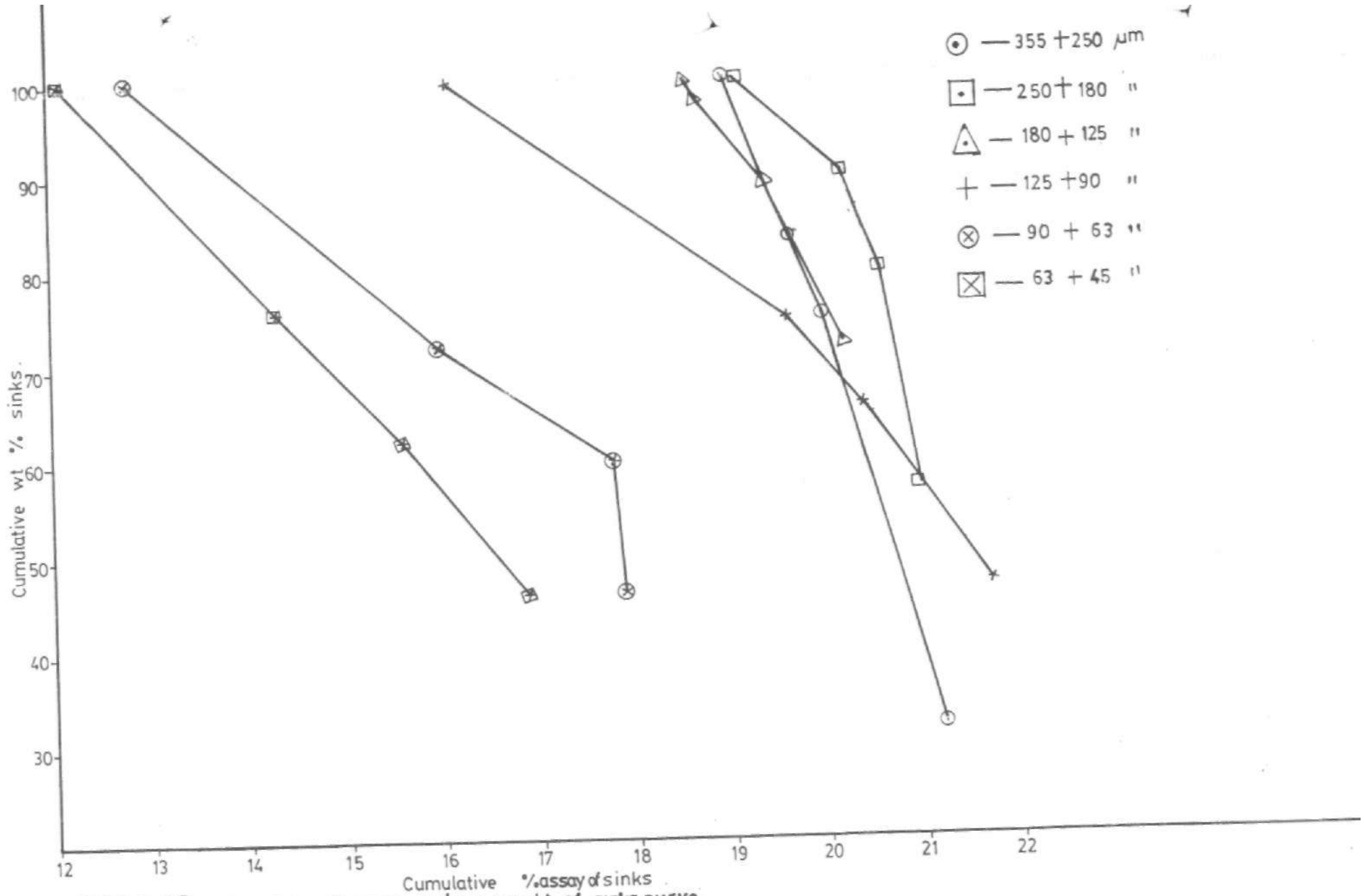


FIG 4.12— Cumulative % assay against weight of sinks curve.

intermittently intergrown with each other.

Tables 3.14 to 3.16 are the release analysis results of the data obtained from the mozley laboratory mineral separator. Figures 4.13 to 4.15 give the Grade - Gradient curves obtained by plotting these results.From a detailed examination and comparison of these curves with theoretical release analysis curves (Figures 2.4), it is clear that the experimental curves obtained for all the three elements/compounds given by experimental curves (Figures 4.13 to 4.15) matched the theoretical curves C and E in Figure 2.4 which are for partial liberation cases. This further confirms the results of the heavy liquid tests on liberation studies carried out and reported in the foreging section.

In order to varify the results of both the heavy liquid and Release Analysis Technique, SEM analysis was carried out in which photomicrographs were taken of the samples under investigation. The photomicrographs are given in Plates iv to x. It can be seen that in some of the micrographs there are more than 60% locked particles indicating that no substantial degree of liberation could be achieved using conventional techniques.

With reference to Plate v to vii, it will be seen that even though most of the mineral particles in the photomicrograph are of particle size range 50µm to 100µm, they constitute more than one phase. In the micrograph of plate viii and ix dark mineral phases can be observed to be the only

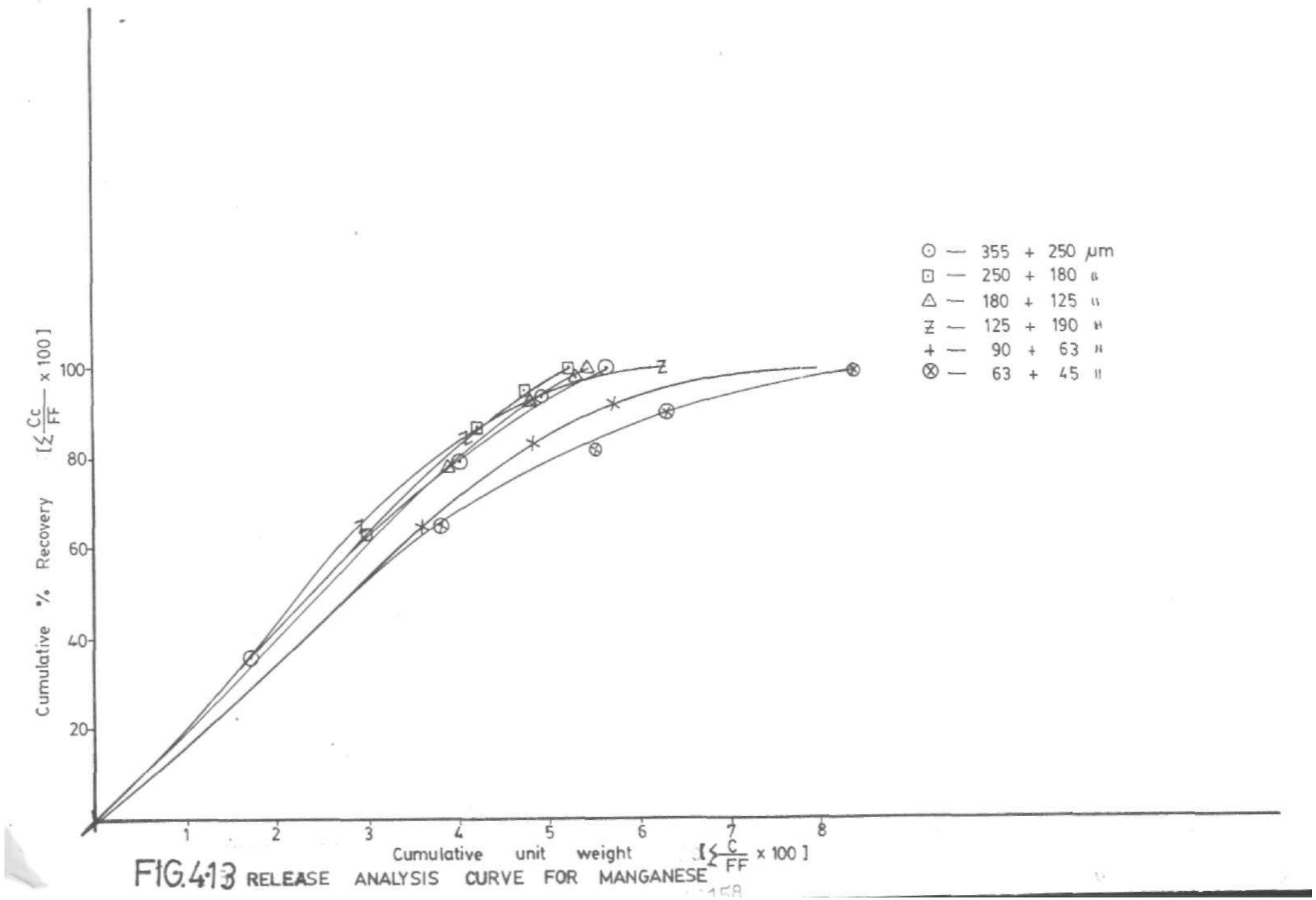


FIG.4.13 RELEASE ANALYSIS CURVE FOR MANGANESE

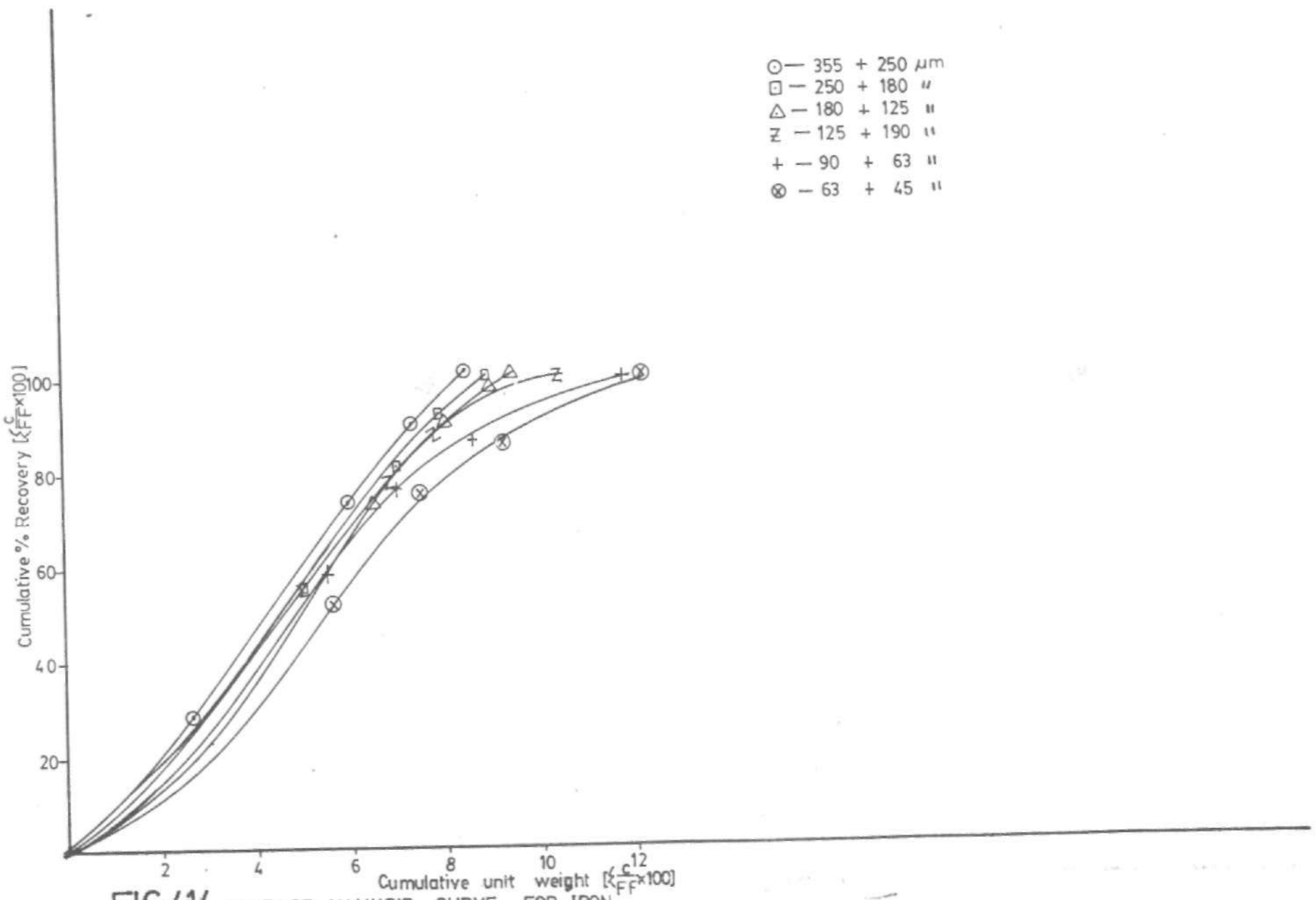


FIG 4.4 RELEASE ANALYSIS CURVE FOR IRON

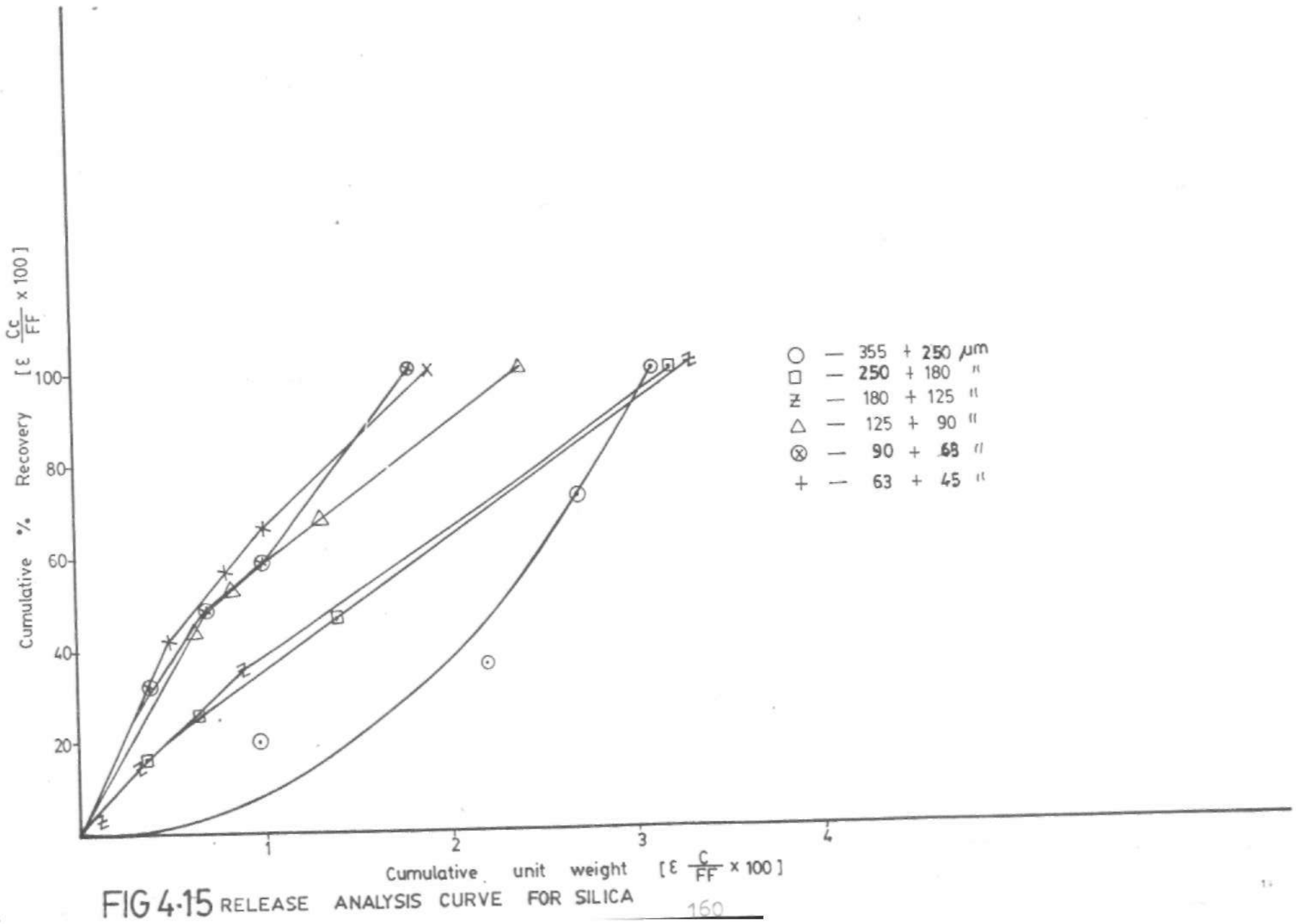


FIG 4·15 RELEASE ANALYSIS CURVE FOR SILICA

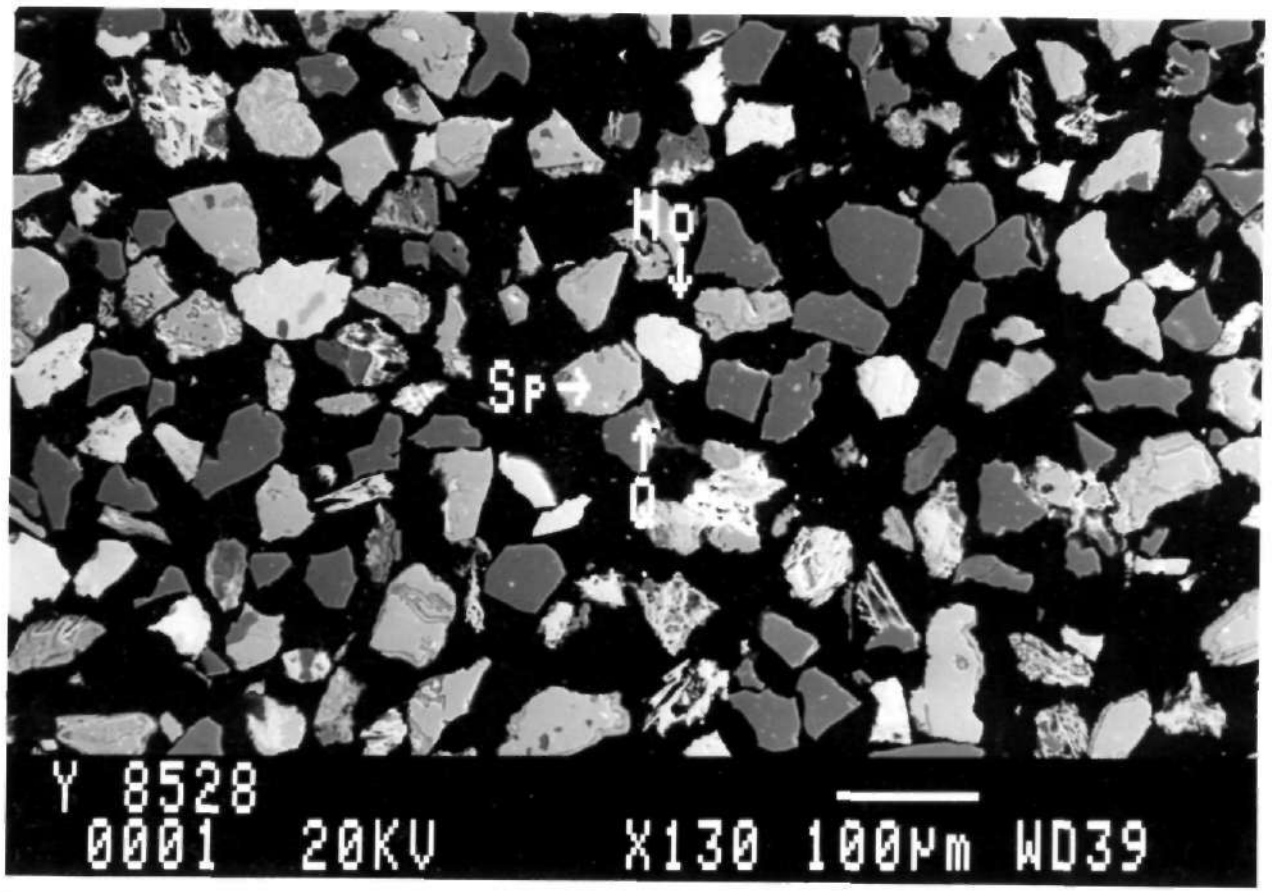


Plate IV: Electron Photomicrograph of the sinks (+3.0) of the simple sink-Float heavy liquid tests at particle size fraction - 63 + 45µm showing

Ho - Hollandite

Sp - Spessartine/almandine

Q - Quartz

NOTE: The Quartz has been liberated while Hollandite and Spessartine/almandine are still locked up.

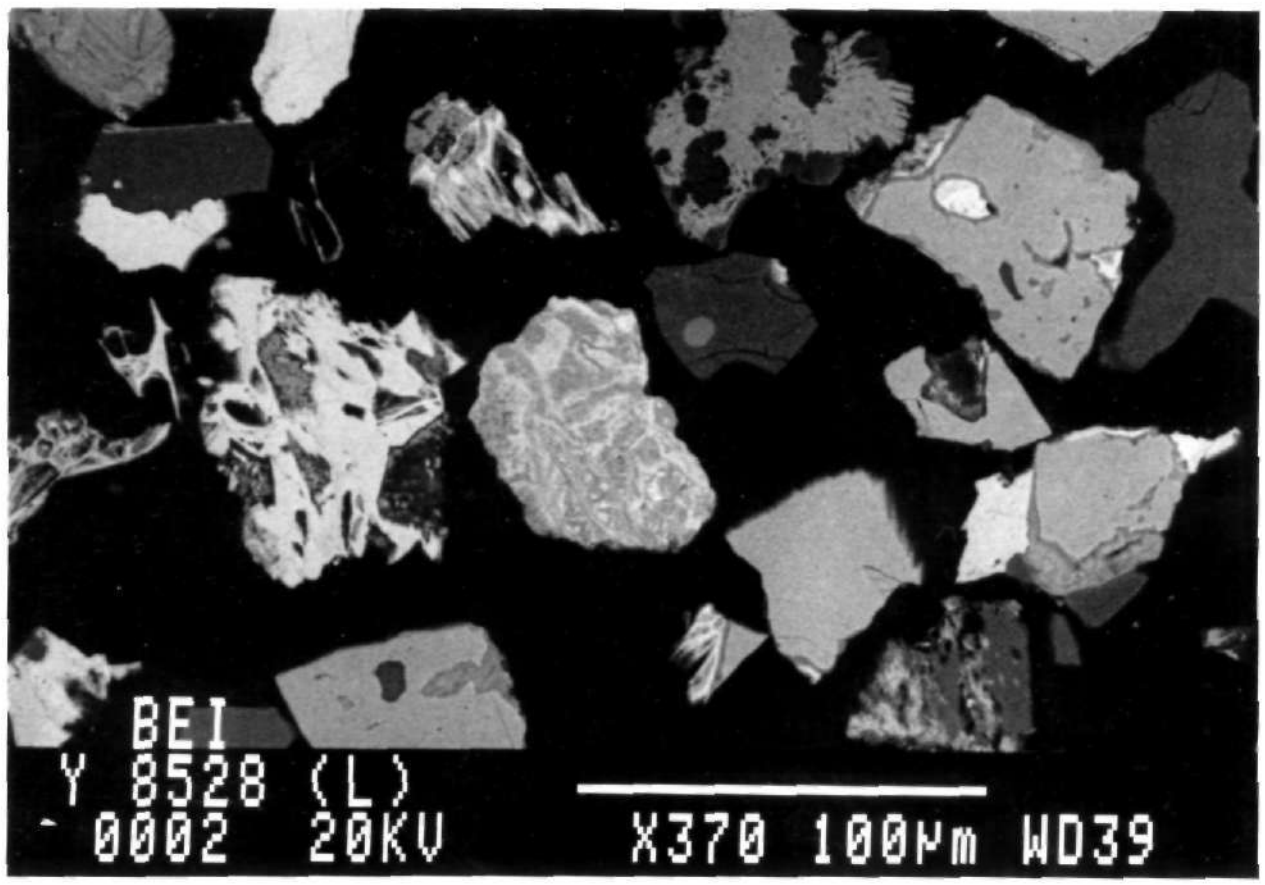


Plate V: Backscattered Electron Image (BEI) of the sinks (+3.0) of the heavy liquid tests showing extreme fineness texture and Mineral intergrowth which makes complete liberation near impossible, using conventional techniques.

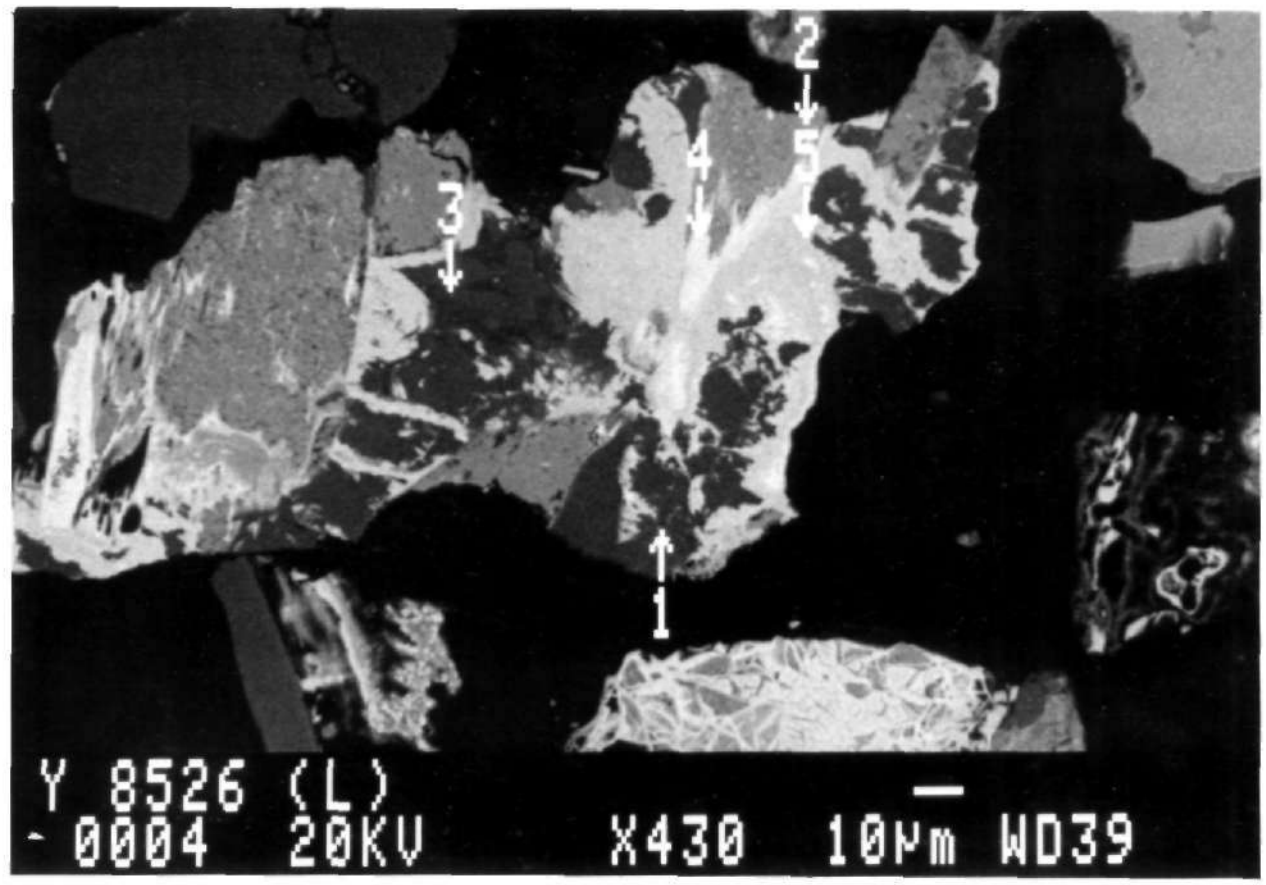


Plate VI: Electron Photomicrograph of the ground ore (-125 + 90µm) showing 100% locking of the Minerals in which

1	-	Dark Phase	-	Quartz
2	-	Light grey phase	-	Lithiophorite
3	-	Hematite	-	Fe_2O_3
4	-	Manganon	-	(Fe, Mn)O

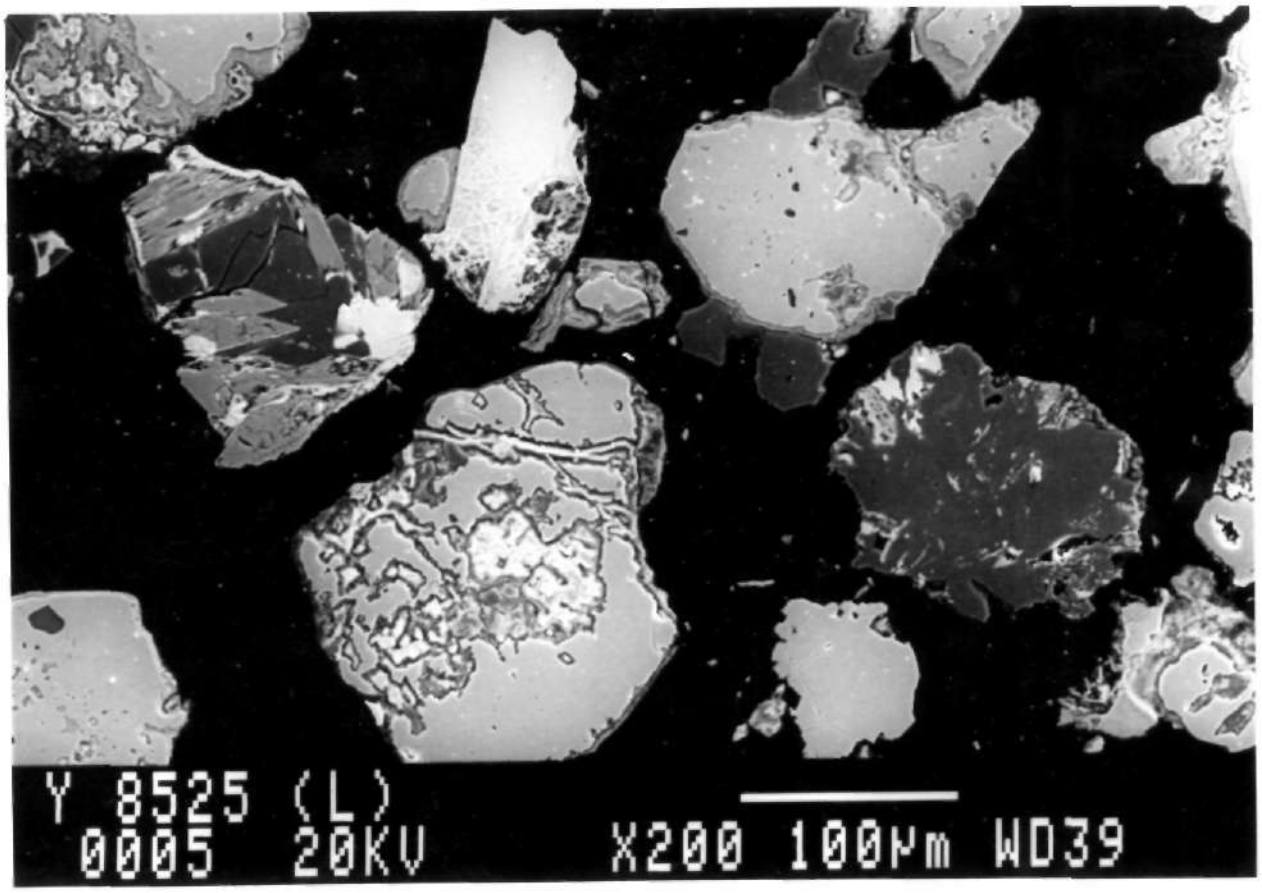


Plate VII: Electron Photomicrograph of the ground ore (-100µm) before Separation showing higher degree of interlocking. The light phase is the Manganese bearing minerals while the dark phase is the Quartz.

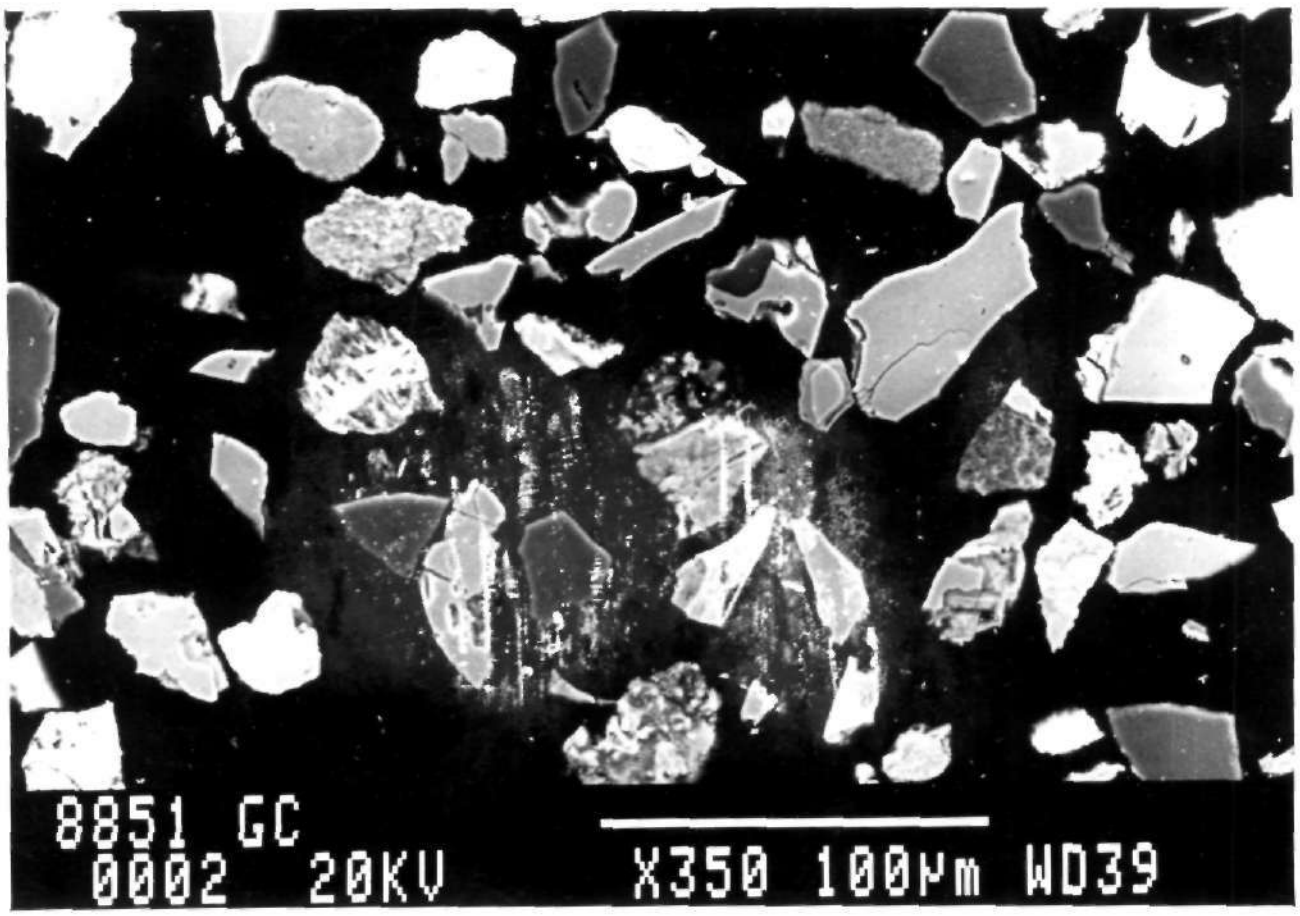


Plate VIII: Electron Photomicrograph of the gravity concentrate (shaken table) at -45µm. Showing higher degree of interlocking of the Manganese bearing minerals and complete liberation of the Quartz.

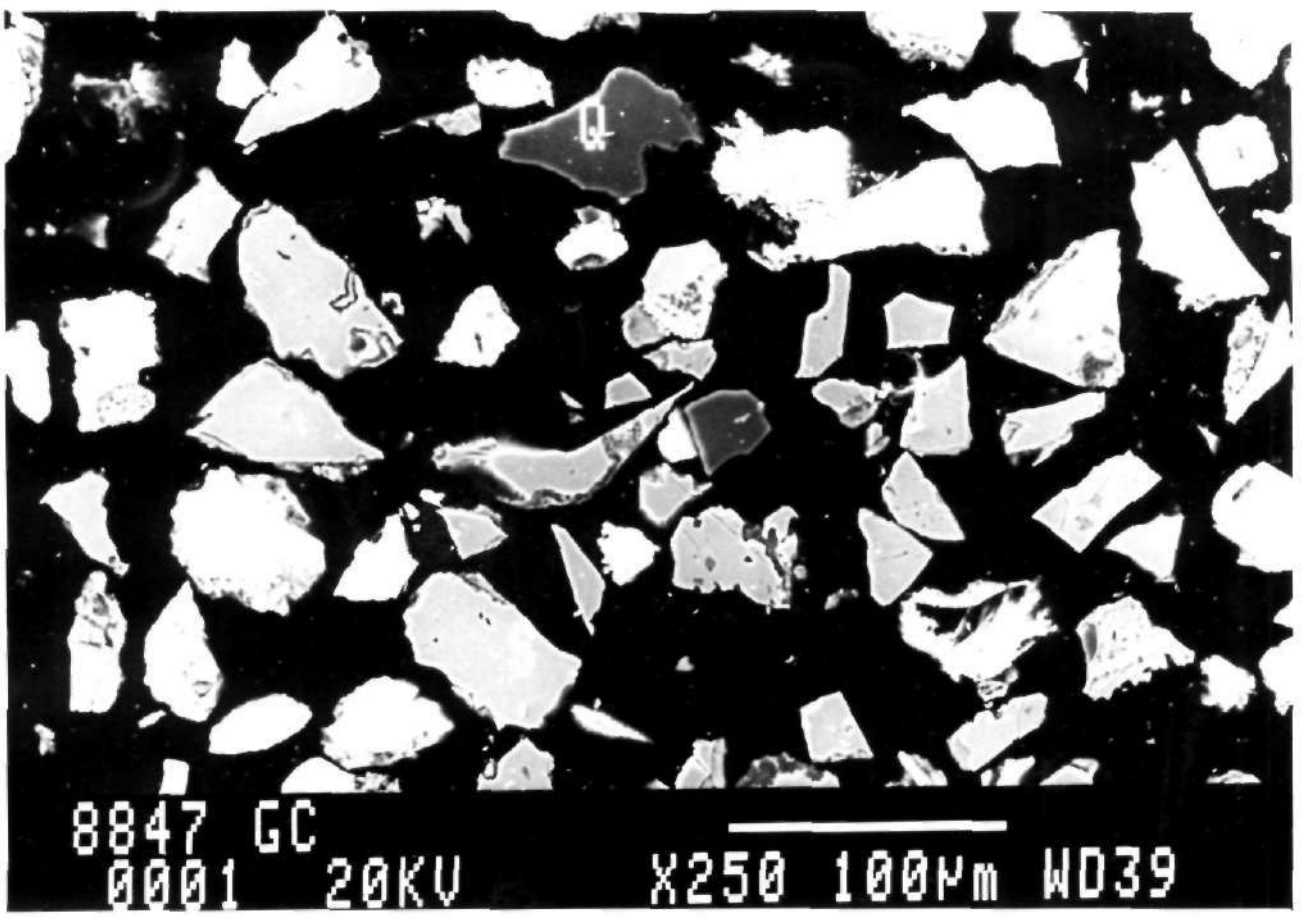


Plate IX: Electron Photomicrograph of the gravity concentrate (Mozley Separator) showing that most of the Free silica has been removed and the concentrate contained mostly manganese bearing minerals.

Q - Quartz

S - Spessartine/almandine

P - Psilomelane

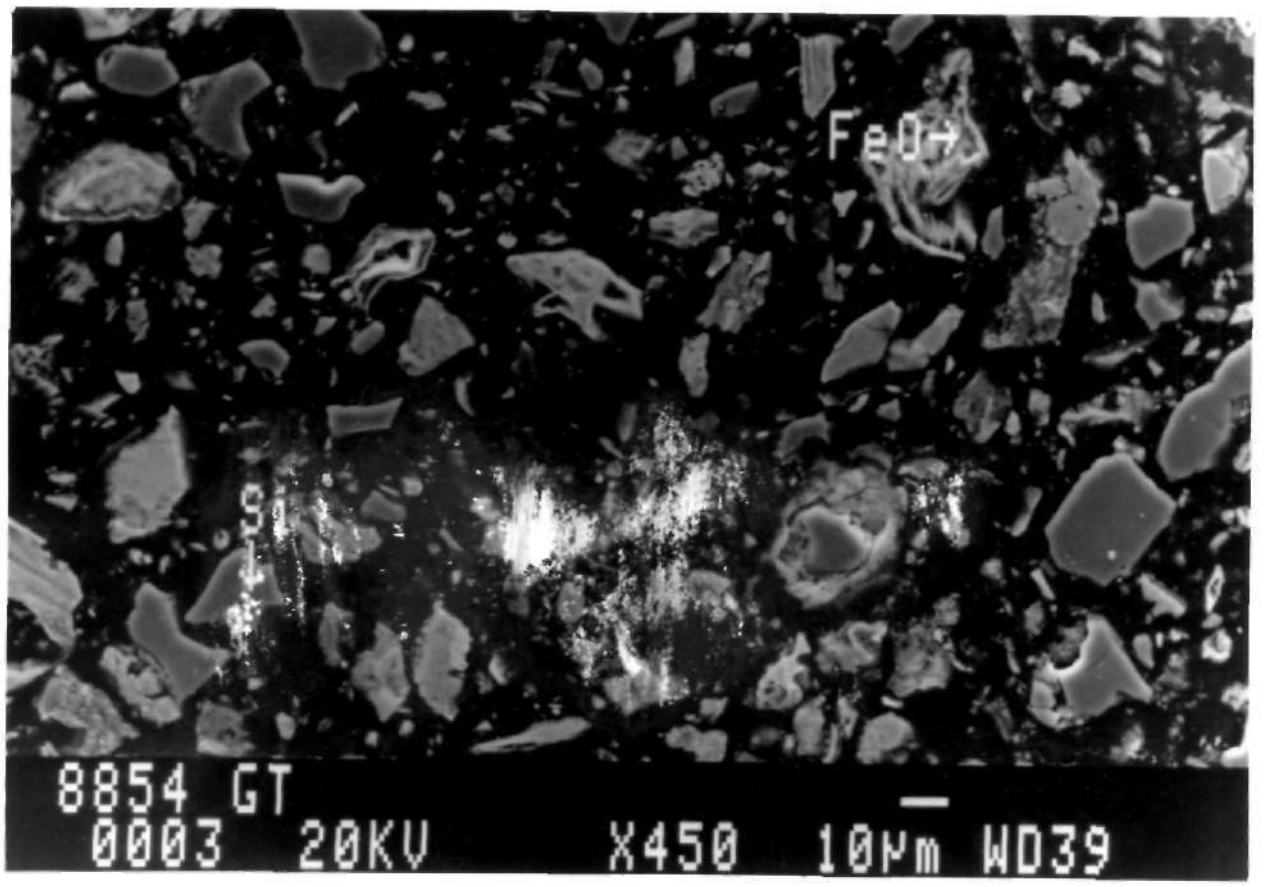


Plate X: Electron Photomicrograph of the Gravity Tailings (Mozley Separator). Showing that the tailings constitute mainly of free silica (Dark phase) and FeO (light phase) in form of slimes.

small proportion in the ore. But a careful examination of the mineral phase at the centre of the photomicrograph of plate vi reveals that, it is made up of three or more phases as identified in the plate . It can also be seen from the micrographs of plates v to viii that in order to achieve complete liberation of each of the mineral phases, there is the need to grind the ore to approximately less than 5µm which is practically impossible because of the economic and other processing considerations.

4.6 GRAVITY SEPARATION TESTS

The gravity separation tests were carried out using a laboratory shaken table for the coarse particle size ranges from - 710µm to +125µm and Mozley laboratory mineral separator for the fine particle size ranges from - 125µm to -45µm.

Tables 3.17 and 3.18 are the metallurgical balance of the separation tests using the Mozley separator for both Mn and SiO_2. From table 3.17, it can be seen that the maximum concentrate grade attainable is only 22.9% Mn with a recovery of only 39.7% which was achieved at a particle size range of -63+45µm. This concentrate at the same particle size range (-63+45µm) assays 34.2% SiO_2 and contains 43.9% of the total Silica in the orginal Ore. The low manganese assay (22.9%Mn) of the concentrate and the high Silica assay of 39.7% SiO_2 make it unsuitable as feed for ferromanganese production. The tailings from this test assay high amount of Manganese (9%Mn)

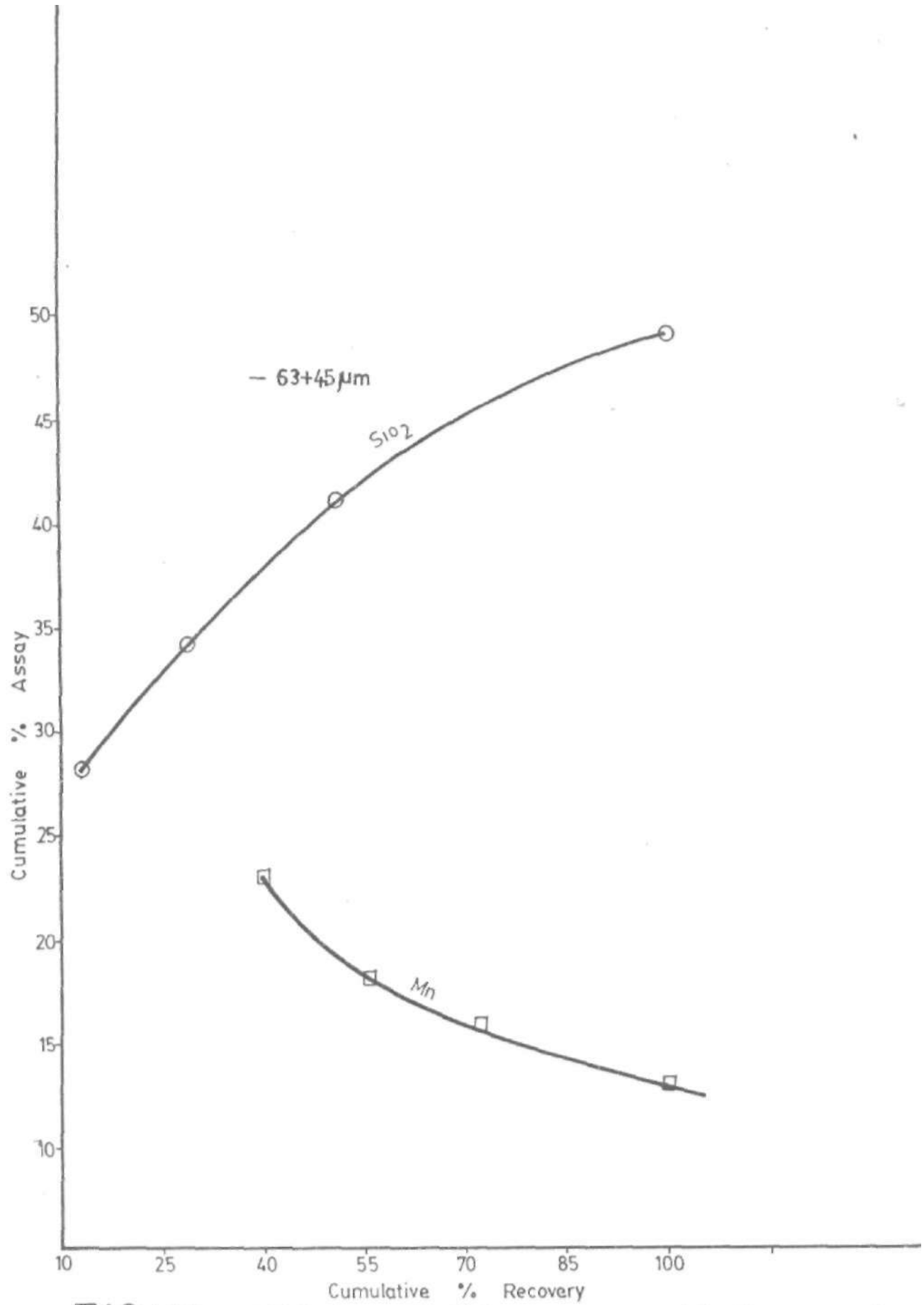


FIG.4.16 — A Plot of cumulative % Assay against cumulative % recovery for Mn & S, O_2 at −63+45 µm size fraction.

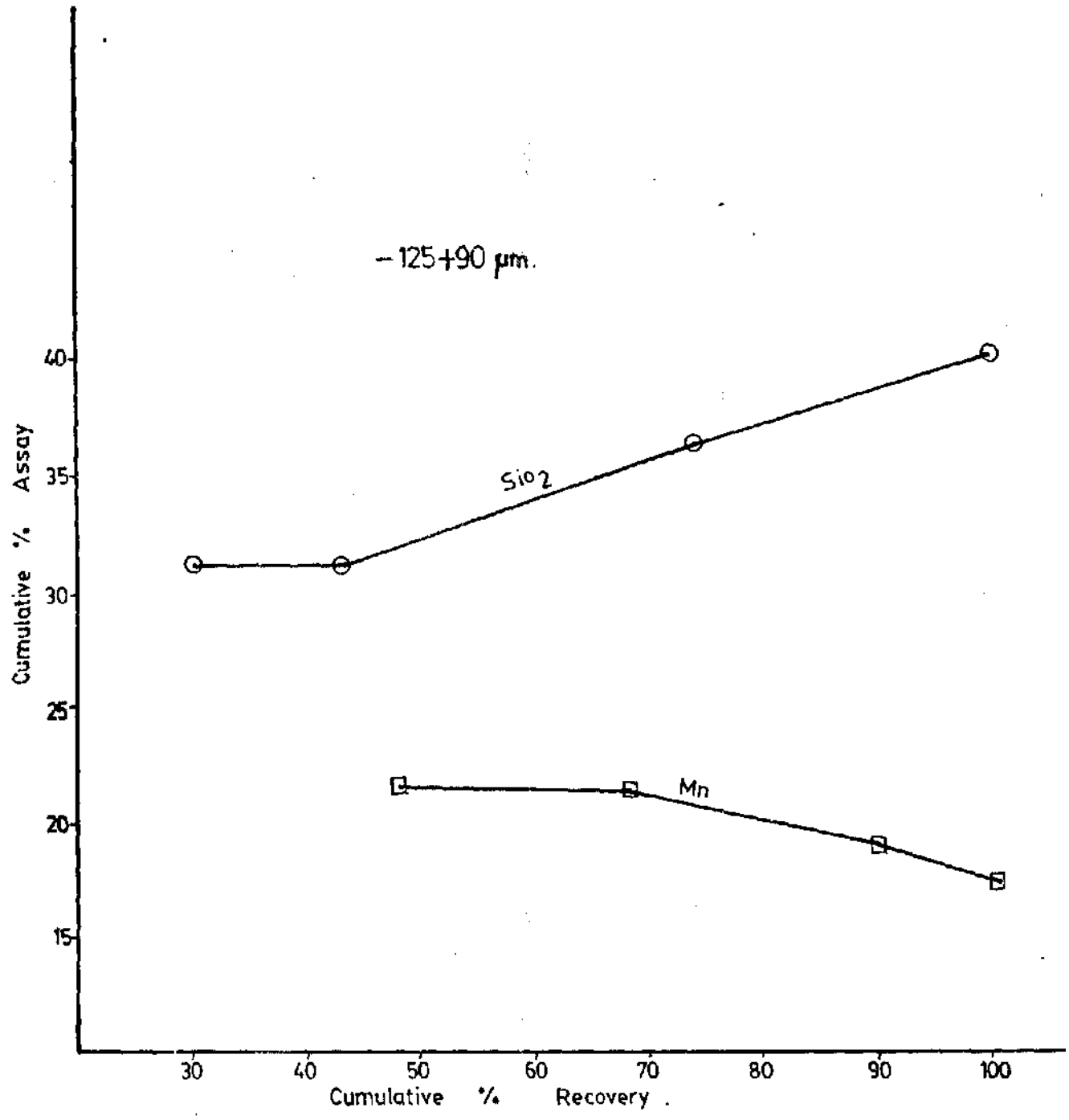


FIG. 4.18 - A Plot of cumulative % Assay against cumulative % recovery for S_iO_2 Mn at -125+90 µm size fraction.

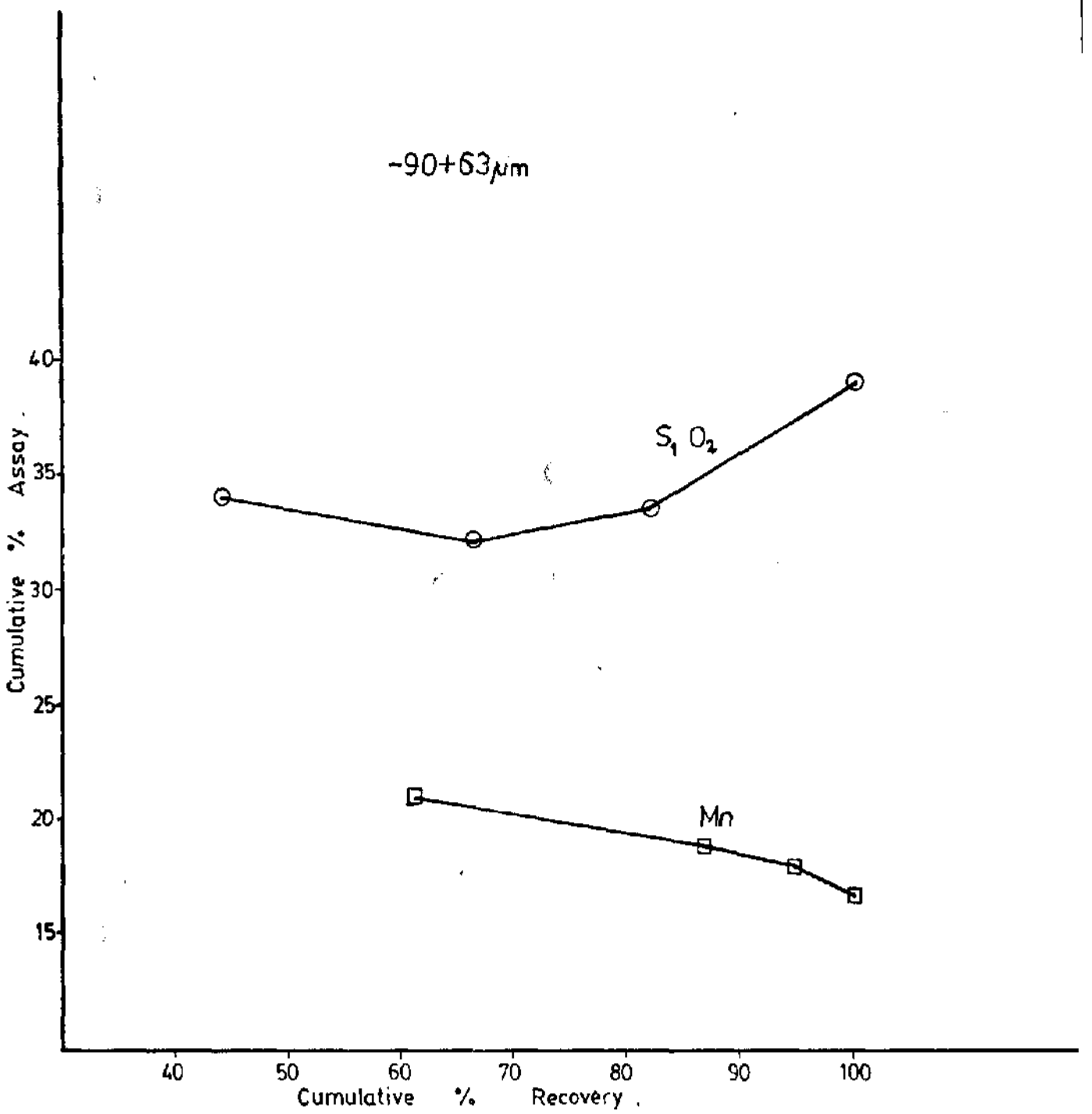


FIG 4.19—A Plot of cumulative % Assay against cumulative % recovery for Mn & $S_i O_2$ a
-90 to 3 μm size.

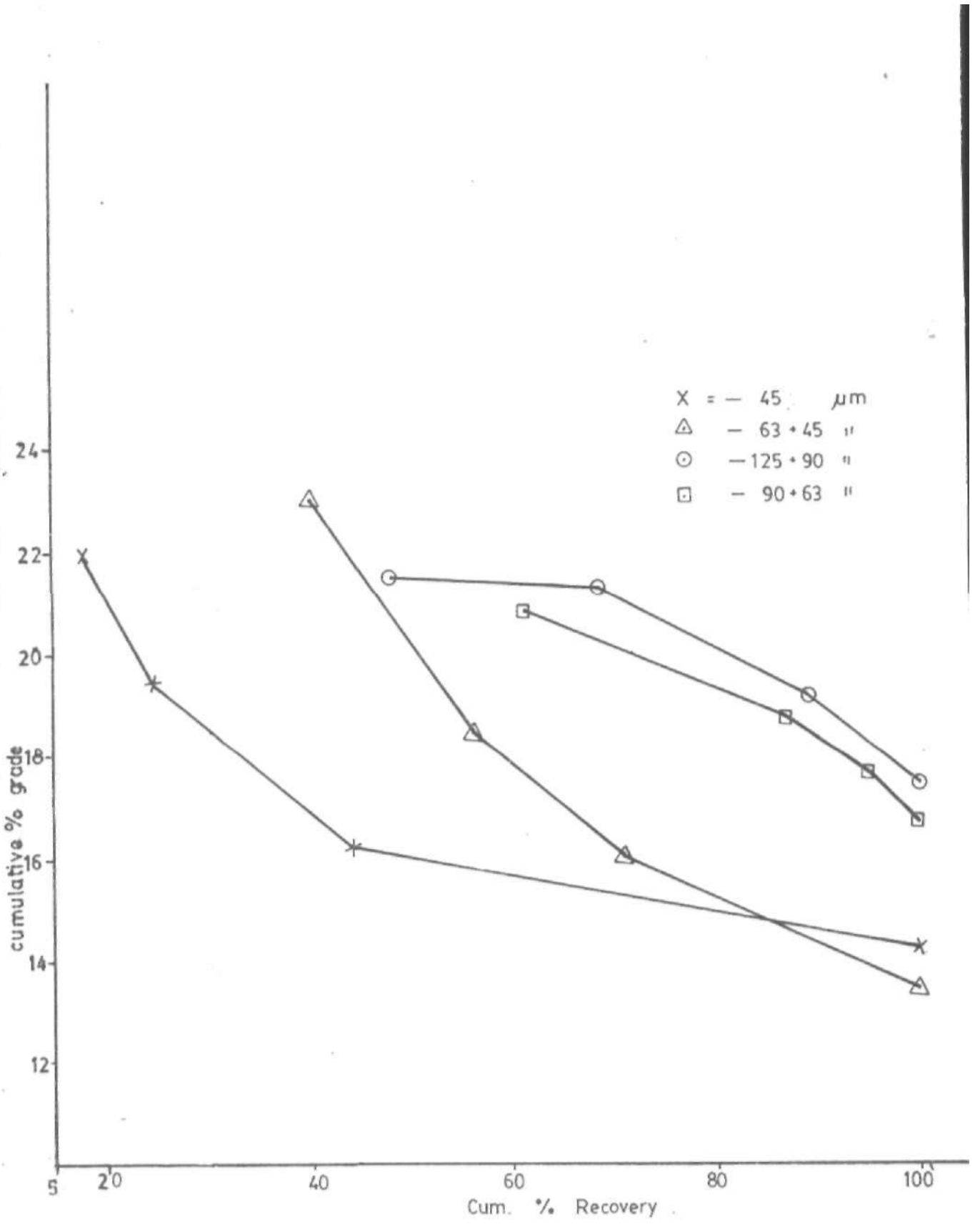


FIG 4.20 — A Plot of cumulative % grade against cumulative % recovery for mangas at various size fraction.

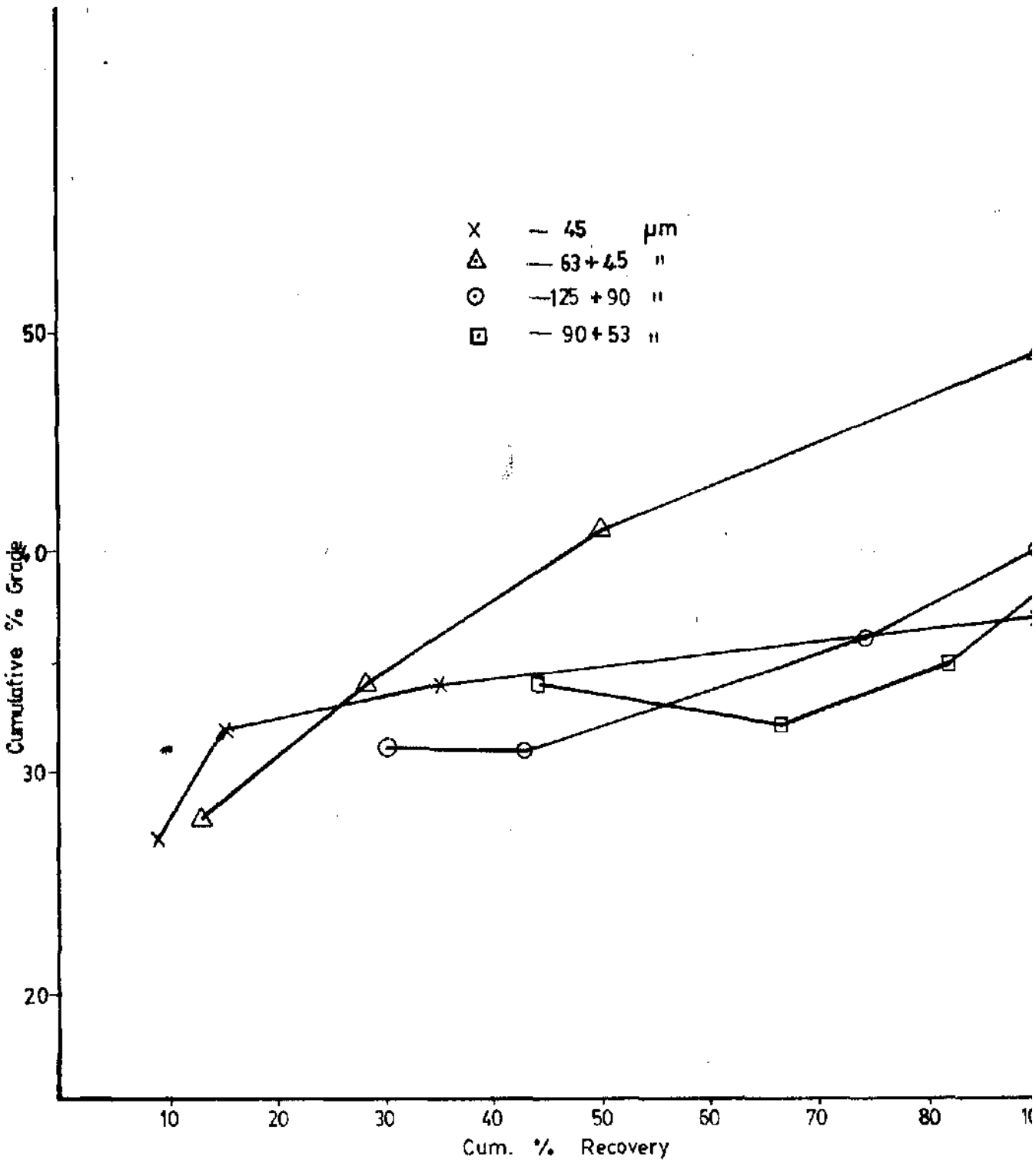


FIG.4.21- A Plot of cumulative % of grade against cumulative of recovery for $Si\,O_2$ at various size fraction.

Tables 3.19 and 3.20 are the metallurgical balances for Manganese and Silica from the separation tests carried out using the laboratory shaken table. From table 3.19 it can be seen that a concentrate with a maximum grade of only 21.2% Mn can be achieved with a recovery of 36% at particle size fraction -355 + 250 µm. The concentrate also assays 29.1% SiO_2 (Table 3.20) at the same particle size. Comparing these results with those obtained from the Mozley mineral separator in which a concentrate with maximum grade of 22.9% Mn was obtained with a recovery of 39.7, Shows that the results obtained from the Mozley mineral separator are better except that the assay of the Silica (34.2%) in the concentrate from the Mozley separator is higher than the 29.1% from the laboratory shaking table.

The most interesting results are those obtained at particle size fractions -180 + 125µm and -355 + 250µm. A concentrate assaying 20.0% Mn was produced with a recovery of 69.3% and containing less amount of Silica 28.7% (Table 3.20) at the particle size -180 + 125µm. Comparing these results with those of particle size fraction -355 + 250µm shows that even though the difference in the assays of the two concentrates, 22.9% Mn and 20.0%Mn for -355 +250µm and -180 + 125Mm particles size, respectively is only 2.9% there is a large difference in the recovery 39.7% and 69.3%. This gives a recovery difference of 29.6% which is very significant. The

separation at particle size fraction - 180 + 125µm produced the optimum results. It must however be born in mind that none of the concentrates produced either by Mozley seperator or shaking table is suitable as a feed for ferromanganese production because all of them contained high amount of Silica far in excess of what is acceptable.

4.7 GRANULATORY TESTS

Appendix 2 are the print outs of the results of malvern master Sizer used for the Granulatory tests. While Table 4.21 is a summary of the results of the tests obtained from these print outs.For each grinding time, 80% passing particle size was obtained from the cumulative curves (Appendix 2) The estimated 80% passing partial size of each grinding time was then plotted against the logarithm of the grinding time to obtain Figure 4.22. This Figure gives the time versus grinding characteristic of the Ore. This is a very important relationship for the comminution and separation processes of the ore. From this graph the time required for the Ore to be ground in order to achieve certain degree of fineness could be estimated. For example, for the flotation tests carried out in this work, the grinding time necessary to achieve a product of 80% - 63µM passing, was determined from this graph to be 4 minutes. In order to achieve that, the ore was ground, in the same set of ball mills under the same conditions as when the test was conducted.

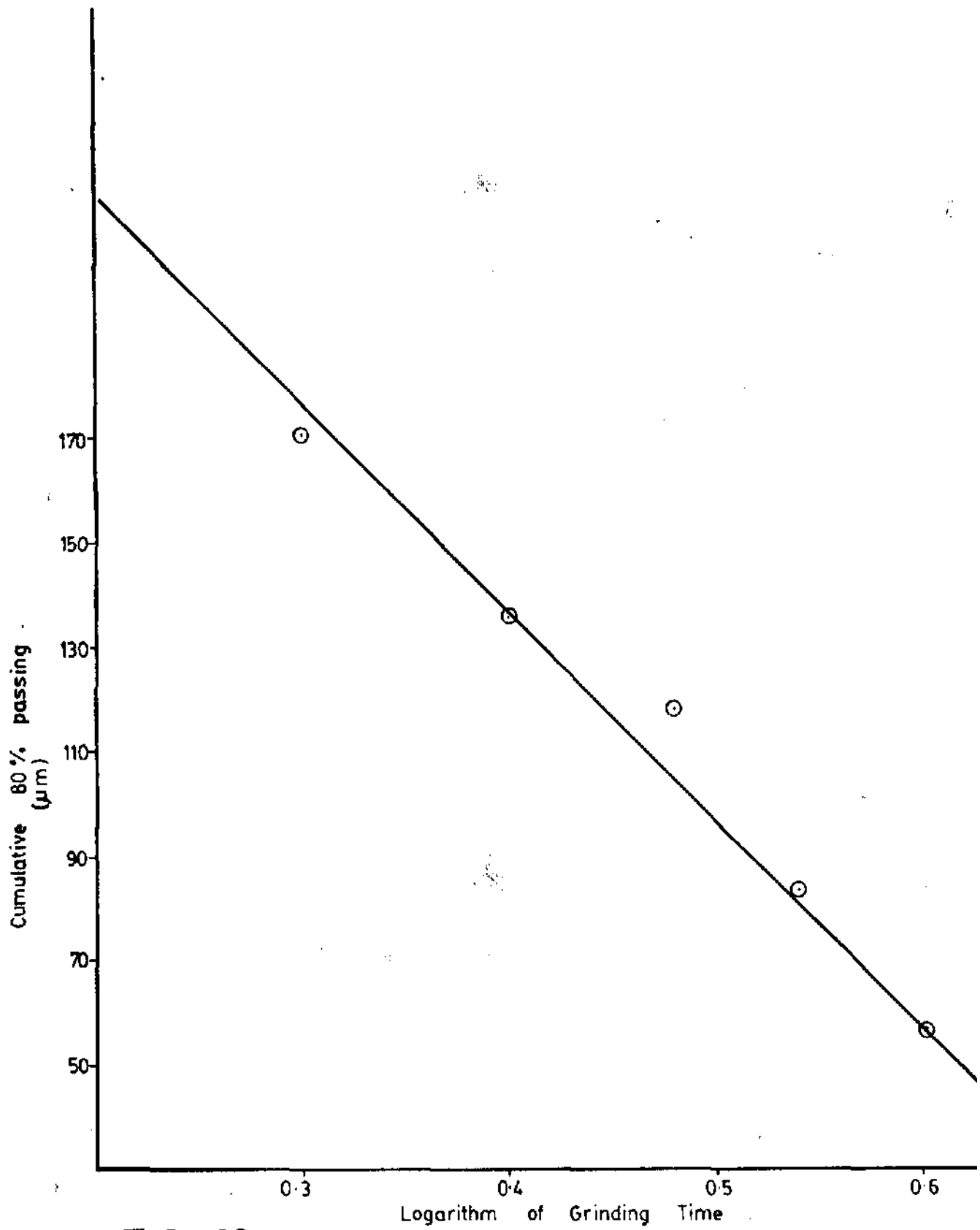


FIG.4·22— A Plot of cumulative 80% passing against log of grinding time.

4.8 FROTH FLOTATION TESTS

Tables 3.22 to 3.24 give the chemical analysis of the concentrates and Tailings Produced from the flotation tests using three different types of reagents Armac(C), Aerofloat 64 and ArmacT, respectively. From these tables it can be seen that for all the three cases, the assays of the manganese in the concentrates (27.49% MnO, 27.35% MnO and 26.52% MnO) are below that required for the metallurgical grade concentrate. The Silica, averaging more than 30% and Alumina, averaging about 15% for all the three cases are also high. Table 4.25 gives the metallurgical balance of the tests. From these results it can be seen that both the tailings and concentrates contain appreciable amounts of silica with the tailings assaying about 70% SiO_2. The high concentration of silica in both the Tailings and concentrate can be explained to be due to the presence of both free and chemically combined silica in the ore. The free together with some ofthe combined silica is floated into Tailings while the major portion of combined silica remained in the concentrate.

Looking at the results (Tables 3.22 to 3.24) of the chemical analyses of the concentrates produced, it is evident that all the three concentrates assay about the same amount of Mn and contained almost the same amount of Aluminium, Iron and Silica in excess of what is acceptable which makes them unsuitable as feeds for the production of ferromanganese.

4.9 GRINDABILITY TEST

Table 3.26 give the particle size analyses of the feed to the Ball Mill for the grindability tests. Figure 4.23 is the semi - logarithmic plot of the percentage weight passing against particle size of the feed. From this plot the 80% passing feed(F_1) and the proportion of material of sizes - 75μM, - 500μM and - 1000μM were estimated and used in getting Tables 3.30 to 3.32.

Tables 3.27 to 3.29 are the particle size analysis of the Ballmill discharges after the tests at the three sizes (75μM, 500μM and 1000μM). Figures 4.24 to 4.26 are the semi - logarithmic plots of the % weight passing against particle size analyses given in Tables 3.27 to 3.29. From these Figures the 80% passing product (P_1) at each size fraction was estimated. Using the value of F_1 determined from Figure 3.22 and the values of P_1 determined from Figures 4.24 to 4.26 at each of the sizes, the work index of the ore at each of the size was calculated using the empirical equation 21. The values of the work index (W_i) calculated using equation 11 for the three sizes 75μM, 500μM and 1000μM are 10.5, 12.83 and 16.02 kwh/st respectively. These values show that the amount of energy required to grind this particular ore from an infinite size to 80% passing 100μM increases with increasing particle size and decreases with decreasing particle size, indicating that the ore is soft at coarse sizes and hard at finer sizes. Also the values of the work index indicate that

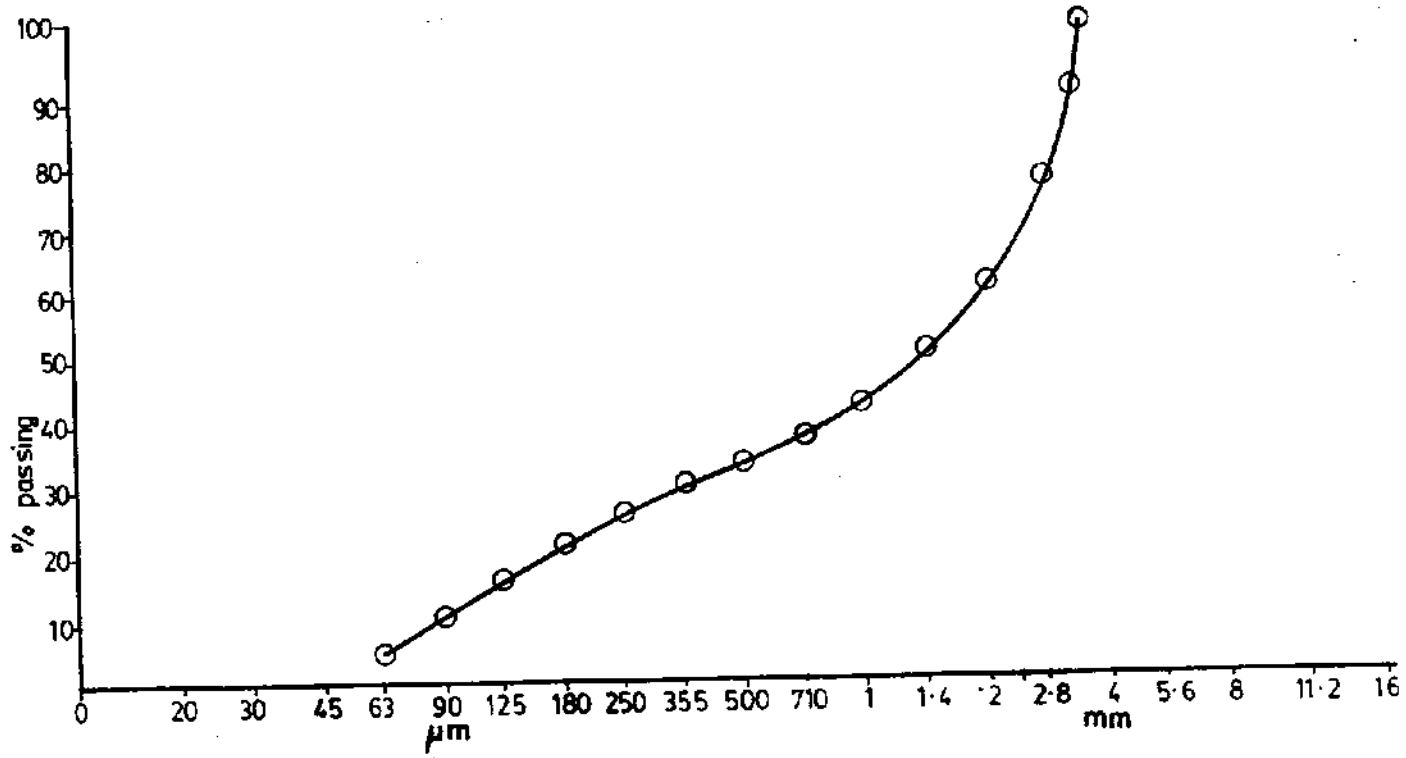


FIG. 4·23—Particle size analysis plot of the feed to the ballmill.

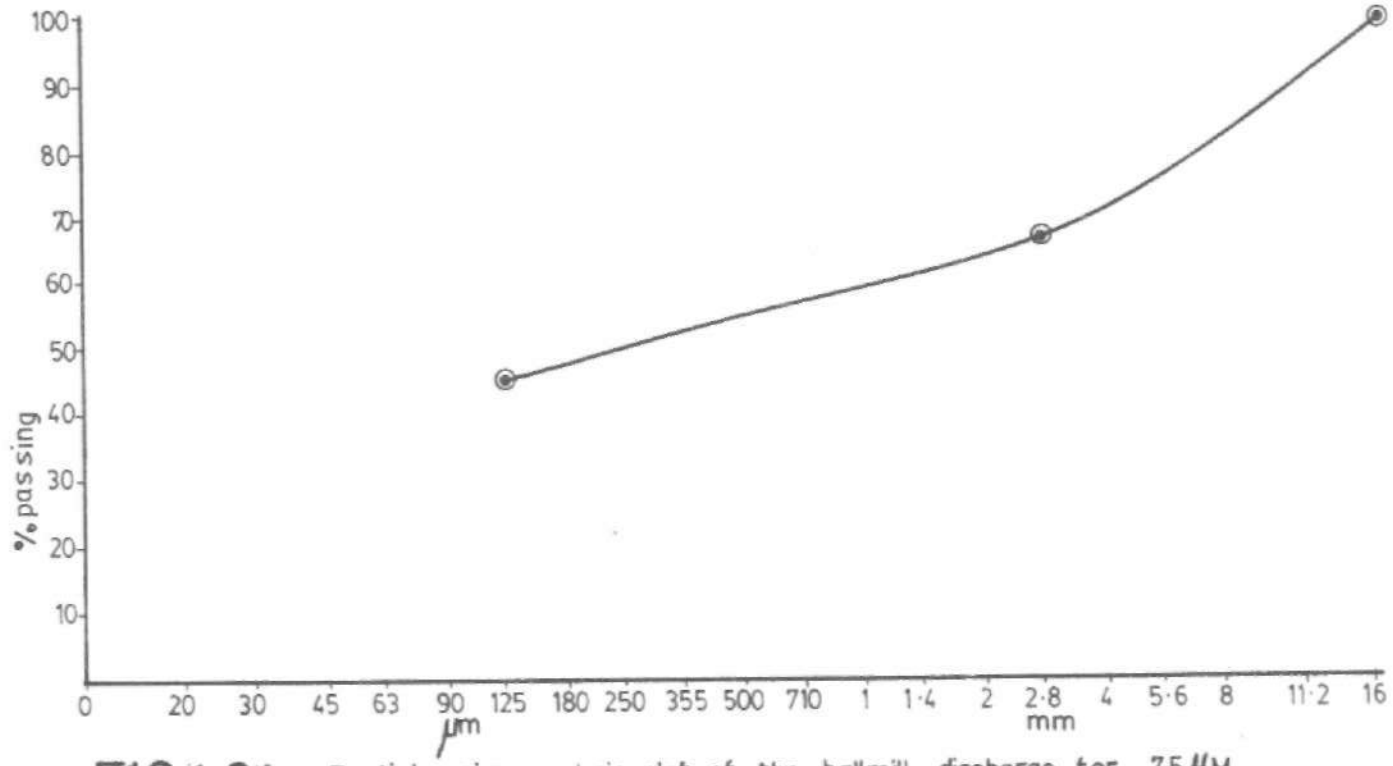


FIG.4·24 - Particle size analysis plot of the ballmill discharge for 75μM

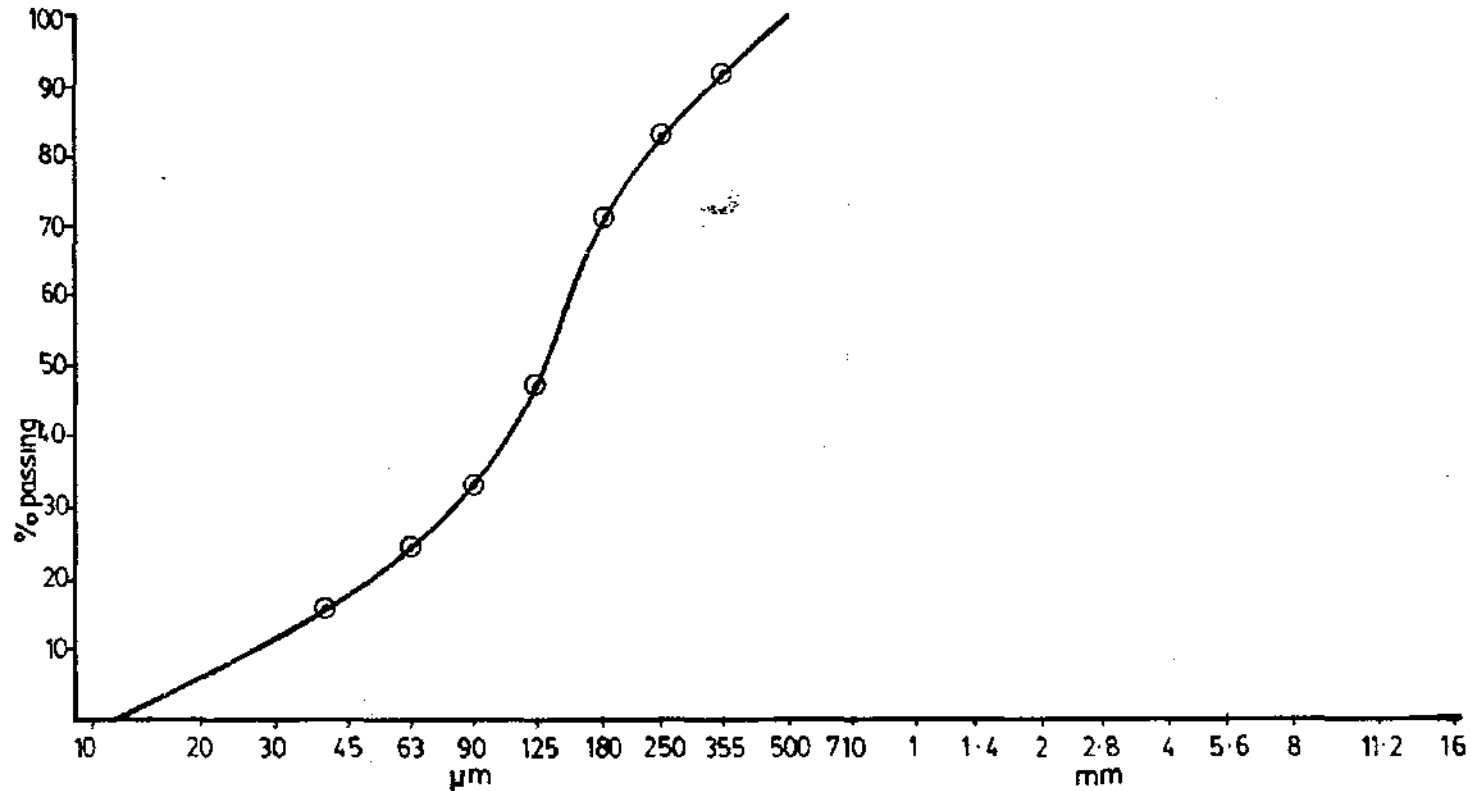


FIG4·25- Particle size analysis plot of ballmill discharge for 500μM

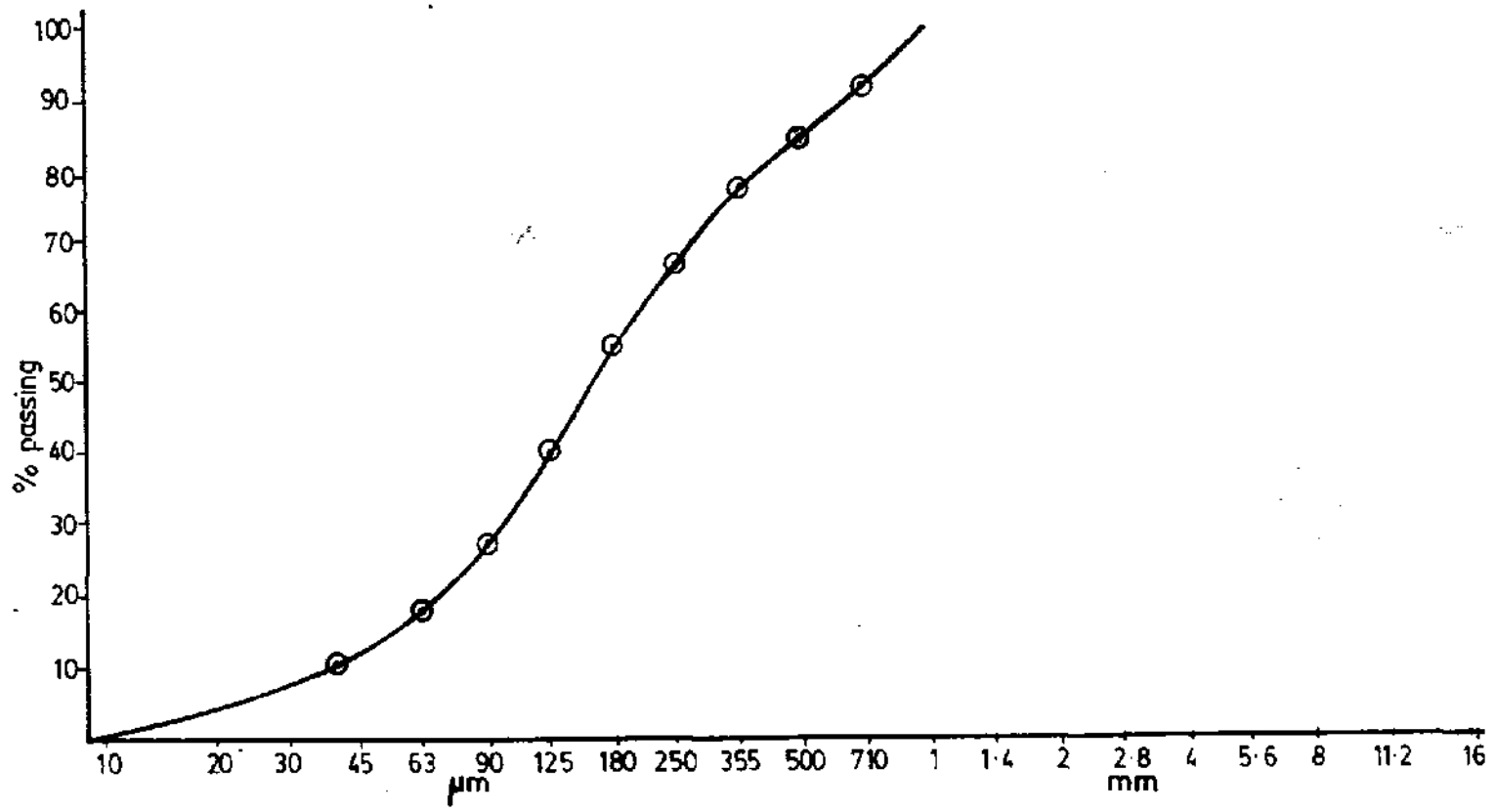


FIG4·26- Particle size analysis plot of the ballmill discharge for 1000μM

the ore is moderately soft.

Figure 4.27 is a graph of the work index against the size fraction. This plot was produced so that it could be used to interpolate or extrapolate values of work index at any given size, which can then be substituted into the Bond's energy equation for purposes of estimating energy requirements in grinding the ore to different particle sizes.

4.10 LIME - CLINKERING PROCESSES

Tables 3.33 and 3.34 give the whole chemical Analyses of the concentrate and Tailings, respectively, produced by the lime-clinkering process. The concentrate assays 38.3% Mn_3O_4 and 8.3% Silica while Alumina is 6.2%. Based on this result, it is a low grade concentrate and hence can be used as feed in the production of spiegeleisen (low grade ferromanganese). This concentrate can also be blended with high grade, low Silica, low Alumina Manganese Ore/concentrate.

From Table 3.34 it can be seen that the tailings assays high Silica (39.6%) and Calcium Oxide (39.1%) with moderate alumina content of about 13.2% . This is expected since the X-ray spectrum of this phase (Figure 4.28) reveals that it consists mainly of Ca and Si in the form of ($CaO.2SiO_2$) followed by another phase of ($Al_2O_3.SiO_2$) in small amounts. The concentrate produced by this process can serve as an excellent feed material for ferromanganese production and subsequently for steel making

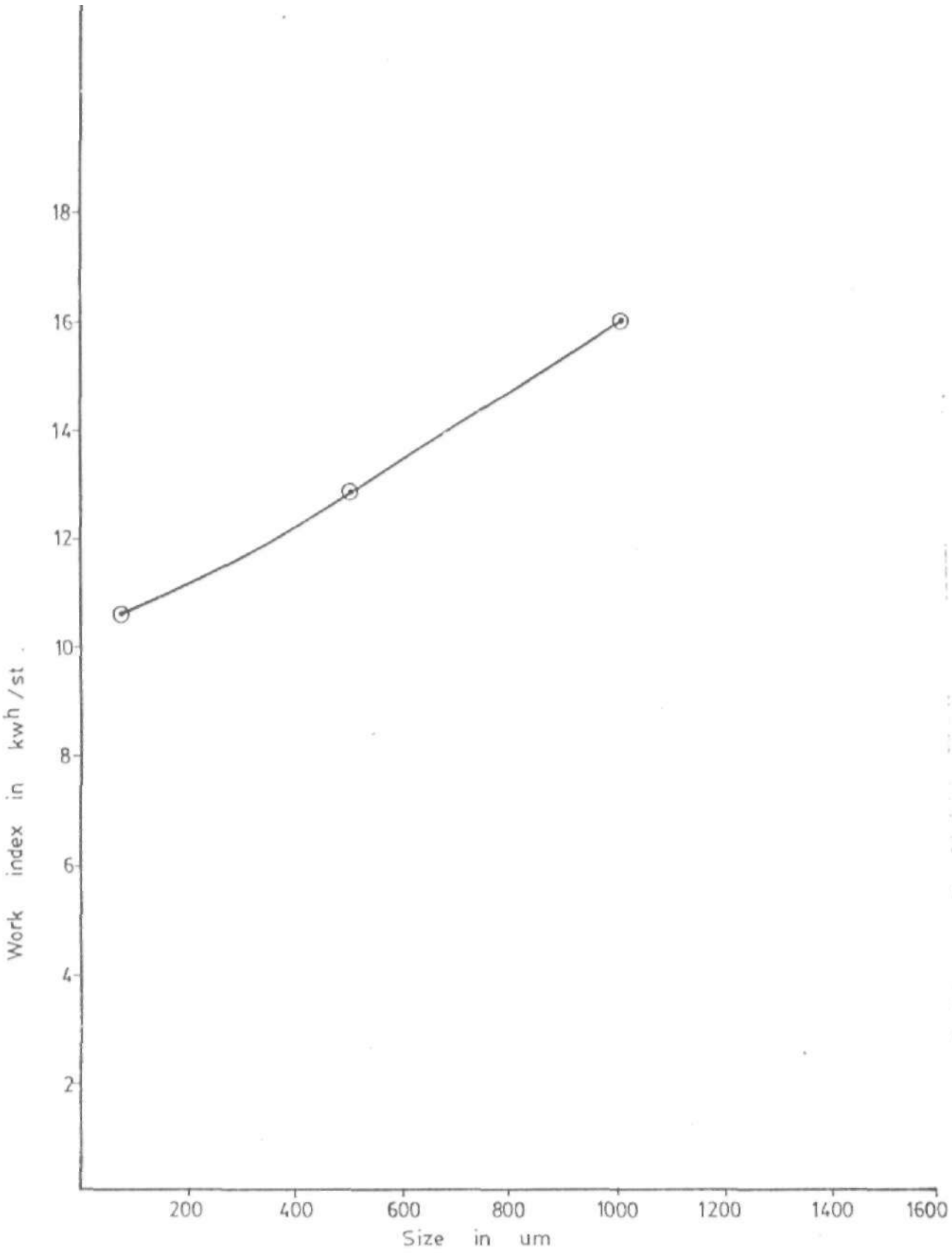


FIG.4·27— Variation of work index with size fraction.

(alloying) since it contains low phosphorus (P_2O_5 = 0.02%) and low sulphur (0.05%).

Figures 4.28 and 4.29 give the x-ray spectra of the tailings and concentrates produced by this process at a

$$\frac{CaO-3(P_2O_5+Al_2O_3)}{SiO_2}$$

ratio of 2.0.From these spectra it can also be observed that the tailings constitute mainly CaO and SiO_2 in the form of ($CaO.SiO_2$) with small amount of Al in the form ofalumino silicate [$Al_2O_3.SiO_2$] and very small amount of (FeMn) entrained in the tailings. thus confirming the results given in Table 4.34. The concentrate contains Fe and Mn in the form of spinel $(Fe.Mn)_2O_3$ with very small amount of Al, Si and Ca in the form of (Cao, $Al_2O_3.SiO_2$) which are entrained in the spinel phase.

Plate xi is the electronphotomicrograph of the clinker produced at a $\frac{CaO-3(P_2O_5+Al_2O_3)}{SiO_2}$ ratio of 2.0 prior to separation into concentrate and tailings. From this Plate it is clear that there are three phases, A, B and C in the clinker. Figures 4.30 to 4.32 show the x-ray spectra of these phases. Phase A, (Figure 4.29) consists of Al, Mn and Fe with trace amount of Ca, Ti and Mg while silica is completely absent in this phase. Phase B, (Figure 4.30) mainly consists of Ca, Si as $CaSiO_3$ with trace amount of Mn and no Iron. This is the slag phase, phase C Figure 4.31 constitute of Al, SiO_2 and Ca with trace amount of Fe and Mn which are entrained in the phase. Further examination of Plate xi reveals that there is more of phase B than Phase A. Both these phases are greater than Phase C. From this Plate it can also be observed that Phase A is metallic.

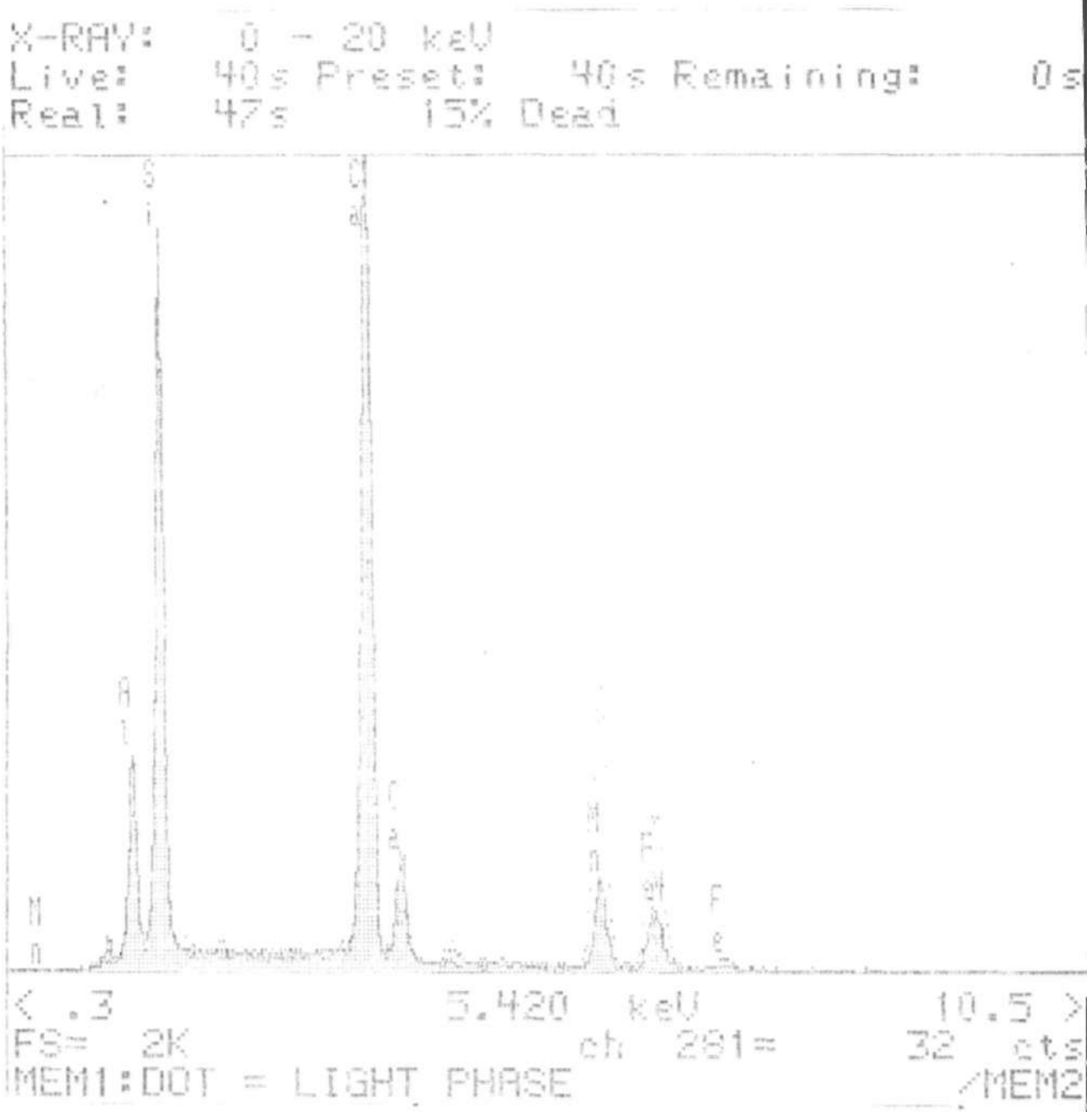


Figure 4.28: X-ray Spectrum of the Tailings of the lime-clinkering process.

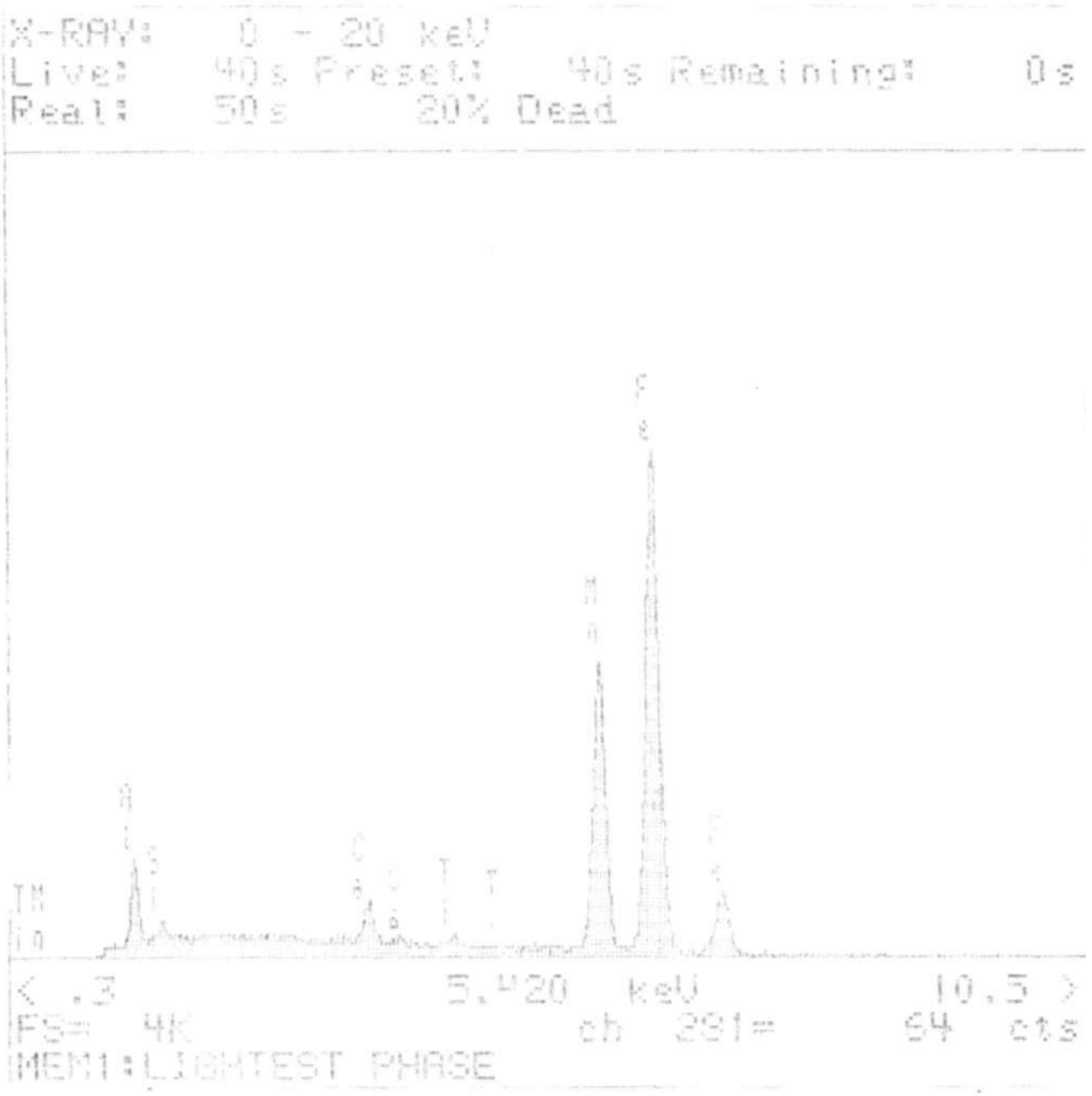


Figure 4.29: X-ray Spectrum of the concentrate of the lime-clinkering process.

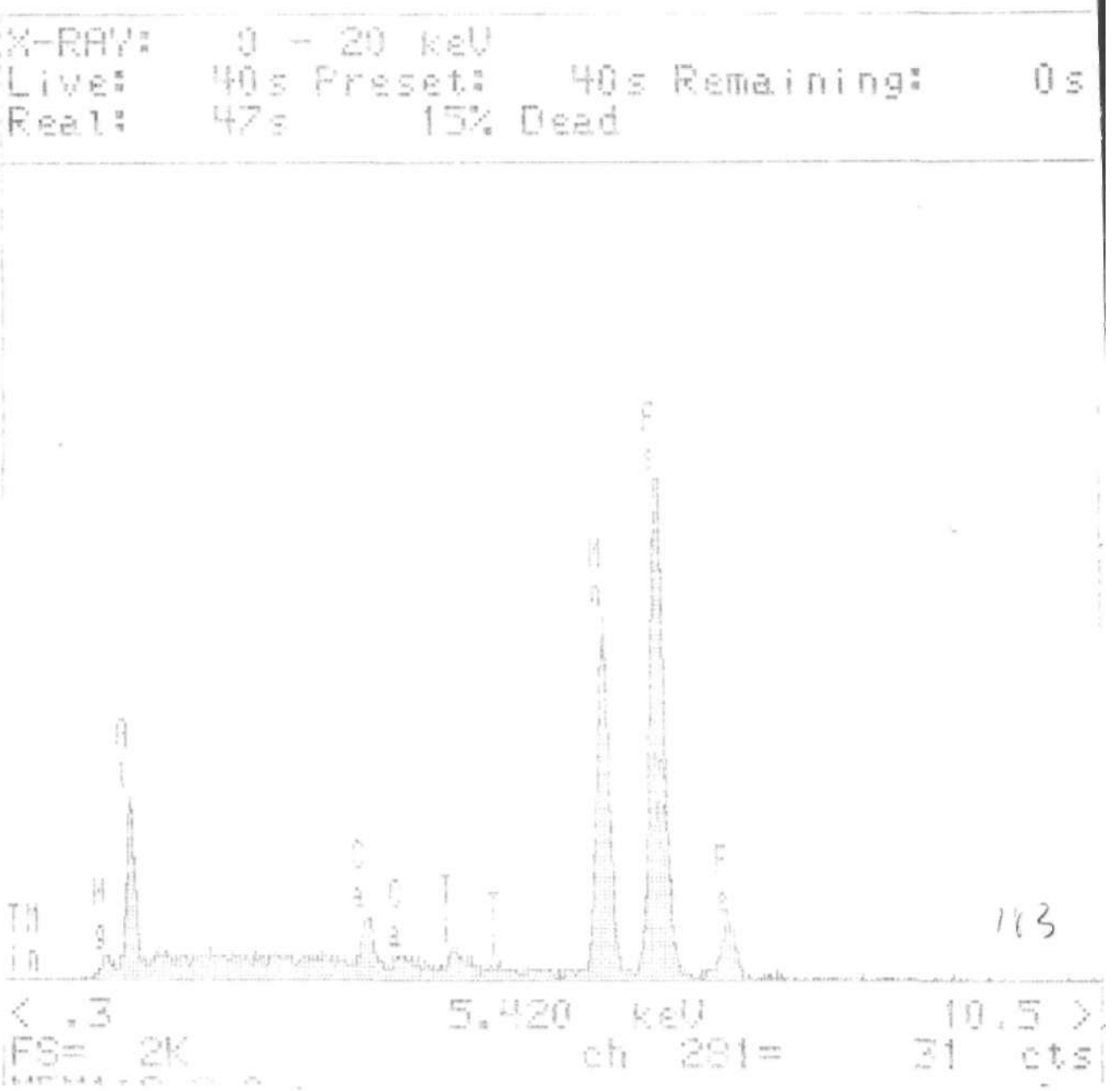


Figure 4.30: X-ray Spectrum of phase A(Light Phase) as identified in plate XIV.

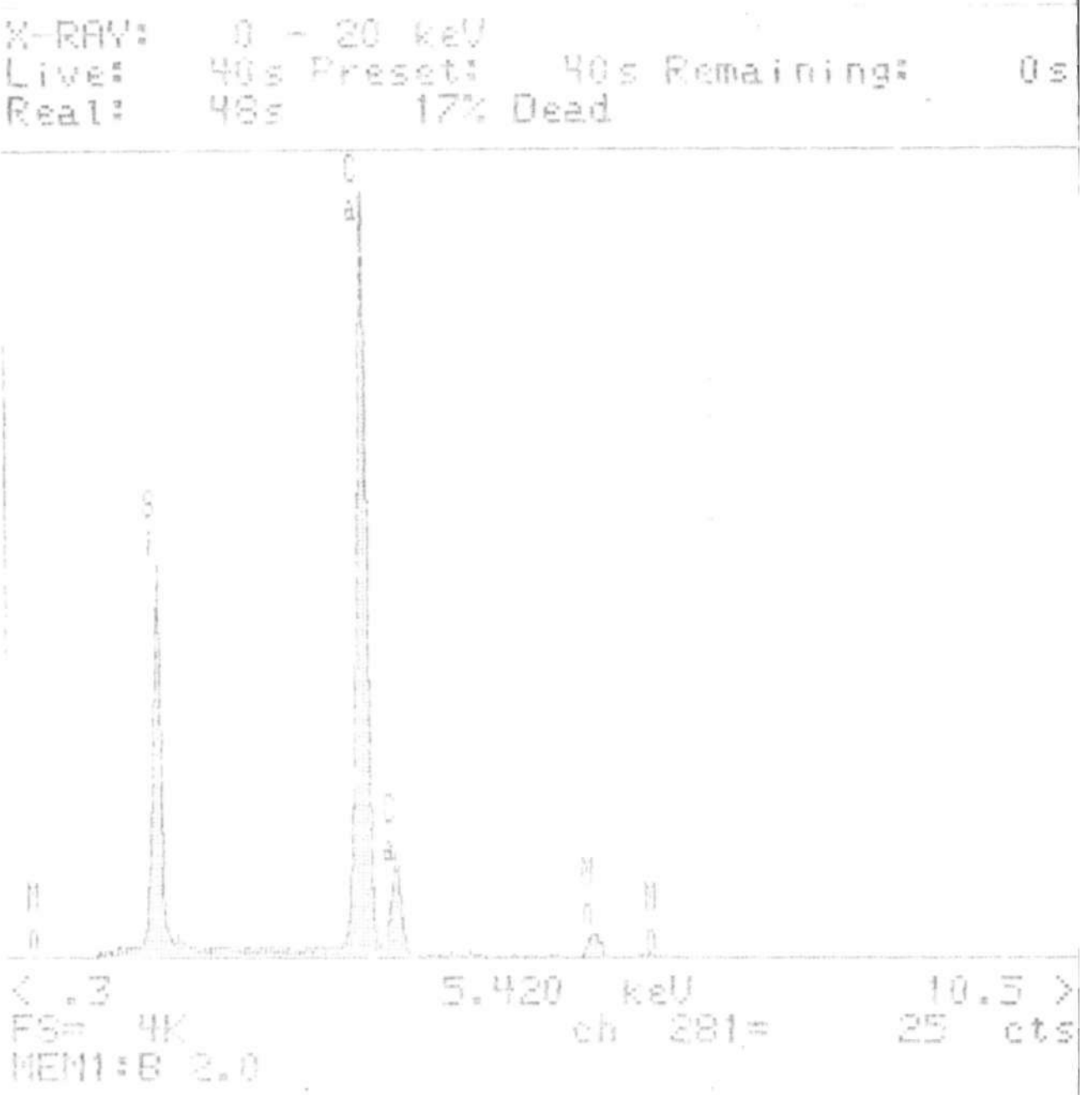


Figure 4.31: X-ray Spectrum of phase B(Grey Phase) as identified in Plate XIV..

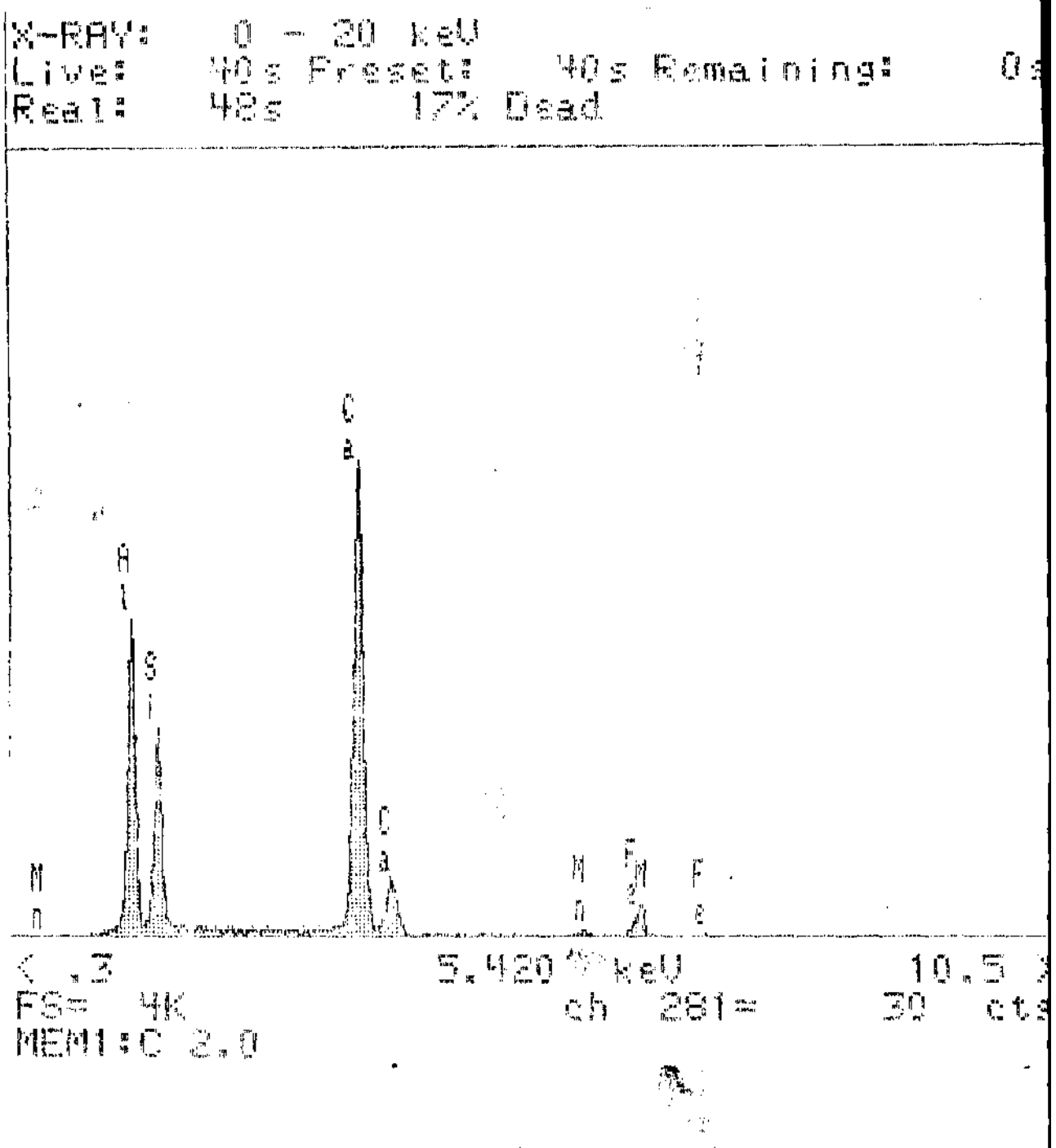


Figure 4.32: X-ray Spectrum of Phase C (Dark Grey Phase) as identified in Phase XI

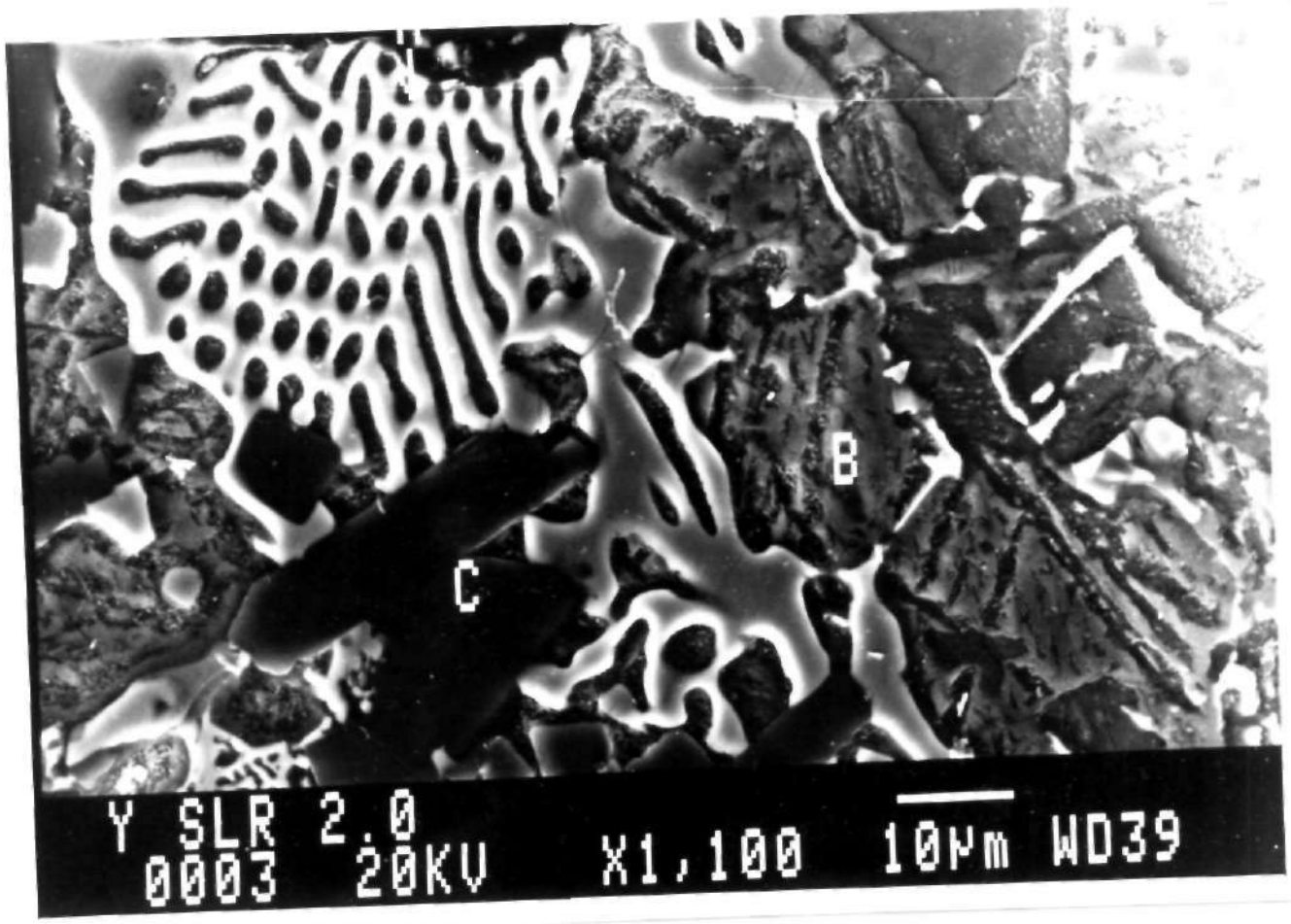


Plate XI: Electron Photomicrograph of the clinker produced at $\frac{CaO-3(P_2O_5+Al_2O_3)}{SiO_2}$=2.0 showing the three formed phases

A - Light Phase - $(Fe,Mn)_2O_3$ Spinel

B - Grey Phase - $(CaO.SiO_2)$ - Tailings

C - Dark Grey Phase - (Ca,Si,Al,Mn,Fe) - Middlings

Plate xii gives the backscattered electron image (BEI) of the same clinker which gives a good view of the clinker structure. The light Phase being the heaviest Phase (Phase A), followed by grey phase (Phase B) and the Dark Phase (Phase C). Plates xiii and xiv are the electron photomicrographs of the clinker produced at $\frac{CaO - 3(P_2O_5 + Al_2O_3)}{SiO_2}$ ratio of 1.4. It can be observed from this Plates that only two phases are formed (Phase A & B). Plate xiii also gives the distribution of the two phases in the clinker structure. From this plate it can be seen that Phase B is bigger in particle size than Phase A and that particles of Phase A are droplets in phase B. Also the particle size distribution of the phases are of wide size range.

Plate xiv shows the individual particles of the phases of the clinker and gives an idea of the approximate particle size to which the clinker will be ground in order to liberate phase A from Phase B. Based on this it is clear that the clinker needs to be ground to an average particle of less than 10 μM in order to unlock the two phases. Plate xv is the electron photomicrograph of the clinker produced at a $\frac{CaO-3(P_2O_5+Al_2O_3)}{SiO_2}$ ratio 1.0. In this plate it can be seen that there is only a single phase and no indication of any reaction that has taken place. This is confirmed by Figure 4.33 which is the x-ray spectrum of the phase. This spectrum reveals that the phase contain of Al, Si, Ca, Mn, Fe which are basically the main elements in the ore.

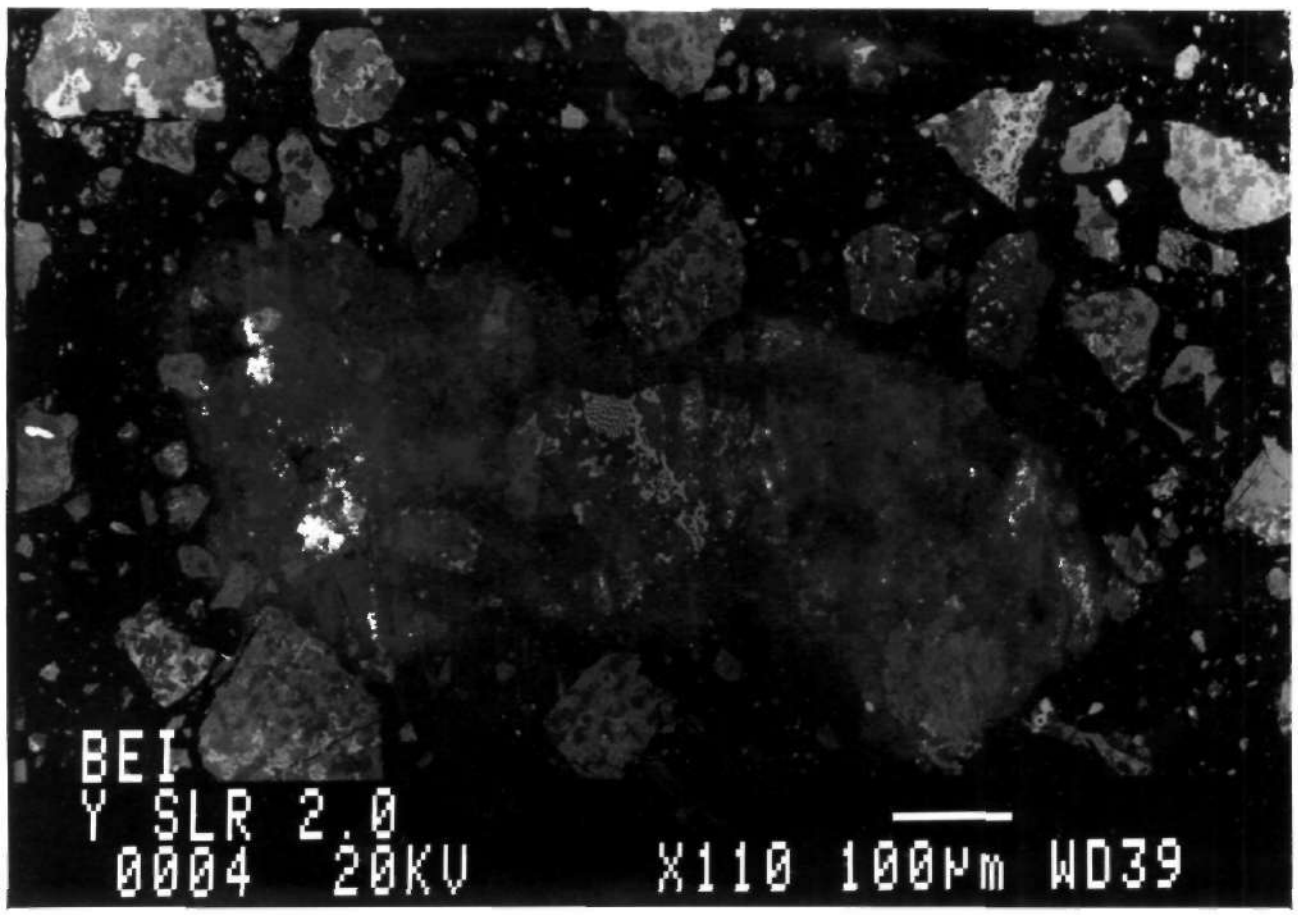


Plate XII: Electron Photomicrograph of the Backscattered Electron Image (BEI) of the clinker produced at $\frac{CaO-3(P_2O_5+Al_2O_3)}{SiO_2}=2.0$ showing the grain size distribution of the Phases in the clinker.

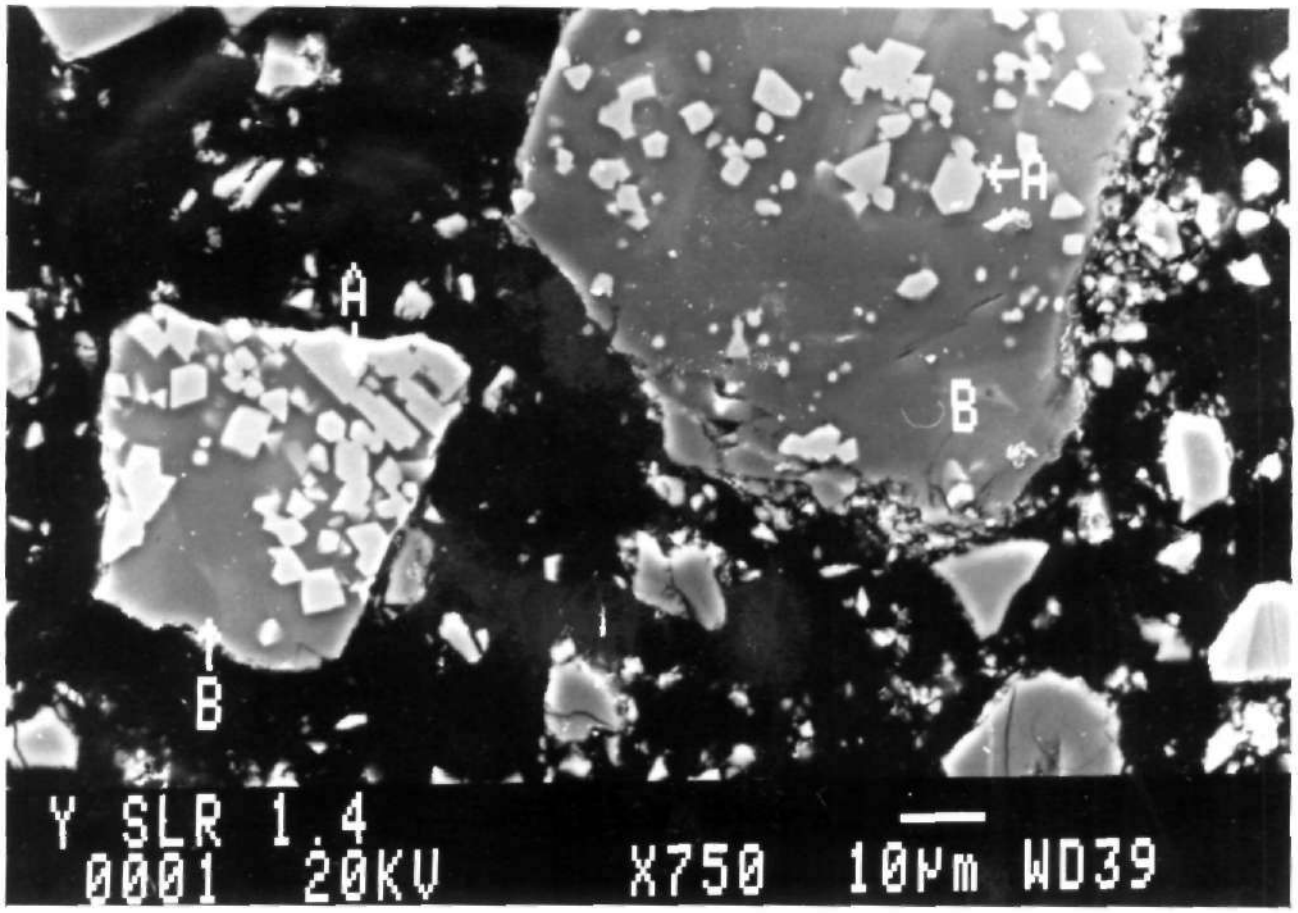


Plate XIII: Electron Photomicrograph of the clinker produced at $\frac{CaO-3(P_2O_5+Al_2O_3)}{SiO_2}$ =1.4 showing the only two phases formed.

Light Phase (A) - $(Fe,Mn)_2O_3$

Dark Phase (B) - (Ca, Si, Al, Mn, Fe)

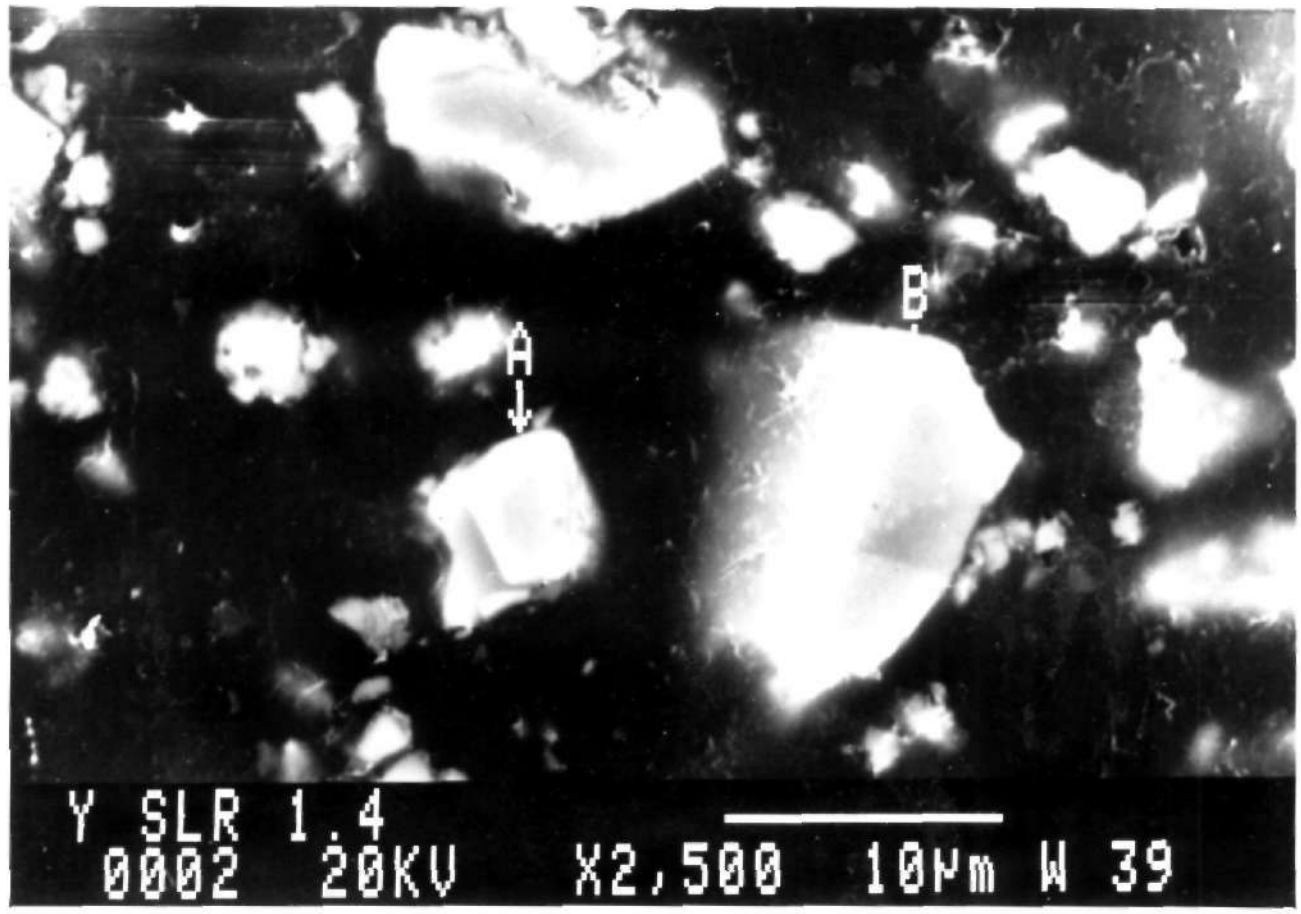


Plate XIV: Electron Photomicrograph of the clinker produced at $\frac{CaO-3(P_2O_5+Al_2O_3)}{SiO_2}$=1.4 showing the grain size of each of the phases formed.

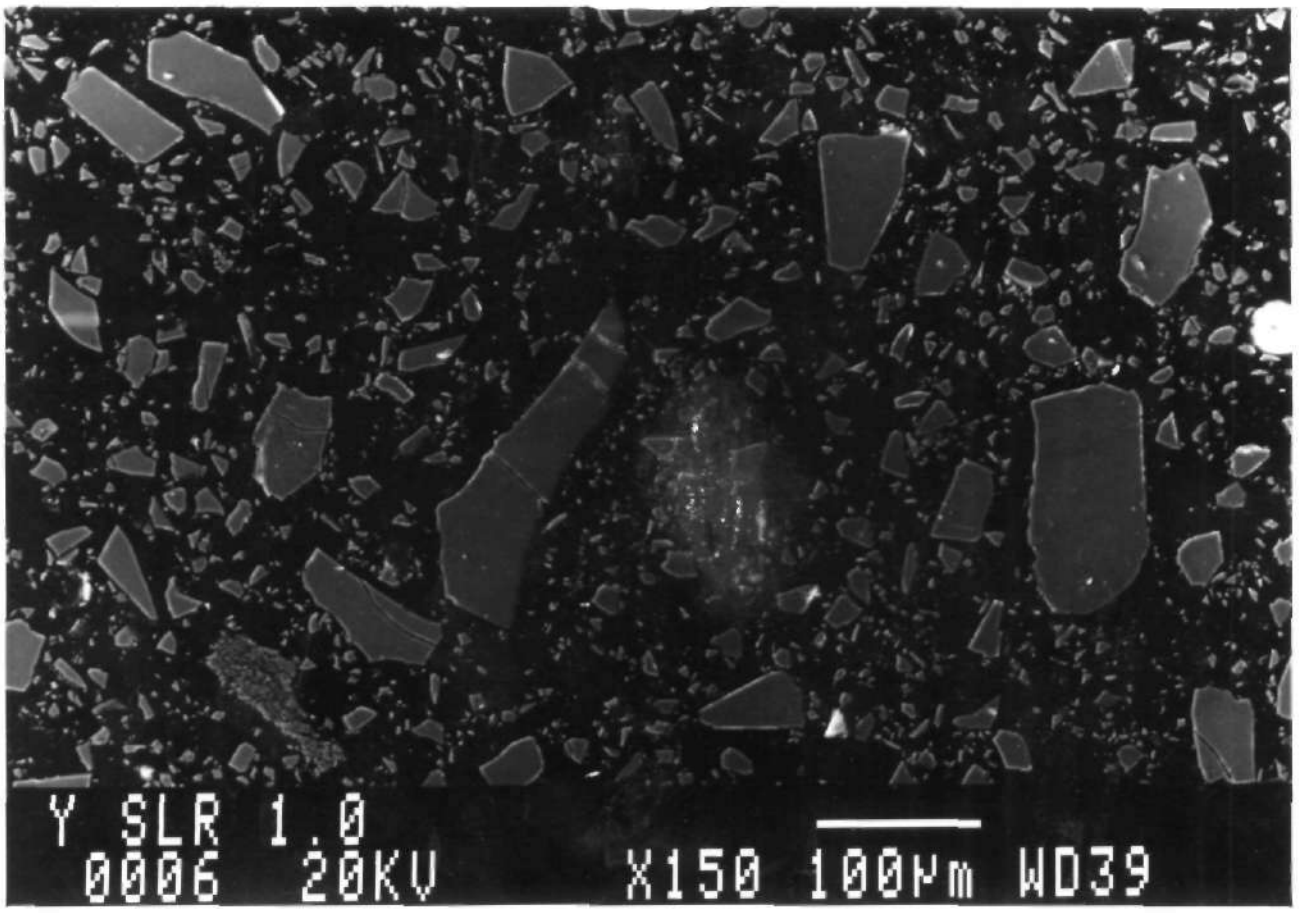


Plate XV: Electron Photomicrograph of the clinker produced at $\frac{CaO-3(P_2O_5+Al_2O_3)}{SiO_2}=1.0$ showing only a single phase formed.

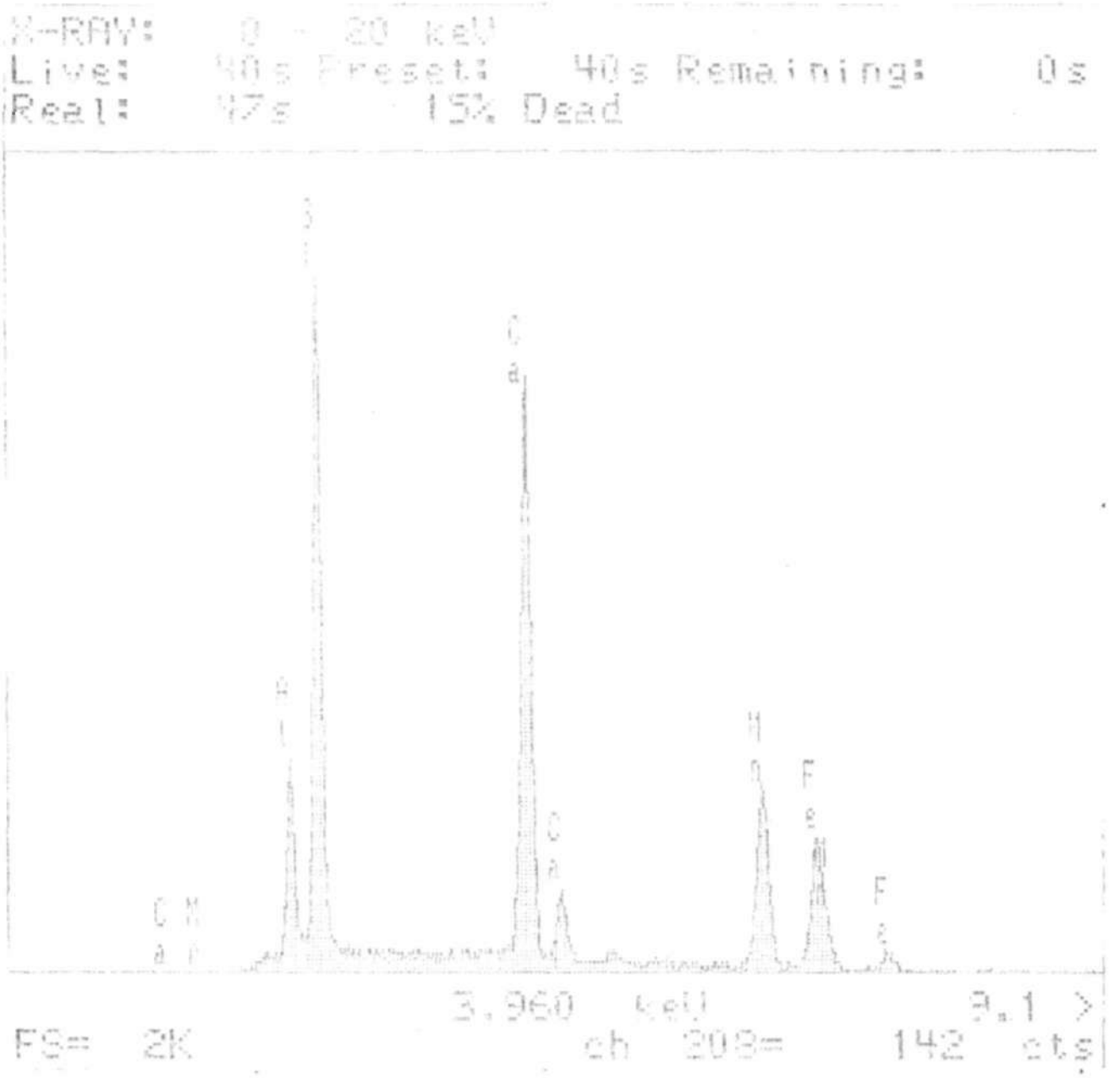


Figure 4.33: X-ray Spectrum of the single phase produced at a ratio of

$$\frac{CaO - 3(P_2O_5 + Al_2O_3)}{SiO_2} = 1.0$$

CHAPTER V

5.0 CONCLUSIONS AND RECOMMENDATIONS

5.1 Introduction

The development of the process route for the upgrading of Mallam Ayuba manganese ore deposit to ferromanganese feed grade was thoroughly investigated and conducted in two phases. The first phase involved carrying out chemical analyses, size/Assay analyses, mineralogical analyses, liberation studies and grindability tests. From these analyses and tests the grade, mineralogy, liberation characterists and work index of the ore were determined.

The second phase of the research involved carrying out concentration tests using mineral processing techniques of gravity separator, froth flotation and the lime-clinkering process. The summary of the results of the concentration tests are given in Table 5.1. Based on the discussion and analyses of the results of the first and second phase of this work, the following conclusion could be drawn:

Table 5.1

Assays of the Concentrates Produced
by the Various Methods of Separation

Separation Technique Used	Initial Assay of the Feed		Assay of the Concentrate Produced	
	% Mn_3O_4	% SiO_2	%Mn_3O_4	%; Sio_2
Gravity Separation (i) Shaken Table	24.7	32.2	27.6	31.2
(ii) Mozley Laboratory Separator	24.1	40.0	30.2	30.2
Froth Flotation	25.3	33.8	28.8	30.4
Lime Clinkering Process	24.4	35.2	38.3	8.3

(1) The Mallam Ayuba Manganese Ore is low grade, assaying only 16% Mn and contains high amount of SiO_2 (36.4%) and Alumina Al_2O_3 (11.0%). Based on the results of chemical analysis it is apparent that the ore does not meet the requirement of metallurgical grade manganese in respect of SiO_2 and Al_2O_3 content. The sulphur and phosphorous (P_2O_5) content of (0.01%) and (0.04%) is however within the requirement of the metallurgical grade manganese Ore.

(2) The size/Assay analyses results show that waste rejection technique cannot be used in rejecting the free Silica in the Ore. This is because it was found that any attempt of rejecting some amount of Silica results in the loss of equal amount of Manganese.

(3) Mineralogical investigation show that in the Mallam Ayuba Manganese ore, most of the Manganese occurs in the Silicates minerals (spessartine) ($3MnO.Al_2O_3.3SiO_2$) with only a small proportion occuring in the mineral psilomelane which is a solid -Solution of Hollandite ($BaMn_8O_{16}$) and Cryptomelane (KMn_8O_{16}).

(4) From investigation, the mineralogy of the ore also revealed that there is a small proportion of Free Silica (Quartz) and that some of the Manganese in the spessartine structure has been substituted by Iron resulting in the formation of spessartine/almandine structure ($3MnO.Al_2O_3.3SiO_2$)/[(FeO,MnO) $Al_2O_3.3SiO_2$]. This could have been responsible for the high amount of Iron

Fe_2O_3(14.0%) obtained in the chemical analysis of the Ore.

(5) The mineralogy of Mallam Ayuba Manganese ore also revealed that the constituent minerals of the ore are finely desiminated and intermittently intergrown with each other.

(6) Liberation studies by heavy liquids and Release Analysis Techniques showed that it is not possible to easily achieve complete liberation of the constituent minerals of the ore. Only partial liberation could be achieved at limits of physical separation techniques . This may be because the constituent minerals of the Ore are finely disseminated and interlocked with each other.

(7) Since it was shown that it was not easy to completely liberate the constituent minerals in the Ore, then conventional physical or physio-chemical separation methods may not be suitable for the beneficiation of the ore.

(8) The concentrate produced by gravity and froth Flotation processes did not meet the requirement for metallurgical grade Ore because of the high Silica content,thus confirming the result of the liberation tests.

(9) The results of grindability tests have shown that the ore is soft with an average work index of about 12Kwh/st for a particle size range between 75µm to 1000µm. This value

of work index means that the energy requirement to grind the Ore is moderate. It was also found that the energy requirements in grinding the Ore increase with increasing particle size.

(10) Based on the results obtained from the lime clinkering process in this study, it can be concluded that the process may be the only means by which this ore can be beneficiated for ferromanganese production.

5.2 RECOMMENDATIONS:

1. The lime-clinkering process is the only promising method so far identified in this work that can be used to produce a manganese concentrate for ferromanganese production. It is recommended that this method be adopted for the beneficiation of the Mallam Ayuba Manganese Ore deposit to ferromanganese feed grade. A flowsheet based on this process has been proposed and is given in figure 5.1.
2. The concentrate produced by the lime clinkering process can also be blended with imported high grade manganese ore/concentrate and smelted to ferromanganese.
3. The concentrate produced by the lime-clinkering processing can also be smelted with the Iron ore concentrate produced at Itakpe in the Blast furnace to produce a high manganese pig iron. The pig iron can then be used in producing Manganese alloy steel.
4. Also based on the chemical composition of the raw Mallam Ayuba Manganese Ore (table 3.1), it is recommended that trial smelting of this ore directly with the Itakpe iron ore concentrate be carried out so as to produce a high manganese pig iron. The benefit of having more manganese in the pig iron will definitely off set the extra cost that will be incurred in using more lime during the smelting.
5. Other manganese ore deposits like those of Tudun Kudu and Ruwan Doruwa in the country should be thoroughly investigated and detailed geological data on them acquired.

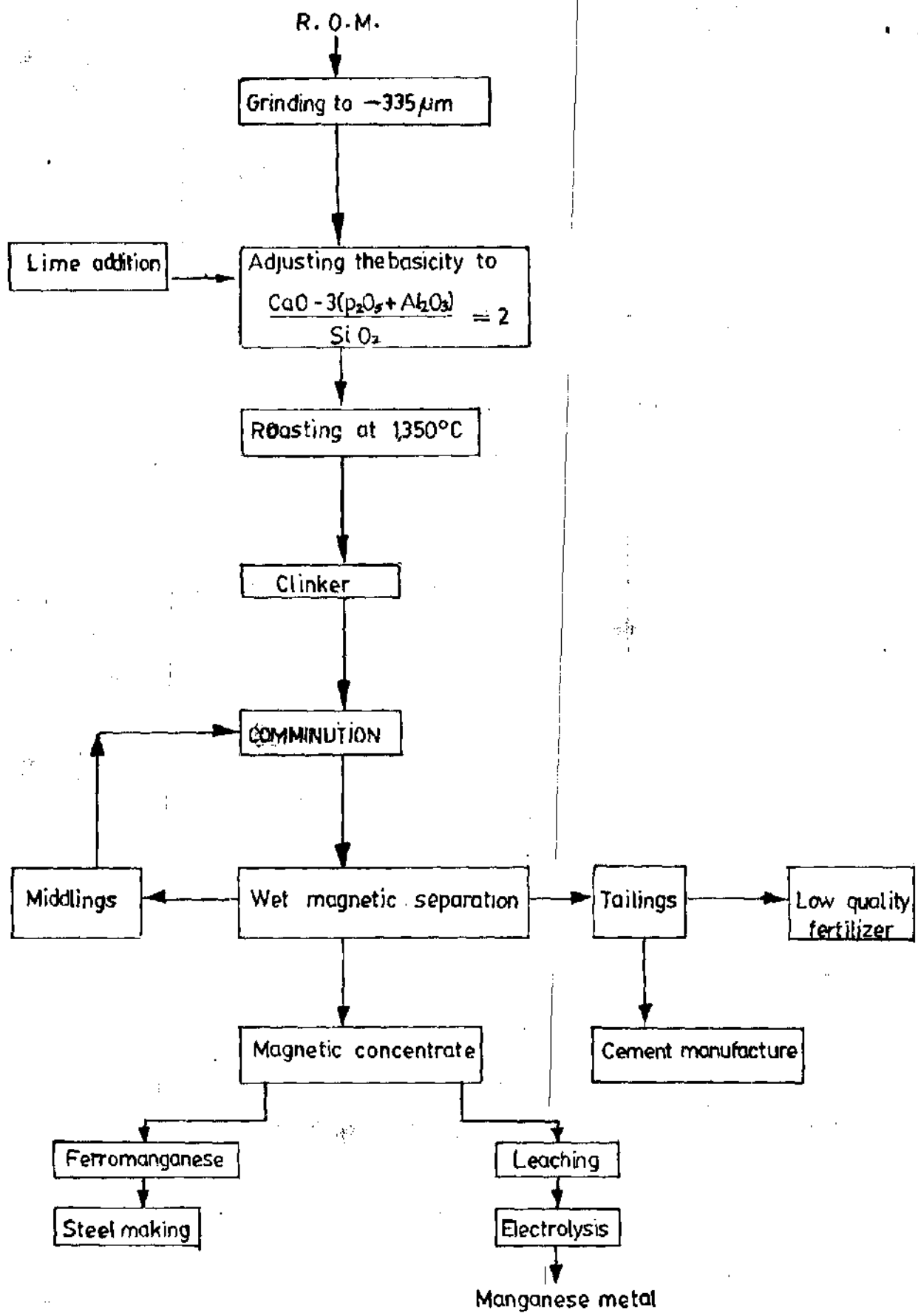


FIG.3·1 PROPOSED FLOW SHEET FOR THE BENEFICIATION OF THE MANGANESE ORE

Researches relating to their beneficiation and possible uses in the metallurgical and non-metallurgical industries should be taken seriously.

6. It is also recommended that the Tailings of the lime clinkering process be used in the production of cement or as refractory material.

7 Further work on the lime clinkering process as regard to optimising the process parameters like. temperature, clinkering time, lime addition etc is highly recommended.

REFERENCES

1. Economics of Manganese Deposits (1991). Roskill Information Services Ltd. Reports (London).

2. Geological survey of Nigeria Annual Reports, 1944-48, 1980.

3. Personal conversation with some staff of the exploration Division of National Steel Council, Kaduna Zonal Office at the Federal Secretariat, Kaduna.

4. Mucke, A. and Okunjeni, C. (1984). Geological and ore macroscopic evidence on the epigenetic origin of the manganese occurences in Northern Nigeria. Journal of Atrican Earth and Sciences Vol. 2, November 3, pp 210-225. Pergamon Press Ltd., Great Bitain.

5. Bator, B.E. and Mucke, A. (1990). The genesis of manganese concretaions in the Igara area of south western Nigeria. Journal of Atrican Earth and Sciences Vo. 10, November 3, pp 292-301 Pergamon Press Ltd., Great Britain.

6. P.C. Moneme, P.W. Scott and A.C. Dunham. Manganese mineralisation at Tudun Kudu, Zaria District, North Central Nigeria. Journal of Mining Geology, Vol. 19, November 2, pp. 30-42, 1982.

7. B. Mason and L.G. Berry. Elements of mineralogy. A series of books in Geology. (Editor: J. Gulluly and A.O. Wootord). W.H. Freeman and Company, 1968.

8. P. Ramdohk. The ore minerals and their intergrowths. International Series in Earth Sciences. (Editor: D.E. Ingerson). 2nd edition, Vol. 35. Pergamon Press, 1980.

9. Mckelvey, V.G., N.A. Wright and R. Rowland. Manganese Nodules resources in the North Eastern equatorial pacitic. Ch. In Marine Geology and Oceanography of the pacitic manganese Nodules province. Edited by S.L. Bischott and D.Z. Piper. Plenum 1979, pp. 747-762.

10. Williams, W.M. Manganese and its importance to Nineteeth Century Metallurgy. Canadian Metallurgical Quarterly, Vol. 19, No. 4, 1981, pp. 403-408.

11. Thomas, S.J. Minerals tacts and problems. Bureau of Mines Bulletin 675. United States Department of the Interior, 1985 edition, pp. 483-498.

12. Matricardi, L.R. and Downing, J.H. Manganese and manganese alloy. Ch. In: Kirkothmer Encyclopedia of chemical Technology Wiley, Vol. 14, 3rd edition, 1981, pp. 824-843.

13. Fuerstenau, D.W. and Him, K.N. Metallurgical and processing of Marine Manganese Nodules. Mineral Processing and Technology Review, Vol. 1, pp. 1-83, 1983.

14. U.S. Geological Survey. "Assessment and Scientific understanding of Hard Mineral Resources in the Economic Exclusion Zone: A National Programme for the Assessment and Development of the U.S. Exclusion Economic Zone. Proceedings of the symposium of the United State Geological Survey, November 15-17, 1984, USGS Circular 929, Washington.

15. Bertin, E.P. Principles and practice of X-ray Spectrometric Analysis, Pergamon Press, 1975.

16. Jenkins, R.J. An introduction to X-ray Spectrometry Analysis, Heyden, 1974.

17. Wills, J.P. The application of X-rays flourescence spectrometry in mineral processing. Proceeding of the International Conference on Mineral Science and Technology; Sandton South Africa, Vol. 2, 1984, pp. 975-980.

18. Williams, K.L. Introduction to X-ray spectrometry, X-ray flourescence and electron microscope analysis. Allen and Urivin Publishers Ltd., London, 1987.

19. Hayat, M.A. Principles and techniques of scanning electron microscopy, Vol. 3, Van Nostrand Reinhood Co., 1980.

20. Glaurt, A.M. Principles and practice of electron microscope operation, Vol. 3, North Holland Publishing, 1974.

21. G. Lawes, Scanning Electron microscopy and X-ray Microanalysis. Analytical chemistry by open learning. {Edited by Norman B. Chapman.} John Wiley and Sons.

22. B.D. Gullity. Element of X-ray Diffraction, Addison, Wesley, 1977.

23. L.S. Denglasser. Crystallography and its applications, Van Nostrand, Reinhood, 1977.

24. D.A. Skoog. Principles of Instrumental analysis, 3rd edition, Sanders College Publishing, 1985.

25. K.C. Brion. X-ray analysors in process control. Elsevier Science Publishers, London, 1986.

26. C. Whiston. X-ray Methods: Analytical chemistry for open learning. (Editor: F.E. Prichard). Section 6, pp. 306-312, John Wiley & Sons.

27. A.J. Lynch: Mineral crushing and grinding circuits. Their simulation, optimisation, design and control. Development in mineral processing [edited: D.W. Fuerstenan]. Vol. 1. Elsevier Scientific Publishers, Amsterdam, Netherlands.

28. B.A. Wills: Mineral processing technology: 5th edition. Pergamon Press. England, 1992.

29. Bond, F.C.: Crushing and grinding calculations Allis-Chalmers Manufacturing Company, Winconsin, 1962. Part 1, 14 pages.

30. Bond, F.C. The third theory of comminution. Transaction of the American Institute of Mining Engineers. Vol. 193, No. 484. 1952.

31. Deister, R.J.: How to determine the Bond work index using Laboratory Ballmill Grindability Tests: Engineering and Mining Journal. pp. 42-45. February 1987.

32. Levin, J. - Observation on the Bond standard grindability test and a proposal for a standard grindability test for fine particles. Journal South African Institution of Mining and Metallurgy 89 (Jan) 13. 1989.

33. N.E. Horst and J.H. Bassarear. Use of simplified ore transaction of Society of Mining Engineers of the American Institute of Mining and Metallurgical Engineers (Grindability to evaluate plant pertormance). Vol. 260, 1977.

34. Smith, R.W. and Lee, K.H. A comparison data from Bond type simulated closed circuit and batch type grindability test transaction of SME/ARME 241, 91 1968.

35. Berry, T.F. and Bruce, R.W. A simple method of determining the grindability of ores. Canadian Mining Journal. No. 63, 1966 (July).

36. Burt, R.O. Gravity concentration from Bench Scale to plant. Paper presented at the Annual Meeting of Canadian Mineral Processing. Ottawa, January 1984. 21pp.

37. D.J. Ottley. Gravity concentration in modern mineral processing. Mineral processing at cross roads. (Edited: B.A. Will and R.W. Barley). NATO ASI series No. 117. Published by Martins Njihoff Publishers Lancarter. pp. 317-413. 1986. Martins Njihoff Publishers.

38. K.B. Bhappu: Strategic Minerals, their impact in mineral processing development. Mineral processing at cross roads (Edited: B.A. Wills and R.W. Barley). NATO ASI series No. 117. Pp. 383-413. 19876. Martins Njihoff Publishers.

39. Burt, R.O. and Mill, C. Gravity concentration Technology Development in Mineral Processing. (Edited: D.W. Fuerstenan). Vol. 5, Elsevier Science Publishers, Netherlands. 1984.

40. Aplan, F.F.: The state of Art and the future of Gravity concentration. (Editors: P. Somasundaran and Fuestenan, D.W.). Research Needs in Mineral Processing. Harriman New York. 1975.

41. Moncrieff, A.G. and Lewis, P.J. The treatment of fine ores. Transaction of the institution of mining and metallurgy.

42. Browning, J.S. Heavy liquids and procedures for laboratory separation of minerals. United States Bureau of Mines Information Circular No. 8007. 14pp.

43. 'O' Connel, W.L. Properties of heavy liquids. Transaction of the American Institute of Mining Engineers, No. 266. pp. 126-132.

44. Smale, D. Density Gradient Column with special reference to their application to model analysis. Mineral Science and Engineering Journal. No. 2, Vol. 2. Pp. 18-23.

45. V.A. Glembotskii, V.I. Klassen and I.N. Planksin. "Flotation" (Edited: H.S. RobinoVich). Tsventriye metally. Primary Sources. New York. 1972.

46. Fuestenau, D.N.: Flotation science and engineering advances and challenges. Proceedings of the XVI International Mineral Processing Congress. Skockholin. (Edited by K.S.E. Forsberg) Vol. A, 63, Elsevier Publishers. 1988.

47. A.J. Lynch, N.W. Johnson, W.V. Manlaping and C.G. Thorne. Mineral and coal flotation circuits, their simulation and control. Development in mineral processing (Edited:

D.W. Fuerstenan). Vol. 3, Elsevier Scientific Publishers. 1981.

48. Crozier, R.D. Plant Reagents: Part 1 - Changing pattern in the supply of Flotation Reagents mining Magazine. 202. 1984.

49. Society of mining engineers of AIME: Column flotation "88" proceeding of an International Symposium on Column Flotation (Edited: K.V.S. Sastry). SME inclusive. January (25-28) 1988.

50. Genski, T. and Coffin, V. Column Flotation Operation at Mines Gaspe *Molebdenum Circuit. Canadian Mining Journal No.* 102, Vol. 28, March 1981.

51. Finch, J.A. and Dobby, G.S. "Column Flotation". Pergamon Press Oxford. 1990.

52. MohnoVskii, V.A. *et al:* Technology of Froth separation and its industrial applications Transactions of 10th Institute of Mineral Processing Congress. Paper 43, 1973.

53. Schulze, H.J. Physiochemical elementary processes in flotation. Elsevier Publisher Amsterdam. 1984.

54. Crozier, R.D. Flotation theory, Reagents and Testing. Pergamon Press, Oxford. 1992.

55. F. Sroboda. Magnetic methods for the treatment of minerals. Development in mineral processing (Edited: D.W. Fuerstenan). Vol. 8, Elsevier Science Publishers, Amsterdam. 1987.

56. J.A. Oberlteuller. Magnetic separation. A review of principles, devices and applications. Pergamon press. 1987.

57. I.J. Corrans: A development in the application of wet high - intensity magnetic separation. "International Symposium on Fine Particles Processing (Edited: P. Somasundaran) Vol. 2. AIME, New York. pp. 1294. 1980.

58. F.K. Dwight: Experimental Technique with general applicability for the study of magnetic phenomena. Journal of Applied Physics. Vol. 38, pp. 15005. 1967.

59. R.R. Birss and M.R. Parker: High intensity magnetic separation. Progress in filteration and separation (Edited: R.J. Walleman) Vol. 2. Elsevier Publisher.

1981.

60. Blake, L.I. and Morsche, L.R. Electrostatic separation process. U.S. Patent 294,032. 1969.

61. Fraas, F. Irreversible changes in response of minerals to electrostatic after heating. U.S. Bureau of Mines Information Circular 5542. 1959.

62. Carpenter, J.H. *et al*. Mining and concentration of ilmenite and associated minerals at Trait Ridge, Florida. Mining Eng. Vol.5. 1953 pp 789-795.

63. Linari-Linholm, A.A. Recovery of diamonds by electrostatic separation. Journal of Chemical Metllurgical Mineral Sciences. South Africa. Vol.50, 1950. pp 131-157.

64. Ralston, O.C. Electrostatic separation of mixed granular solids. Amsterdam. Elsevier Science Publishers. 1961.

65. Subramaya, G.V. and P.I.A. Narayanan. Benefication of low-grade manganese ores with particular reference to Semi-pilot plant studies on a low-temperature magnetising reduction process for ferruginous mangenese ores. Proceeeding of International Mineral Processing Congress of IMM, 1960, pp 919-934.

66. Applan, F.F. Manganese: SME Mineral Processing Handbook [edited: N.L. Welss]. Vol.2 section 27-6. SME. New York.

67. Spurgeon, R.C. and 'O' Connel, E.J. "South River Ships a tough manganese ore problem in Virgina. Engineering & Mining Journal. Volume 159, No. 5. May 1958. pp 106-111.

68. Dept. of Mines & Technical Surveys, Ottawa, Canada - USSR Exchange Visits, 1964. The Iron industry. Canadian Group report. 1965, Ottawa.

69. Yuderich, G.I. Concentration of Iron and manganese ores metallurgizdal. 1955.

70. Ren Zhumin: Test report on processing flowsheet for obtaining high quality concentrate of manganese carbonate from Tonghioging, Zunyi Mine. Chagsha, Mining and Metallurgical research Institute. 1985.

71. Basmanov, V.A. An investigation of the susceptibility to concentration of manganese slimes in chiatura. Gornoobogatite' ny. Zhumol. 1937, No.6.

72. Fuerstenau, M.G. and Rice, D.A. Transaction of AIME, Vol. 241, No. 453, 1968.

73. Palmer, A.C. *et al*: Flotation of manganese bearing silicates. Advances in mineral processing [Edited: P. Somasundaran] AIME/SME inclusive pp 116-126. 1984.

74. Fuerstenau, M.G., K.N. Han and J.D., Miller. Flotation Behaviour of Chromium in Mineral processing [Editor: P. Somasundaran]. AIME/SME inclusive. pp 289-306. 1986.

75. Kharlamov, V.S. Kurnosov, E.G. IZr. Vyeshuchelo. Zared, Corn Zhr 9(11) 163 1966.

76. LIUYAO, FENG QIUZH, ZHANG YONGLAI: Benefication of clean manganese ore in Zunyi Mine Chine. Proceeding of the XVI International Mineral Processing Congress held at Stockholm, Sweden. Part B, pp 1357-1368. 1988.

77. Norcross, F.S. Development of lo-grade manganese ores of Cuba. Transaction of AIME Vol. 153, pp. 97 - 110. 1943.

78. Taggart, A.F. Handbook of Mineral Dressing John Wiley. New York 1945, Sec.2 pp 2-5.

79. Narayanan, P.I.A. and Subramanya, G.V. Laboratory studies on the benefication of some ferruginous manganese ores of India for the production of ferrumanganese Transaction of IMM. Bulletin No. 77, pp 49-68. 1958.

80. LALKAKA, R.D.: Utilisation of low-grade manganese ores for production of standard ferrumanganese by Reeplex Smelting Metter. Vol.11, No.101, 1988.

81. A process for the concentration of manganese ore high in iron. Indian Patent No. 51625. March 1955.

82. Hans-Dieter, W. and Dieter, Z. Benefication of Iron and Manganese ores and recycling og metal bearing slags by means of air-pulsated BATAC Jigs. Process in mineral processing Technology [Editeds: H. Demirel and S. Ersayin].

83. Leaver, E.S. Hydrometallurgy of manganese. Ch. in manganese: Its occurrence, mining and metallurgy part III. Bureau of Mines Information Circular 6770. 1934 pp 167-192.

84. U.S. Congress. Benefication and utilisation of manganese Deposits in the United States. Hearings before subcommittee on minerals, materials and fuels of senate committee on interior and insular Affairs. 84th Congress, 1st session. 1955 pp. 138-145.

85. Cotter, L.W. Nitric leach has Advantages: Section in Atomic-Age metal extraction Chemical Engineering Journal. Vol.65, No.2. 1958 pp. 114-115.

86. Marshall, W.E. Method of producing concentrates of iron and manganese from low-grade ores and slags. U.S. Patent. 2,709,132, 1955.

87. Macmillan, R.T. and T.L. Turner: Development of chloride volatalisation process for manganese ores from Awostook country, Maine Progress Report. Bereau of Mines Report of Investigation 5281, 1956.

88. Skow, M.L., R.C. Kirby and J.E. Conley. Chloridisation of Marine Manganese Ore. Preliminary Batch-fluidisation Tests on Maple Mountain, Hovey Mountain samples. Bureau of Mines Report of Investigation 5271, 1956.

89. Conley, J.E. Metallurgical investigations. Ch. in Maple Mountain, Hovey Mountain Project, Bureau of Mines Report of Investigation 4921, 1952. pp.20-22.

90. Bradley, Wilson: Process for recovery manganese values. U.S. Patent 1,937,508. 1933.

91. Dear, R.S. Aqueous solution containing manganese in a complex iron and processes of making the same and making manganese from ores. Bureau of Mines Report of Investigation 3626. 1942.

92. Fox, A.L., Back, A.E., Chindgren, C.J., K.E. Tame and D. Kantman. Semi-pilot-plant investigations of Nitrogen Dioxide process for Beniticiation of manganese ores. Bureau of Mines Report 674, 1945.

93. Sharma, T. Physico-chemical processing of low-grade manganese ore. Internal Journal of Mineral Processing. Volume 35, Elseview Science Publichers. pp191-203. 1992.

94. Nossen, L.S. Manganese concentration from low-grade Domestic ore, Industrial and Engineering Chemical Journal. Volume 43, No.7. 1931. pp.1693-1700.

95. Macmillan, R.T. and T.L. Turner. Recovery of manganese from ores of Aroostook country. Maine. Bureau of Mines Report of Investigation 5082. 1954. pp. 23.

96. Leaute, K.M. Manganese Electrolyte Purification. United States Patent 2,334,210. 1943.

97. Dean, R.S. Aqueous solutions containing manganese in a complex ton and the process of making the same and making

manganese compounds therefrom. United States patent 2,608,463. 1952.

98. Heindle, R.A., J.A. Ruppert, M.L. Skow and J.E. Conley: Manganese from steel-plant slags by a lime-clinkering and carbonate leaching process. Part. Laboratory Development. Bureau of Mines Report of Investigation 5124, 1955.

99. Van Arsdale, G.D. and Mair C.G. Process for treatment of Manganese ores. U.S. patent 1, 348, 068.

100. Welsh, J.Y. and D.W. Peterson. Managanese from low-grade ores by the ammonium carbonate process. Journal of Metals, Vol.9, No.6. 1957.

101. Bradley, Wilson: Process for recovering manganse values. U.S. Patent 1,951,341. 1934.

102. Bradley, Wilson: Winning manganese values. United State Patent 1,947,457. 1934.

103. Stringham, W.S. and G.N. Summers. Method for Beneficiation manganese containing materials U.S. Patent 2,724,646. 1955.

104. Sweet, A.T. Method for Beneficiation manganese ores. U.S. Patent No. 2,724,645. 1955.

105. Weld, C.M. *et. al.* Manganese, uses, preparation, mining costs and the production of ferro-alloys. Bureau of Mines Bulletin 173. 1920.

106. Dean, R.S., E.S. Leaver and T.L. Joseph. Manganese: Its occurence, milling and metallurgy. Bureau of Mines Information Circular 6770. 1934, pp180-184.

107. Van Barneveld, C.E. Leaching of manganese ores with sulphur dioxide. Ch. in manganese, uses, preparation, mining costs and the production of Ferro-alloys. Bureau of Mines Bulletin 173. 1920. pp.57-70.

108. Allen, L.N. Recovery of manganese from low-grade ores. Chemical Engineering Progressive. Volume 50, No.1, 1954. pp.9-13.

109. Revite, S.F. *et al.*: The Semi-pilot-plant tests on treatment of manganese silver ores by the Dithionate process. *Bureau of Mines Technical, paper 723*, 1949.

110. Furman, W.H. and R.F. Whitesides. Manganese ore treatment. U.S. Patent 2,539,823.

111. Whitehouse, I.P. and M.E. Graham. Process of Selectively chloridising manganese in the treatment of minerals containing iron and manganese. U.S. Patent 2,658,813. 1953.

112. De Hutt, G.L. Manganese. Ch.in Minerals facts and problems. Bureau of Mines Bulletin 585, 1960. pp.493-510.

113. De Hutt, G.L. and Teresa, F. Manganese. Bureau of Mines Minerals Year Book. Volume 1, pp. 759-782. 1960.

114. F. Habashi. A Textbook of hydrometallurgy. 3rd edition, Metallurgic Extractive Quebel. Canada pp.239-242. 1993.

115. Broken Hill Proprietary Company Ltd. Process for the recovery of manganese from metallurgical slags. Australlan Patent 151,653.

116. Hosking, H.W. and J.A. Gregory: A process for the recovery of manganese from open hearth slags. Australian Engineering Journal. pp.44-55. 1953.

117. Udy, M.L. Process for the production of ferromanganese from low-grade manganese bearing materials. U.S. Patent 2,830,890. 1955.

118. Banning, L.H. E.E. Anable and E.F. Hergert. Experimental Electric Furnace smelting of silicious manganiferous materials. Bureau of Mines Report of Investigation 5515. 1959.

119. Torgeson, D.R. *et al.*: Matte smelting of chamber lain, 5. Dokota manganese ore. Bureau of Mines Report of Investigation 3917. 1946.

120. Lostquist, Helge. (Concentration of manganese from liquid spiegeleisen in sulphide oxide slag. Jernkontorets Annual Journal Vol.13, 1947. pp. 493-517.

121. Lostquist, Helge. Process for metallugical concentration of Raw Materials. U.S. Patent 1,927,240.

122. Harris, V., J.D. Holmgre, S. Korman and C. Sheer. Arc Decomposition of Rhodenite Journal of Electrochemical Society. Vol. 106. No.10 1959. pp. 874-876.

123. Schoenaub, R.A. Recovery of manganese from compound silicate material. U.S. Patent 2,539,485. 1951.

124. Ruppert, J.A. Manganese concentrates from open-hearth slags by lime-clinkering (Sylvester) process. Bureau of Mines Report of Investigation 4847.

125. Carosella, M.C. Method for preparing manganese - bearing materials for extraction of manganese. British Patent 785,307.

126. Scortecci, A. and A. Palazzi. Non-traditional processes for iron ore reduction. Journal of Iron and Steel Institution. Volume 195, pp. 267-277. 1960.

127. Rogers, R.R.: Direct Reduction of Iron. Canada Dept. of Mines and Technology Surveys. Mines Branch Information Circular 109, 1958.

128. Buehl, R.C. and M.B. Royers: Production of spiegeleisen from open hearth slag in an experimental Blast Furnace. Transaction of AIME. Vol. 194, pp. 1294, 1952.

129. Royers M.B. and R.C. Buehl: Production of high manganese slags by selective oxidation of spiegeleisen. Transaction of AIME. Volume 194, pp. 1295-1300. 1952.

130. Veglio, F., Schippa, G. and Toro, L. Leaching of pyrolusite concentrate of in industrial interest using sucrose in sulphuric acid solution. Proceedings of the 4th Symposium on Mining Chemistry [Edited: L.K. Attunina]. Hungarian Academy of Sciences. pp. 369-373. 1992.

131. E.C. Parkins and Novielli, F. Bacterial leaching of manganese ores. U.S. Bureau of Mines Report 6102.

132. Madgwick, J.C. Microbial processing of manganese. Australian Journal of Biotechnology. Volume 1 No.2. pp. 41-43, 1987.

133. Ehrlich, H.L. Manganese oxide reduction as a form of anaerobic respiration. Journal of Geomicrobiology. No.5, Vol.3&4. pp. 423-431, 1987.

134. Gupta, A. and Ehrlich, H.L. Selective and Non-selective bioleaching of manganese from a manganese containing silver ore. Journal of Biotechnology No.9, pp. 287-304, 1989.

135. Agate, A.D. and Deshpando, H.A. Leaching of manganese ores using Arthrobacter species. Gesellschaft Fier Biotechnologieche Forschung. [Editors: W. Schwartz and M.R. Kular]. GBF monographic series. Verlag Chemie, New York. pp. 243-250, 1977.

136. Hart, M.J. and Madgwick, J.C. Biodegradation of manganese dioxide tailings. Bulletin of the proceeedings of Australian Institution of Mining Metallurgy. Vol. 291, No.3. pp. 61-64, 1986.

137. F. Veglio and L. Toro. Reductive leaching of a concentrate manganese dioxide ore in acid solution. Stoichiometry and Preliminary Kinetic analysis. International Journal of Mineral Processing. Vol. 4, No.3. Elsevier Science Publishers, pp. 257-272. 1994.

138. Heindle, R.A., J.A. Ruppert, M.L. Skow and J.E. Conley. Manganese from steel plant slags by a lime-clinkering and carbonate leaching process. Part II, Pilot plant Development. Bureau of Mines Report of Investigation 5142. 1955.

139. Weld, C.M. *et al.*: Manganese. Uses, preparation, mining costs and the production of ferro-alloys. Bureau of Mines Bulletin 173. 1920.

140. Wright, E.C. More manganese from American ores and slags. Metal progress. Volume 59, 1951. pp. 347-353.

141. E.A. Herson: Hanbook of Non-ferrous metallurgy recovery of the metals. [Edited: D.M. Liddeli]. 2nd edition McGraw - Hill Book Company. pp. 566-582. 1945.

142. Chilton, C.H. High purity manganese via Electrolysis. Chemical Engineering Volume 65. No. 10. pp. 497-498. 1958.

143. Hunter, *et al.*: First two years of operations of the Bureau of Mines Electrolytic manganese pilot plant at Boulder City, Navada. A.I.M.M.E. Technical paper 1717. New York. 1944.

144. Normal, L.D. and Kirby, R.C. Review of major proposed processes for recovering manganese from United States Resources. Part II, Choloride and Fixed Nitrogen processes. Bureau of Mines Information Circular 8160. 1963.

145. Ravitz, S.F., E.F. Wayman, A.E. Back and K.E. Tame. The Dithiorite process for recovery of manganese from low-grade ores. Transactions of AIME volume 182, pp. 286-295. 1986.

146. Jukkola, W.W. Manganese ore treatment. U.S. Patent 2,340,188.

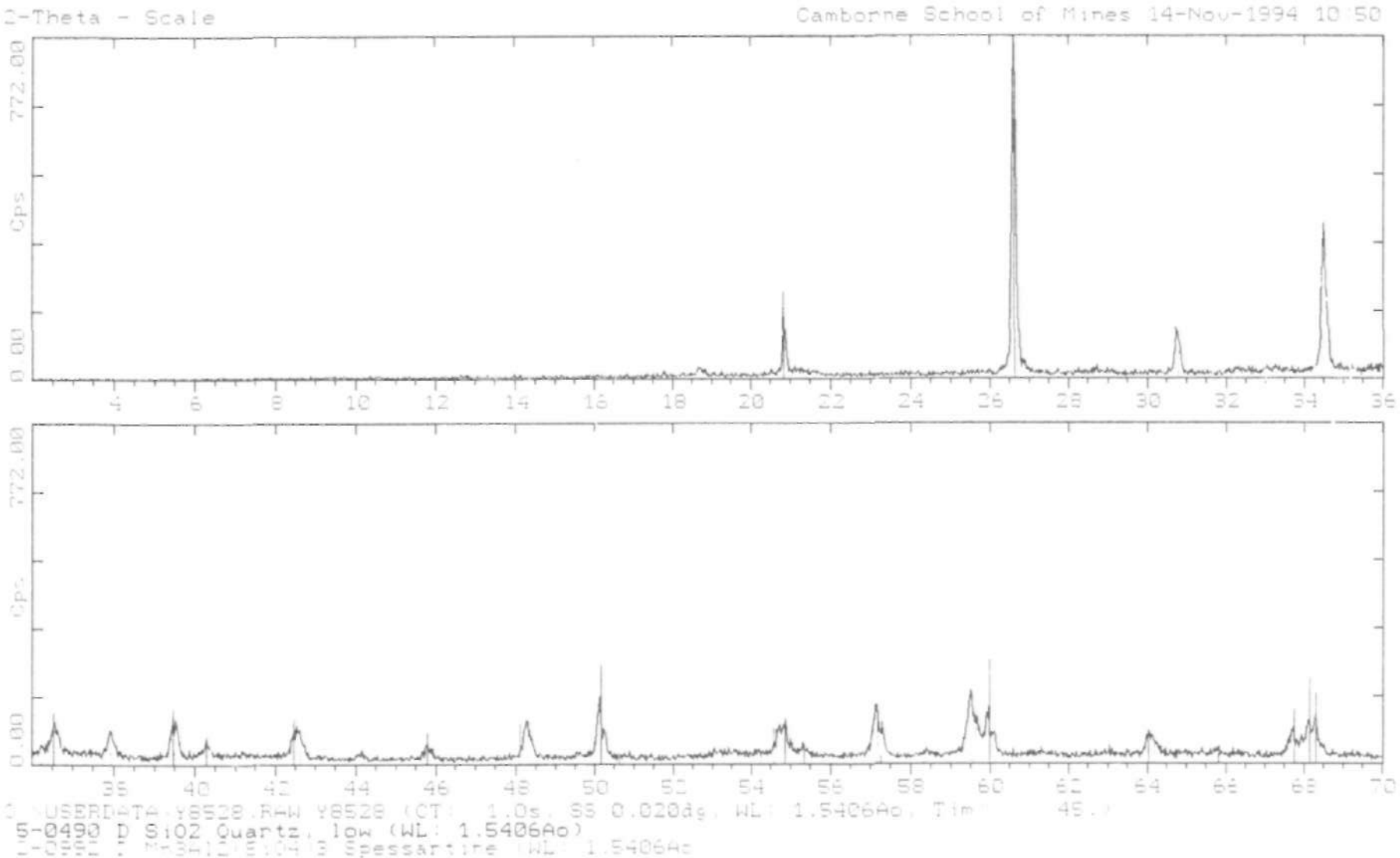
147. Hoak, R.D. and J. Cowell. Recovery of manganese from low-grade ores. Iron age. Volume 165. No.3. pp. 81-82.

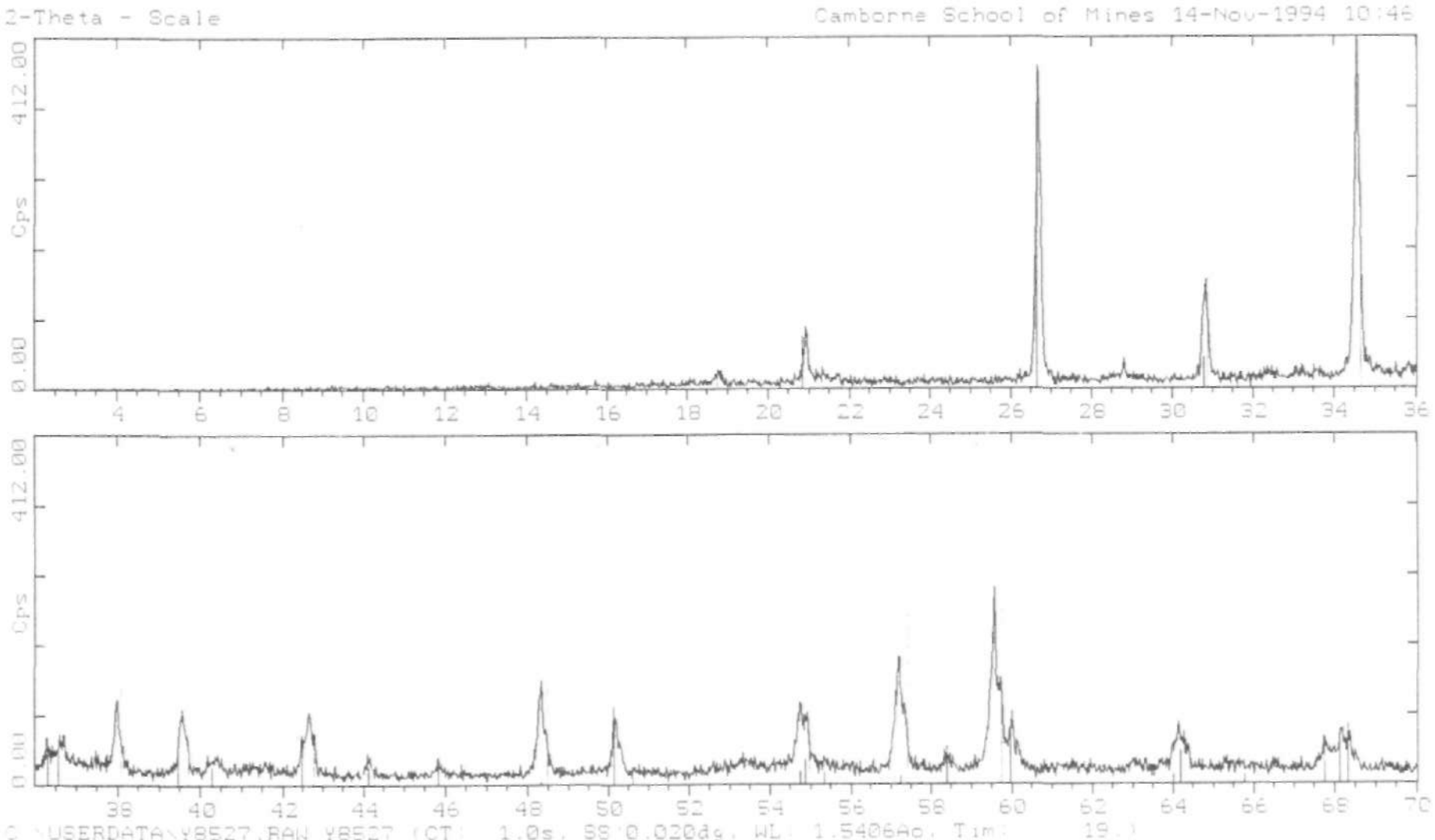
148. Hoak, R.D. and J. Covll. Recovery of manganese from low-grade ores: Chemical Engineering Progressive. Vol.46, No.3. pp. 158-168.

149. Van Ardale, G.D. and C.G. Mair. Process of extracting manganese and making sulphuric acid and manganese dioxide. U.S. Patent 1,304,222.

150. Normal, L.D. and R.C. Kirby. Review of Major proposed processes for recovering manganese from United States Resources. Part I. Pyrometallurgical processes. Bureau of Mine Information Circular 8138, 1962.

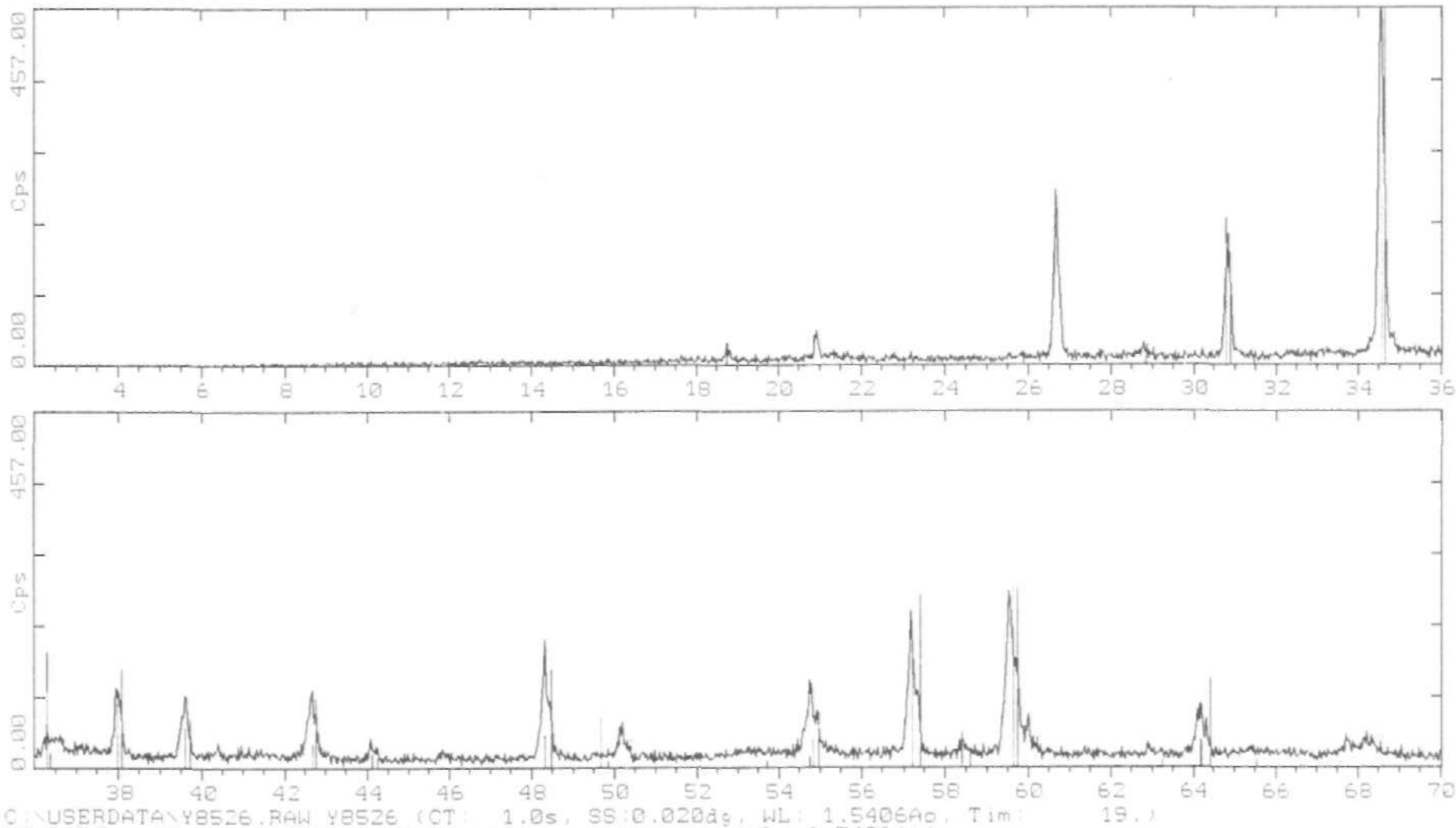
APPENDICES


2-Theta - Scale
Camborne School of Mines 14-Nov-1994 10:50
772.00
Cps
0.00
4 6 8 10 12 14 16 18 20 22 24 26 28 30 32 34 36
772.00
Cps
0.00
38 40 42 44 46 48 50 52 54 56 58 60 62 64 66 68 70
C:\USERDATA\Y8528.RAW Y8528 (CT: 1.0s, SS 0.020d, WL: 1.5406Ao, Tim 45.)
5-0490 D SiO2 Quartz, low (WL: 1.5406Ao)
Spessartine (WL: 1.5406Ao


2-Theta - Scale
Camborne School of Mines 14-Nov-1994 10:46
412.00
Cps
0.00
4
6
8
10
12
14
16
18
20
22
24
26
28
30
32
34
36
412.00
Cps
0.00
38
40
42
44
46
48
50
52
54
56
58
60
62
64
66
68
70
C:\USERDATA\Y8527.RAW Y8527 (CT: 1.0s, SS:0.020dg, WL: 1.5406Ao, Tim: 19.)
33-1161 * SiO2 Quartz, syn (WL: 1.5406Ao)
29-0880 * MnAl2O4 Galaxite, syn (WL: 1.5406Ao)

2-Theta - Scale

Camborne School of Mines 14-Nov-1994 10:42

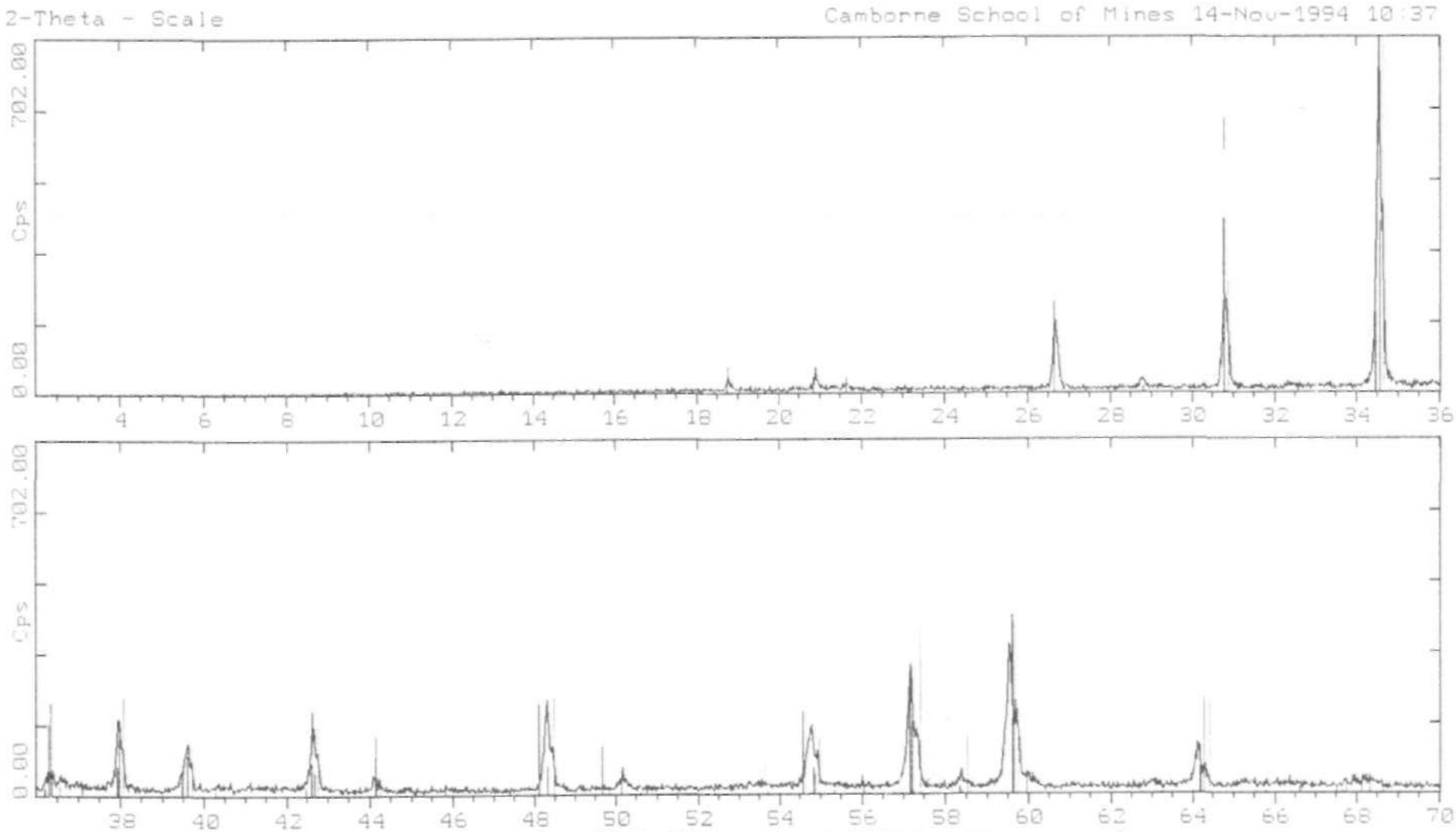


C:\USERDATA\Y8526.RAW Y8526 (CT: 1.0s, SS:0.020dg, WL: 1.5406Ao, Tim: 19.)

33-0658 * (Fe,Mn)3Al2(SiO4)3 Almandine, manganoan (WL: 1.5406Ao)

35-0536 I Mg3Cr2(SiO4)3 Knorringite, syn (WL: 1.5406Ao) x ?

29-0880 * MnAl2O4 Galaxite, syn (WL: 1.5406Ao)



C:\USERDATA\Y8525.RAW Y8525 (CT: 1.0s, SS:0.020deg, WL: 1.5406Ao, Tim: 19.)

35-0536 I Mg3Cr2(SiO4)3 Knorringite, syn (WL: 1.5406Ao)

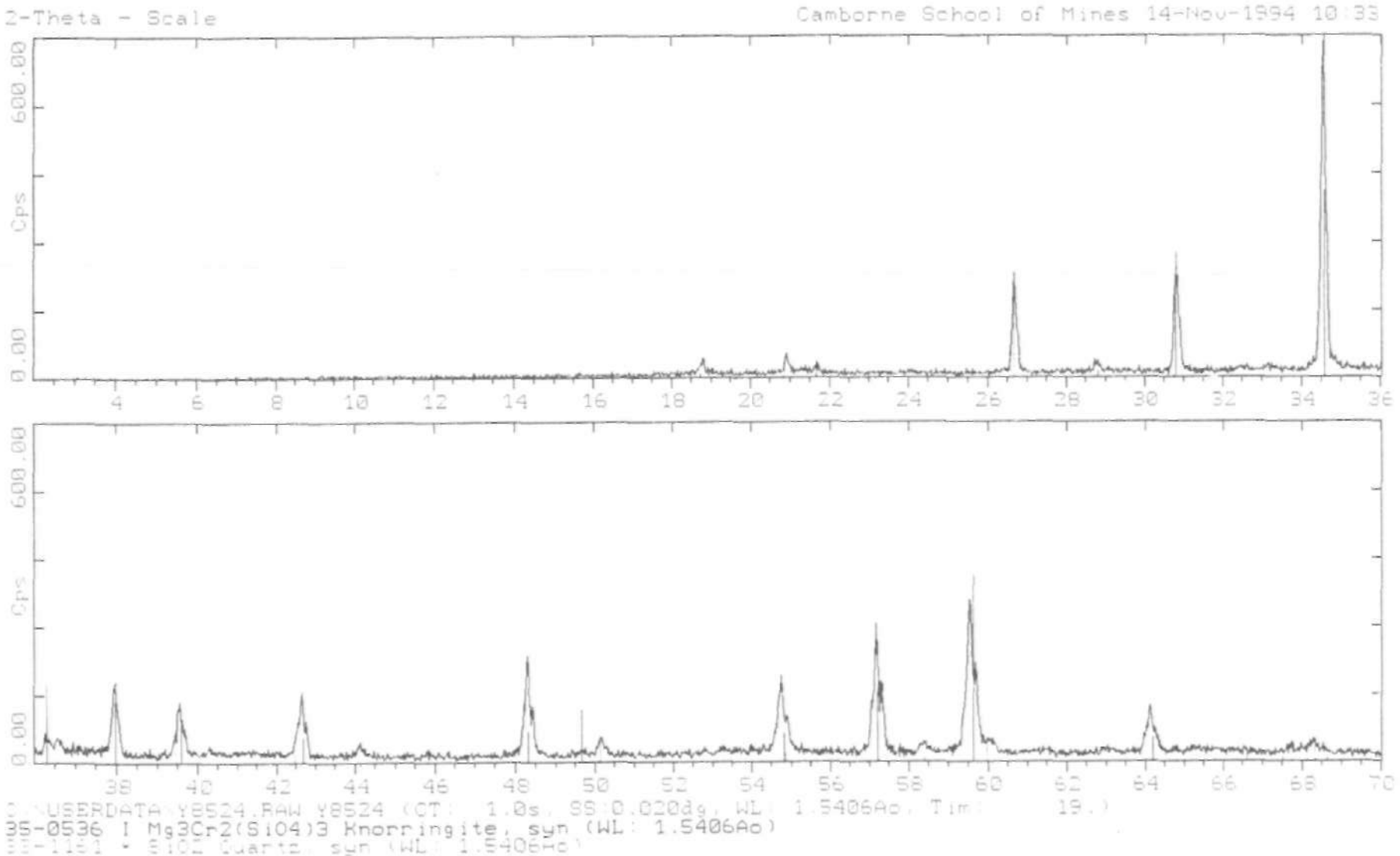
~~33-0658 * (Fe,Mn)3Al2(SiO4)3 Almandine, manganoan (WL: 1.5406Ao)~~

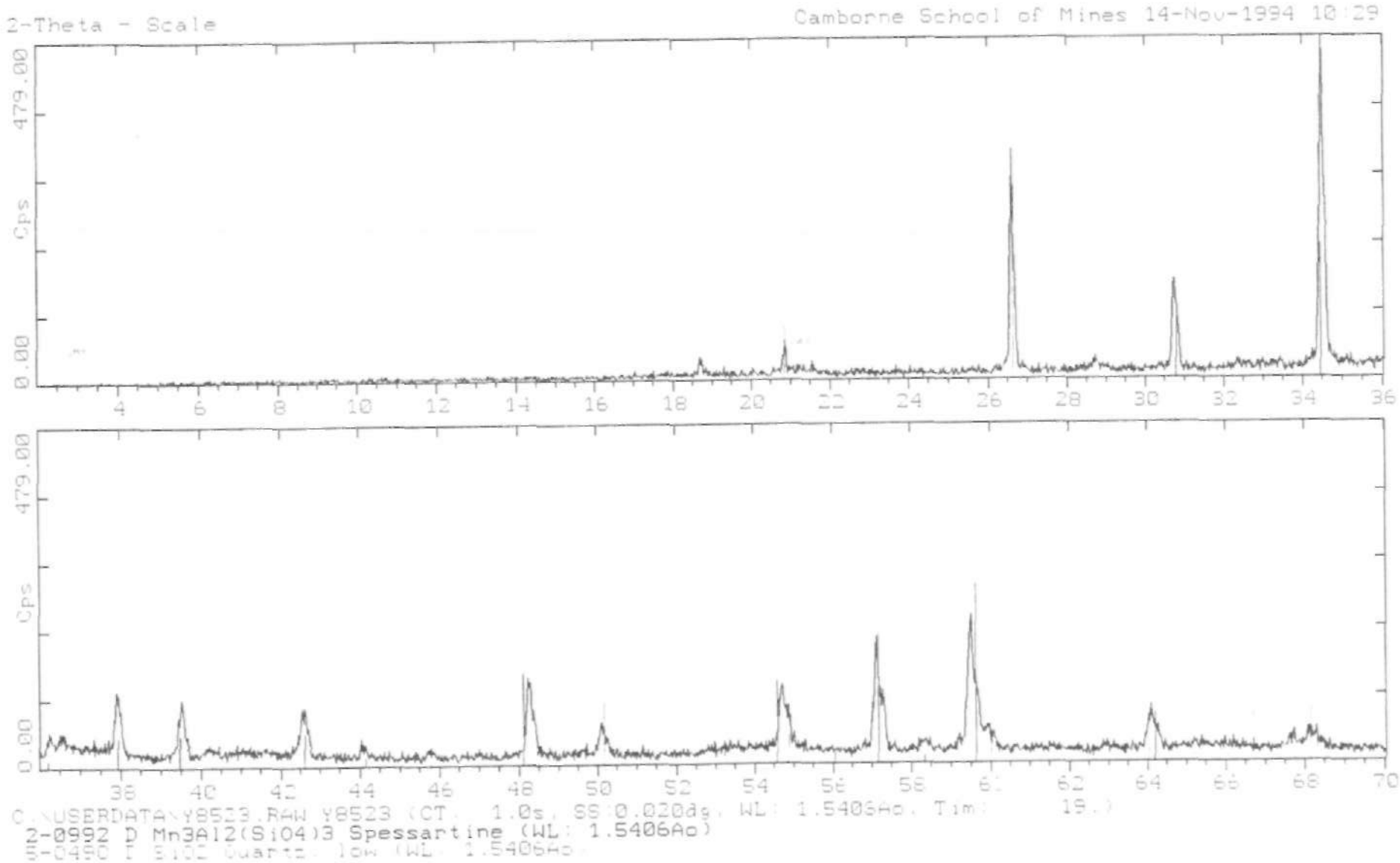
2-0992 D Mn3Al2(SiO4)3 Spessartine (WL: 1.5406Ao)

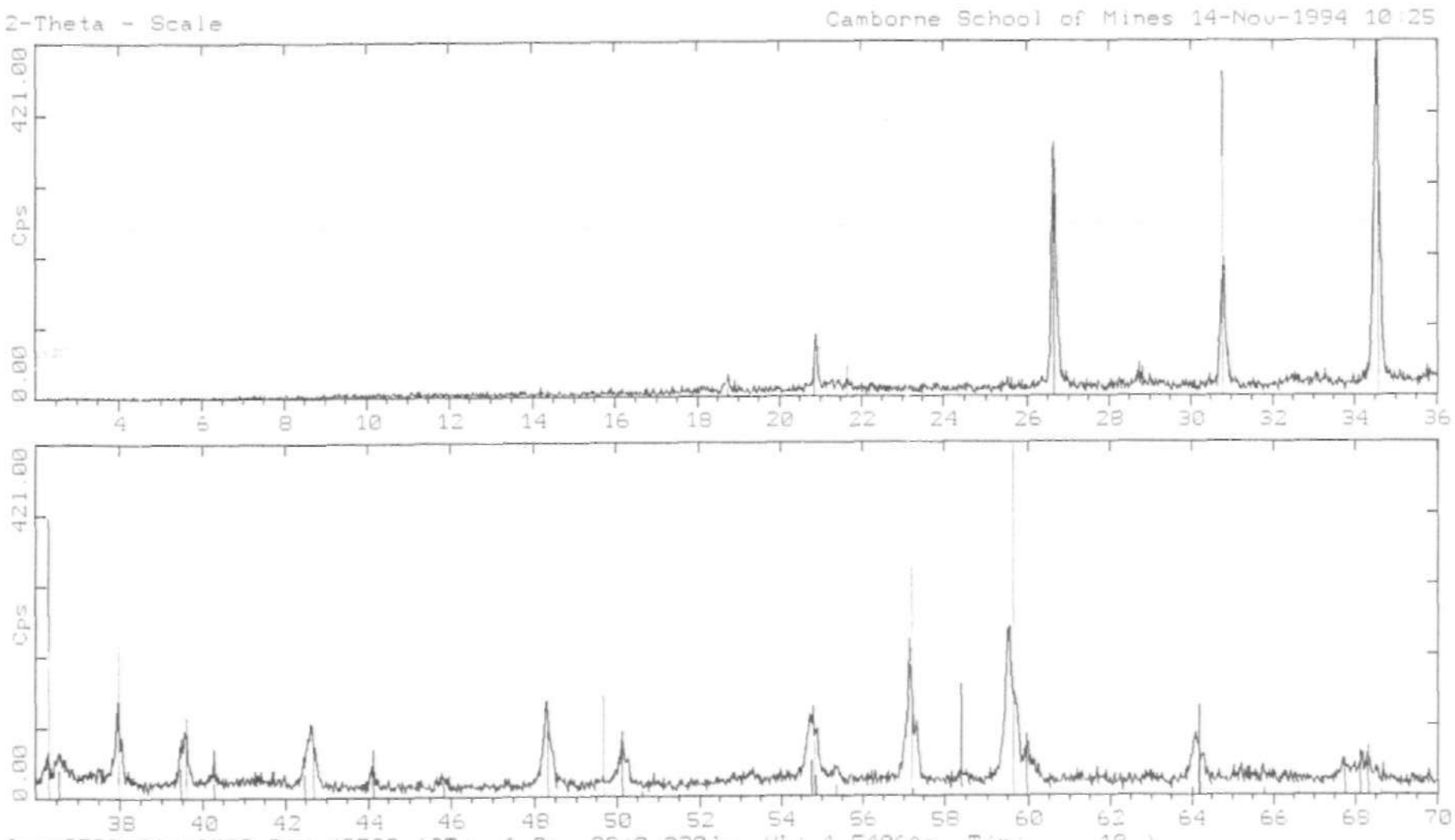
~~[illegible]~~

33-1161 * SiO2 Quartz, syn (WL: 1.5406Ao)

21-0540 I Mg(Al,Fe)2O4 Spinel, ferrian (WL: 1.5406Ao)


2-Theta - Scale
Camborne School of Mines 14-Nov-1994 10:33
600.00
Cps
0.00
4
6
8
10
12
14
16
18
20
22
24
26
28
30
32
34
36
600.00
Cps
0.00
38
40
42
44
46
48
50
52
54
56
58
60
62
64
66
68
70
C:\USERDATA\Y8524.RAW Y8524 (CT: 1.0s, SS:0.020dg, WL: 1.5406Ao, Tim: 19.)
35-0536 I Mg3Cr2(SiO4)3 Knorringite, syn (WL: 1.5406Ao)


2-Theta - Scale
Camborne School of Mines 14-Nov-1994 10:29
Cps
479.00
0.00
4
6
8
10
12
14
16
18
20
22
24
26
28
30
32
34
36
38
40
42
44
46
48
50
52
54
56
58
60
62
64
66
68
70
C:\USERDATA\Y8523.RAW Y8523 (CT: 1.0s, SS:0.020dg, WL: 1.5406Ao, Tim: 19.)
2-0992 D Mn3Al2(SiO4)3 Spessartine (WL: 1.5406Ao)
5-0490 I SiO2 Quartz, low (WL: 1.5406Ao)


2-Theta - Scale
Camborne School of Mines 14-Nov-1994 10:25
Cps
421.00
0.00
4
6
8
10
12
14
16
18
20
22
24
26
28
30
32
34
36
38
40
42
44
46
48
50
52
54
56
58
60
62
64
66
68
70
C:\USERDATA\Y8522.RAW Y8522 (CT: 1.0s, SS:0.020dg, WL: 1.5406Ao, Tim: 18.)
33-1161 * SiO2 Quartz, syn (WL: 1.5406Ao)
35-0536 I Mg3Cr2(SiO4)3 Knorringite, syn (WL: 1.5406Ao)
29-0880 * MnAl2O4 Galaxite, syn (WL: 1.5406Ao)

APPENDIX 2

MALVERN Instruments SB.0C 23 Nov 1994 11:29 am

manganese
23/11/94
ground for 20mm 000000082 00000000000000001295 0000001000003745000003748

END

3850 stnd lm10337s

Upper	in	Lower	Under
		124	6.1 101 65.2
		101	5.3 83.3 59.3
		83.3	4.5 68.3 55.4
		68.3	4.2 56.1 51.2
699	0.2 432	55.1	4.0 45.0 47.2
432	0.5 404	46.0	4.2 37.8 43.0
404	1.2 332	37.8	4.3 31.0 38.7
332	2.7 272	31.0	4.4 25.5 34.2
272	4.5 224	25.5	4.2 20.9 30.0
224	5.1 183	20.9	3.8 17.1 26.2
183	6.7 151	17.1	3.3 14.1 22.9
151	6.9 124	14.1	2.9 11.6 20.0

Upper	in	Lower	Under
11.6	2.3	9.48	17.4
9.48	2.3	7.78	15.1
7.78	2.2	6.39	12.9
6.39	2.1	5.24	10.8
5.24	2.0	4.30	8.8
4.30	1.8	3.53	7.0
3.53	1.6	2.90	5.4
2.90	1.4	2.38	4.0
2.38	1.1	1.95	2.9
1.95	0.9	1.60	1.9
1.60	0.9	1.32	1.0
1.32	1.0	0.50	0.0

Source = :Sample	Beam length = 2.4 mm	Model indp
	Residual = 0.912 %	
Focal length = 300 mm	Obscuration = 0.1045	Volume Conc. = 0.0187%
Presentation = stnd	Volume distribution	Sp.S.A 0.4640 m²/cc.

Span 3.99

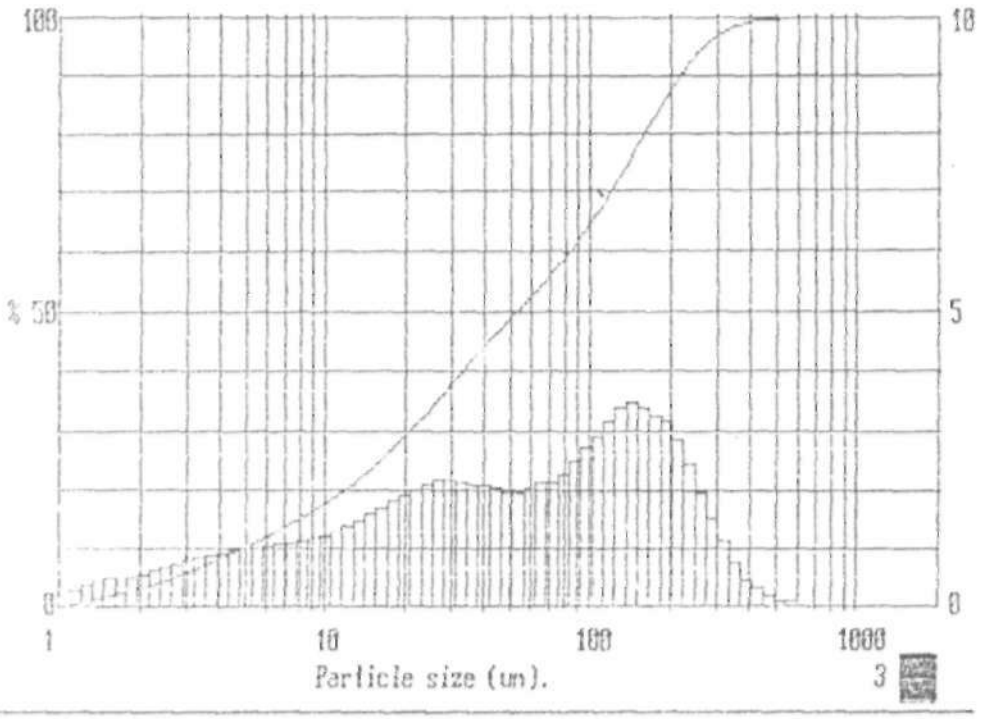
D[4,3] 87.26µm

D[3,2] 12.93µm

D[v,0.9] 215.94µm

D[v,0.1] 4.86µm

D[v,0.5] 52.93µm



Malvern Instruments

MALVERN Instruments SB.8C 22 Nov 1994 3:58 pm

manganese
22/11/94
ground for 2½ mins

00000082 00000000000000001295 0000001000003744

End

3850 stnd lm10337s

Upper	in	Lower	Under
600	3.0	432	97.0
432	2.3	404	94.7
404	2.1	332	92.6
332	2.2	272	90.5
272	2.4	224	88.0
224	2.7	183	85.3
183	3.1	151	82.1
151	3.4	124	78.8

Upper	in	Lower	Under
124	3.7	101	75.1
101	3.9	83.3	71.2
83.3	4.2	68.3	67.1
68.3	4.5	56.1	62.6
56.1	4.8	46.0	57.8
46.0	4.9	37.8	52.9
37.8	5.0	31.0	47.9
31.0	4.9	25.5	43.0
25.5	4.7	20.9	38.2
20.9	4.4	17.1	33.9
17.1	4.0	14.1	29.7
14.1	3.6	11.6	26.1

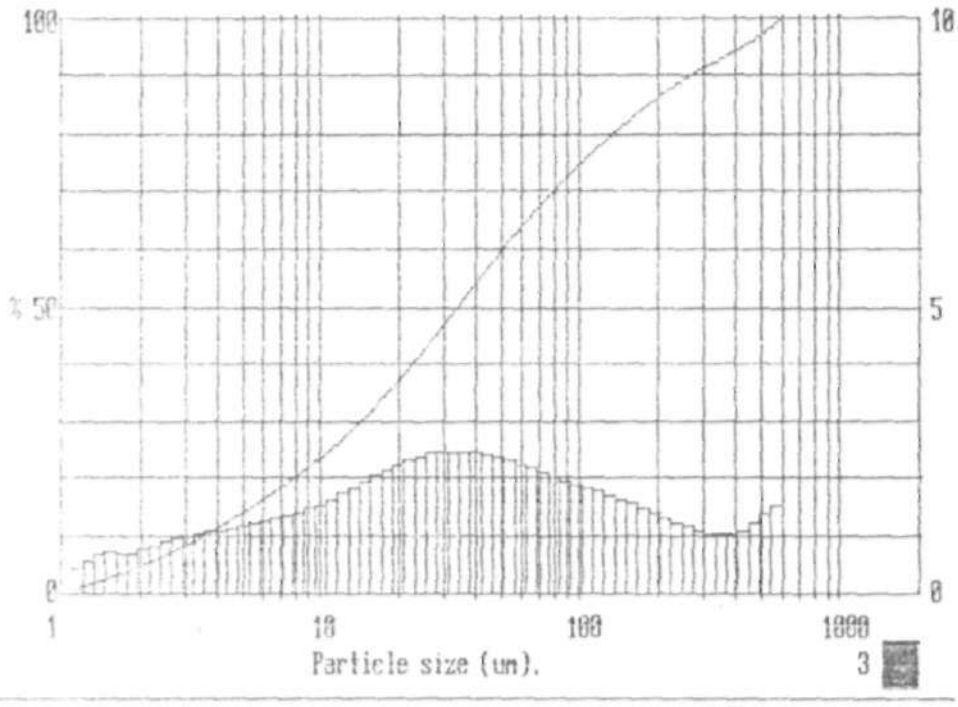
Upper	in	Lower	Under
11.6	3.2	9.48	22.9
9.48	2.9	7.78	20.0
7.78	2.7	6.39	17.3
6.39	2.5	5.24	14.8
5.24	2.4	4.30	12.4
4.30	2.2	3.53	10.2
3.53	2.0	2.90	8.2
2.90	1.9	2.38	6.3
2.38	1.7	1.95	4.6
1.95	1.4	1.60	3.2
1.60	1.4	1.32	1.7
1.32	1.7	0.50	0.0

Span
7.67
D[4,3] 87.56µm
D[3,2] 9.60µm
D[v,0.9] 262.01µm
D[v,0.1] 3.46µm
D[v,0.5] 33.69µm

Source = :Sample
Focal length = 300 mm
Presentation = stnd

Beam length = 2.4 mm
Residual = 0.274 %
Obscuration = 0.1613
Volume distribution

Model indp
Volume Conc. = 0.0222%
Sp.S.A 0.6251 m²/cc.



Malvern Instruments

40

MALVERN Instruments SB.0C 23 Nov 1994 12:27 pm

manganese
23/11/94
ground for 30min

000000082 00000000000000001295 0000001000003745000003749

3850 stnd lm10337s

Upper	in	Lower	Under
600	0.0	492	100
492	0.1	404	99.9
404	0.5	332	99.4
332	1.4	272	98.0
272	2.7	224	95.2
224	3.9	183	91.3
183	4.6	151	86.7
151	5.0	124	81.7

Upper	in	Lower	Under
124	4.9	101	76.8
101	4.8	83.3	72.0
83.3	4.7	68.3	67.3
68.3	4.8	56.1	62.6
56.1	4.8	46.0	57.7
46.0	4.8	37.8	52.9
37.8	4.8	31.0	48.1
31.0	4.8	25.5	43.3
25.5	4.8	20.9	38.5
20.9	4.5	17.1	34.0
17.1	4.1	14.1	29.9
14.1	3.6	11.6	26.3

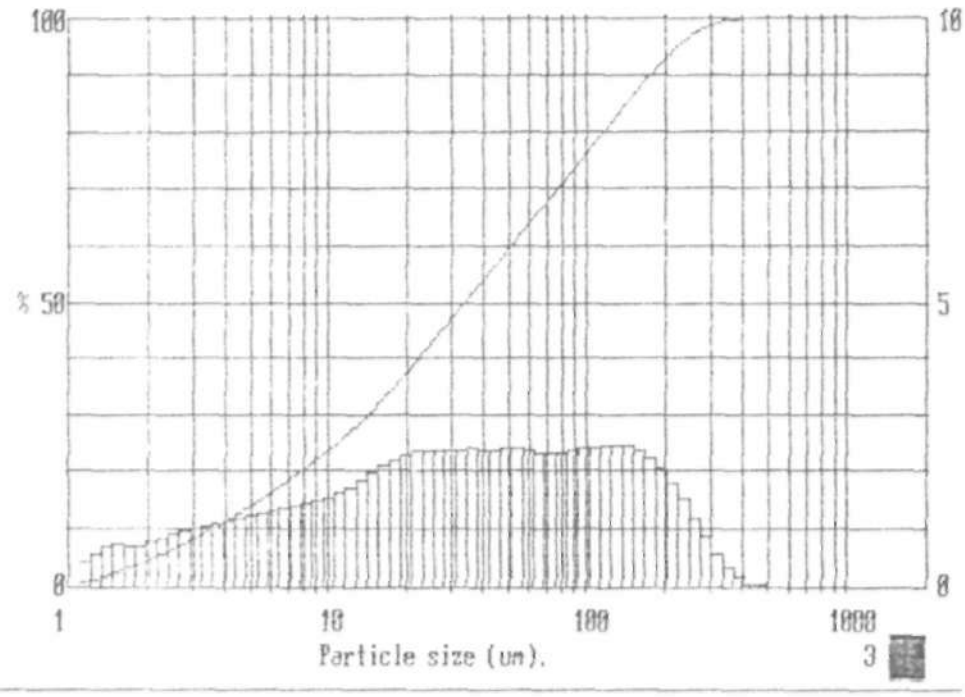
Upper	in	Lower	Under
11.6	3.2	9.48	23.1
9.48	3.0	7.78	20.1
7.78	2.8	6.39	17.3
6.39	2.6	5.24	14.7
5.24	2.4	4.30	12.3
4.30	2.3	3.53	10.1
3.53	2.1	2.90	8.0
2.90	1.9	2.38	6.1
2.38	1.6	1.95	4.5
1.95	1.4	1.60	3.1
1.60	1.4	1.32	1.7
1.32	1.7	0.50	0.0

Span
5.05
D[4,3] 63.96µm
D[3,2] 9.63µm
D[v,0.9] 172.98µm
D[v,0.1] 3.51µm
D[v,0.5] 33.54µm

Source = :Sample
Focal length = 300 mm
Presentation = stnd

Beam length = 2.4 mm
Residual = 1.640 %
Obscuration = 0.1510
Volume distribution

Model indp
Volume Conc. = 0.0207%
Sp.S.A 0.6230 m²/cc.



Malvern Instruments

MALVERN Instruments SB.BC 22 Nov 1994 4:14 pm

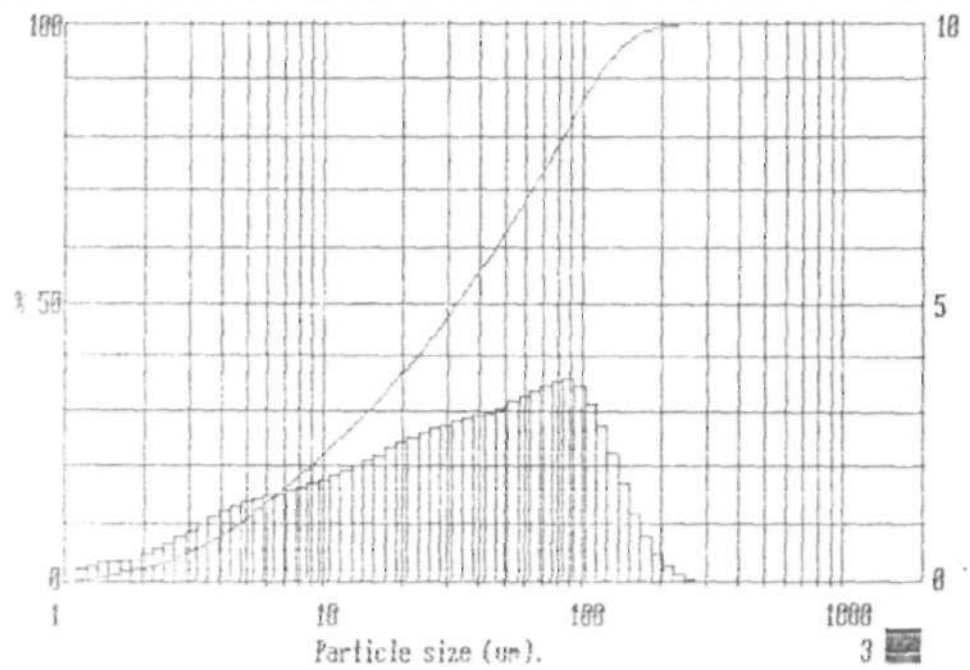
manganese
22/11/94 B.S.Mair
ground for 9min 000000082 0000000000000001295 0000001000003745

END

3850 stnd l=10337s

Upper	in	Lower	Under	Upper	in	Lower	Under	Upper	in	Lower	Under	Span
				124	5.9	101	87.1	11.6	3.6	9.48	21.2	3.26
				101	7.1	83.3	80.0	9.48	3.4	7.78	17.8	D[4,3]
				83.3	7.0	68.3	73.0	7.78	3.1	6.39	14.7	47.19µm
				68.3	6.6	56.1	66.4	6.39	3.0	5.24	11.7	
600	0.0	492	100	56.1	6.2	46.0	60.2	5.24	2.7	4.30	9.0	D[3,2]
492	0.0	404	100	46.0	5.9	37.8	54.3	4.30	2.4	3.53	6.6	11.85µm
404	0.0	332	100	37.8	5.7	31.0	48.5	3.53	1.9	2.90	4.7	
332	0.0	272	100	31.0	5.4	25.5	43.1	2.90	1.5	2.38	3.3	D[v,0.9]
272	0.2	224	99.8	25.5	5.2	20.9	37.9	2.38	1.0	1.95	2.2	111.00µm
224	0.7	183	99.1	20.9	4.8	17.1	33.8	1.95	0.7	1.60	1.5	
183	2.0	151	97.1	17.1	4.3	14.1	28.8	1.60	0.7	1.32	0.8	D[v,0.1]
151	4.0	124	93.0	14.1	4.0	11.6	24.8	1.32	0.8	0.50	0.0	4.63µm

Source = :Sample	Beam length = 2.4 mm	Model indp	D[v,0.5]
	Residual = 1.658 %		32.64µm
Focal length = 300 mm	Obscuration = 0.1439	Volume Conc. = 0.0240%	
Presentation = stnd	Volume distribution	Sp.S.A 0.5063 m²/cc.	



MALVERN Instruments S8.0C 23 Nov 1994 10:25 am

manganese
23/11/94 4-0
ground for 0.5min 000000082 00000000000000001295 00000010000037450000037460

END

3850 stnd lm10337s

Upper	in	Lower	Under	Upper	in	Lower	Under	Upper	in	Lower	Under
				124	2.6	101	91.3	11.6	4.3	9.48	33.4
				101	3.2	83.3	88.1	9.48	4.0	7.78	29.4
				83.3	3.7	68.3	84.5	7.78	3.8	6.39	25.6
				68.3	4.3	56.1	80.1	6.39	3.6	5.24	22.0
600	0.1	492	99.9	56.1	4.7	46.0	75.5	5.24	3.4	4.30	18.6
492	0.1	404	99.9	46.0	5.2	37.8	70.2	4.30	3.1	3.53	15.5
404	0.2	332	99.7	37.8	5.3	31.0	64.9	3.53	2.8	2.90	12.7
332	0.4	272	99.3	31.0	5.7	25.5	59.2	2.90	2.5	2.38	10.3
272	0.7	224	98.6	25.5	5.7	20.9	53.5	2.38	2.1	1.95	8.2
224	1.0	183	97.6	20.9	5.7	17.1	47.8	1.95	1.7	1.60	6.5
183	1.6	151	96.0	17.1	5.3	14.1	42.5	1.60	1.7	1.32	4.7
151	2.1	124	93.9	14.1	4.8	11.6	37.7	1.32	4.7	0.50	0.0

Source = :Sample	Beam length = 2.4 mm	Model indp	
	Residual = 0.982 %		
Focal length = 300 mm	Obscuration = 0.1514	Volume Conc. = 0.0138%	
Presentation = stnd	Volume distribution	Sp.S.A 0.9820 m²/cc.	

Span 4.90

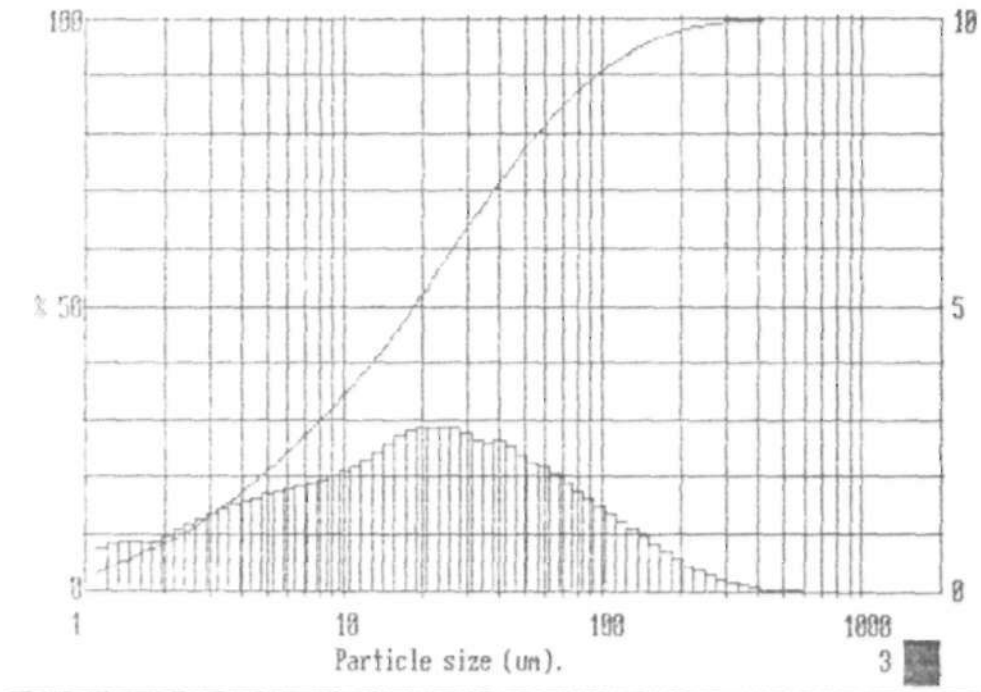
D[4,3] 36.69µm

D[3,2] 6.11µm

D[v,0.9] 93.18µm

D[v,0.1] 2.33µm

D[v,0.5] 18.53µm



MALVERN Instruments SB.0C 21 Nov 1994 2:33 pm

MANGANESE ORE
21/11/94
GROUND 6 Min.

0000000B2 00000000000000001295 0000001000033741

3850 stnd 1m10337s

Upper	in	Lower	Under
800	0.0	492	100
492	0.0	404	100
404	0.1	332	99.9
332	0.3	272	99.6
272	0.8	224	98.9
224	1.7	183	97.2
183	3.1	151	94.1
151	4.5	124	89.7

Upper	in	Lower	Under
124	5.6	101	84.1
101	6.1	83.3	77.9
83.3	6.4	68.3	71.5
68.3	6.2	56.1	65.3
56.1	5.9	46.0	59.4
46.0	5.7	37.8	53.6
37.8	5.7	31.0	48.0
31.0	5.5	25.5	42.5
25.5	5.1	20.9	37.3
20.9	4.6	17.1	32.7
17.1	4.1	14.1	28.6
14.1	3.4	11.6	25.2

Upper	in	Lower	Under
11.6	2.9	9.48	22.3
9.48	2.6	7.78	19.7
7.78	2.4	6.39	17.3
6.39	2.3	5.24	15.0
5.24	2.2	4.30	12.8
4.30	2.1	3.53	10.7
3.53	2.0	2.90	8.7
2.90	1.9	2.38	6.8
2.38	1.7	1.95	5.0
1.95	1.5	1.60	3.5
1.60	1.6	1.32	1.9
1.32	1.9	0.50	0.0

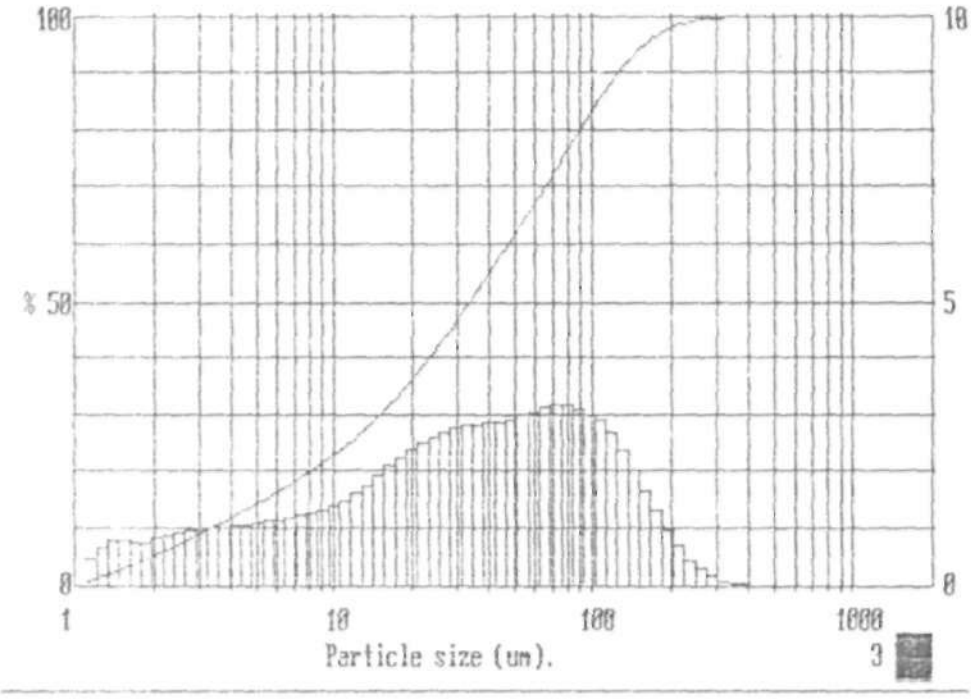
Span
3.66
D[4,3] 51.49µm
D[3,2] 9.28µm
D[v,0.9] 125.15µm
D[v,0.1] 3.31µm
D[v,0.5] 33.31µm

Source = :Sample
Focal length = 300 mm
Presentation = stnd

Beam length = 2.4 mm
Residual = 0.618 %
Obscuration = 0.1328
Volume distribution

Model indp

Volume Conc. = 0.0174%
Sp.S.A 0.6467 m²/cc.



APPENDIX 3

TABLE: SPECIFICATIONS FOR CHEMICAL - GRADE MANGANESE ORE/CONCENTRATE

	ASSAY	
CONSTITUENT	TYPE A (%)	TYPE B (%)
MnO_2, Minimum	80.0	82.0
Mn, Minimum	50.0	53.0
Fe, Maximum	3.0	3.0
Si, Maximum	-	5.0
Al, Maximum	-	3.0
P, Maximum	-	0.20
As, Maximum	-	0.10

Sources: Economics of Manganese, 1991, by Roskill Information Services.

TABLE: SPECIFICATIONS FOR BATTTERY - GRADE MANGANESE:

ASSAY	%
MnO_2	85% Minimum
Mn	58 Minimum
H_2O	2 Maximum
Fe	0.3 Maximum
SiO_2	0.5 Maximum
Total Heavy Metals	0.3 Maximum
Pb	0.2

Sources: Economics of Manganese 1991, by Roskill Information Services.